CONSOLIDATION AND MANTLE EVOLUTION OF THE SINOKOREAN CRATON IN EARLY PRECAMBRIAN TIME

By

MIN SUN

B.Sc., Peking University,1982
M.Sc., The University of British Columbia, 1985

A THESIS SUBMITTED IN PARTIAL FULFILMENT OF

THE REQUIREMENTS FOR THE DEGREE OF

DOCTOR OF PHILOSOPHY

in

THE FACULTY OF GRADUATE STUDIES

(Department of Geological Sciences)

We accept this thesis as conforming

to the required standard

THE UNIVERSITY OF BRITISH COLUMBIA

November 1991

Department of Geological Sciences

The University of British Columbia
Vancouver, Canada

Date Nov. 4, 1991

ABSTRACT

The oldest nuclei of the Sinokorean Craton are the 3.5 Ga amphibolites and grey gneisses of the Qianxi Complex and the ≥3.0 Ga Qingyuan Complex that may extend to the Anshan area to include the ≥3.0 Ga Tiejiashan and Lishan granites. Other high-grade metamorphic complexes of the Sinokorean Craton are mostly between 2.7 and 2.8 Ga in age - the Anshan, Longgang, Jianping, Taishan, Jiaodong, and Taihua complexes. The high-grade Fuping Complex formed about 2.6 Ga ago in an environment like a modern island arc: it is not one of the earliest nuclei. The medium-grade Wutai Complex formed by 2.5 Ga ago, mostly in a tectonic setting similar to that of Fuping Complex, with the exception that one volcanic cycle formed in an environment like a modern MOR and one unit formed in an environment transitional between modern within-plate and plate margin settings. There is no evidence for continental crust older than 2.6 Ga in the Wutaishan and Taihangshan regions. The Sm-Nd systems for metabasaltic rocks in the Wutaishan and Taihangshan region, are all significantly disturbed, in contrast with the undisturbed Sm-Nd system reported for rocks older than 2.6 Ga in the Sinokorean Craton.

High-grade rocks of the Sanggan and Dengfeng complexes, and some granulites in the Qianxi Complex are ≥2.5 Ga in age. Available Nd isotopic data show that rocks older than 2.5 Ga in the Sinokorean Craton are derived from a mantle source more depleted than that defined by DePaolo's depleted mantle evolution curve. Granitic magmatism peaked 2.5 Ga ago in the

Sinokorean Craton, affecting all the previously formed rocks. Nd isotopic data show significant crustal involvement in formation of some ~2.5 Ga granites in the Sinokorean Craton.

Early Proterozoic mafic volcanic rocks of the 2.3 to 2.4 Ga Kuandian Complex in Liaoning Province and the Hutuo Complex in Shanxi Province, formed in a intra-continental environment. Kuandian granites have an anorogenic granite character. The early Proterozoic mantle magma source in the eastern Liaoning Province is less depleted than the mantle of DePaolo's (1981) average mantle evolution curve. This can be explained by contamination of Archean basement or derivation from a different mantle source.

TABLE OF CONTENTS

LIST OF TABLES

LIST OF FIGURES

ACKNOWLEDGEMENTS

I wish to express sincere appreciation to Dr. Richard Lee Armstrong, thesis supervisor, for his support, supervision, advice and encouragement throughout the study.

I am also grateful for supervision and support from Dr. Richard St J. Lambert during sample collection in China and isotopic analyses at the University of Alberta.

Financial support was provided by graduate fellowships from the University of British Columbia and the University of Alberta, an NSERC Operating Grant to R. St J. Lambert and an NSERC Operating Grant to R. L. Armstrong.

Thanks also to Drs. Xinhua Zhou, Molan E, Jiliang Li, Kaiyi Wang, Chunchao Jiang, Chaolei Xu, Jiahong Wu, Guangsheng Feng and Yinghui Li for their help and discussion during the field work.

ACKNOWLEDGEMENTS

I wish to express sincere appreciation to Dr. Richard Lee Armstrong, thesis supervisor, for his support, supervision, advice and encouragement throughout the study.

I am also grateful for supervision and support from Dr. Richard St J. Lambert during sample collection in China and isotopic analyses at the University of Alberta.

Financial support was provided by graduate fellowships from the University of British Columbia and the University of Alberta, an NSERC Operating Grant to R. St J. Lambert and an NSERC Operating Grant to R. L. Armstrong.

Thanks also to Drs. Xinhua Zhou, Molan E, Jiliang Li, Kaiyi Wang, Chunchao Jiang, Chaolei Xu, Jiahong Wu, Guangsheng Feng and Yinghui Li for their help and discussion during the field work.

I. INTRODUCTION

The Sinokorean Craton (30-45°N, and 105-128°E) includes much of the oldest crystalline basement in Asia. It contains rocks as old as 3.5 Ga, and was largely stabilized 2.4-2.5 Ga ago. The Early Precambrian rocks have generally undergone high- to medium- grade metamorphism in Archean and Early Proterozoic times. The main exposures along the north border of the craton are, from west to east, in Inner Mongolia, eastern Hebei, eastern Liaoning and southeastern Jilin provinces; exposures of the centre of the craton in Shanxi, and Shandong provinces and near to the south border of the craton, small exposures along northern slope of the Qinling Mountain Range in Henan and adjacent provinces (Fig. 1-1 and 1-2).

Recent geochemical and geochronological studies of the Early Precambrian rocks in the Sinokorean Craton have substantially improved our understanding of its Precambrian history. However, conventional stratigraphic divisions are still widely used for Archean and Early Proterozoic systems in China and great effort has been made to correlate the stratigraphic groups and formations for different areas (e.g. Wang, 1988; Zhao, 1988). Such conventional stratigraphic divisions often create contradictions even when applied to small areas, due to erasure of original petrology by superimposed high-grade metamorphism. Moreover stratigraphic schemes based solely on metamorphic grade or structural complexity are generally not substantiated by firm geochronological data. For example, when

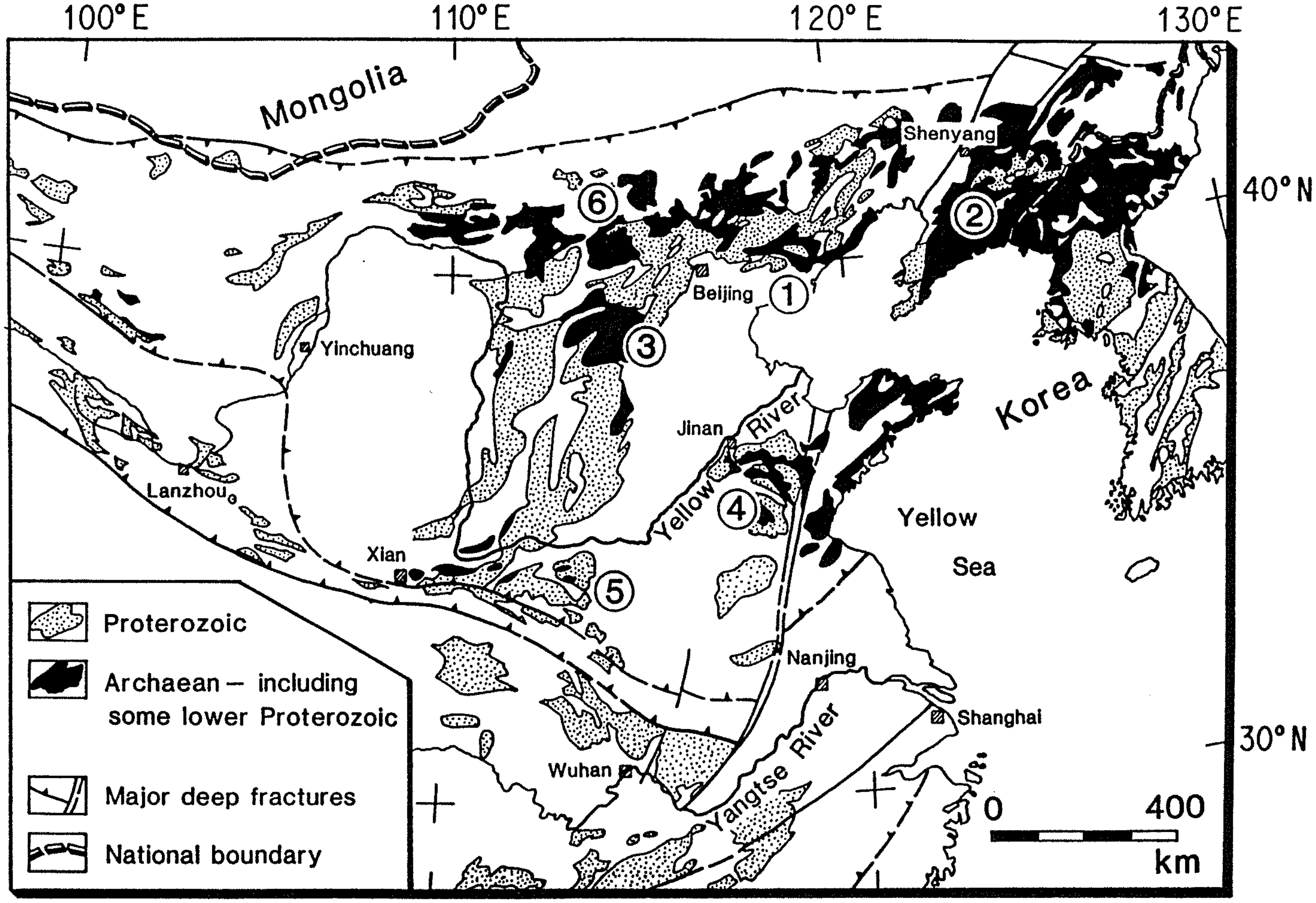

Figure 1-1. Exposures of Early Precambrian rocks in the Sinokorean Craton (adopted from Jahn, 1990a). Numbered regions are 1: eastern Hebei Province; 2: Liaoning and Jilin provinces; 3: Shanxi Province; 4: Shandong Province; 5: Henan Province; 6: Inner Mongolia.

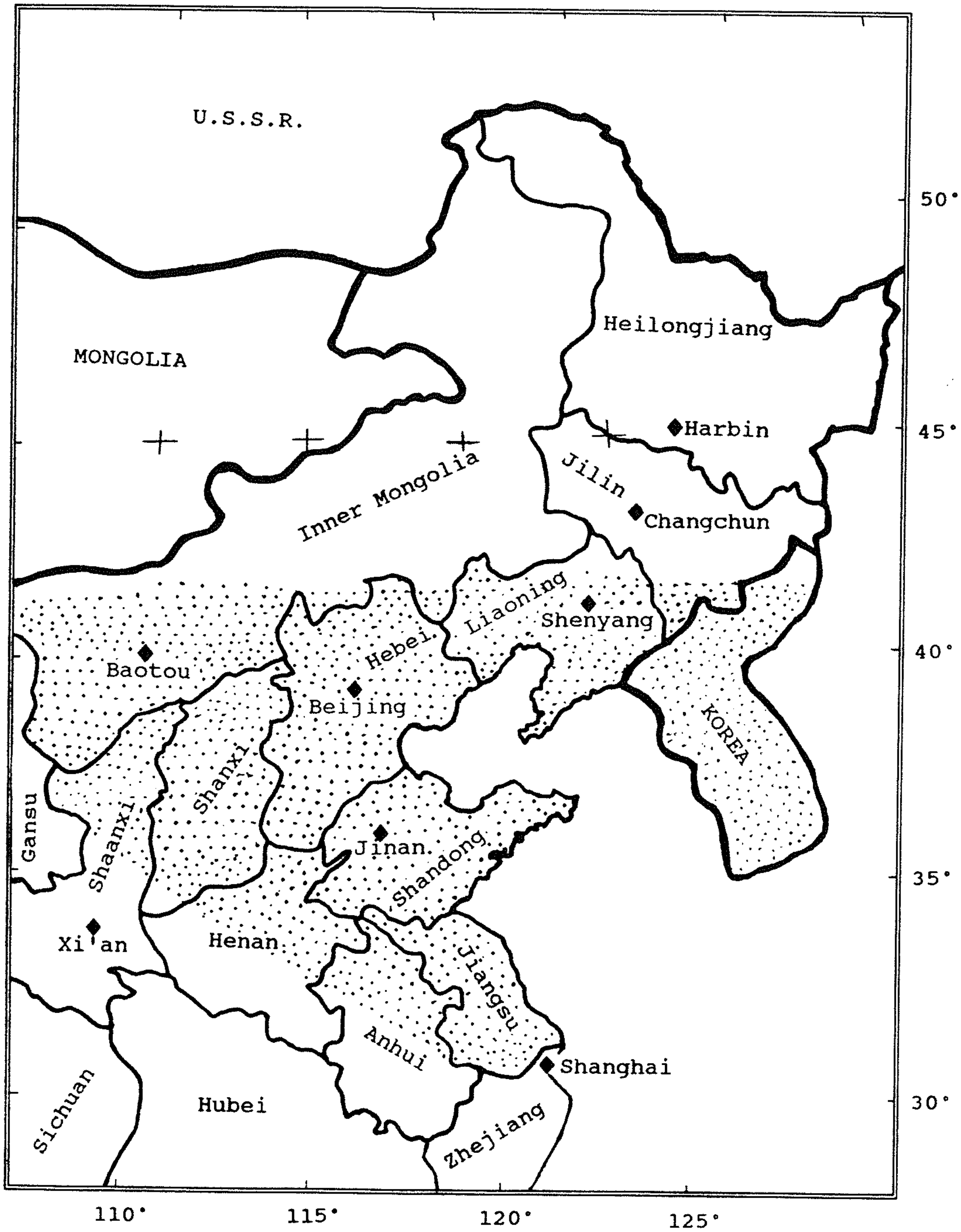

Figure 1-2. Political divisions of northern China showing their relationship to Sinokorean Craton (stippled). The map is simplified from CAGS, 1973.

compared with the Precambrian rocks in Liaoning and Jilin provinces, the "Fuping Group" in Shanxi Province has been correlated either to the "Anshan Group" (Wang, 1988), or to the "Longgang Group" that was placed below the "Anshan Group" (Zhao, 1988), or to the "Kuandian Group" which overlies the "Anshan Group" (Jiang, 1987).

Many Precambrian studies including our recent work (Sun et al., 1991a and 1991b) have revealed that Early Precambrian rocks even in vicinity locations may have formed in different tectonic environments and in different times, they may or may not have the same lithological associations. Large proportion of meta-igneous rocks also invalidates stratigraphic divisions. Thus the conventional stratigraphic divisions only lead to misunderstanding of new data and of geological history.

This thesis synthesizes published data and our own work to describe the Early Precambrian crustal accretion history and mantle evolution for the entire Sinokorean Craton. We abandon the conventional stratigraphic divisions where they are no longer appropriate, instead the term "complex" has been used in this study to refer to a rock system identified in the field by a close association of distinctive lithologies of similar age. Well-identified granitic intrusions are not included as members of the named complexes but are named separately as plutons.

Samples of our own analyses are described in Appendix 1. Methods for Rb-Sr, Sm-Nd and Pb-Pb isotopic analyses are described in Appendix 2. Measured $^{87}Sr/^{86}Sr$, and $^{143}Nd/^{144}Nd$ ratios have been normalized to $^{86}Sr/^{88}Sr = 0.1194$, and $^{146}Nd/^{144}Nd =$

0.7219, respectively. The U-Pb zircon analyses follow the method described in van der Heyden (1989). Tables of Rb-Sr, Sm-Nd, Pb-Pb, and U-Pb zircon isotopic data are incorporated in appropriate chapters. All errors reported are 2σ.

A York (1969) regression program was used for isochron calculations in the course of this study. Sr and Nd depleted mantle model dates calculated according to DePaolo (1981) are listed in Rb-Sr and Sm-Nd tables. Nd model dates calculated according to Allegre and Rousseau (1984) are very similar to those of DePaolo (1981) so are not tabulated. The nominal single, first stage growth μ value is determined from the intersection of the whole rock Pb-Pb isochron and the 4.57 Ga geochron. This μ value is that of single-stage growth in a uniform source, or is an overall average μ of a multi-stage growth history prior to differentiation into rocks of diverse U/Pb ratios.

The following Rb-Sr, Sm-Nd, and U-Pb constants have been used in this study: $\lambda_{^{87}Rb} = 1.42\times10^{-11}/yr$, $\lambda_{^{147}Sm} = 0.654\times10^{-11}/yr$, $(^{147}Sm/^{144}Nd)_{CHUR} = 0.1967$, $(^{143}Nd/^{144}Nd)_{CHUR} = 0.512626$, $\lambda_{^{238}U} = 1.55125\times10^{-10}/yr$, $\lambda_{^{235}U} = 9.8485\times10^{-10}/yr$, $^{238}U/^{235}U = 137.88$ atom ratio. Primeval $^{206}Pb/^{204}Pb = 9.3066$ and $^{207}Pb/^{204}Pb = 10.293$.

II. EARLY PRECAMBRIAN ROCKS IN EASTERN HEBEI PROVINCE

II-1. Qianxi Complex

Geological background

Because of its granulite-facies metamorphism (which was formerly thought to be restricted to the lowermost unit of the basement), the oldest Rb-Sr and Sm-Nd dates reported in China, and economic importance (BIF), the Qianxi Complex has been the focus of many recent papers on the early stages of Sinokorean Craton history (e.g. Zhao, 1988; Wang, 1988; Liu et al., 1990; Wang, 1990; Jahn, 1990a and b).

The Qianxi Complex is mainly distributed in Qianan, Qianxi and Zunhua counties, Hebei Province (Fig. 1-1 and 1-2). The Complex contains amphibolite, fuchsite quartzite, banded iron formation (BIF), kinzigite, diopsidite, fine-grained gneiss (the term "leptynite" and "leptite" are widely used in China), grey gneiss, biotite- and/or plagioclase-bearing pyroxene granulite and marble. Qianxi rocks have undergone polyphase metamorphism and deformation, and been intruded by multiphase granitic rocks which include gabbroic diorite, monzodiorite, granodiorite, K-rich granite, and charnockite.

Most amphibolites have basic compositions and occur as layers intercalated with fuchsite quartzite, BIF, marble and diopsidite, or as enclaves in grey gneiss, either isolated meter to decimeter-sized blocks or meter-sized disrupted boudins. The intercalated amphibolites have been considered to be, together with the gneisses, of a bimodal volcanic suite. The amphibolite blocks/boudins have been considered either disrupted pieces of the same origin or disrupted dykes (Liu et al., 1990).

Granulite-facies rocks have basic, intermediate, acid and ultrabasic igneous compositions (Jahn and Zhang, 1984).

<u>Isotopic dating of the Qianxi Complex and associated granitic rocks</u>

Isotopic dates for the Qianxi Complex and the associated granitic rocks are summarized in Table 2-1.

a. Amphibolite:

A 3.5 Ga Sm-Nd isochron, with an initial $\epsilon_{Nd}(T) = +3$, has been obtained by three research groups (Huang et al., 1986; Qiao et al., 1987; Jahn et al., 1987).

b. Fuchsite-quartzite

Zircons from the Qianxi fuchsite-quartzite give 3.65 to 3.67 Ga single zircon evaporation dates (Liu et al., 1990). These are the oldest dates reported so far for the Sinokorean Craton.

c. Grey gneiss:

Four biotite-plagioclase-gneiss samples plot on the 3.5 Ga Sm-Nd isochron for the Qianxi amphibolite (Qiao et al., 1987). The Nd depleted mantle model dates (T_{DM}, all cited T_{DM}'s have been recalculated according to DePaolo, 1981) for these samples are between 3.32 and 3.46 Ga, except for one 2.10 Ga. Three quartz-diorite gneisses fall close to the 3.5 Ga amphibolite Sm-Nd isochron (Huang et al., 1986), with T_{DM}'s between 3.22 and 3.36 Ga. One sample in the same study, off the 3.5 Ga isochron, has

Table 2-1. Isotopic dates for Early Precambrian rocks from eastern Hebei Province

Rock type	Date (Ga±2σ)	Method	Source
Qianxi amphibolite	3.50±0.08 @ϵNd=+3.3±0.3	Sm-Nd isochron	Huang et al., 1986
	3.47±0.11 @ϵNd=+2.7±0.6	Sm-Nd isochron	Jahn et al., 1987
	3.50±0.02 @ϵNd=+3.1±1.3	Sm-Nd isochron	Qiao et al., 1987
Qianxi grey gneiss	3.12 to 3.46 (& one 2.1 & one 3.76)	T_{DM}	Huang et al., 1986 Jahn et el., 1987 Qiao et al., 1987
	2.64±0.07	U-Pb zicon upper intercept	Liu et al., 1990
	2.8, 2.6 and 2.3	single zircon evaporation	Liu et al., 1990
	2.31±0.12 @0.7020±8	Rb-Sr isochron	Sun et al., 1986
Qianxi fine-grained gneiss	3.3, 2.9-3.0, ~2.5	single zircon evaporation	Liu et al., 1990
Qianxi fuchsite-quartzite	3.65-3.67	single zircon evaporation	Liu et al., 1990
Qianxi granulite	~3.0	Rb-Sr isochron	Sun et al., 1986
	2.79±0.07 @ϵNd=+3.6±0.8	Sm-Nd isochron	Jahn et al., 1990b
	2.48±0.13 @ϵNd=+2.7±2.2	Sm-Nd isochron	Jahn et al., 1990b
	2.53±0.06 @I_{Sr}=0.70166±9	Rb-Sr isochron	Compston et al., 1983
	2.48±0.07 @I_{Sr}=0.70174±6	Rb-Sr isochron	Jahn and Zhang, 1984
	2.51±0.02	U-Pb zircon upper intercept	Pidge, 1980
	2.4±0.3 @I_{Sr}=0.7018±4	Rb-Sr isochron	Sun et al., 1986
	2.40 and 2.45	Nd T_{DM}	this study
Qianxi charnockite	2.73±0.03	U-Pb zicon upper intercept	Liu et al., 1990
	2.65±0.05 @I_{Sr}=0.7022±2	Rb-Sr isochron	Wang et al., 1985
	2.513±0.008	U-Pb zircon upper intercept	Liu et al., 1990
	~2.5	U-Pb zircon upper intercept	Yin, 1988

continued

Qianxi K-rich granite	3.0±0.1	U-Pb zircon upper intercept	Liu et al., 1990
	2.980±0.008 and ~2.5	sigle zircon evaporation	Liu et al., 1990
	2.596±0.009	U-Pb zircon upper intercept	Liu et al., 1990
Qianxi granodiorite	2.494±0.002	U-Pb zircon upper intercept	Liu et al., 1990
	2.48±0.01	single zircon evaporation	Liu et al., 1990
	2.45±0.03	U-Pb zircon upper intercept	Liu et al., 1990
Qianxi gabbroic diorite	2.498±0.003	sigle zircon evaporation	Liu et al., 1990
	2.45±0.03	U-Pb zircon upper intercept	Liu et al., 1990
Qianxi monzodiorite	2.495±0.001	U-Pb zircon upper intercept	Liu et al., 1990
Dantazi-Zhuzhangzi metabasaltic rock	~2.2	Rb-Sr isochron	Lu and Huang, 1987
Dantazi-Zhuzhangzi fine-grained gneiss	2.4 to 2.5	Rb-Sr isochrons	Liu et al., 1981 Shen et al., 1981 Luo et al., 1982
Quartz diorite	~2.4	Rb-Sr isochron	Lu and Huang, 1987

T_{DM} = 3.76 Ga.

Two granodioritic gneisses give a 3.12 and a 3.13 Ga T_{DM} (Jahn et al., 1987).

Single-zircon evaporation dates of 2.8, 2.6 and 2.3 Ga, and a 2.64 ± 0.07 Ga U-Pb upper intercept date have been reported for the grey gneiss (Liu et al., 1990). Sun et al. (1986) have obtained a 2.31 ± 0.12 Ga Rb-Sr isochron, with $(^{87}Sr/^{86}Sr)_0$ = 0.7020 ± 0.0008, for the Qianxi gneiss.

d. Fine-grained gneiss:

Four zircons from the Qianxi fine-grained gneiss have yielded 3.3, 2.9, and ~2.5 Ga single-zircon evaporation dates (Liu et al. 1990).

e. Granulite-facies rocks and charnockite:

A 2.79 ± 0.07 Ga Sm-Nd isochron, with $\epsilon_{Nd}(T)$ = +3.6 ± 0.8, has been obtained by Jahn (1990a) for the Qianxi granulitic rocks. Three basic enclaves in charnockite plot on the 3.5 Ga amphibolite Sm-Nd isochron (Jahn et al., 1987). A 2.73 ± 0.03 Ga U-Pb zircon upper intercept date (Liu et al., 1990) and a 2.65 ± 0.05 Ga Rb-Sr isochron (Wang et al., 1985) have been reported for charnockites in the region. Rb-Sr study of Sun et al. (1985) also gave a hint of ~3.0 Ga history for the Qianxi granulitic rocks. However, date around 2.5 Ga (from Sm-Nd, Rb-Sr and U-Pb) seems still prevailing for the granulite rocks (Pidgeon, 1980; Compston et al., 1983; Jahn and Zhang, 1984; Sun et al., 1985; 2.40 and 2.45 Ga Nd T_{DM} in this study, Table 2-2) and for the charnockite (Yin, 1988; Liu et al., 1990).

Table 2-2. Sm-Nd isotopic data with 2σ errors for samples from Qianxi Complex

Sample		Sm ppm+	Nd ppm	$^{147}Sm/^{144}Nd$	$^{143}Nd/^{144}Nd$	$\epsilon Nd(0)$	T_{DM}*
Qianxi Complex							
HTB-4		7.628	37.45	0.1229	0.511606	-19.9	2.40
	+/-	0.006	0.02	0.0002	0.000012	0.1	0.02
HTB-5		1.316	10.85	0.0732	0.510778	-36.0	2.45
	+/-	0.002	0.04	0.0004	0.000020	0.1	0.07

+ Sm and Nd concentrations were determined by isotopic dilution on a VG-30 mass spectrometer, $^{143}Nd/^{144}Nd$ ratios were measured by a VG-354 at the University of Alberta. 2 sigma errors listed in this table do not include calibration and replication uncertainties. 0.005% and 1.0% were used for $^{143}Nd/^{144}Nd$ and $^{147}Sm/^{144}Nd$ in regression calculations.

* T_{DM}: depleted mantle model date of DePaolo (1981), errors are propagated from standard deviations of $^{147}Sm/^{144}Nd$ and $^{143}Nd/^{144}Nd$.

f. Archean granitic intrusions associated with the Qianxi Complex:

Liu et al. (1990) obtained the following U-Pb zircon dates for granitic rocks associated with the Qianxi Complex: 2.980 ± 0.008 and ~2.5 Ga single-zircon evaporation dates, 3.0 ± 0.1 and 2.6 Ga U-Pb zircon upper intercept dates for K-rich granites, and many ~2.5 Ga U-Pb zircon upper intercept dates and single-zircon evaporation dates for granodiorite, monzodiorite, and gabbroic diorite.

Discussion

The well-defined 3.5 Ga Sm-Nd isochron for the Qianxi amphibolite evidently records an important crustal differentiation event in the area. The mantle source of the magma of the amphibolite has very depleted Nd isotopic character as revealed by a positive $\epsilon_{Nd}(T)$. The 3.5 Ga amphibolites and their associated metasediments have been regarded as the earliest supracrustal rocks in Sinokorean Craton (e. g. Zhao, 1988).

The 3.3 Ga single-zircon evaporation date for the fine-grained gneiss has been considered as an evidence that the fine-grained gneiss is nearly as old as the amphibolite and together they represent an Archean bimodal volcanic suite (Liu et al., 1990). Minimum age of the grey gneiss is defined by the 2.8 Ga single-zircon evaporation date. The T_{DM} values of the grey gneiss, between 3.12 and 3.46 Ga, will be older if a more depleted mantle source, as indicated by Sm-Nd isochron of the amphibolites, is used in calculation of the model dates. Because of its close field relationship with the amphibolites, its chemical similarity to the fine-grained gneiss, and its T_{DM} values, the grey gneiss has likewise been inferred to be an acid member of an Archean bimodal magmatic suite (Jahn et al., 1987).

The 3.65 Ga old detrital zircon from the fuchsite-quartzite implies the existence of an early Archean sialic crust in the Sinokorean Craton, although the field relationship suggests contemporaneous formation of the quartzite and the 3.5 Ga amphibolite. The Cr in fuchsite is likely derived from detrital chromite which is eventually derived from ultramafic-basaltic rocks (Fabries and Latouche, 1973). Liu et al. (1990) consequently inferred an Early Archean greenstone belt as the source. Wang et al. (1990) considered the association of shallow water sediments (quartzite, marble and BIF) and pointed out that this is similar to the Isua supracrustal rocks and thus implies the existence of an even older, yet undiscovered sialic basement.

Most investigators have concluded that the granulitic rocks and charnockite were emplaced and metamorphosed in rapid succession about 2.5 Ga ago (Compston et al., 1983; Jahn and Zhang, 1984; Liu et al., 1990). Based on the Nd isotopic data, however, we infer that the granulitic rocks in the region formed at more than two times, one group at least 2.8 Ga ago and another around 2.5 Ga ago, and metamorphosed to granulite-grade 2.5 Ga ago. Granitic intrusions also formed predominantly in at least two periods, ~ 3 Ga and 2.5-2.6 Ga ago.

II-2. Dantazi-Zhuzhangzi Group

Dantazi-Zhuzhangzi Group (Zhao, 1988) overlies the Qianxi Complex in the north and east of the Qianxi Complex, in Chengde, Qinglong, Luanxian and Funing counties, Hebei Province. This group is made of metavolcanic, volcanoclastic, pelitic and silicic rocks and BIF, which have undergone amphibolite to greenschist facies metamorphism. Presently these are amphibolite, fine-grained gneiss, schist, quartzite and BIF.

Liu et al. (1981), Shen et al. (1981) and Luo et al. (1982) reported 2.5 to 2.4 Ga Rb-Sr isochrons for fine-grained gneiss (Table 2-1). Lu and Huang (1987) obtained a 2.2 Ga Rb-Sr isochron for metabasaltic rocks of the Dantazi-Zhuzhangzi Group. A quartz diorite, intruding the Dantazi-Zhuzhangzi Group, gives a 2.4 Ga Rb-Sr isochron date (Lu and Huang, 1987). We infer that the Dantazi-Zhuzhangzi Group is older than 2.4 Ga, but younger than 2.5 Ga granulite-facies rocks of the Qianxi Complex.

III. EARLY PRECAMBRIAN ROCKS IN LIAONING AND JILIN PROVINCES

III-1. Qingyuan Complex

We use the term "Qingyuan Complex" for the high-grade greenstone-granite association in the Qingyuan area, Liaoning Province (Fig. 1-1 and 1-2). The same rock suite has been referred to "Qingyuan Group" (Yan et al., 1981), or "Anshan Group" (e.g. Zhang, 1984; Jahn, 1990b).

The Qingyuan Complex contains granitic gneisses, metavolcanic and metasedimentary rocks. The granitic gneisses possess tonalite-trondhjemite-granodiorite (TTG) and monzonitic composition (Zhai et al., 1985) and have undergone granulitic metamorphism. The granitic gneisses are believed to be overlain by amphibolitic rocks with ultramafic-basaltic and calcakaline compositions, and fine-grained gneiss, schist, marble and quartzite (Yan and Li, 1981; Zhai et al., 1985).

Isotopic dates for the Qingyuan Complex and associated granitic rocks are summarized in Table 3-1.

Wang et al. (1987) obtained a 2.98 ± 0.07 Ga K-Ar and two 2.99 Ga $^{40}Ar/^{39}Ar$ plateau dates for hornblendes separated from the Qingyuan amphibolite. The Qingyuan amphibolite also gave 2.61 ± 0.1 Ga (Zhai et al., 1985) and 2.4 ± 0.1 Ga (Sun et al., 1989) Rb-Sr isochrons.

The Qingyuan tonalitic gneiss gave 2.88 ± 0.17 Ga U-Pb zircon and 2.90±0.09 Ga K-Ar biotite dates (Zhai et al., 1985).

Sun et al. (1989) obtained a 2.4 ± 0.1 Ga Rb-Sr isochron

Table 3-1. Isotopic dates for Early Precambrian rocks from Liaoning and Jilin provinces

Rock type	Date (Ga±2σ)	Method	Source
Qingyuan amphibolite	2.98±0.07	K-Ar hornblende	Wang et al., 1987
	~2.99	$^{40}Ar/^{39}Ar$	Wang et al., 1987
	2.61±0.03	Rb-Sr isochron	Zhai et al., 1985
	2.4±0.1 @I_{Sr}=0.7019±4	Rb-Sr isochron	Sun et al., 1989
Qingyuan tonalitic gneiss	2.88±0.17	U-Pb zircon upper intercept	Zhai et al., 1985
	2.90±0.09	K-Ar biotite	Zhai et al., 1985
Qingyuan granulite	~2.9 and ~2.6	Rb-Sr isochron	R.G.Sun & Armstrong unpublished data
	2.47 and 2.51	Nd T_{DM}	this study
Qingyuan charnockite	2.4±0.1 @I_{Sr}=0.7038±14	Rb-Sr isochron	Sun et al., 1989
Lijiapuzi granite	2.71±0.14	Rb-Sr muscovite	Zhai et al., 1985
Hongshilazi granite	2.73±0.16	U-Pb zircon	Zhai et al., 1985
Yangwangbizi granite	2.76±0.16	Th-Pb monazite	Zhai et al., 1985
Tiejiashan Granite	3.3 to 3.4	U-Pb upper intercept	Chen and Zhong, 1981
	2.83±0.06 @I_{Sr}=0.7026±11	Rb-Sr isochron	Zhong, 1984
	2.86±0.05	Pb-Pb isochron	Zhong, 1984
	2.97	U-Pb zircon micro-probe	Zhong, 1984
Lishan Granite	2.97 to 3.34	Nd T_{DM}	this study
	3.1±0.1 @μ=8.55	Pb-Pb isochron	this study
Anshan amphibolite	2.66±0.08 @ϵNd=+4.4±0.5	Sm-Nd isochron	Jahn et al., 1990
	2.73±0.25 @ϵNd=+3.0±5.0	Sm-Nd isochron	Qiao et al., 1990
	2.72±0.10 @ϵNd=+3.2±2.2	Sm-Nd isochron	Qiao et al., 1990
	3.1±0.1 @μ=9.13	Pb-Pb isochron	This study

continued

Anshan fine grained gneiss	2.72	Nd T_{DM}	This study
	2.4±0.1 @μ=8.5	Pb-Pb isochron	This study
	1.9±0.4 @I_{Sr}=0.7092±57	Rb-Sr isochron	This study
Anshan schist	2.50 to 2.79 (& one 2.0 & one 3.0)	Nd T_{DM}	Qiao et al., 1990
Anshan Gneissic Granite	2.5±0.2 @ϵNd=-8.7±2.9	Sm-Nd isochron	Qiao et al., 1990
	3.22 to 3.61	Nd T_{DM}	Qiao et al., 1990
	~2.5	U-Pb zircon upper intercept	Peucat et al., 1986
	~2.5	$^{40}Ar/^{39}Ar$ plateau	Wang et al., 1986
Longgang gneiss	2.97±0.19 @I_{Sr}=0.7009±8	Rb-Sr isochron	Jiang, 1987
	2.5±0.1	U-Pb zircon upper intercept	Jiang, 1987
Longgang gneiss & granulite	2.56 to 2.78 (one 2.27)	Nd TDM	this study
	3.3±0.1 @μ=8.58	Pb-Pb isochron	this study
Jianping amphibolite	2.68±0.16 @I_{Sr}=0.7012±4	Rb-Sr isochron	this study
	2.85±0.08 @ϵNd(T)=+5.0	Nd isochron	this study
	2.58 to 2.63	Nd T_{DM}	this study
Kuandian amphibolite & granite	2.32±0.06 @ϵNd=+1.3±0.5	Sm-Nd isochron	this study
	2.10±0.04 @μ=8.21	Pb-Pb isochron	this study
	1.91±0.06 @I_{Sr}=0.7056±7	Rb-Sr isochron	this study
	1.7-1.9	K-Ar dates	Jiang, 1987
	~2.2	Rb-Sr	Liu et al., 1981

continued

Kuandian amphibolite	2.46 to 2.75	Nd T_{DM}	this study
	1.96±0.22 @ I_{Sr}=0.705±1	Rb-Sr isochron	this study
	2.46±0.14 @ϵNd=+1.8±0.8	Sm-Nd isochron	this study
	1.85±0.12	Sm-Nd mineral isochron	this study
	0.23±0.02	Rb-Sr mineral isochron	this study
Kuandian granite	2.36 to 2.53	Nd T_{DM}	this study
	>2.14	U-Pb zircon upper intercept	this study
	1.8±0.1 @I_{Sr}=0.717±11	Rb-Sr isochron	this study
	2.4±2 @ϵNd=+2.3±1.7	Sm-Nd isochron	this study
	1.8, 2.1 and 2.3	U-Pb zircon upper intercepts	Jiang, 1987
Caohe Group	2.23 & 2.53	Nd T_{DM}	this study
	~2.0	Pb-Pb isochron	Chen and Zhong, 1981
	1.86 and 1.90	Rb-Sr isochron	Jiang, 1987
	1.8	K-Ar muscovite	Jiang, 1987
Liaoyang Group	1.55±0.06 @I_{Sr}=0.7168±25	Rb-Sr isochron	this study
	2.54 & 2.73	Nd T_{DM}	this study
	1.48 and 1.45	Rb-Sr isochrons	Jiang, 1987
	1.6	K-Ar muscovite	Jiang, 1987
Shisi Granite	2.44 & 3.07	Nd T_{DM}	this study
Mafeng Granite	2.17 & 2.58	Nd T^{DM}	this study
	0.210±0.025 @I_{Sr}=0.7167±3	Rb-Sr isochron	this study
	0.16±0.10 @ϵNd=-20.3±0.9	Sm-Nd isochron	this study
Felsi dyke	~0.120	U-Pb zirocn upper intercept	this study

for charnockite from the Qingyuan Complex, their unpublished Rb-Sr data also indicate a ~2.9 and a ~2.6 Ga date for the Qingyuan biotite granulites (personal communication). We have derived 2.47 and 2.51 Ga Nd T_{DM} for the Qingyuan biotite granulite (Table 3-2).

Granitic rocks intruding the Qingyuan Complex (Lijiapuzi, Hongshilazi, and Yangwangbizi granites) gave a 2.71 ± 0.14 Ga Rb-Sr muscovite, a 2.73 ± 0.16 Ga U-Pb zircon and a 2.76 ± 0.16 Th-Pb monazite dates (Zhai et al., 1985).

We interpret that the Qingyuan Complex formed about 3.0 Ga ago and was intruded by 2.7 Ga granites.

II-3. Tiejiashan and Lishan granites

Geological setting and geochemistry

The Tiejiashan and Lishan gneissic granites are exposed in Anshan City, Liaoning Province. They are overlain by the Anshan supracrustal rocks, and thus are considered to be basement for the Anshan supracrustal rocks.

The Tiejiashan Granite plots in the granite field in the normative An-Ab-Or diagram (Fig. 3-1). This granite has an S-type granite character in major element composition with exception of lower Al_2O_3, and higher Na_2O (Table 3-3). In contrast, it has an A-type granite character in high field strength trace elements (HFS), e.g. Zr, Nb, Y, and Ce (Table 3-4), and falls in the WPG field in Rb - (Y+Nb) plot (Fig. 3-2).

The Lishan Granite plots in the trondhjemite field in the normative An-Ab-Or diagram (Fig. 3-1). Its major composition is

Table 3-2. Sm-Nd isotopic data with 2σ errors for samples from Liaoning and Jilin provinces

Sample		Sm ppm+	Nd ppm	$^{147}Sm/^{144}Nd$	$^{143}Nd/^{144}Nd$	$\epsilon_{Nd}(0)$	T_{DM}*
Qingyuan Complex							
LG-2		5.453	34.21	0.0962	0.511134	-29.1	2.47
	+/-	0.024	0.17	0.0006	0.000008	0.2	0.12
LG-3		2.164	16.68	0.0783	0.510813	-35.4	2.51
	+/-	0.004	0.02	0.0002	0.000012	0.2	0.04
Lishan Granite							
r86-159		2.985	24.91	0.0723	0.510056	-50.1	3.25
	+/-	0.004	0.02	0.0002	0.000008	0.2	0.04
r86-163		3.287	23.68	0.0837	0.510227	-46.8	3.34
	+/-	0.002	0.02	0.0001	0.000016	0.3	0.04
r86-164		5.733	43.69	0.0792	0.510280	-45.8	3.15
	+/-	0.001	0.04	0.0001	0.000060	1.2	0.08
r86-165		3.452	26.04	0.0800	0.510328	-44.8	3.12
	+/-	0.004	0.12	0.0004	0.000006	0.1	0.14
r86-166		3.199	26.19	0.0737	0.510328	-44.8	2.97
	+/-	0.004	0.06	0.0002	0.000008	0.2	0.06
Anshan Complex							
A86-129		0.761	2.24	0.2053	0.512834	4.1	--
	+/-	0.001	0.00	0.0005	0.000008	0.2	--
A86-130		1.680	5.12	0.1980	0.512717	1.8	3.38
	+/-	0.000	0.00	0.0000	0.000042	0.8	0.36
A86-136		1.885	5.89	0.1933	0.512817	3.7	1.57
	+/-	0.008	0.00	0.0008	0.000024	0.5	0.35
A86-144		4.198	23.04	0.1100	0.511196	-27.9	2.72
	+/-	0.001	0.02	0.0001	0.000008	0.2	0.04
Longgang Complex							
LG-001		5.558	35.80	0.0937	0.511251	-26.8	2.27
	+/-	0.005	0.00	0.0001	0.000012	0.2	0.03
LG-003		12.482	81.32	0.0926	0.511012	-31.5	2.56
	+/-	0.033	0.24	0.0004	0.000006	0.1	0.14
LG-009		7.099	42.60	0.1006	0.511011	-31.5	2.74
	+/-	0.011	0.03	0.0002	0.000006	0.1	0.07
LG-034		0.885	6.16	0.0867	0.510854	-34.6	2.63
	+/-	0.001	0.00	0.0001	0.000014	0.3	0.05
LG-035		1.793	9.47	0.1143	0.511235	-27.1	2.78
	+/-	0.002	0.00	0.0001	0.000016	0.3	0.05

continued

Jianping Complex							
6341		0.563	1.54	0.2203	0.513324	13.6	--
	+/-	0.000	0.00	0.0000	0.000038	0.7	--
6354		4.025	19.90	0.1221	0.511493	-22.1	2.58
	+/-	0.000	0.00	0.0000	0.000008	0.2	0.01
6441		7.466	39.02	0.1155	0.511347	-24.9	2.63
	+/-	0.001	0.02	0.0001	0.000006	0.1	0.02
6496		9.154	42.25	0.1307	0.511624	-19.5	2.61
	+/-	0.001	0.01	0.0000	0.000006	0.1	0.01
Kuandian Complex							
K86-027		8.370	49.80	0.1015	0.511206	-27.7	2.49
	+/-	0.004	0.04	0.0001	0.000004	0.1	0.04
K86-086		7.736	35.59	0.1313	0.511729	-17.5	2.42
	+/-	0.032	0.10	0.0006	0.000012	0.2	0.26
K86-088		8.639	42.00	0.1242	0.511577	-20.5	2.49
	+/-	0.046	0.10	0.0008	0.000008	0.2	0.28
K86-089		6.989	39.87	0.1059	0.511290	-26.1	2.47
	+/-	0.008	0.08	0.0002	0.000008	0.2	0.10
K86-090		9.174	56.92	0.0973	0.511184	-28.1	2.43
	+/-	0.038	0.10	0.0004	0.000012	0.2	0.18
K86-091		9.238	41.84	0.1333	0.511706	-17.9	2.53
	+/-	0.042	0.04	0.0006	0.000010	0.2	0.24
K86-093		3.381	17.90	0.1141	0.511493	-22.1	2.36
	+/-	0.006	0.01	0.0002	0.000018	0.4	0.10
K86-083		3.043	10.97	0.1676	0.512222	-7.9	2.71
	+/-	0.004	0.01	0.0002	0.000008	0.2	0.12
K86-084		4.425	15.86	0.1686	0.512258	-7.2	2.64
	+/-	0.014	0.01	0.0006	0.000018	0.4	0.22
K86-243		3.398	12.98	0.1581	0.512140	-9.5	2.46
	+/-	0.004	0.01	0.0002	0.000006	0.1	0.08
K86-244		2.422	9.05	0.1616	0.512164	-9.0	2.56
	+/-	0.002	0.02	0.0006	0.000008	0.2	0.22
K86-246		3.329	11.76	0.1710	0.512272	-6.9	2.75
	+/-	0.001	0.02	0.0004	0.000006	0.1	0.16
K86-248		5.329	25.56	0.1259	0.511561	-20.8	2.57
	+/-	0.002	0.02	0.0001	0.000006	0.1	0.04

continued

K244 plag	1.045	6.52	0.0967	0.511429	-23.4	2.09
+/-	0.001	0.01	0.0001	0.000022	0.4	0.04
K244 hbl	1.948	6.12	0.1922	0.512591	-0.7	3.36
+/-	0.001	0.01	0.0001	0.000032	0.6	0.34
Caohe Group						
C87-020	14.908	85.18	0.1056	0.511451	-22.9	2.23
+/-	0.010	0.08	0.0002	0.000026	0.5	0.06
C87-076	4.096	22.45	0.1101	0.511321	-25.5	2.53
+/-	0.004	0.02	0.0002	0.000008	0.2	0.06
Liaoyang Group						
L86-213	4.459	22.18	0.1214	0.511505	-21.9	2.54
+/-	0.002	0.01	0.0001	0.000028	0.5	0.06
L86-218	3.966	18.59	0.1287	0.511522	-21.5	2.73
+/-	0.006	0.02	0.0002	0.000006	0.1	0.10
Shisi Granite						
r86-173	3.935	20.54	0.1156	0.511082	-30.1	3.07
+/-	0.002	0.02	0.0002	0.000008	0.2	0.06
r86-174	1.522	10.03	0.0916	0.511083	-30.1	2.44
+/-	0.004	0.02	0.0002	0.000056	1.1	0.12
Mafeng Granite						
r86-183	2.502	14.57	0.1036	0.511465	-22.6	2.17
+/-	0.002	0.02	0.0002	0.000008	0.2	0.08
r86-187	0.359	1.78	0.1218	0.511484	-22.3	2.58
+/-	0.002	0.01	0.0006	0.000010	0.2	0.24

+ Sm and Nd concentrations were determined by isotopic dilution on a VG-30 mass spectrometer, $^{143}Nd/^{144}Nd$ ratios were measured by a VG-354 at the University of Alberta. 2 sigma errors listed in this table do not include calibration and replication uncertainties. 0.005% and 1.0% were used for $^{143}Nd/^{144}Nd$ and $^{147}Sm/^{144}Nd$ in regression calculations.

* T_{DM}: depleted mantle model date of DePaolo (1981), errors are propagated from standard deviations of $^{147}Sm/^{144}Nd$ and $^{143}Nd/^{144}Nd$.

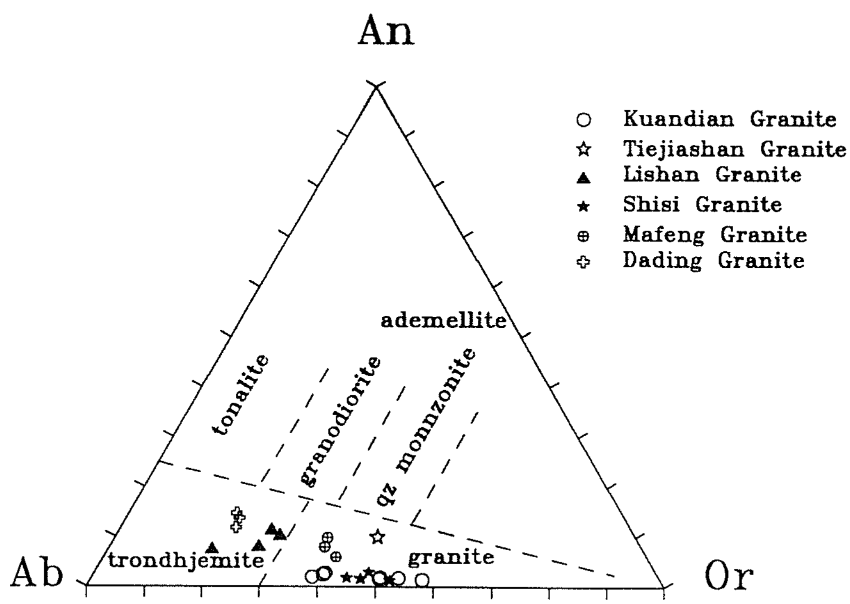

Figure 3-1. An - Ab - Or plot for Tiejiashan, Lishan, Kuandian granites and some other granitic bodies from the eastern Liaoning Province. The dividing lines are from O'Connor (1965).

Table 3-3. Major element analyses for samples from Liaoning and Jilin provinces

Sample	SiO_2*	TiO_2	Al_2O_3	Fe_2O_3(as ΣFe)	MnO	MgO	CaO	Na_2O	K_2O	P_2O_5	L.O.I.+
Anshan Complex											
A86-121	70.0	0.42	13.5	5.8	0.07	1.93	1.59	3.54	2.99	0.12	1.33
A86-130	52.3	0.87	14.4	13.2	0.24	6.72	8.87	2.85	0.35	0.06	1.21
A86-144	70.2	0.38	13.6	5.0	0.09	1.99	2.54	4.12	2.03	0.13	1.63
Longgang Complex											
LG-001	60.9	0.56	16.5	7.0	0.11	2.06	4.62	4.53	3.36	0.30	0.11
LG-003	60.3	0.61	16.9	6.8	0.12	2.28	4.88	4.75	2.97	0.32	0.13
LG-009	60.4	0.60	16.6	7.1	0.11	2.29	4.86	4.58	3.08	0.31	0.17
LG-011	62.9	0.58	16.0	6.4	0.11	1.90	4.06	4.29	3.56	0.28	0.20
LG-014	62.2	0.54	16.1	6.6	0.12	2.08	4.59	4.19	3.29	0.28	0.49
LG-033	74.8	0.23	12.8	2.5	0.05	0.54	2.88	3.75	2.35	0.03	0.26
LG-034	69.8	0.70	14.3	4.3	0.08	1.51	3.07	4.07	2.11	0.07	0.15
LG-035	72.7	0.47	12.2	5.7	0.07	0.68	3.47	3.43	1.26	0.11	0.19
Kuandian Complex											
K86-027	74.7	0.27	11.4	4.4	0.07	0.10	0.53	3.30	5.16	0.03	0.35
K86-086	72.8	0.31	11.8	4.8	0.09	0.04	1.28	3.17	5.68	0.04	0.21
K86-088	73.9	0.30	11.7	4.5	0.07	0.06	0.63	3.37	5.34	0.03	0.37
K86-089	73.7	0.23	12.5	3.6	0.07	0.09	0.95	4.30	4.46	0.03	0.22
K86-090	74.1	0.30	11.6	4.7	0.07	0.05	1.06	3.95	4.18	0.03	0.00
K86-091	73.4	0.29	11.5	5.1	0.08	0.06	0.72	2.88	6.01	0.03	0.22
K86-093	75.1	0.11	12.7	2.3	0.07	0.04	0.61	4.53	4.40	0.09	0.34
K86-084	50.4	1.29	14.7	14.1	0.25	6.04	9.65	2.41	1.07	0.11	0.85
K86-244	48.9	1.05	15.3	12.7	0.18	6.65	10.31	2.38	2.46	0.10	0.42
K86-246	49.1	0.95	14.4	11.8	0.20	8.99	11.30	2.21	0.96	0.08	0.85
K86-248	74.3	0.58	11.9	2.9	0.08	1.19	5.80	2.78	0.32	0.13	0.32
K87-079	69.1	0.66	16.7	7.6	0.20	1.19	0.61	1.19	2.59	0.17	3.17
K87-125	64.3	0.47	13.7	6.3	0.12	3.72	5.06	3.20	2.77	0.26	0.81
Caohe Group											
C86-207	33.8	0.17	3.6	1.7	0.05	7.07	51.68	0.94	0.96	0.09	33.20
C87-020	65.5	0.75	18.0	7.2	0.13	2.04	0.38	0.50	5.34	0.11	4.47
C87-076	57.2	0.40	9.7	3.3	0.05	12.35	11.49	1.68	3.71	0.08	3.97
C87-091	62.8	0.65	21.3	7.4	0.03	1.63	0.27	0.87	4.94	0.12	3.69
C87-098	56.7	0.68	27.2	6.6	0.02	1.53	0.22	0.80	6.14	0.12	4.63
Liaoyang Group											
L86-213	63.5	0.71	17.2	11.1	0.09	3.19	0.54	1.38	2.23	0.10	3.52
L86-218	64.9	0.75	16.9	10.1	0.08	2.37	0.61	1.55	2.64	0.10	3.09
L86-222	59.9	0.67	17.3	14.6	0.07	4.96	0.15	0.20	2.03	0.09	4.54
L87-107	61.7	0.65	22.0	7.3	0.04	2.37	0.11	0.65	5.14	0.06	4.04
L87-108	61.1	0.64	21.6	8.1	0.05	2.24	0.30	0.90	5.03	0.09	4.39
Tiejiashan Granite											
T1	69.9	0.52	12.8	5.9	0.07	0.57	2.01	3.15	4.88	0.15	0.78
Lishan Granite											
r86-159	72.7	0.27	14.3	2.8	0.08	0.39	1.70	4.65	3.02	0.09	0.61
r86-163	73.5	0.24	13.9	2.4	0.09	0.37	1.26	5.10	3.05	0.08	0.65
r86-164	73.6	0.29	14.4	2.5	0.08	0.59	1.16	5.32	1.98	0.11	0.90
r86-165	73.5	0.20	14.1	2.2	0.08	0.33	1.55	4.67	3.30	0.07	0.63
Shisi Granite											
r86-173	76.1	0.09	12.3	1.8	0.08	0.10	0.47	3.79	5.27	0.02	0.33
r86-174	76.5	0.07	12.5	1.4	0.05	0.08	0.33	4.03	5.01	0.02	0.90
r86-175	78.0	0.12	11.1	1.6	0.08	0.13	0.54	3.11	5.30	0.04	0.32
r87-116	75.6	0.12	12.4	1.8	0.07	0.11	0.81	3.82	5.24	0.03	0.28
r87-118	74.8	0.08	13.1	1.6	0.06	0.11	0.77	3.84	5.58	0.02	0.48

continued

Mafeng Granite											
r86-183	74.0	0.17	13.9	1.8	0.06	0.20	1.48	4.09	4.31	0.04	1.32
r86-187	74.2	0.13	13.6	2.1	0.12	0.13	1.16	4.18	4.34	0.03	1.11
r86-188	76.1	0.05	13.0	1.0	0.06	0.04	1.12	4.00	4.55	0.02	0.59
Dading Granite											
rD-002	72.7	0.09	15.5	1.8	0.06	0.27	1.76	5.39	2.42	0.04	0.61
rD-005	72.5	0.10	15.2	1.6	0.06	0.30	2.35	5.39	2.44	0.04	0.86
rD-008	72.6	0.10	15.3	1.6	0.06	0.30	2.32	5.34	2.30	0.03	0.54

* All major element analyses are by a Philips PW-1400 XRF spectrometer, on ground fused glass pellets (Michael and Russell, 1989), reported in wt% and calculated to 100% volatile free. Estimated accuracy (1 sigma) from duplicated runs: SiO_2, 1%; K_2O, TiO_2, 2%; Fe_2O_3, 7%; Al_2O_3, MgO, CaO, Na_2O, 5%; MnO, P_2O_5, ±0.01.

\+ L.O.I. = weight loss between 120 and 900°C.

Table 3-4. Trace element analyses for samples from Liaoning and Jilin provinces

	Ba*	Cr	Nb	Ni	Rb	Sr	V	Y	Zr
ERROR+	7.	8.	1.	5.	1.	6.	37.	1.	3.
Anshan Complex									
A86-121	831.	162.	6.	50.	100.	292.	65.	15.	138.
A86-122	774.	167.	6.	42.	93.	282.	71.	14.	134.
A86-130	129.	123.	4.	72.	20.	123.	176.	17.	57.
A86-144	667.	137.	7.	44.	76.	301.	63.	15.	137.
Longgang Complex									
LG-001	1016.	28.	9.	18.	72.	1114.	89.	17.	171.
LG-003	835.	34.	13.	20.	65.	979.	86.	29.	162.
LG-009	930.	25.	8.	17.	72.	1100.	88.	21.	173.
LG-011	1195.	27.	8.	11.	102.	1064.	88.	12.	224.
LG-014	1110.	39.	6.	14.	71.	947.	89.	19.	187.
LG-033	718.	14.	6.	7.	59.	575.	21.	1.	143.
LG-034	502.	77.	11.	17.	80.	602.	59.	4.	55.
LG-035	196.	21.	7.	10.	58.	427.	58.	10.	240.
Kuandian Complex									
K86-027	913.	13.	18.	5.	152.	66.	27.	50.	324.
K86-086	1183.	12.	20.	6.	222.	87.	34.	66.	298.
K86-088	1015.	17.	18.	2.	200.	74.	29.	55.	270.
K86-089	649.	15.	15.	3.	166.	106.	21.	41.	220.
K86-090	741.	3.	20.	5.	162.	114.	22.	51.	261.
K86-091	1142.	12.	16.	10.	202.	75.	31.	61.	349.
K86-093	491.	23.	11.	0.	161.	70.	8.	20.	59.
K86-084	315.	97.	6.	42.	48.	255.	221.	27.	92.
K86-244	250.	215.	5.	38.	131.	233.	185.	22.	75.
K86-246	144.	534.	5.	109.	25.	202.	176.	16.	60.
K86-248	93.	69.	11.	17.	5.	260.	50.	26.	224.
K87-079	451.	60.	11.	32.	159.	126.	77.	43.	158.
K87-125	800.	168.	6.	45.	115.	439.	75.	14.	127.
Caohe Group									
C86-207	301.	31.	4.	4.	30.	700.	22.	16.	152.
C87-020	1235.	80.	15.	30.	188.	72.	111.	35.	289.
C87-076	277.	76.	8.	20.	172.	149.	78.	23.	159.
C87-091	594.	116.	13.	44.	246.	90.	89.	37.	158.
C87-098	768.	138.	12.	33.	280.	103.	108.	39.	150.
Liaoyang Group									
L86-213	229.	161.	6.	70.	71.	104.	100.	22.	123.
L86-218	232.	155.	6.	63.	89.	128.	110.	22.	127.
L86-222	162.	166.	6.	87.	56.	46.	98.	19.	119.
L87-107	540.	119.	12.	37.	216.	40.	95.	40.	138.
L87-108	654.	116.	12.	36.	218.	43.	97.	30.	141.
Tiejiashan Granite									
T1	1358.	154.	26.	16.	156.	116.	68.	80.	429.
Lishan Granite									
r86-159	1585.	5.	3.	-3.	166.	513.	52.	6.	185.
r86-163	1356.	6.	11.	0.	157.	326.	45.	7.	151.
r86-164	859.	15.	8.	2.	139.	249.	33.	11.	246.
r86-165	1136.	14.	7.	2.	184.	382.	36.	10.	139.
Shisi Granite									
r86-173	302.	32.	11.	2.	274.	85.	2.	13.	86.
r86-174	292.	25.	9.	-4.	202.	91.	-3.	12.	79.
r86-175	348.	16.	15.	1.	276.	92.	7.	22.	109.
r87-115	329.	23.	12.	-0.	278.	116.	0.	16.	78.
r87-116	331.	20.	14.	3.	300.	108.	2.	19.	91.
r87-118	553.	16.	13.	2.	264.	94.	12.	26.	79.

continued

Mafeng Granite									
r86-183	1234.	13.	9.	-1.	115.	473.	32.	14.	115.
r86-187	1077.	33.	9.	8.	136.	402.	23.	26.	107.
r86-188	655.	20.	6.	-0.	135.	328.	7.	10.	63.
Dading Granite									
rD-002	1288.	18.	3.	2.	97.	702.	32.	3.	81.
rD-005	1234.	14.	3.	3.	97.	724.	26.	7.	85.
rD-008	1240.	16.	4.	3.	98.	713.	26.	5.	80.

* All trace element analyses are by a Philips PW-1400 XRF spectrometer, on pressed powder pellets (Armstrong and Nixon, 1980), reported as ppm.
+ 1 sigma error estimated from scatter of standards about working curve.

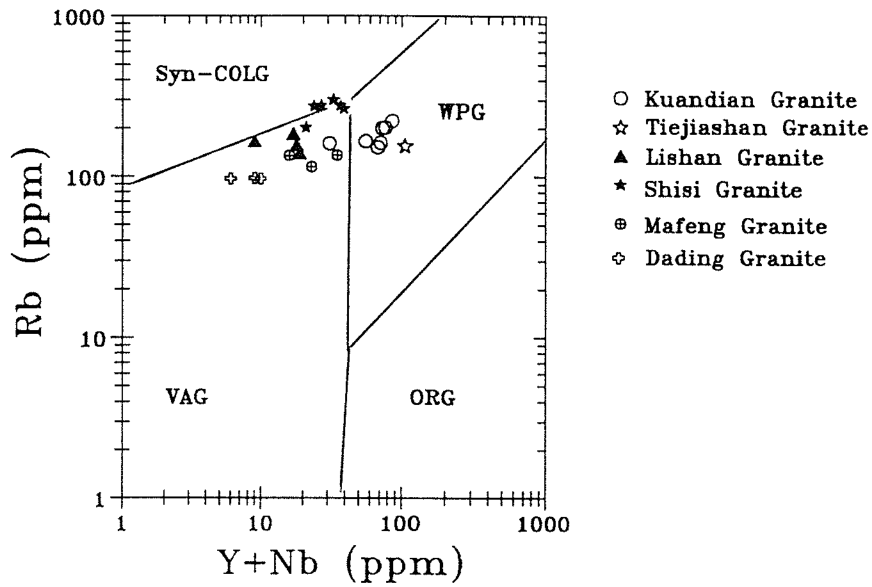

Figure 3-2. Rb - (Y+Nb) plot Tiejiashan, Lishan, Kuandian granites and some other granitic bodies from the eastern Liaoning Province. The dividing lines are from Pearce et al. (1984).

similar to I-type granite, but ΣFe_2O_3 and Na_2O are higher, and Rb is lower than the average value of Whalen et al. (1987). It plots in the VAG field in Rb-(Y+Nb) diagram (Fig. 3-2).

Isotopic dating of the Tiejiashan and Lishan Granite

Chen and Zhong (1981) published a 3.3 to 3.4 Ga U-Pb zircon upper intercept date for the Tiejiashan Granite. Zhong (1984) reported a 2.83 Ga Rb-Sr, a 2.86 Ga Pb-Pb whole rock isochron, and a nearly concordant 2.97 Ga date by zircon ion probe analyses for the Tiejiashan Granite (Table 3-1).

Four Rb-Sr data from the Lishan Granite plot on a line which corresponds to 2.05 ± 0.09 Ga with $(^{87}Sr/^{86}Sr)_0 = 0.7147 \pm 0.0016$ (Table 3-5, Fig. 3-3). One sample is far from the isochron. The Sr depleted mantle model dates are around 3.0 Ga for this granite (Table 3-5). Five whole rock samples are scattered in a Sm-Nd isochron diagram, but plot around 3.0 Ga reference line through CHUR (Table 3-2 and Fig. 3-4). The Nd depleted mantle model dates are between 2.97 and 3.34 Ga. Five whole rock samples mostly plot right of the geochron, and define a Pb-Pb isochron of 3.1 ± 0.1 Ga, with a single stage, first stage growth $\mu = 8.55$ (Table 3-6 and Fig. 3-5), second stage μ's are equal to or greater than 8.55.

Discussion

The minimum age of the Tiejiashan Granite is 2.97 Ga, the ion probe U-Pb zircon concordia date.

Table 3-5. Rb-Sr isotopic data for samples from Liaoning and Jilin provinces

Sample		Rb ppm+	Sr ppm	$^{87}Rb/^{86}Sr$	$^{87}Sr/^{86}Sr$	T_{DM}*
Lishan Granite						
r86-159		164.76	508.34	0.941	0.74282	3.1
	+/-	0.34	0.42	0.002	0.00023	0.4
r86-163		152.00	298.44	1.473	0.75728	2.7
	+/-	1.71	1.96	0.007	0.00048	0.8
r86-164		134.83	241.85	1.615	0.78232	3.5
	+/-	0.08	2.44	0.019	0.00011	0.9
r86-165		180.90	305.91	1.721	0.76644	2.6
	+/-	0.30	0.24	0.003	0.00016	0.6
r86-166		165.92	473.80	1.017	0.74462	3.0
	+/-	0.44	0.14	0.003	0.00017	0.6
Anshan Complex						
A86-002		3.56	28.70	0.359	0.72483	4.7
	+/-	0.01	0.00	0.001	0.00029	0.2
A86-005		142.84	226.83	1.832	0.76126	2.3
	+/-	0.30	0.10	0.004	0.00007	0.9
A86-129		25.87	125.44	0.599	0.74874	5.6
	+/-	0.05	0.03	0.001	0.00023	0.2
A86-130		17.25	128.06	0.391	0.72909	5.1
	+/-	0.05	0.07	0.001	0.00010	0.2
A86-136		16.59	385.15	0.125	0.71497	7.9
	+/-	0.03	4.53	0.003	0.00019	0.6
A86-120		81.88	298.02	0.797	0.72734	2.3
	+/-	0.16	0.17	0.002	0.00030	0.3
A86-121		102.61	292.41	1.018	0.73652	2.4
	+/-	0.22	0.09	0.002	0.00012	0.5
A86-143		132.96	304.62	1.268	0.74589	2.5
	+/-	0.22	5.79	0.024	0.00059	0.9
A86-144		75.55	288.79	0.759	0.73251	2.9
	+/-	0.13	0.16	0.001	0.00017	0.3
A86-147		124.85	162.83	2.230	0.76312	1.9
	+/-	0.29	0.10	0.005	0.00016	0.9

continued

Longgang Complex						
LG-001		68.70	878.10	0.226	0.70803	1.9
	+/-	0.12	0.33	0.001	0.00002	0.1
LG-003		65.18	828.99	0.228	0.70882	2.2
	+/-	0.14	0.21	0.001	0.00001	0.1
LG-009		74.61	929.40	0.232	0.71107	2.9
	+/-	0.12	3.91	0.001	0.00017	0.8
LG-033		60.42	530.82	0.330	0.71320	2.5
	+/-	0.29	0.29	0.002	0.00007	0.3
LG-034		81.05	605.26	0.388	0.71798	3.0
	+/-	0.14	0.17	0.001	0.00002	0.1
LG-035		53.64	404.69	0.384	0.71550	2.5
	+/-	0.08	0.50	0.001	0.00016	0.2
Jianping Complex						
6302		5.19	212.99	0.071	0.70403	2.3
	+/-	0.01	0.12	0.000	0.00006	0.1
6303		10.10	258.77	0.113	0.70597	2.8
	+/-	0.09	0.06	0.001	0.00004	0.2
6341		1.72	56.63	0.088	0.70427	1.9
	+/-	0.01	0.05	0.001	0.00023	0.3
6354		8.79	104.76	0.243	0.71042	2.5
	+/-	0.14	0.02	0.004	0.00007	0.8
6441		76.88	706.22	0.315	0.71275	2.5
	+/-	0.12	0.02	0.001	0.00002	0.1
6496		17.40	173.88	0.296	0.71317	2.8
	+/-	0.05	0.02	0.001	0.00006	0.2
Kuandian Complex						
K86-026		169.32	68.92	7.237	0.89439	1.9
	+/-	0.38	0.04	0.017	0.00006	0.7
K86-027		145.67	62.00	6.916	0.88517	1.9
	+/-	0.26	0.06	0.014	0.00026	0.9
K86-086		209.74	78.94	7.888	0.92889	2.0
	+/-	0.36	0.74	0.029	0.00001	0.8
K86-088		197.08	76.63	7.570	0.91253	2.0
	+/-	1.98	0.01	0.033	0.00015	0.9
K86-089		168.67	94.99	5.210	0.85237	2.0
	+/-	0.40	0.08	0.003	0.00020	0.6
K86-090		153.88	98.89	4.561	0.83621	2.1
	+/-	0.26	1.22	0.014	0.00061	0.8
K86-091		188.16	67.65	8.239	0.93351	2.0
	+/-	0.32	0.14	0.028	0.00094	1.0
K86-093		154.26	61.15	7.435	0.89864	1.9
	+/-	0.30	0.04	0.002	0.00019	0.4

continued

K86-083		93.81	309.57	0.878	0.72811	2.1
	+/-	0.36	1.40	0.001	0.00007	0.2
K86-084		53.18	273.33	0.564	0.72441	2.9
	+/-	0.10	0.06	0.001	0.00008	0.2
K86-243		31.92	184.63	0.501	0.71648	2.1
	+/-	0.06	0.06	0.001	0.00024	0.2
K86-244		133.10	234.20	1.652	0.75289	2.2
	+/-	0.40	0.44	0.004	0.00020	0.8
K86-246		29.69	199.30	0.419	0.73248	---
	+/-	0.56	1.63	0.001	0.00045	---
K86-248		5.26	248.29	0.061	0.70748	---
	+/-	0.02	0.58	0.003	0.00023	---
K87-079		153.13	120.45	3.714	0.80654	2.0
	+/-	0.38	0.10	0.010	0.00035	0.9
K87-125		104.19	374.11	0.808	0.73106	2.6
	+/-	0.28	0.44	0.002	0.00004	0.6
K244 plag		563.18	598.54	2.740	0.77501	1.9
	+/-	2.94	1.18	0.015	0.00006	0.8
K244 hbl		16.57	22.75	2.121	0.77302	2.4
	+/-	0.04	0.01	0.004	0.00006	0.9
Caohe Group						
C86-019		3.90	16.28	0.696	0.73743	3.7
	+/-	0.02	0.06	0.008	0.00608	0.9
C86-020		2.00	26.74	0.217	0.73799	---
	+/-	0.01	0.08	0.001	0.00267	---
C86-032		217.01	146.72	4.323	0.81204	1.8
	+/-	0.40	0.20	0.010	0.00048	0.9
C86-037		159.67	239.74	1.940	0.77797	2.8
	+/-	0.30	0.26	0.004	0.00032	0.9
C86-098		4.38	17.54	0.725	0.73068	2.8
	+/-	0.01	0.14	0.001	0.00156	0.2
C86-099		2.01	11.32	0.514	0.73984	5.3
	+/-	0.01	0.02	0.002	0.00086	0.2
C86-207		25.43	531.18	0.137	0.70898	4.0
	+/-	0.08	0.20	0.001	0.00006	0.1
C87-020		172.66	71.05	7.126	0.84674	1.4
	+/-	0.34	0.24	0.028	0.00027	0.8
C87-076		140.57	108.48	3.779	0.79006	1.6
	+/-	0.30	0.04	0.008	0.00005	0.5
C87-091		251.05	135.31	5.487	0.93522	3.0
	+/-	0.84	1.04	0.046	0.00086	0.9

continued

C87-098		267.73	128.17	6.171	0.92222	2.5
	+/-	0.66	0.16	0.020	0.00008	0.7
Liaoyang Group						
L86-213		72.26	106.27	1.977	0.75972	2.1
	+/-	0.30	0.24	0.001	0.00033	0.1
L86-218		83.23	121.35	1.995	0.76307	2.2
	+/-	0.57	0.68	0.029	0.00089	0.9
L86-222		54.17	42.65	3.707	0.79634	1.8
	+/-	0.22	0.22	0.001	0.00028	0.1
L87-107		215.35	34.49	18.793	1.11874	1.6
	+/-	1.28	0.04	0.001	0.00076	0.1
L87-108		219.38	44.28	14.833	1.06330	1.7
	+/-	0.52	0.16	0.067	0.00038	0.9
Shisi Granite						
r86-172		253.08	79.17	9.457	0.93645	1.7
	+/-	0.52	0.10	0.022	0.00012	0.9
r86-173		262.19	75.21	10.331	0.95627	1.7
	+/-	0.62	0.18	0.030	0.00070	1.0
r86-174		201.44	90.79	6.509	0.85499	1.7
	+/-	0.42	0.28	0.198	0.00033	1.0
r86-175		265.49	124.43	6.190	0.73672	0.4
	+/-	0.50	0.56	0.012	0.00096	1.0
Mafeng Granite						
r86-180		120.87	403.61	0.867	0.71933	1.4
	+/-	0.26	0.24	0.002	0.00007	0.4
r86-183		114.25	461.07	0.718	0.71904	1.7
	+/-	0.28	0.60	0.002	0.00020	0.4
r86-184		111.72	453.73	0.713	0.71883	1.7
	+/-	0.24	0.32	0.002	0.00014	0.4
r86-187		131.80	376.99	1.013	0.71955	1.2
	+/-	0.24	2.08	0.006	0.00040	0.9
r86-188		131.06	296.49	1.281	0.72069	1.0
	+/-	0.22	0.24	0.002	0.00021	0.6

\+ Rb and Sr concentrations were determined by isotopic dilution on a VG-30 spectrometer at the University of Alberta. 2 sigma errors listed in this table do not include calibration and replication uncertainties. 0.026% and 2% were used for $^{87}Sr/^{86}Sr$ and 87Rb/^{86}Sr in regression calculations.

* T_{DM}: depleted mantle model date of DePaolo (1981), errors are propagated from standard deviations of $^{87}Rb/^{86}Sr$ and $^{87}Sr/^{86}Sr$.

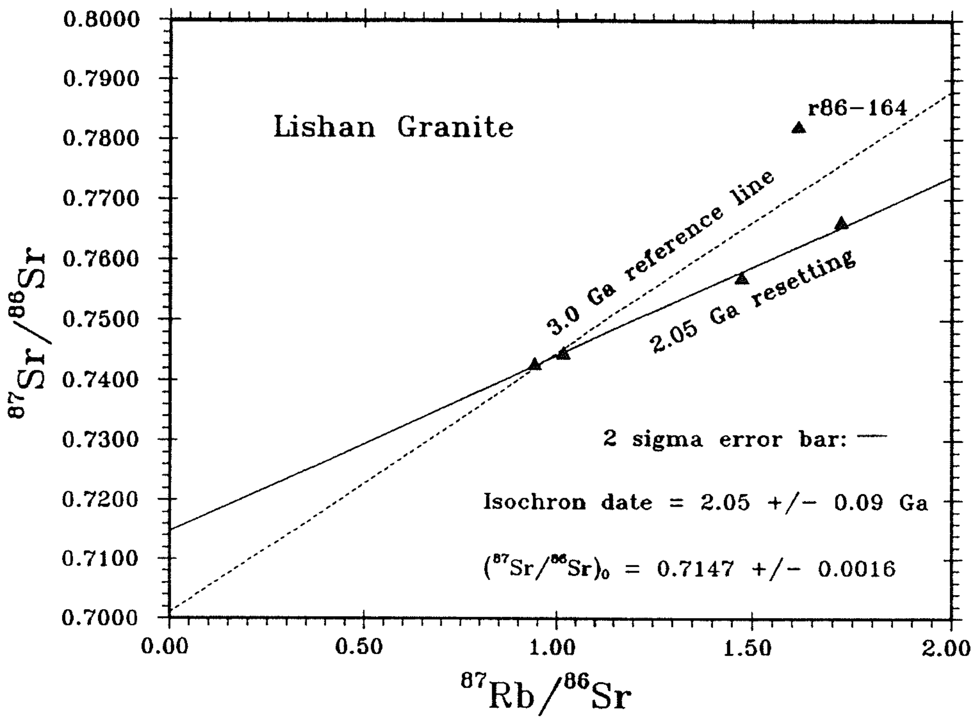

Figure 3-3. Rb - Sr isochron plot for samples from the Lishan Granite.

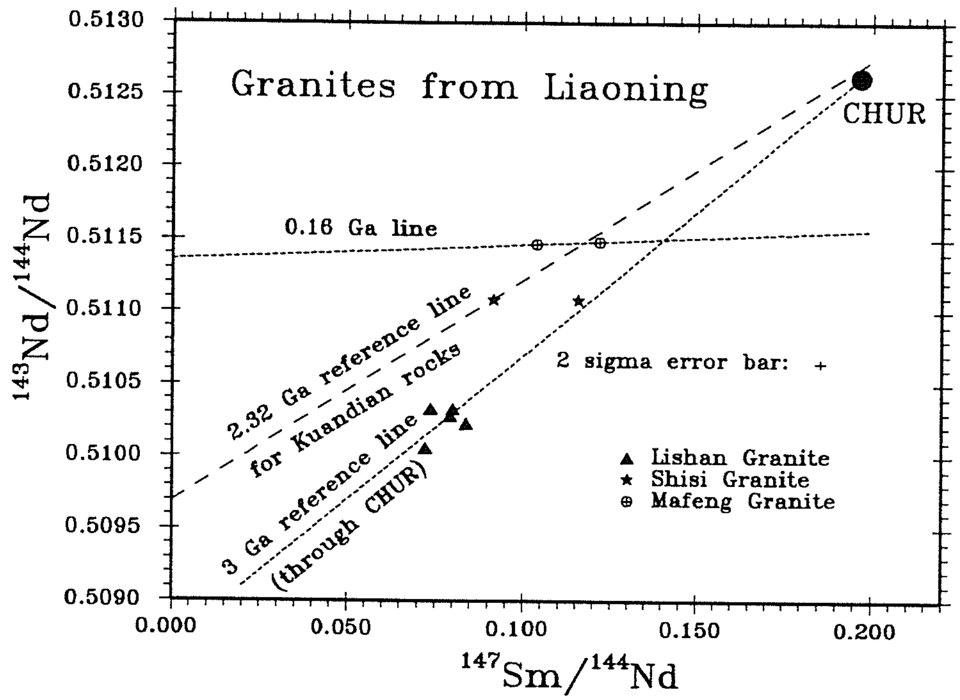

Figure 3-4. Sm - Nd isochron plot for the Lishan, Shisi, and Mafeng granites.

Table 3-6. Pb isotopic data for samples from Liaoning and Jilin provinces

Sample	$^{206}Pb/^{204}Pb$#	$^{207}Pb/^{204}Pb$	$^{208}Pb/^{204}Pb$
Anshan amphibolite			
A86-128	19.21	16.27	37.44
A86-129	18.55	16.15	37.09
A86-130	18.53	16.10	37.25
A86-133	21.30	16.82	38.45
A86-136	17.81	15.96	36.70
A86-137	18.69	16.26	37.07
Anshan fine grained gneiss			
A86-120	18.28	15.85	37.91
A86-121	19.18	15.96	38.81
A86-143	19.26	15.96	38.27
A86-144	20.14	16.14	38.86
A86-147	21.67	16.36	39.99
Longgang Complex			
LG-001	14.47	14.89	34.87
LG-003	14.43	14.90	34.50
LG-009	14.48	14.84	35.13
LG-033	15.15	15.07	34.51
LG-034	15.65	15.18	36.32
LG-035	15.17	15.09	34.73
Kuandian Complex			
K86-026	48.46	19.56	72.78
K86-027	34.52	17.82	53.45
K86-086	26.60	16.70	50.12
K86-089	34.08	17.85	72.95
K86-093	21.30	16.04	42.56
K86-083	17.34	15.57	36.49
K86-084	17.43	15.51	37.46
K86-243	23.96	16.47	44.08
K86-244	21.88	16.19	41.91
K86-248	28.70	16.86	51.82
K244 plag	17.62	15.71	38.44
K244 hbl	18.69	15.67	38.79
Lishan Granite			
r86-159	18.81	15.99	40.85
r86-163	18.09	15.82	40.90
r86-164	19.93	16.26	45.01
r86-165	19.88	16.20	39.68
r86-166	18.69	15.92	40.59
Mafeng Granite			
r86-180	17.40	15.54	38.12
r86-183	17.42	15.56	38.21
r86-187	17.56	15.57	38.20
r86-188	17.61	15.51	38.16

The 2 sigma errors for $^{206}Pb/^{204}Pb$, $^{207}Pb/^{204}Pb$ and $^{208}Pb/^{204}Pb$ are 0.10, 0.15, and 0.16%, respectively. Error correlation coefficient (R) between $^{206}Pb/^{204}Pb$ and $^{207}Pb/^{204}Pb$ is 0.8.

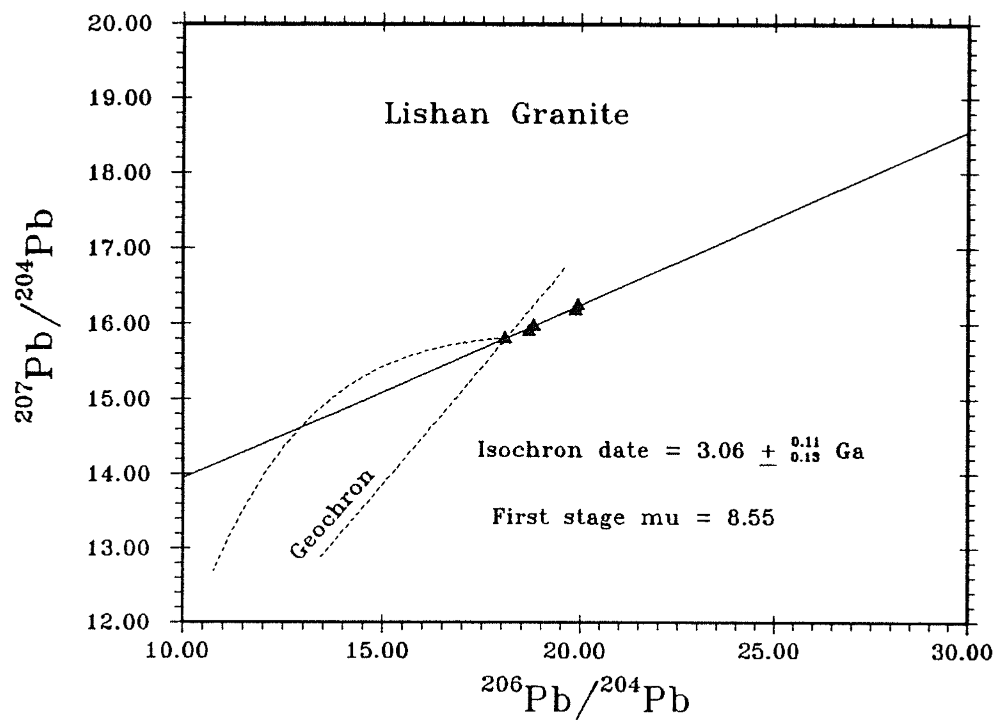

Figure 3-5. Whole rock Pb plot for samples from the Lishan Granite. The 4.57 Ga geochron is plotted for reference. A nominal single, first stage growth μ, 8.55, is calculated from the intersection of geochron and Pb-Pb isochron. This μ value is that of single-stage growth in a uniform source, or is an overall average μ of a multi-stage growth history prior to differentiation into rocks of diverse U/Pb ratio. Second stage μ's are equal to or greater than 8.55.

The 2.97 to 3.34 Ga Nd depleted mantle model dates for the Lishan Granite indicate a mantle source older than the 2.7 Ga Anshan Complex, which is the oldest supracrustal rock exposed in the area. The 2.05 ± 0.09 Ga Rb-Sr isochron date cannot be a differentiation age because the Anshan Complex overlies the Lishan Granite. This young date is partly due to isotopic resetting, and the high initial Sr isotopic ratio is consistent with this interpretation. The Sr depleted mantle model dates are consistent with a pre-Anshan age. The 3.06 Ga whole rock Pb-Pb isochron date is probably close to the true age of the Lishan Granite. First stage growth μ equals 8.55 and all the data plot to right of the geochron. This indicates a relatively high U/Pb source and an overall enrichment of U/Pb in the rock suite at the time of differentiation. In conclusion, we infer that the Tiejiashan and Lishan granites are at least 3.0 Ga old.

III-3. Anshan Complex and Anshan gneissic granite

Geological background

The Anshan Complex is exposed in Anshan city and Benxi county, Liaoning Province (Fig. 1-1 and 1-2). It overlies the Tiejiashan and Lishan gneissic granites, and is composed of mainly supracrustal rocks, i.e. amphibolites with komatiitic, calc-alkaline basaltic compositions (Zhang, 1984), fine-grained gneiss, schist with greywacke and pelite compositions, quartzite, and BIF. In general, the BIF is closely associated with amphibolites, and makes a high proportion of China's iron ore. The rocks have undergone amphibolite (north) to greenschist-facies metamorphism (south).

The Anshan Complex is intruded by the Anshan gneissic granite. Presently, the Anshan Complex occur as giant to small lenses within the Anshan gneissic granite.

Isotopic dating of the Anshan Complex and the Anshan gneissic granite

Published isotopic dates and our results for the Anshan Complex and the Anshan gneissic granite are listed in Table 3-1.

a. Amphibolites:

Jahn and Ernst (1990) have obtained a 2.66 ± 0.08 Ga Sm-Nd isochron, with $\epsilon_{Nd}(T)$ = +4.4 ± 0.5, for the Anshan amphibolite. Qiao et al. (1990) have analyzed two suites of amphibolitic samples that are associated with two different BIF formations in the Anshan area, and derived Sm-Nd isochrons of same date, 2.7 Ga, with similar $\epsilon_{Nd}(T)$, about +3. Our Sm-Nd data for three amphibolites from two drill holes in the Anshan area plot close to the 2.7 Ga Sm-Nd reference line (Table 3-2 and Figure 3-6).

Our six Pb isotopic data for the Anshan amphibolites from two drill holes give a 3.1 ± 0.1 Ga Pb-Pb isochron, with a single stage μ = 9.13 (Table 3-6, Fig. 3-7).

Our Rb-Sr data for amphibolite are scattered (Table 3-5, Fig. 3-8), same as in the case of Qiao et al (1990).

b. Fine-grained gneiss:

One fine-grained gneiss sample with a granodioritic composition (Appendix 1) has a T_{DM} of 2.72 Ga and falls close to

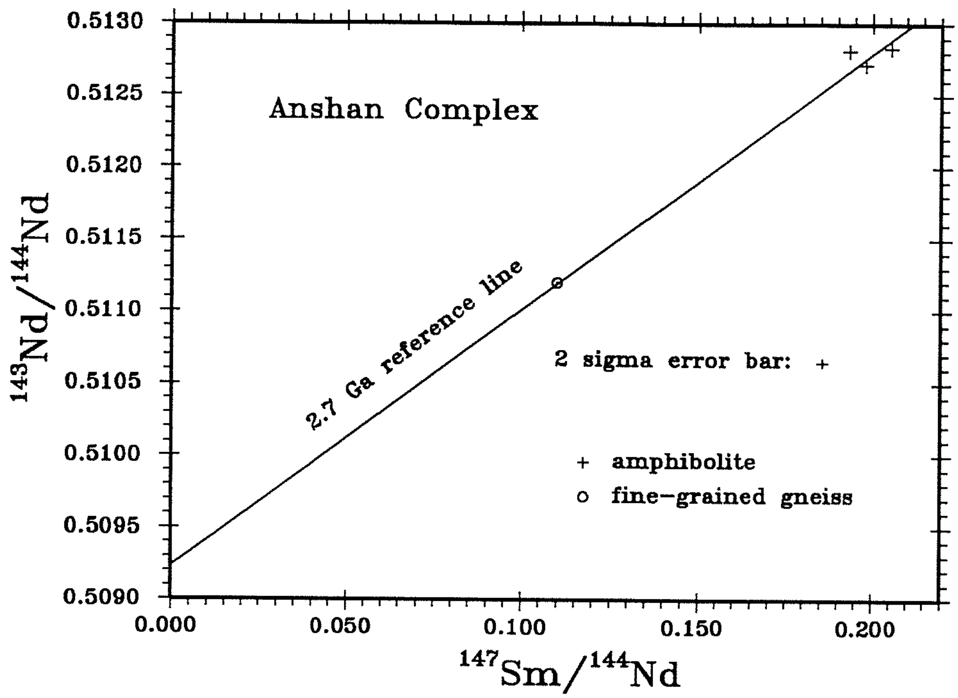

Figure 3-6. Sm-Nd isochron plot for the Anshan amphibolite and fine grained gneiss.

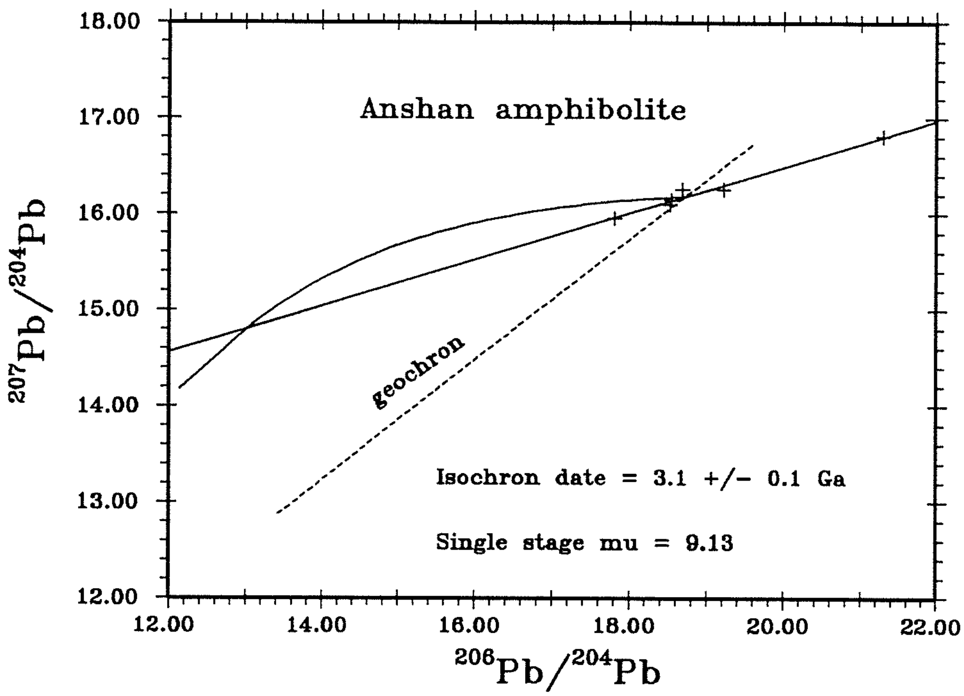

Figure 3-7. Pb-Pb isotopic plot for the Anshan amphibolites. The 4.57 Ga geochron is plotted for reference. Meaning of single stage μ, 9.13, is same as for the Lishan Granite (Figure 3-5). Second stage μ's are either smaller or greater than 9.13.

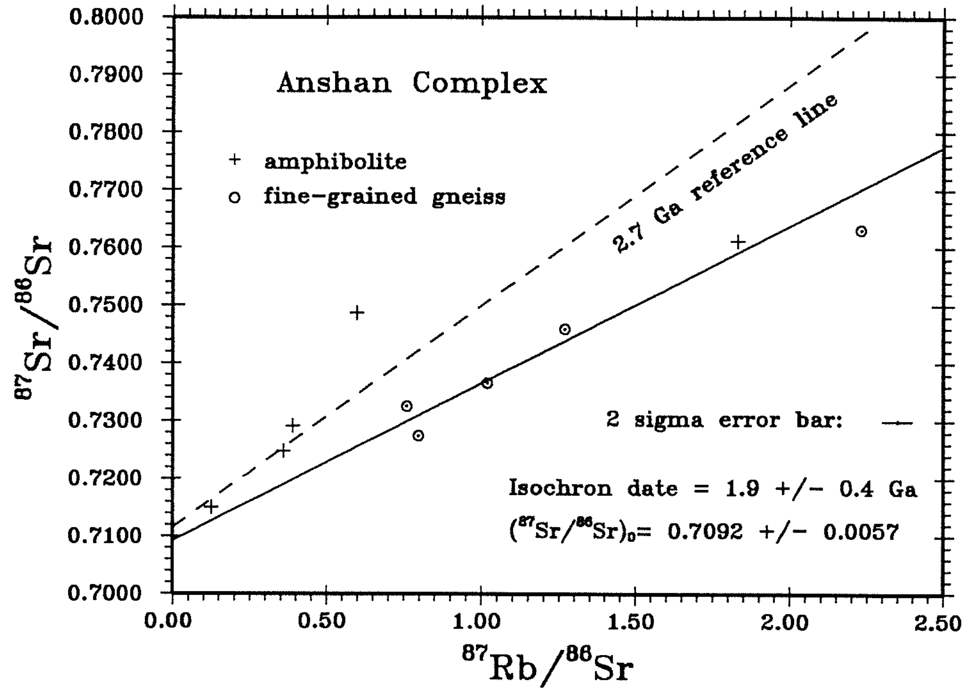

Figure 3-8. Rb-Sr isochron plot for the Anshan amphibolite and fine-grained gneiss. 1.9 Ga errochron date is calculated for the fine-grained gneiss.

the 2.7 Ga Sm-Nd reference line (Table 3-2 and Fig. 3-6).

Five fine-grained gneisses all plot right to the 4.57 Ga geochron. This may imply that a U/Pb depleted component has been left since formation of the fine-grained gneiss, or this is due to metamorphic U enrichment of the fine-grained gneiss. The five data define a 2.4±0.1 Ga Pb-Pb isochron, with a single stage μ = 8.5 (Table 3-6, Fig. 3-9). These five samples poorly defined a Rb-Sr isochron of 1.9 ± 0.4 Ga, with initial $(^{87}Sr/^{86}Sr)_0$ = 0.7092 ± 0.0057 (Table 3-5, Fig. 3-8).

c. Pelitic schist

Qiao et al. (1990) published five Sm-Nd data for the Anshan metapelitic rocks. The T_{DM}'s of these rocks are between 2.50 and 2.79 Ga, except for one 2.0 and one 3.0 Ga.

d. Anshan gneissic granite

Qiao et al. (1990) obtained a 2.5 ± 0.2 Ga Sm-Nd isochron, with $\epsilon_{Nd}(T)$ = -8.7 ± 2.9, for the Anshan gneissic granite. The T_{DM}'s of these rocks are between 3.22 to 3.61 Ga. 2.5 Ga dates have also been obtained by U-Pb zircon (Peucat et al., 1986) and $^{40}Ar/^{39}Ar$ methods (Wang et al., 1986).

Discussion

The 2.7 Ga Sm-Nd isochron, with a very depleted initial Nd isotopic ratio, reveals that the Anshan amphibolites are mainly derived from the mantle 2.7 Ga ago. Their tectonic environment has been inferred to be similar to modern island arcs (Zhai et al., 1990).

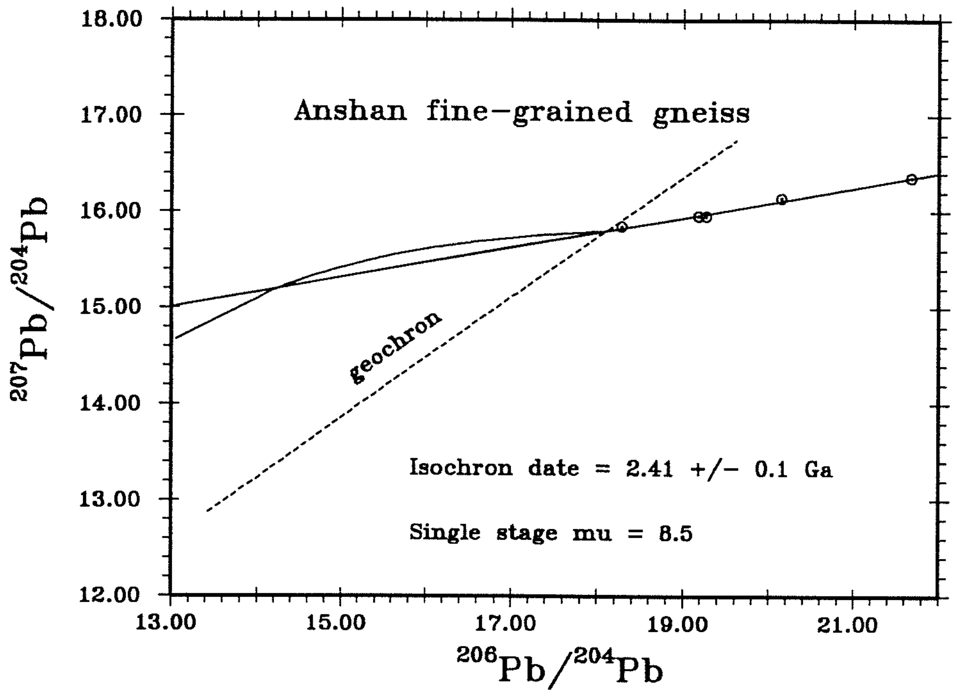

Figure 3-9. Pb-Pb isotopic plot for the Anshan fine-grained gneisses. Meaning of single stage μ, 8.5, is same as for the Lishan granite (Figure 3-5). Second stage μ's are all greater than 8.5. This may imply that these rocks came from a U/Pb enriched source, or this is due to metamorphic U enrichment of the fine-grained gneiss.

The fine-grained gneiss and other supracrustal rocks most likely were also formed/deposited about 2.7 Ga ago. The Anshan supracrustal rocks are intruded by 2.5 Ga Anshan gneissic granite, which was largely derived from partial melting of the existed continental crust as evidenced by the Nd depleted mantle model dates.

III-4. Longgang Complex

Geology and isotopic dating

The Longgang Complex is exposed in the Huadian-Jingyu area, Jilin Province (Fig. 1-1 and 1-2). It has also been referred to "Baishanzhen Group" (Jiang and Shen, 1980), "Anshan Group" (e.g. Jahn, 1990), or "Longgang Group" (Jiang, 1987).

The Longgang Complex comprises amphibolite, grey gneiss, fine-grained gneiss, quartzite, Hyp-Hb-granulite and Cpx-Opx-granulite. The amphibolite and granulite have basic to intermediate compositions (Jiang, 1987).

Jiang (1987) obtained a 2.97 ± 0.19 Ga Rb-Sr isochron, with $(^{87}Sr/^{86}Sr)_0$ = 0.7009 ± 0.0008, and a 2.5 ± 0.1 Ga U-Pb zircon upper intercept date for the Longgang grey gneisses (Table 3-1).

We have done Rb-Sr, Sm-Nd and Pb-Pb isotopic analyses for the Longgang grey gneiss and Longgang granulite with intermediate compositions (Table 3-3).

The Rb-Sr and Sm-Nd data are scattered (Fig. 3-10 and 3-11). The Nd T_{DM}'s for these rocks are between 2.56 and 2.78 Ga, except for one 2.27 Ga. Pb isotopic compositions for the

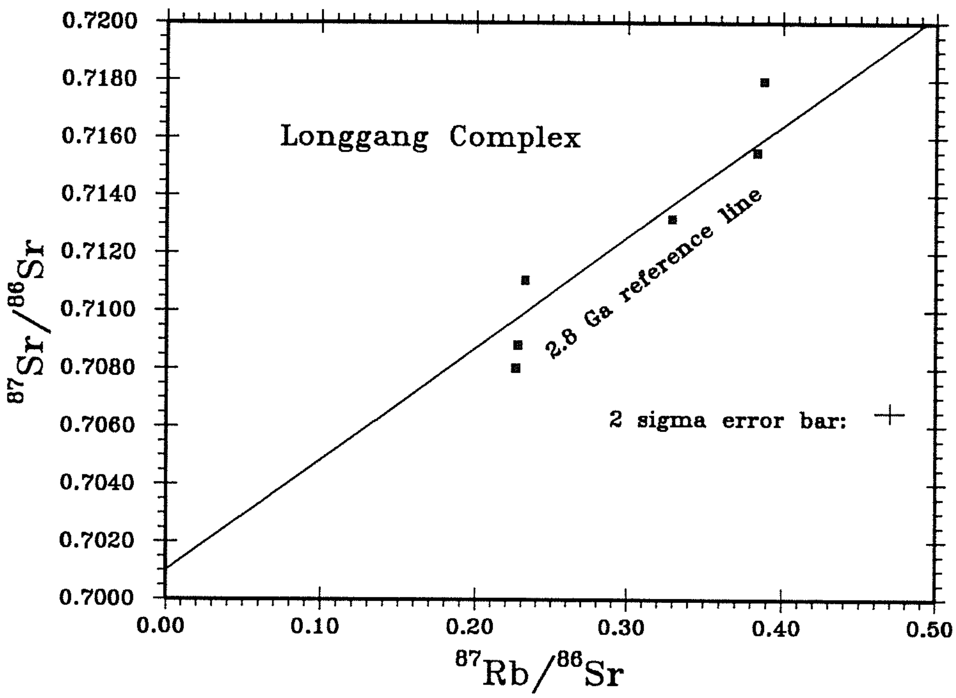

Figure 3-10. Rb-Sr isochron plot for the Longgang Complex.

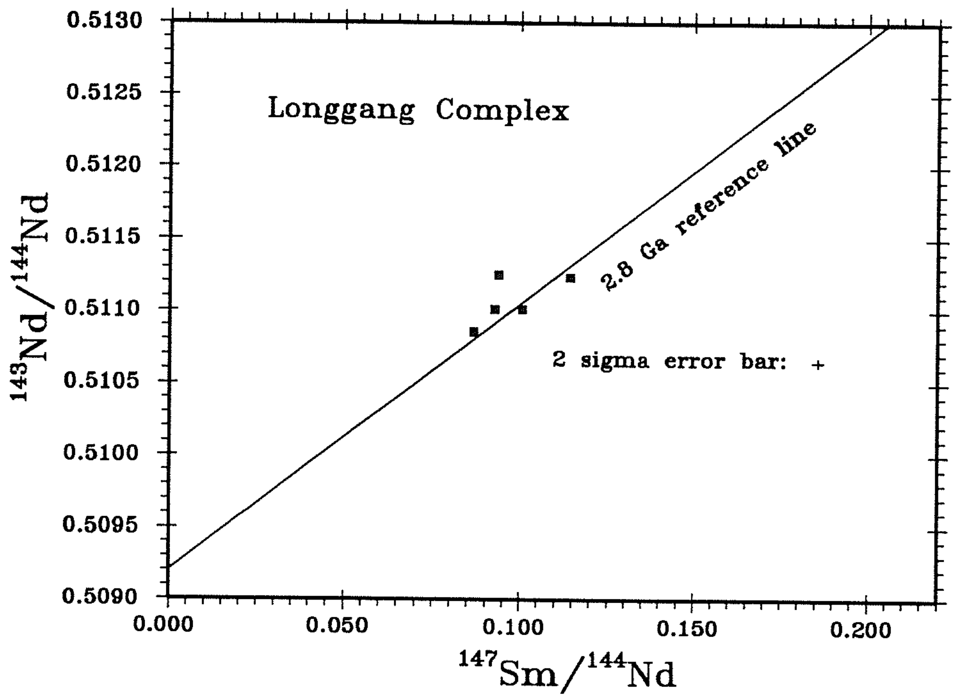

Figure 3-11. Sm-Nd isochron plot for the Longgang Complex.

Longgang granulite are nearly identical, and together with data of grey gneiss plot on a 3.3 ± 0.1 Ga Pb-Pb line (Fig. 3-12). All these Pb data plot left of the geochron, the same as granulites from the Qianxi Complex (Sun, 1987). This indicates that the Longgang Complex has a U/Pb depleted character which is perhaps related to the granulite-facies metamorphism.

Discussion

The maximum formation age of the Longgang Complex is indicated by the maximum Nd T_{DM}, 2.78 Ga. The only possibility that the Longgang Complex is older than 2.78 Ga, is that it is derived from a mantle source more depleted than DePaolo's (1981) average mantle curve as seen in other Archean rocks of the Sinokorean Craton. The 3.5 Ga Qianxi amphibolites have initial Nd +2.0 ϵ units higher than the mantle curve (Huang et al., 1986; Jahn et al., 1987; Qiao et al., 1987), 2.7 Ga Anshan amphibolites posses an initial Nd + 1.8 ϵ units higher than the mantle curve (Jahn et al., 1990; Qiao et al., 1990), and 2.7 Ga Taishan amphibolites have initial Nd + 1.1 ϵ units higher than the mantle curve (Jahn et al., 1988). However, even if the mantle source for the Longgang Complex is + 2 higher than the average mantle curve, the calculated Nd T_{DM} is still not greater than 3.0 Ga.

We infer that the Longgang Complex was formed around 2.8 Ga ago and metamorphosed 2.5 Ga ago. The 3.3 ± 0.1 Ga Pb-Pb isochron is considered as a mixing line between unrelated end members and thus of no age significance.

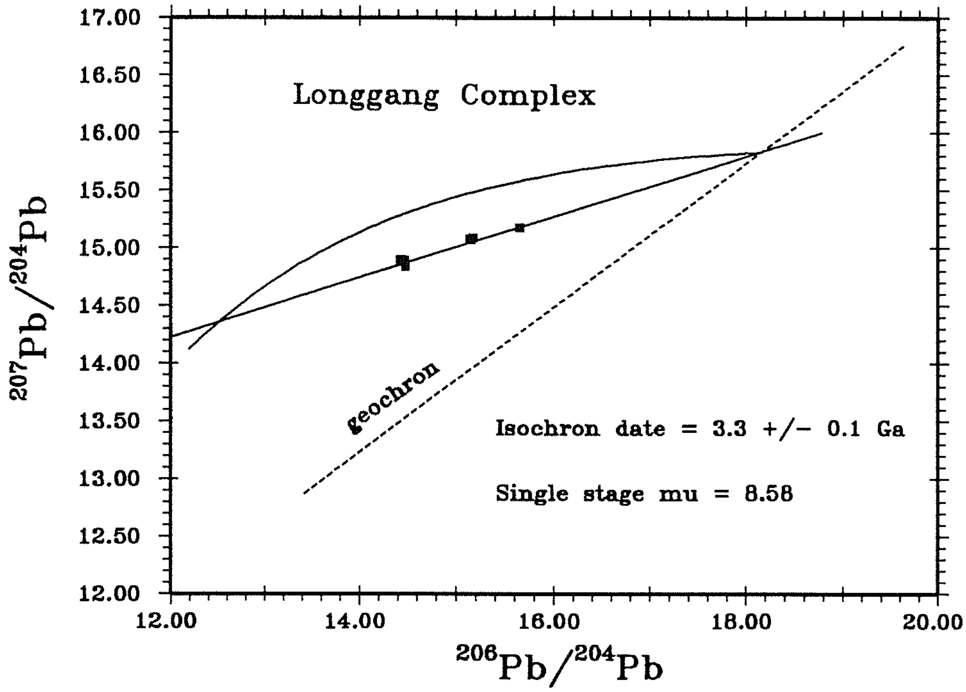

Figure 3-12. Pb-Pb isotopic plot for the Longgang Complex. Meaning of single stage μ, 8.58, is same as for the Lishan Granite (Figure 3-5). Second stage μ's are all smaller than 8.58. This indicates that the Longgang Complex has a U/Pb depleted character which is perhaps related to the granulite-facies metamorphism.

III-5. Jianping Complex

Early Precambrian rocks exposed in the western Liaoning Province, west of the Tan-Lu Fault, have been named the Jianping Complex (Fig. 1-1 and 2-2), which has also been referred as "Anshan Group" (Chinese Academy of Geological Sciences, 1973). The Jianping rocks have undergone granulitic-facies metamorphism and are considered, together with the Qianxi Complex, as part of the "granulitic belt" which continues west to the Yinshan region of Inner Mongolia (Sanggan Complex) and east to the Jilin Province (the Longgang Complex).

Rocks in the Jianping Complex are mainly amphibolite, hornblendite, pyroxenite, gneiss and granulites with basic to intermediate compositions. Our Rb-Sr data of amphibolitic samples from the Jianping Complex define a 2.68 ± 0.16 Ga isochron, with $(^{87}Sr/^{86}Sr)_0$ = 0.7012 ± 0.0004 (Table 3-5, Fig. 3-13). Our four Sm-Nd samples lie on a 2.85 ± 0.08 Ga line, with $\epsilon_{Nd}(T)$ = + 5.0±0.3 (Table 3-2, Fig. 3-14). The Nd T_{DM}'s for three of the four samples are between 2.58 and 2.63 Ga (Table 3-2). One with a high Sm/Nd ratio (6341) does not give a reasonable T_{DM}. Thus we infer that the Jianping Complex has formed 2.7 to 2.85 Ga ago, perhaps contemporaneous with or not much older than the Anshan supracrustal rocks.

II-6. Kuandian Complex and associated rocks

A Proterozoic mobile belt is well exposed in the eastern Liaoning Province and southern Jilin Province, China (Fig. 1-1,

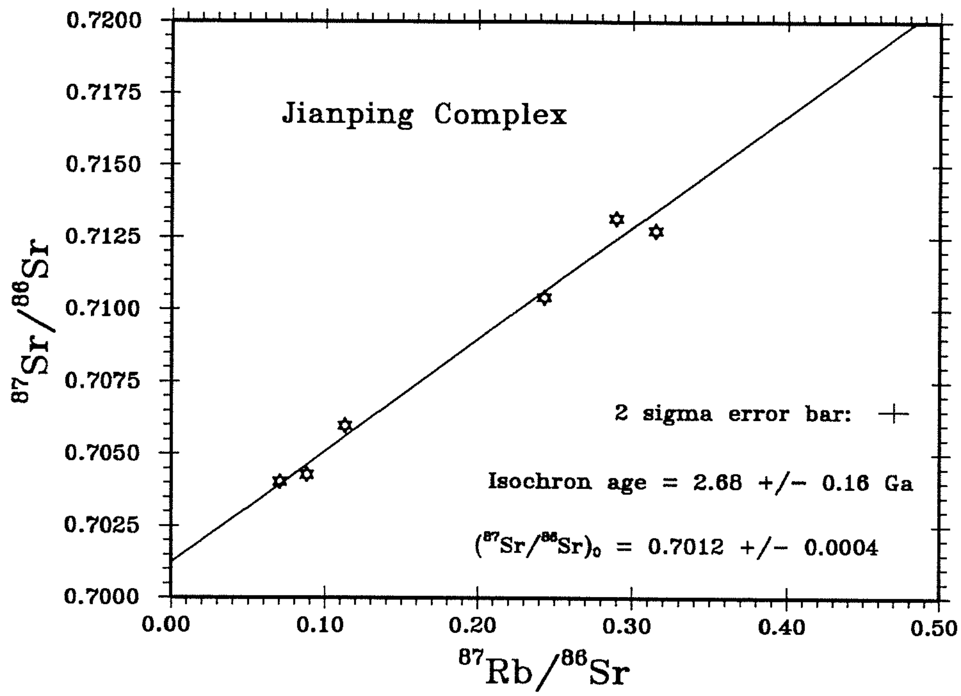

Figure 3-13. Rb-Sr isochron plot for the Jianping Complex.

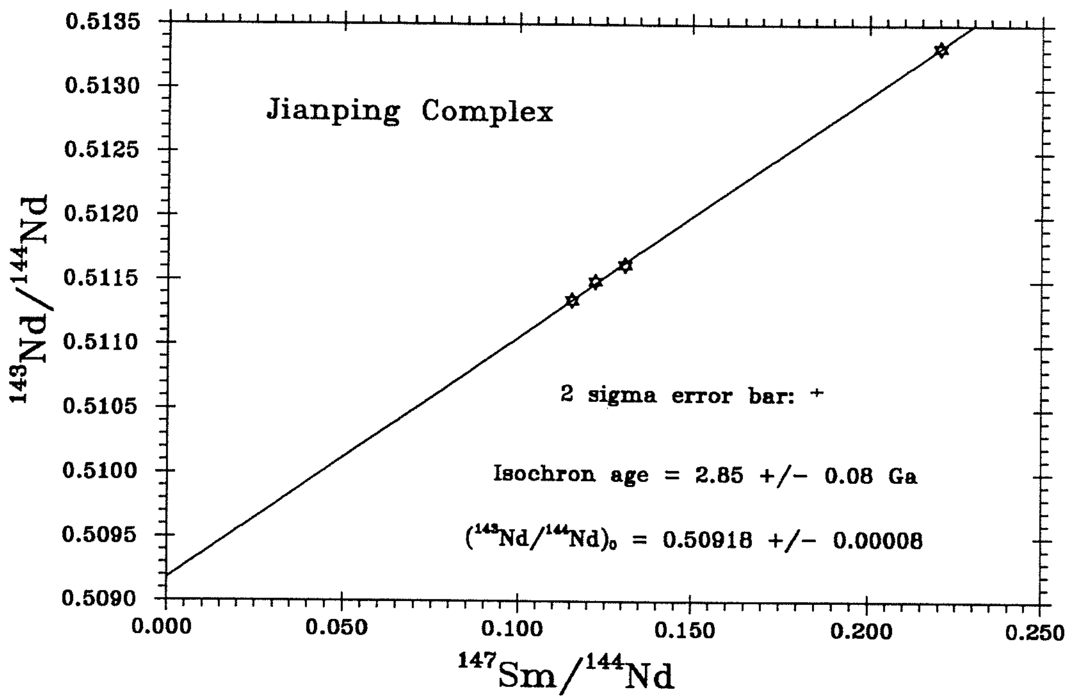

Figure 3-14. Sm-Nd isochron plot for the Jianping Complex.

1-2 and 3-15). The belt is bounded by the Archean Anshan Complex to the north and south, Tan-Lu Fault to the west, and continues into Korea on the east. The name, Liaohe Group, has been used for decades for the Proterozoic rocks in the area. Zhang (1984) pointed out that metapelitic, carbonate rocks are found in the north and that intrusive, volcanic rocks and turbidite are found in the south of the Proterozoic belt. He proposed that a miogeosyncline ("North-Liaohe") coexisted with an eugeosyncline ("South-Liaohe", or "Liaojitite") in the Early Proterozoic in the area. Jiang and his colleagues, however, subdivided the Proterozoic rocks into the following complex and groups (Fig. 3-16): Kuandian Complex, Caohe Group, Dalizi Group, Liaoyang Group, and Xutun Group (e.g. Jiang, 1987). The Kuandian Complex is composed of high grade metamorphosed rocks, such as gneiss and amphibolite, and granite. The other Proterozoic groups are medium or low grade metasediments. They observed unconformities between the adjacent rock systems in the above sequence, and concluded that these rocks formed in the Early to the Middle Proterozoic (Jiang, 1981) or from Late Archean to the Middle Proterozoic (Jiang, 1984; 1987) time. Figure 3-17 shows in more detail the distribution of Proterozoic rocks in the study area, East Liaoning Province, and our sample localities.

Geological background and previous isotopic work

Kuandian Complex:

The Kuandian Complex unconformably overlies the Archean Anshan Complex (Jiang, 1984). The Kuandian Complex contains

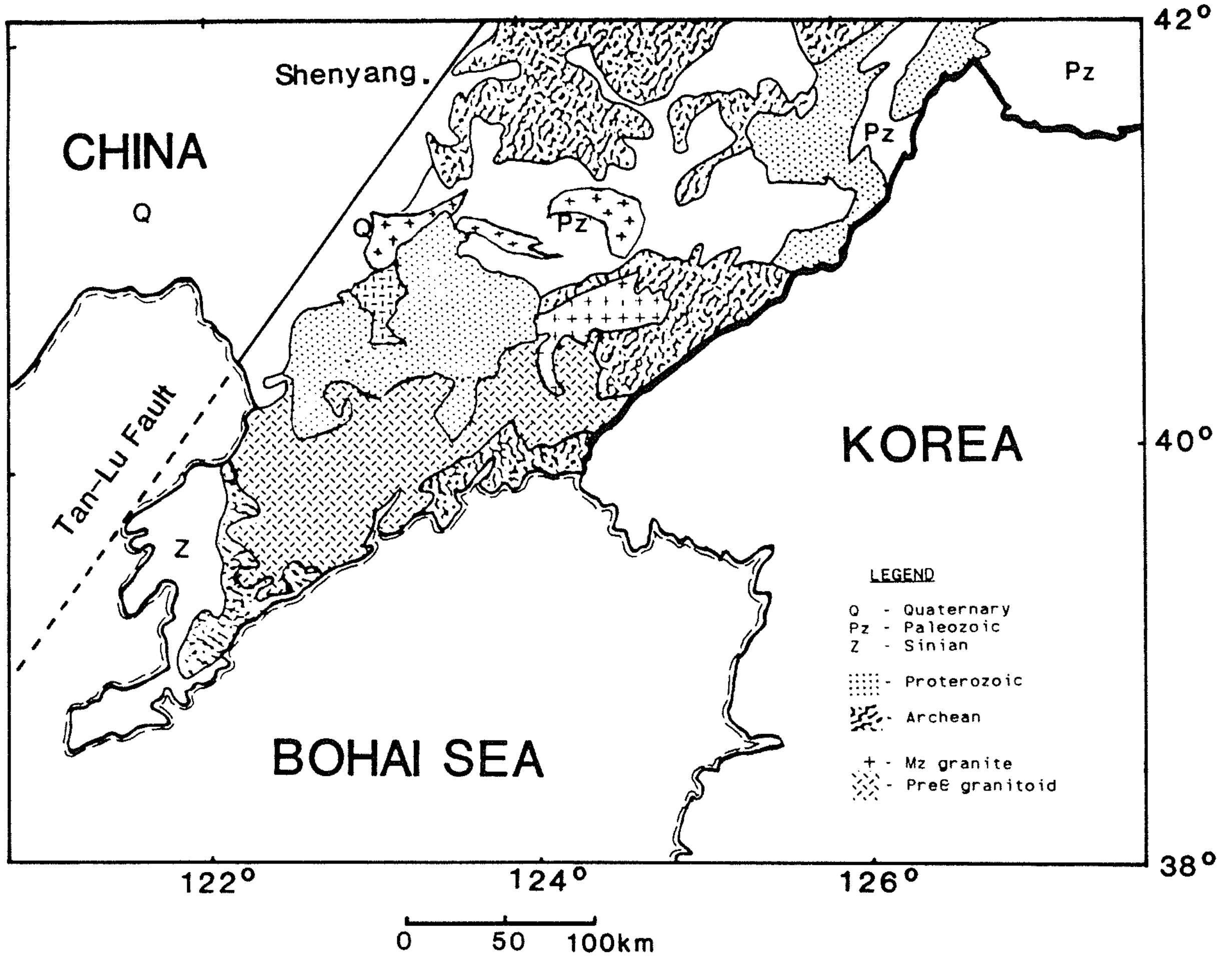

Figure 3-15. Simplified geological map of eastern Liaoning Province, China. Jilin Province is north of 41°N and east of 126°E. The Proterozoic mobile belt is bounded by Archean rocks to the north and south, the Tan-Lu Fault to the west, and continues into Korea on the east (simplified from CAGS, 1973 and unpublished map of Jiang, 1987).

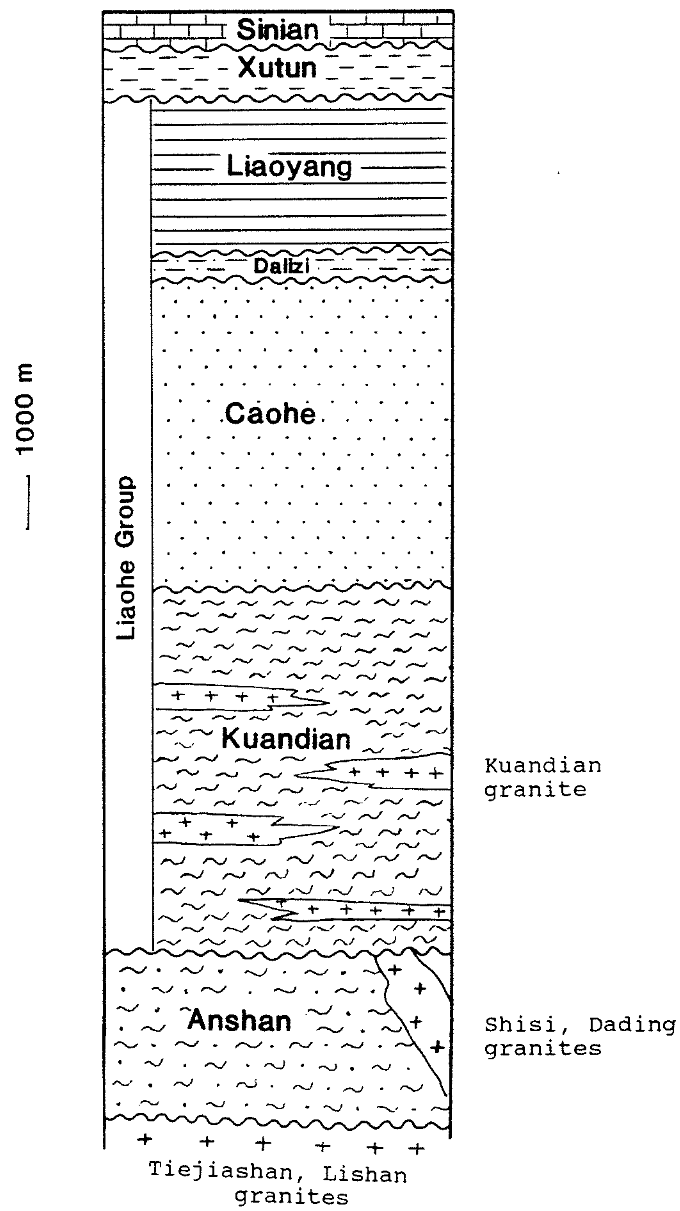

Figure 3-16. Schematic stratigraphic section showing the relationships of the Proterozoic geological systems in the East Liaoning Province, China. The "thicknesses" are compiled from Jiang (1987). Unconformities have been observed between the different systems. The Archean Anshan Complex unconformably lies on Tiejiashan Granite, and is mainly composed of amphibolites and gneisses. The Kuandian Complex consists of amphibolite, granite, limestone and fine-grain gneiss. The Caohe Group is intermediate grade rocks of meta-flysch facies and metapelite. Dalizi Group is mainly low-grade phyllite and meta-siltstone. Liaoyang Group is slate and carbonate. Xutun Group is slate, phyllite and quartzite.

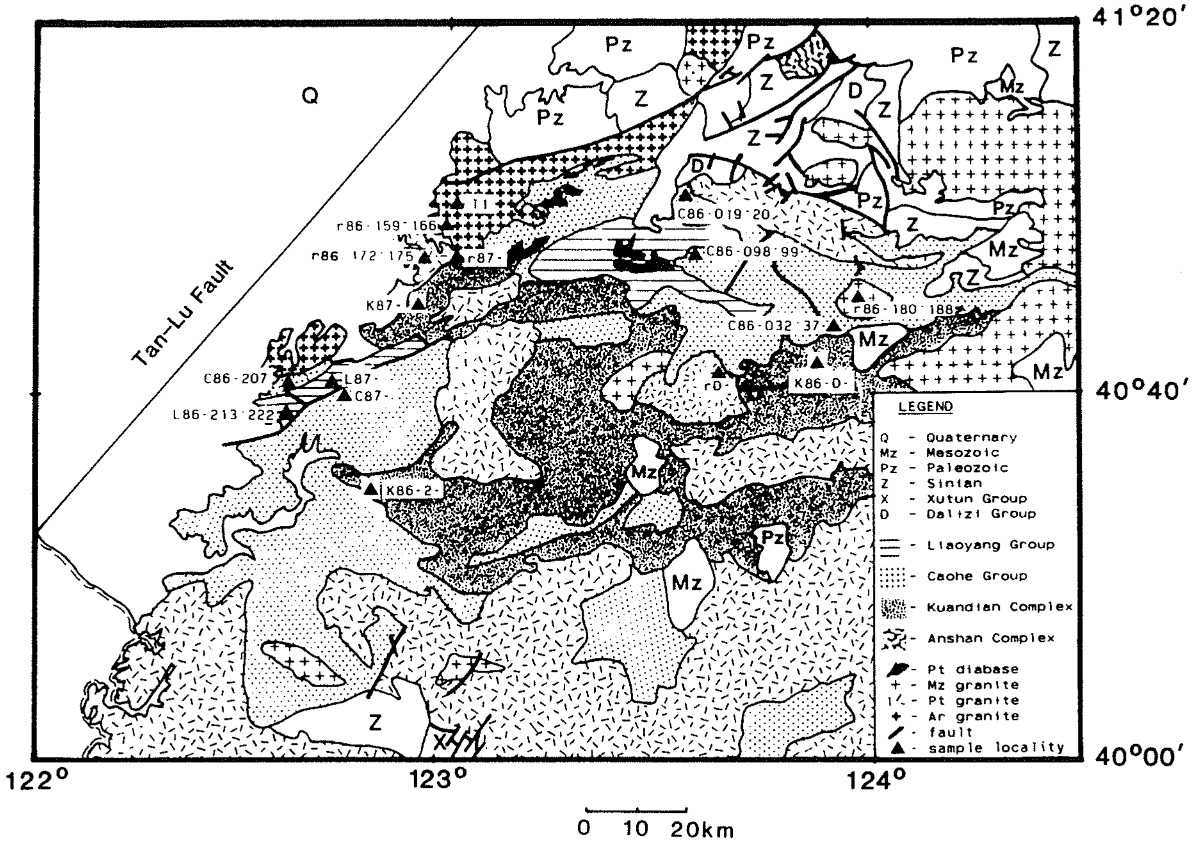

Figure 3-17. Geological map showing sample localities. The map shows the field occurrences of the Archean Anshan Complex, Proterozoic Kuandian complex, Caohe, Liaoyang, Dalizi, and Xutun groups, and granitic bodies of various ages (simplified from unpublished map of Jiang, 1987).

fine-grained gneiss, amphibolite, olivine-phlogopite-marble and granite with a low-Mg character.

Protoliths of fine-grained gneisses are rocks with turbidite rhythmic layers, which consist of immature sandstone, siltstone, greywacke, and some pyroclastic rocks/components (Zhang, 1984; Jiang, 1987). The amphibolites are made of fine or medium grain-sized hornblende and plagioclase, with well developed lineation and foliation.

Controversy exists regarding the nature of the Kuandian granite. The granite occurs as sheets or layers intercalated with amphibolite and gneiss. Jiang (1987) named the granite as layered migmatite and implied a metamorphic origin. Zhang (1984), however, proposed an igneous origin for the granite. Our petrographic study indicates that the granite is hololeucocratic, mainly composed of fine to intermediate grain-sized microcline, oligoclase and quartz. Mafic minerals are around 5%, which include biotite, blue amphibole (riebeckitic?) and locally dark green (aegirine?) augite. Magnetite, apatite and zircon are the main accessory minerals. No fluorite has been observed. Quartz usually shows undulatory extinction. Fractures are found inside zircon grains. K-feldspar porphyroclasts appear in one thin section. Perthitic textures are common in microclines, the exsolved albite has a stringer shape and is distributed regularly through the K-feldspar. Gneissic texture is conspicuous for the granite. From the above observations and rock chemistry discussed below, we infer that the Kuandian granite has an igneous origin, either an orthogneiss or metavolcanic rock.

The previously published K-Ar dates are between 1.7 to 1.9 Ga (compiled by Jiang, 1987). Liu et al. (1981) reported a 2.2 Ga Rb-Sr whole rock isochron for the Kuandian gneissic rocks. U-Pb zircon upper intercept dates for the Kuandian granite are around 1.8, 2.1, and 2.3 Ga (compiled and recalculated by Jiang, 1987). Based on these isotopic data, Jiang and his colleagues once placed the Kuandian Complex in the Early Proterozoic (e.g. Jiang, 1981). However, by comparison of petrochemistry and lithologic assemblages with the Fuping Complex in the Taihangshan region, Shanxi and Hebei provinces, they later tentatively placed the Kuandian Complex in the Late Archean (Jiang, 1984; 1987).

The Kuandian Complex contains two important type of boron deposits, i.e. ascharite type and ludwigite type, also massive Fe of metasediment type, fine-grained stratiform Pb-Zn, magnesite, and talc.

Caohe Group:

The Caohe Group unconformably overlies the Kuandian Group. Conglomerates are observed overlying the contact. The Caohe Group consists of intermediate grade rocks of meta-flysch facies and metapelite, now mainly fine-grained gneiss, schist and carbonate. Chen and Zhong (1981) reported a 2.0 Ga Pb-Pb whole rock isochron. Jiang (1987) obtained 1.90 and 1.86 Ga Rb-Sr whole rock isochrons for the Caohe Group and a 1.8 Ga K-Ar date for muscovite from a pegmatite intruding the Caohe Group. They proposed that the Caohe Group was deposited between 2.1 and 1.85

Ga, and underwent a metamorphic event at 1.85 ± 0.05 Ga.

Dalizi Group:

The Dalizi Group mainly crops out in the southeastern Jilin Province. This group consists of low grade phyllite and meta-siltstone. The phyllite has a pelitic composition. Jiang (1987) reported a 1.73 Ga Rb-Sr whole rock isochron and interpreted the date as a metamorphic age. They presumed that the Dalizi Group was deposited between 1.8 to 1.7 Ga. Dalizi stratiform iron deposit is confined in this group.

Liaoyang Group:

The Liaoyang Group is mainly made of slate and thick and massive carbonates. The slate has a pelitic composition. Jiang (1987) obtained 1.48 and 1.45 Ga Rb-Sr whole rock isochrons and a 1.6 Ga K-Ar date for muscovite from a pegmatite intruding the Liaoyang Group. They interpreted the Rb-Sr isochron date as a metamorphic age and proposed that the Liaoyang Group was deposited between 1.7 to 1.5 Ga. Important magnesite, talc, and metasedimentary phosphorus deposits are found in this group.

Xutun Group:

The Xutun Group consists of slate, phyllite, and quartzite. The slate and phyllite have a pelitic composition. No isotopic ages have been reported for this group to date. Field relationships indicate that it is older than the Sinian.

In summary, previous geochronological studies generally agree on an Early Proterozoic age for the Kuandian Complex and Caohe Group, probable Early Proterozoic age for the Dalizi Group, and possible Middle Proterozoic age for the Liaoyang

Group.

Granitic intrusions:

Granitic bodies of different ages are widely distributed in the area, but very little isotopic dating has been done on the granites.

Pre-Kuandian granites:

The Shisi Granite and the Dading Granite are overlain by the Kuandian Complex and contain inclusions of the Anshan Complex. There are no isotopic data for these bodies.

Post-Kuandian granite:

The Mafeng granite was previously mapped as a Proterozoic granite. Our new field observations indicate that the Mafeng Granite intrudes the Kuandian Complex. The isotopic data of this study indicate a Mesozoic age.

Petrochemistry of Kuandian Complex and associated rocks

We have done major and trace element XRF analyses for 4 amphibolites, 7 granites, and 2 metasediments from the Kuandian Complex, 5 metasediments from the Caohe Group, 5 metasediments from the Liaoyang Group, and 12 samples from associated granitic bodies (Tables 1 and 2). Immobile elements have been given special attention.

(1). Kuandian amphibolites

Essential Classification:

Volcanic rocks usually fall into basaltic, andesitic, and rhyolitic categories according to their SiO_2 concentrations.

They can be classified as subalkaline, alkaline, and peralkaline, according to their alkali contents. The subalkaline rocks can be further subdivided into tholeiitic and calc-alkaline series based on iron enrichment trends and Al_2O_3 contents (Irvine and Baragar, 1971).

Amphibolites from the Kuandian Complex are mostly basaltic, except for one sample, K86-248, of very different composition. This sample has high SiO_2 (74.3%), but extremely low K_2O (0.32%) and Rb (5 ppm). CaO is higher than rocks with high SiO_2. It is from a leucocratic microlayer inside the foliated melanocratic amphibolite, and is mainly composed of fine grained quartz, minor alkali feldspar, hornblende, sphene, and apatite, with a mylonitic fabric. The protolith of this rock is probably a SiO_2-enriched sediment, perhaps impure chert or siliceous exhalite, and is excluded from any further discussion.

Major element data indicate that most of the Kuandian amphibolites have the chemical signature of subalkaline rocks (Figs. 3-18 and 3-19). The only exception is one sample, K86244, that plots at the boundary of alkaline and subalkaline rocks in Alkali-Si_2O diagram (Fig. 3-18) and falls in the alkaline field in Ol'-Ne'-Q' plot (Fig. 3-19). Trace elements show a subalkaline character for all the amphibolites from the Kuandian Complex, e.g. Y/Nb > 1.

All the Kuandian amphibolites fall in the tholeiitic field in Al_2O_3 -normative plagioclase plot (Fig. 3-20) and AFM diagram (Fig. 3-21).

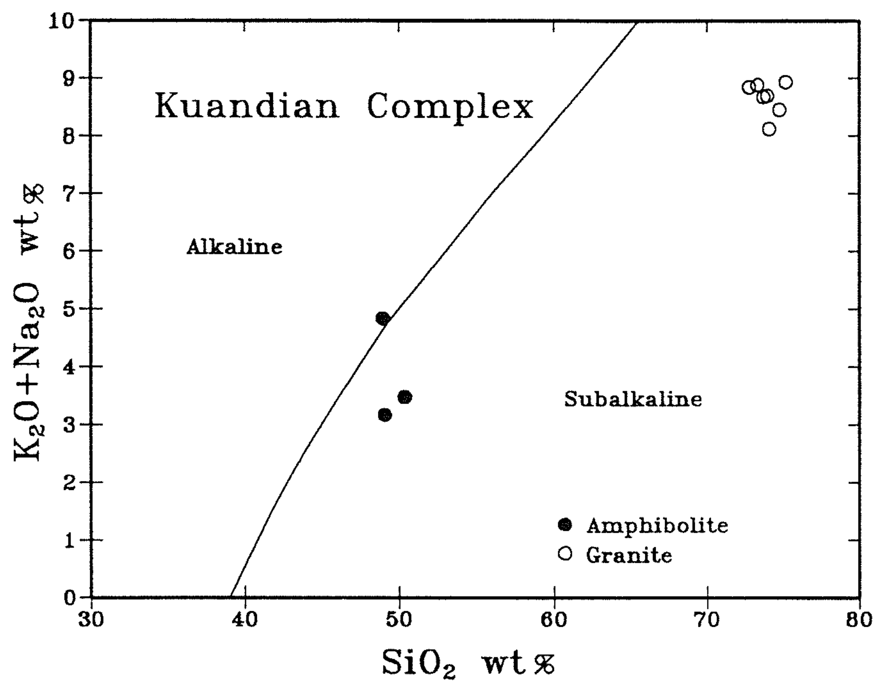

Figure 3-18. Total alkali - SiO_2 plot showing that Kuandian amphibolites and granites fall in the subalkaline field with the exception that one amphibolite plots near to the boundary of alkaline and subalkaline fields. The dividing line is from Irvine and Baragar (1971).

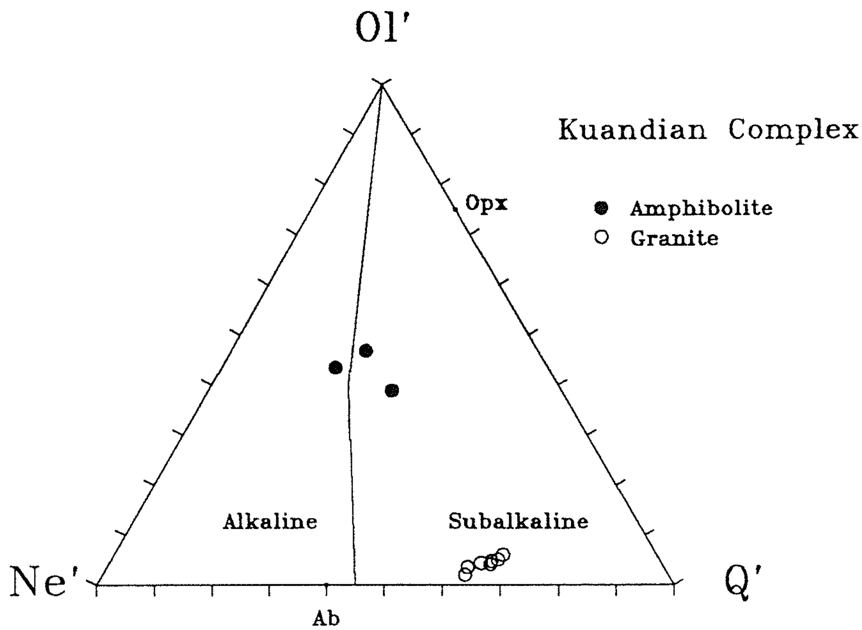

Figure 3-19. Ol'-Ne'-Q' plot showing that Kuandian amphibolites and granites fall in the subalkaline field with the exception that one amphibolite plots slightly in the alkaline field. The dividing line is from Irvine and Baragar (1971). Ol'=Ol+3/4Opx, Ne'=Ne+3/5Ab, Q'=Q+2/5Ab+1/4Opx, cation norms.

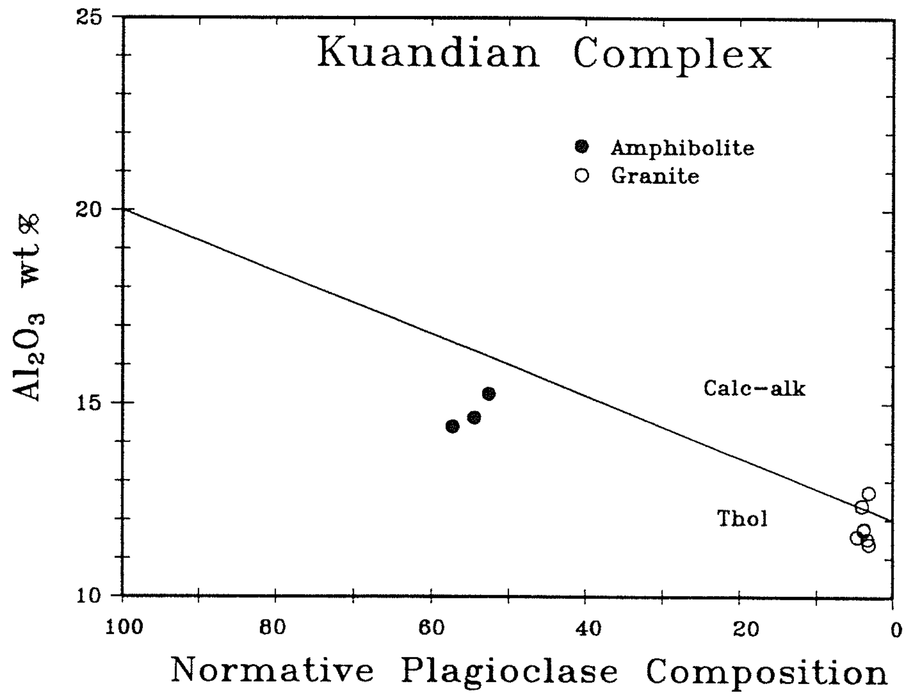

Figure 3-20. Al_2O_3 - Plagioclase plot for Kuandian Complex. All the amphibolites fall in the tholeiitic field.

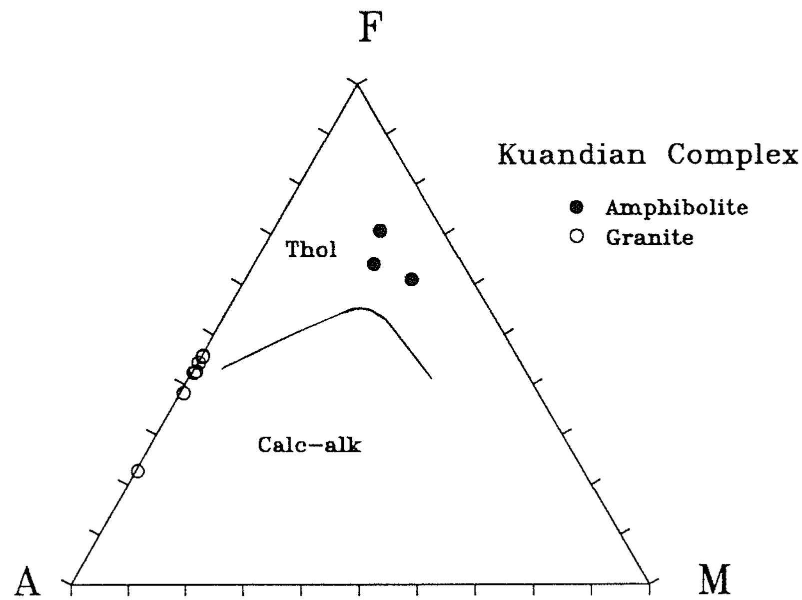

Figure 3-21. AFM plot for Kuandian Complex. All amphibolites fall in the tholeiitic field. The dividing line is from Irvine and Baragar (1971). A=K_2O+Na_2O, F=ΣFeO, M=MgO, all in wt%.

In summary, the Kuandian amphibolites have basaltic compositions, and are subalkaline to transitional (subalkaline-alkaline) with a tholeiitic character.

Tectonic Discriminant Plots:

The tectonic settings for modern volcanic rocks are well defined and numerous discriminant diagrams based on major and trace elements have been proposed (e.g. Pearce, 1982). These may not be exactly appropriate for Precambrian time but nevertheless provide a basis for comparison between Precambrian magmatic suites and between Precambrian and modern analogues.

Glassley (1974) proposed a FeO^*/MgO - TiO_2 diagram to distinguish tholeiitic rocks formed in the environments of mid ocean ridge (MORB), ocean island (OIB) and island arc (IAT). Two amphibolites from the Kuandian Complex plot in the IAT field, and one in the MORB field (Fig. 3-22).

Pearce (1976) proposed diagrams using discriminant functions F_1, F_2, and F_3, calculated from major element data. In F_2-F_1 plot, two amphibolites plot in the field of CAB+LKT, and one more alkaline sample falls in the field of SHO (Fig. 3-23). In F_3-F_2 plot, two amphibolites plot in the LKT field, and the one with more alkaline composition falls near to the SHO field (Fig. 3-24).

Pearce (1982) introduced N-type MORB normalized trace element patterns ("spider diagrams") for comparison of MORB, WPB, and VAB. The Kuandian amphibolites are highly enriched in K, Rb, Ba, and Th; slightly enriched in Nb and Ce; P, Zr, Hf, Sm, Ti, Y, Yb, and Sc are close to 1. The pattern is between

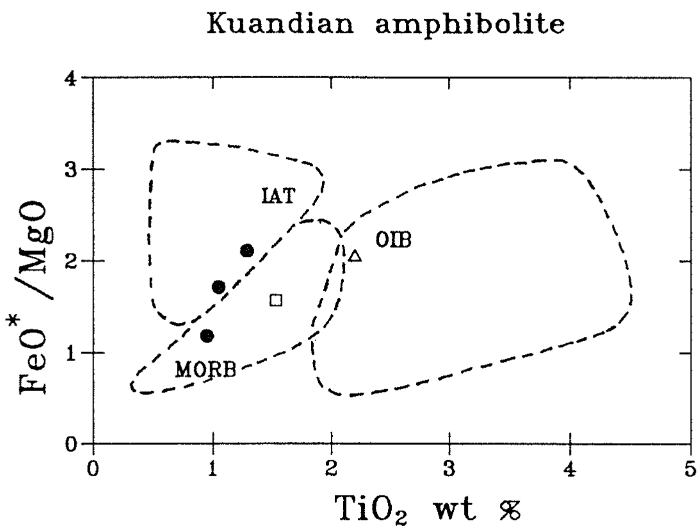

Figure 3-22. FeO^*/MgO - TiO_2 plot for tholeiitic basalts (Glassley, 1974). FeO^* represents total iron in FeO form, all in wt%. Tholeiites can be discriminated as MORB, IAT, and OIB in this diagram. Two tholeiitic amphibolites from the Kuandian Complex fall in the IAT filed, one in the MORB field. Condie (1982)'s average value of continental rift and flood basalts is indicated by an open triangle. Average value of the high-Mg Picture George basalt (BVSP, 1981; Bailey, 1989) is shown by an open square.

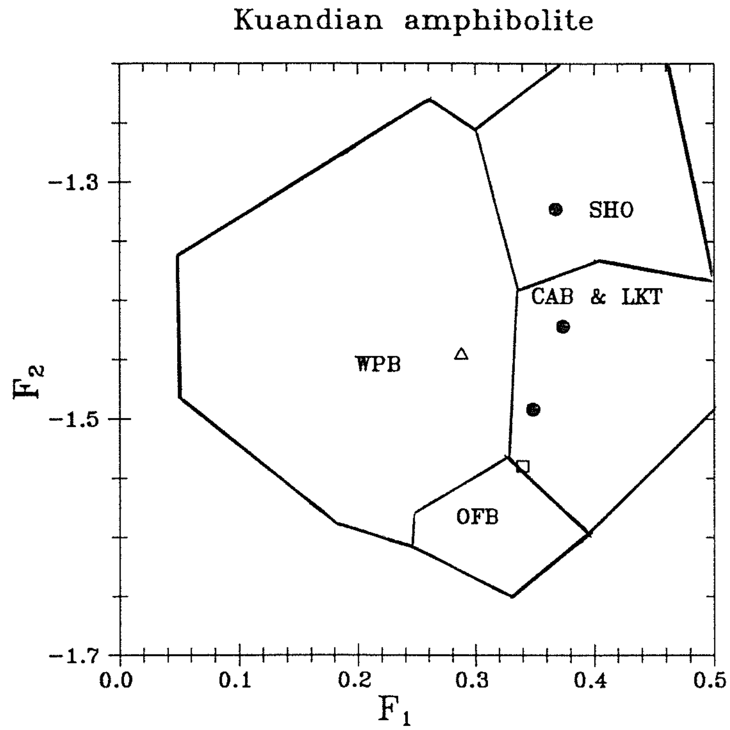

Fig. 3-23. F_2 - F_1 plot for basaltic rocks (Pearce, 1976). Two basaltic amphibolites from Kuandian Complex fall in the field of CAB+LKT. One with more alkaline composition plots in SHO field. $F_1 = 0.0088SiO_2 - 0.0774TiO_2 + 0.0102Al_2O_3 + 0.0066FeO - 0.0017MgO - 0.0143CaO - 0.0155Na_2O - 0.0007K_2O$, $F_2 = -0.0130SiO_2 - 0.0185TiO_2 - 0.0129Al_2O_3 - 0.0134FeO - 0.00300MgO - 0.0204CaO - 0.0481Na_2O + 0.0715K_2O$. $Fe_2O_3 = TiO_2 + 1.5$ was assumed in calculating FeO. Meanings of open triangles and squares are the same as on Figure 3-22.

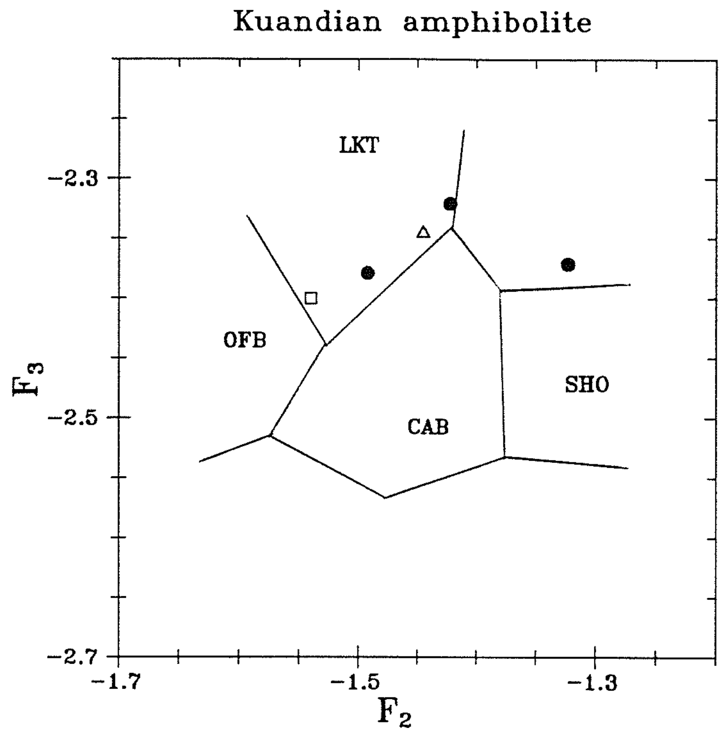

Figure 3-24. F_3 - F_2 plot for basaltic rocks (Pearce, 1976). Two basaltic amphibolites from Kuandian Complex fall in the LKT field, one with more alkaline composition plots near to SHO field. F3 = $-0.0221SiO_2 - 0.0532TiO_2 - 0.036Al_2O_3 - 0.0016FeO - 0.0310MgO - 0.0237CaO - 0.0614Na_2O - 0.0289K_2O$. Meanings of open triangles and squares are the same as on Figure 3-22.

typical calc-alkaline and typical arc tholeiitic basalts (Fig. 3-25).

Some trace element diagrams are effective in discriminating WPB from non-WPB, e.g. Ti/Y - Nb/Y (Pearce, 1982), Ti/100 - Zr - Y*3 (Pearce and Cann, 1973), Zr/Y - Zr (Pearce and Norry, 1979), and Ti-Zr (Pearce, 1982) diagrams. All the amphibolites from the Kuandian Complex plot in the fields of non-WPB (Figs. 3-26, 3-27, 3-28, and 3-29).

Ti/100 - Zr - Sr/2 (Pearce and Cann, 1973) and Ni - Y (Capedri et al., 1980) have been suggested for the further discrimination of non-WPB. In a Ti/100 - Zr - Sr/2 diagram, all the amphibolites plot in the LKT field (Fig. 3-30). In Ni - Y diagram, two amphibolites plot in the LKT field, and one falls in the MORB field (Fig. 3-31).

In summary, the Kuandian amphibolites mostly show the character of island arc Low-K tholeiites in the above major and trace element tectonic discriminant diagrams. Nevertheless high K_2O in the Kuandian amphibolites is strongly inconsistent with the low-K tholeiite character. If this could be attributed to K-enrichment in a later metamorphic event, however, the low Al_2O_3 and high ΣFeO characters of Kuandian amphibolite would still be inconsistent with island arc low-K tholeiites. Comparing with arc low-K tholeiite (e.g. Sun, 1980), the Kuandian amphibolite is also enriched in Rb, Ba, Sr, Cr, Ni, Y, and Zr. Sr/Nd ratios of the Kuandian amphibolite are between 14.2 and 25.9, which are also smaller than island arc basalts (30 to 35, McDonough, 1990).

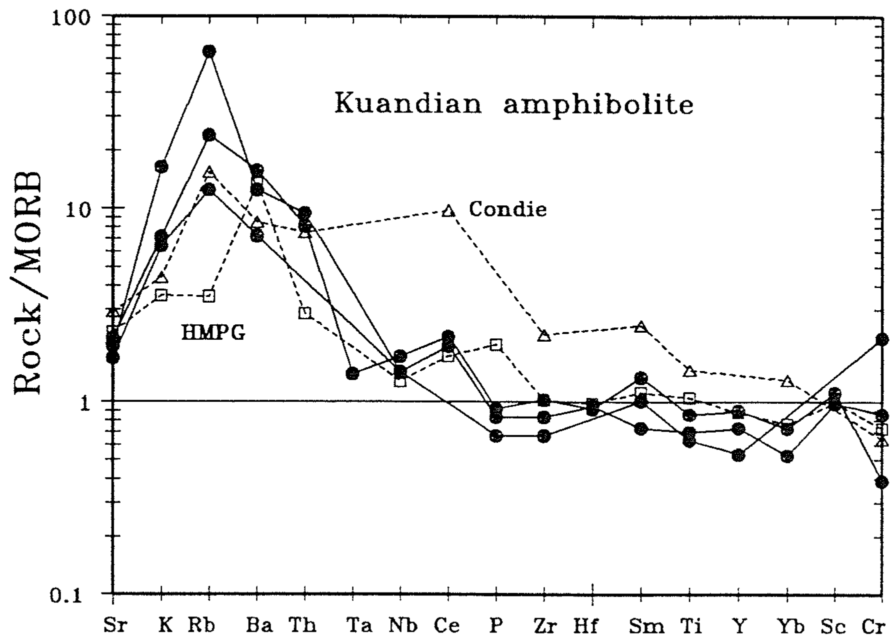

Figure 3-25. Trace element plots (spider diagrams) for basaltic amphibolites from Kuandian Complex. Meanings of open triangles and squares are the same as on Figure 3-22.

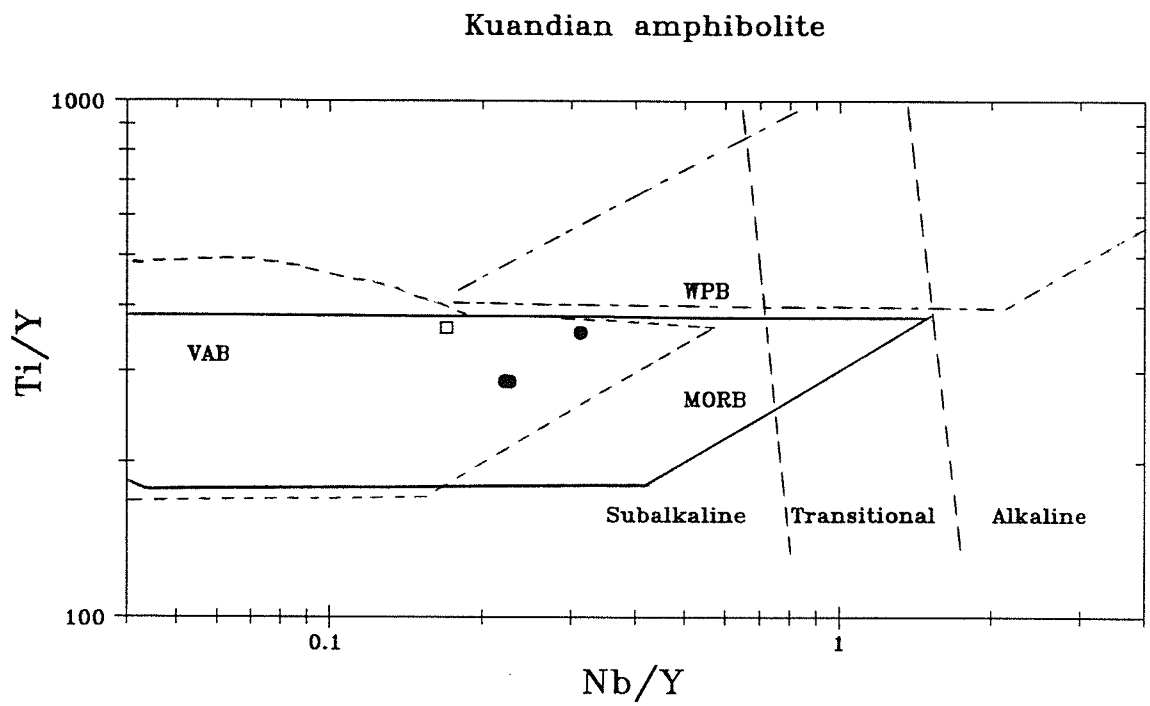

Figure 3-26. Ti/Y - Nb/Y plot for tholeiitic and alkaline basalts (Pearce, 1982). Fields are divided into subalkaline, transitional, and alkaline mainly according to Nb/Y ratios. WPB can be easily discriminated from the non-WPB that includes VAB and MORB. But VAB and MORB fields largely overlap. The Kuandian amphibolites are non-WPB and subalkaline, in accord with major element plots. Meanings of open squares is the same as on Figure 3-22.

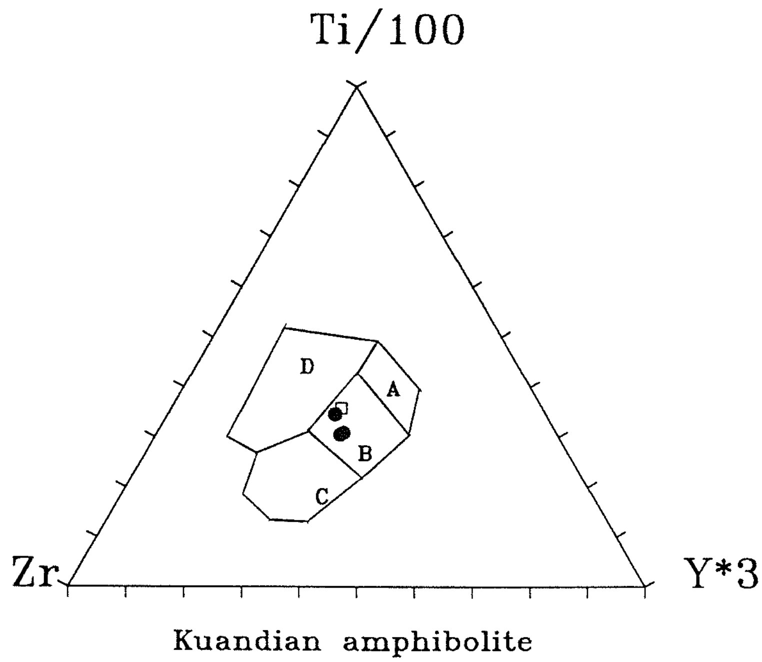

Figure 3-27. Ti/100 - Zr - Y*3 plot for basaltic rocks (Pearce and Cann, 1973). WPB plots uniquely in the field D, thus can be discriminated from non-WPB. The Kuandian amphibolites plot in non-WPB fields. Meaning of open squares is the same as on Figure 3-22.

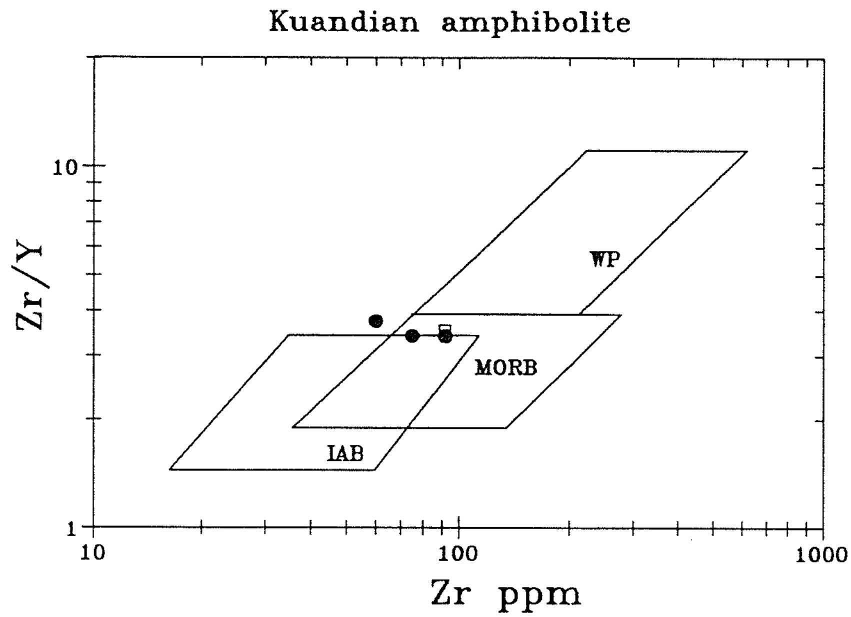

Figure 3-28. Zr/Y - Zr plot for basaltic rocks (Pearce and Norry, 1979). WPB can be distinguished from non-WPB, but the fields of MORB and IAB partly overlap. The Kuandian amphibolites plot in non-WPB fields. Meaning of open squares is the same as on Figure 3-22.

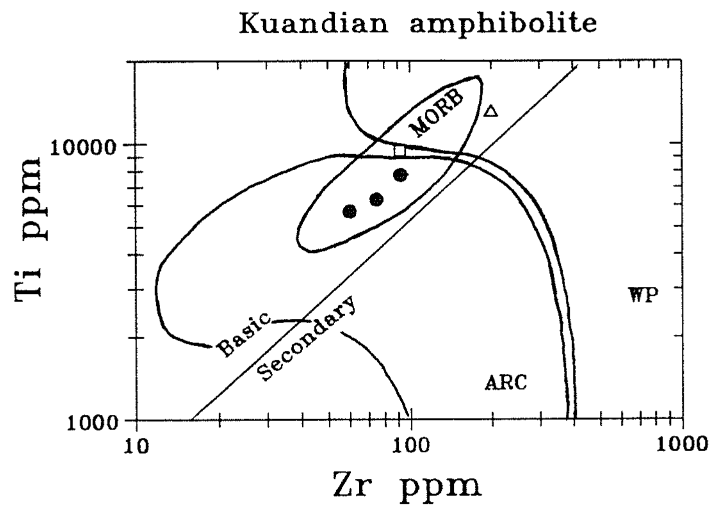

Figure 3-29. Ti-Zr plot for basalts and secondary rocks (Pearce, 1982). The Kuandian amphibolites plot in the non-WPB field. Meaning of open triangles and squares are the same as on Figure 3-22.

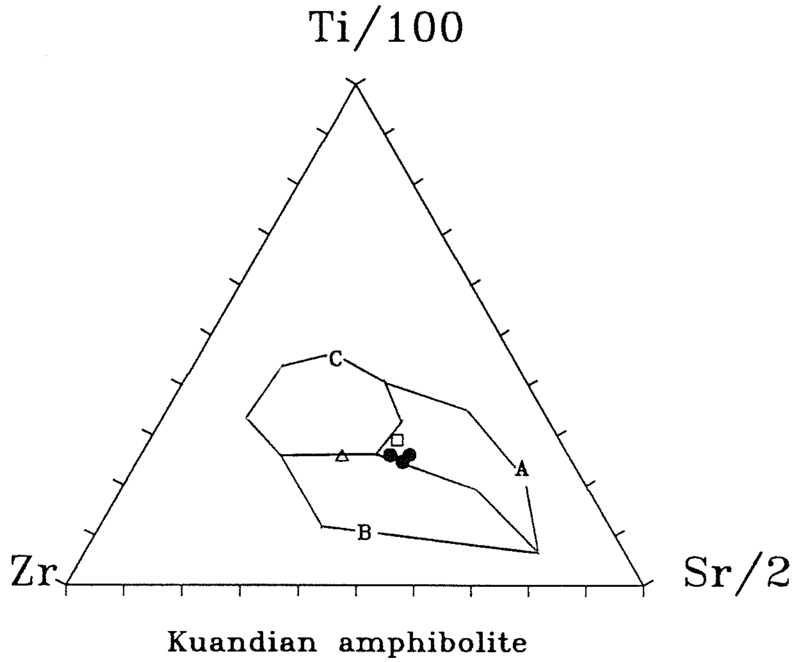

Figure 3-30. Ti/100 - Zr - Sr/2 plot for non-WPB basalts (Pearce and Cann, 1973). Basalts formed in non-WP settings can be easily distinguished, but subject to much uncertainty because of Sr mobility in metamorphic rocks. LKT plots in field A, CAB in field B, and OFB in field C. The Kuandian amphibolites plot in the LKT field. Meaning of open triangles and squares are the same as on Figure 3-22.

Kuandian amphibolite

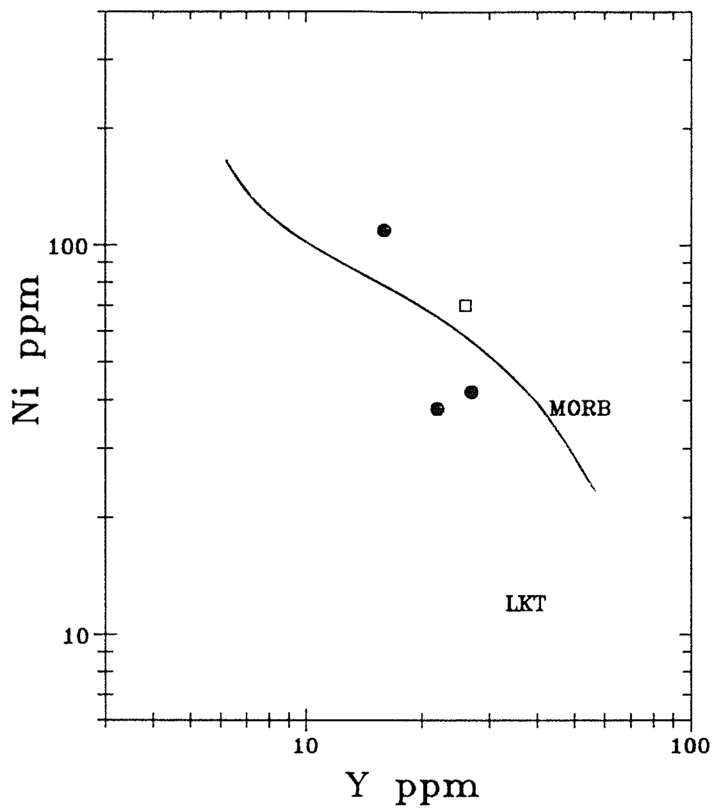

Figure 3-31. Ni - Y plot for TH basalts (Capedri et al., 1980). The fields are divided into MORB and LKT. Two basaltic amphibolites from Kuandian Complex plot in the LKT field, and one in the MORB field. Meaning of open squares is the same as on Figure 3-22.

The REE pattern of the Kuandian amphibolites is relative flat, with a slight enrichment of LREE (Fig. 32, unpublished data from Wu). No Eu anomaly was observed. This is also different from the arc low-K tholeiite. The latter has a slight LREE depletion (BVSP, 1981).

The REE pattern of the Kuandian amphibolites is, however, similar to one of the most primitive members of the Columbia River Basalt Group (BVSP, 1981). Their major and other trace elements also resemble the High-Mg Picture George basalt (BVSP, 1981; Bailey, 1989), except for higher K_2O and Rb and lower P_2O_5 in the Kuandian amphibolites.

In terms of K_2O and Rb, the Kuandian amphibolites are even more enriched than many continental rift and continental flood basalts, e.g. those from Afar Rift in Ethiopia (Barberi et al., 1975), Southern Gregory (Kenya) Rift (Barker et al., 1977), Isle of Skye in Scotland (Thompson et al., 1972; 1980), Proterozoic Keweenawan basalt in the Lake Superior district (BVSP, 1981), basalt from Iceland (Wood, 1978; Sigvaldason and Oskarsson, 1986), as well as Snake River basalt (Thompson et al., 1983). The basaltic formations in the 2.76 Ga Fortescue Group of Australia share the high K_2O and Rb character but the latter are generally higher in SiO_2, lower in MgO, CaO and Al_2O_3 (Glikson et al., 1986).

Compared with the above mentioned continental rift and continental flood basalts (CFB), the Kuandian amphibolites are also in some degree enriched in ΣFeO (similar to Snake River basalt, but the latter has a lower SiO_2), and depleted in Zr, Nb

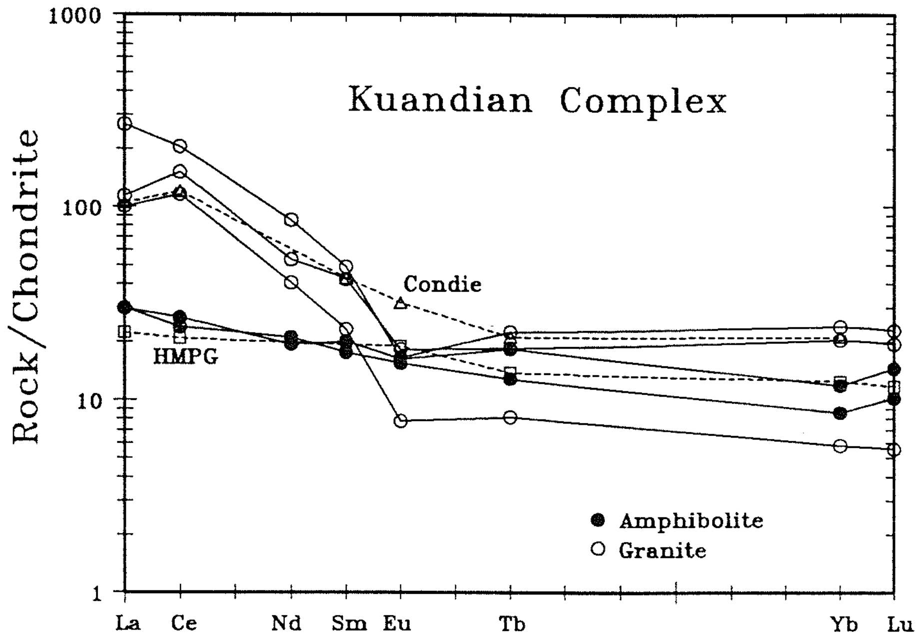

Figure 3-32. Chondrite normalized REE plot for the Kuandian amphibolites and granites. Meanings of open triangles and squares are the same as on Figure 3-22.

and Ti. This can explain why the Kuandian amphibolite falls in the LKT fields in tectonic discriminant diagrams.

In conclusion, the Kuandian amphibolites are most likely flood basalts, and thus hot-spot related melts, incorporating continental lithosphere (Duncan and Richards, 1991).

(2). Kuandian granite

Samples from the Kuandian granite are metaluminous and plot in the granite field in the normative An-Ab-Or diagram (Fig. 3-1). They are chemically similar to A-type granite (Whalen et al., 1987; Eby, 1990), except that Ba and V are high, and Th and Zn are low. K_2O is often even higher, Al_2O_3, MgO/ΣFeO and MgO are even lower, K/Rb ratio is higher, and Rb/Sr and Rb/Ba ratios are lower than the average A-type granite. Zr, Nb, and Y are compatible with A-type granite, although generally lower than the average value of Whalen et al. (1987) and White and Chappell (1983).

The Kuandian granites show a REE pattern of enriched LREE, flat HREE, with slightly negative Eu anomaly (Fig. 3-32, unpublished data from Wu). This REE pattern is similar to the A-type granite (e.g. Collins et al., 1982), although ΣREE is lower.

The Rb - (Y+Nb) diagram of Pearce et al. (1984) has been used to discriminate tectonic environments of the Precambrian granites in this study. The Kuandian granites mostly plot in the WPG field in the Rb - (Y+Nb) diagram (Fig. 3-2).

Compared with world-wide Proterozoic anorogenic granites (Anderson, 1983), except for higher ΣFeO and Sr, the Kuandian granites are close in composition to the Wolf River batholith, Wisconsin; Trial Creek granite, Wyoming; Ragunda biotite granite, Sweden; the average Finish rapakivi granites; and Snegamook Lake biotite granite, Labrador.

The Kuandian granites also show higher K_2O and ΣFeO, lower Al_2O_3 and MgO character when compared with the Cenozoic rhyolites (>69% SiO_2) from predominantly bimodal mafic-silicic volcanic associations (Ewart, 1979), e.g. those from Yellowstone and Snake River Plain, western U. S. A.; Medicine Lake Centre, and Salton Sea Centre, California; Iceland (also see Wood, 1978); Western Scotland and Northern Ireland, Southern Queensland (also see Ewart, 1982); and Kenya Rift (Macdonald et al., 1987).

(3). Other granitic bodies from the area

The Shisi Granite falls in the granite field in the normative An-Ab-Or diagram (Fig. 2-1). It is chemically similar to A-type granite in major elements and Ba, Sc and V, but depleted in Zr, Nb, Y, La, and Ce, which are critical for A-type granite classification. So we interpret that the Shisi Granite is a highly evolved I-type granite, instead of A-type granite. Its location on the boundary of VAG and Syn-COLG in the Rb - (Y+Nb) diagram (Fig. 3-2), also substantiates this interpretation.

The Dading Granite plots in the trondhjemite field in normative An-Ab-Or diagram (Fig. 3-1). It has an I-type granite chemistry except for high Na_2O and low MgO and Rb. It plots in the VAG field in Rb - (Y+Nb) plot (Fig. 3-2).

The Mafeng granite plots in the granite field in the normative An-Ab-Or diagram (Fig. 3-1). This granite has an I-type chemistry, except for high Na_2O, and low MgO and Rb. It falls in the VAG field in Rb - (Y+Nb) plot (Fig. 3-2).

Combined with chemistry of the Archean Tiejiashan and Lishan granites, we conclude that the granitic bodies from the eastern Liaoning Province have a variety of compositions, some with contradictory major and trace elements signatures: (a) the Archean Tiejiashan Granite has an S-type character in term of major elements and an A-type character in term of trace elements. We make this observation without providing any explanation. (b) the Archean Lishan Granite, Proterozoic Dading Granite, and Mesozoic Mafeng Granite all have an I-type character. (c) the Proterozoic Shisi Granite has an A-type character in major elements and I-type granite character in trace elements. We tentatively infer that these b and c category granites are normal to extremely evolved I-type granites. (d) the Kuandian granite has a unique A-type granite character for both major and trace elements.

Isotopic results

Published isotopic dates and our own results for the Kuandian Complex and associated rocks are summarized in Table 3-1.

Kuandian Complex:

Five amphibolites and eight granites define a Rb-Sr isochron of 1.91 ± 0.06 Ga, with $(^{87}Sr/^{86}Sr)_0$ = 0.7056 ± 0.0007 (Table 3-5 and Fig. 33). One amphibolite (K86-246) was rejected from the regression calculation. Two metasediments also plot on the isochron. Hornblende and plagioclase separated from an amphibolite, K86-244, plot near to the isochron. The two-mineral isochron date is 0.23 ± 0.02 Ga with $(^{87}Sr/^{86}Sr)_0$ = 0.7662 ± 0.0006. The reason that the two mineral separates plot above the whole rock could be due to epidote alteration. Higher Rb/Sr ratio of plagioclase than the hornblende is tentatively attributed to a possible K-feldspar component in the plagioclase separate. The low mineral isochron date is probably due to isotopic resetting by Mesozoic magmatic activity in the region. Separate regression of amphibolites and granites gives 1.96 ± 0.22 and 1.8 ± 0.1 Ga, with $(^{87}Sr/^{86}Sr)_0$ = 0.705 ± 0.001 and 0.717 ± 0.011, for the amphibolites and granites respectively.

Six amphibolites and seven granites define a straight line in the Sm-Nd plot. The isochron date is 2.32 ± 0.06 Ga with $(^{143}Nd/^{144}Nd)_0$ = 0.50969 ± 0.00005 or $\epsilon_{Nd}(T)$ = +1.3 ± 0.5 (Table 3-2 and Fig. 34). Hornblende separated from an amphibolite, K86-244, falls on the isochron, while plagioclase from the same sample plots above the isochron. The two-mineral isochron date is 1.85 ± 0.12 Ga with $(^{143}Nd/^{144}Nd)_0$ = 0.51025 ± 0.00014. Separate regression of amphibolites and granites gives 2.46 ± 0.14 and 2.4 ± 0.2 Ga, with $(^{143}Nd/^{144}Nd)_0$ = 0.5095 ± 0.0001 and 0.5096 ± 0.0001 or $\epsilon_{Nd}(T)$ = +1.8 ± 0.8 and +2.3 ± 1.7, for the amphibolites and granites respectively. Nd depleted mantle model

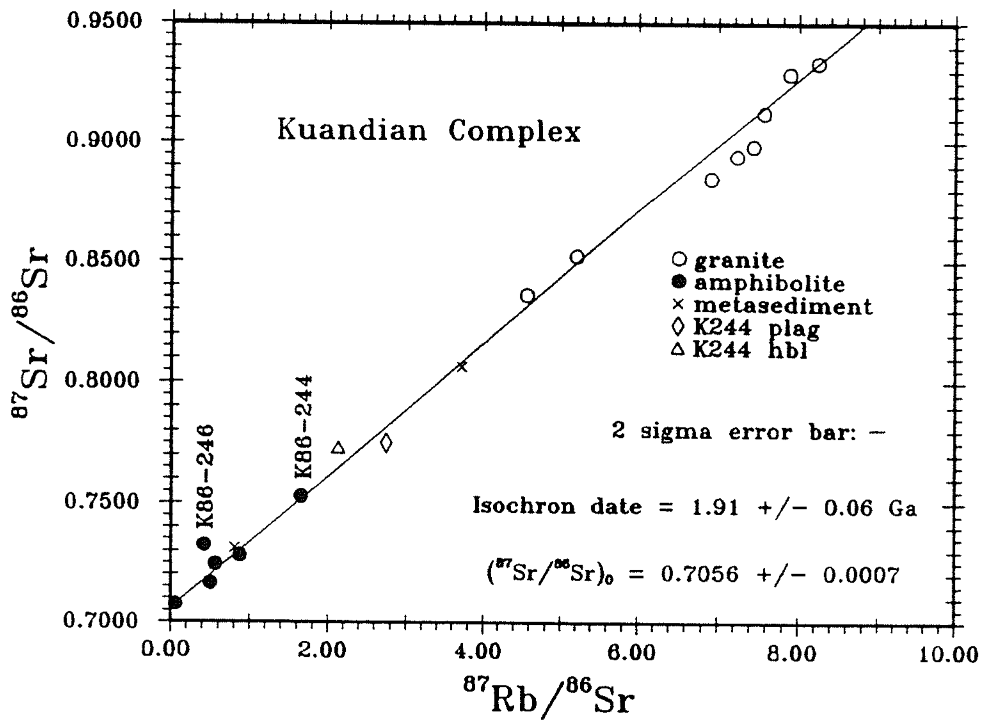

Figure 3-33. Rb - Sr isochron plot for the Kuandian Complex.

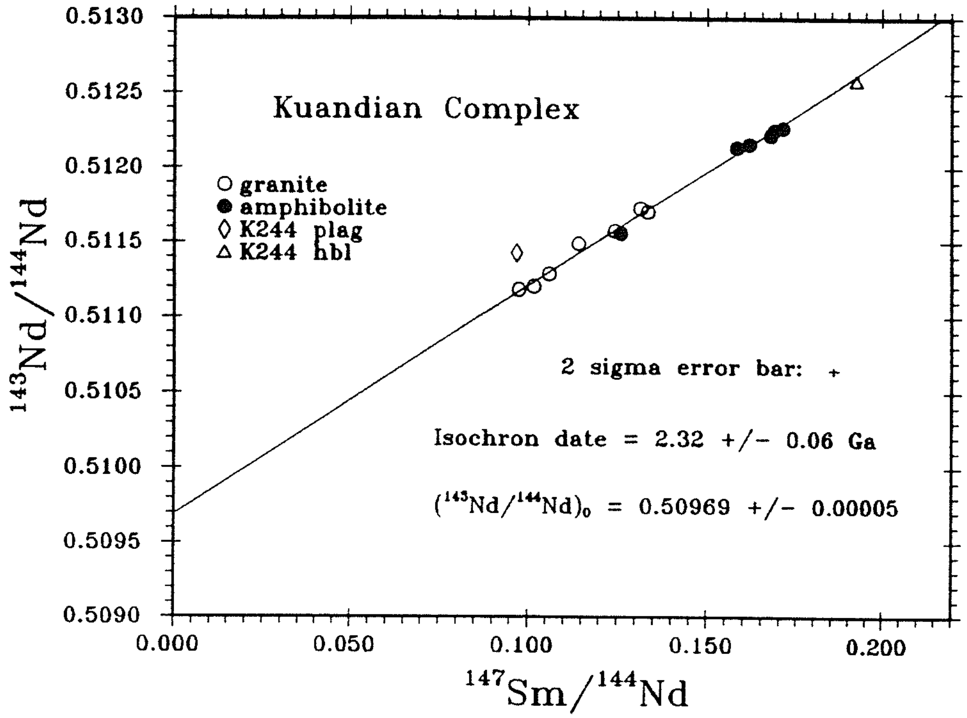

Figure 3-34. Sm-Nd isochron plot for the amphibolites and granites from the Kuandian Complex.

dates for amphibolites are 2.46 to 2.75 Ga, those for granites are 2.36 to 2.53 Ga.

Five amphibolites and five granites define a Pb-Pb isochron of 2.10 ± 0.04 Ga (Table 3-6 and Fig. 3-35). The 4.57 Ga geochron has been plotted as a reference. Two amphibolites plot close to the geochron, others plot far to the right of the geochron. The calculated single, first stage growth μ = 8.21, second stage μ's are equal to or greater than 8.21.

Zircons from the Kuandian granite are euhedral, prismatic, with dark or light pink colour or colourless. Length/width ratio is 1 to 3. No evidence is found from our analyses for inherited Pb, but our results show multiple Pb loss events. At least two, one Proterozoic and one modern Pb loss event, are needed to explain the data. Abrasion of coarse-grained zircons resulted in drastic decreases in U and Pb concentrations and improved concordance (Table 3-7). If the U-gain in zircons is a recent event, it would be difficult to explain the correlated high Pb content and high radiogenic Pb of unabraded samples. So we infer that zircons from the Kuandian granite have undergone an ancient U-gain event, which is probably related to Proterozoic metamorphism.

Four coarse grain-sized (>149 μ) zircon fractions from the Kuandian granite with different colour, abraded or non-abraded, give an upper intercept date of 2.142 ± 0.005 Ga and a lower intercept date of 0.438 ± 0.129 Ga. Two abraded coarse, one unabraded intermediate, and two unabraded fine gain-sized zircons give a highly suspect upper intercept date of 2.25 ±

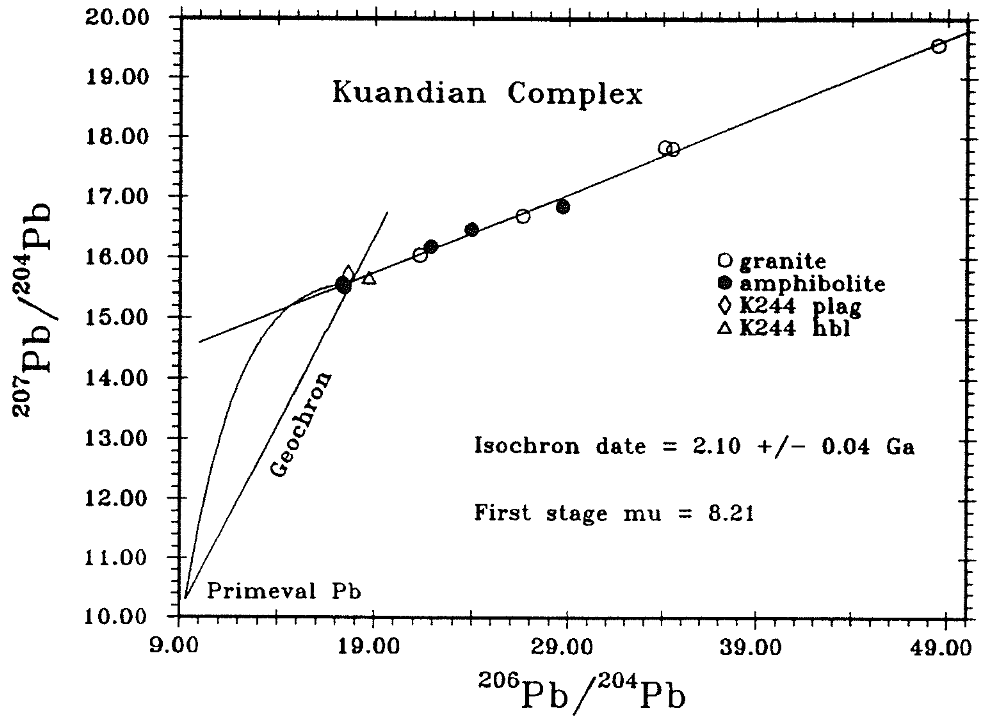

Figure 3-35. Whole rock Pb plot for the amphibolites and granites from the Kuandian Complex. The first stage μ same as for the Lishan Granite (Figure 3-5). Second stage μ's are equal to or greater than 8.21.

Table 3-7. U-Pb analyses of zircon fractions from Kuandian granite and a felsic dike (all Ma, and 2σ)

#	Split	wt(mg)	ppm U	ppm Pb	^{207}Pb	^{208}Pb	^{204}Pb	Measured $^{206}Pb/^{204}Pb$	$^{206}Pb/^{238}U$	Date	$^{207}Pb/^{235}U$	Date	$^{207}Pb/^{206}Pb$	Date
						$^{206}Pb=100$								
T88104 (Kuandian granite)														
1	NM 1.5A/3° >149μ, purple	0.8	975	366	13.236	10.4989	0.0040	23617	0.3527±0.0072	1947±34	6.412±0.130	2034±18	0.13183±0.00008	2122.5±1.2
2	NM 1.5A/3° >149μ, pink	0.3	1775	503	12.691	7.6411	0.0091	10471	0.2734±0.0094	1558±48	4.739±0.161	1774±28	0.12572±0.00016	2038.9±2.4
3	M 1.5A/3° 64-74μ, pink	0.3	609	226	12.798	8.1699	0.0073	12412	0.3558±0.0101	1962±48	6.231±0.18	2009±26	0.12702±0.00010	2057.2±1.6
4	M 1.5A/3° 64-74μ, purple	0.1	376	140	12.773	8.1165	0.0011	20972	0.3574±0.0018	1970±8	6.288±0.030	2017±4	0.12758±0.00008	2064.9±1.2
5	NM 1.5A/3° >149μ,single grain purple, abraded	~0.015	642	267	13.480	12.9350	0.0153	3483	0.3810±0.0032	2081±16	6.975±0.066	2108±8	0.13279±0.00040	2135.2±5.4
6	NM 1.5A/3° >149μ,3 grains purple, abraded	~0.04	674	264	13.215	9.4884	0.0004	18811	0.3717±0.0026	2037±12	6.770±0.042	2082±6	0.13210±0.00012	2126.0±1.6
7	NM 1A/5° 74-149μ, pink	0.2	374	143	12.969	8.5629	0.0049	14899	0.3664±0.0024	2012±12	6.519±0.042	2049±6	0.12905±0.00010	2085.0±1.4

continued

<u>T88102</u> (Felsic dike)														
1 NM 1.5A/3° 74-149μ, clear	0.35	1789	36.4	5.0060	20.325	0.0098	6472.0	0.0188±0.0002	120.2±1.0	0.1262±0.0012	120.7±1.0	0.04861±0.00012	129.2±6.2
2 M 1.5A/3° 64-74μ, clear	0.4	1661	34.9	5.0111	20.234	0.0090	8286.5	0.0195±0.0002	124.2±0.8	0.1309±0.0010	124.9±0.8	0.04878±0.00006	137.4±3.4

U and Pb concentrations are corrected for blank Pb.

Isotopic composition of 100 picogram blank is ^{206}Pb:^{207}Pb:^{208}Pb:^{204}Pb=17.75±0.19:15.50±0.17:37.30±0.29:1.00.

Common Pb assumed to be Stacey and Kramers (1975) model Pb of 2200±100 and 120±5 Ma ages for T88104 and T88102, respectively.

IUGS conventional decay constants (Steiger and Jäger, 1977) are: $^{238}U=1.55125\times10^{-10}a^{-1}$, $^{235}U=9.8485\times10^{-10}a^{-1}$, $^{238}U/^{235}U$=137.88 atom ratio.

0.05 Ga (Fig. 3-36). This array of analyses is probably the combined result of Proterozoic and modern Pb loss so that the apparent upper intercept has no geological significance. We consider the minimum crystallization age of the Kuandian granite is close to the 2.14 Ga upper intercept date from the coarse-grained zircons.

Caohe Group:

Eleven metasediment samples are scattered in a Rb-Sr isochron plot (Fig. 3-37). This is likely due to different provenance and variable resetting. Two metasediments produce Nd depleted mantle model dates of 2.23 and 2.53 Ga. In the Sm-Nd isochron plot (Fig. 3-38), they are close to the isochron of Kuandian igneous rocks, so the provenance of Caohe sediments could have a large component of Kuandian rocks or other rocks with similar age.

Liaoyang Group:

Four metapelitic samples give a Rb-Sr isochron of 1.55 ± 0.06 Ga with $(^{87}Sr/^{86}Sr)_0$ = 0.7168 ± 0.0025 (Fig. 3-39). Two samples produce Nd depleted mantle model dates of 2.54 and 2.73 Ga. In Sm-Nd isochron diagram (Fig. 3-38), they are close to the isochron of Kuandian igneous rocks, this could indicate that the Kuandian rocks remain as an important source for Liaoyang sediments.

Pre-Kuandian granite:

Shisi Granite:

Four whole rock samples are scattered in a Rb-Sr diagram (Fig. 3-40). Three of these give a 1.7 Ga depleted mantle model

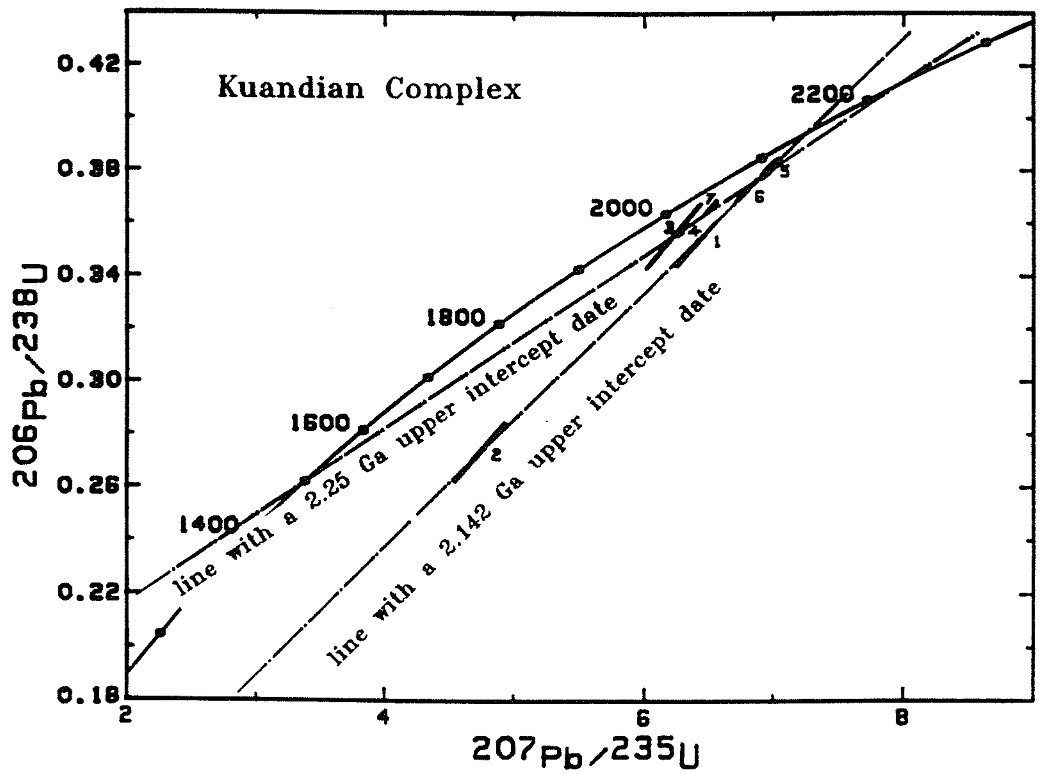

Figure 3-36. U-Pb concordia plot for zircons from the Kuandian granites. Zircon fractions: 1 and 2, unabraded >149μ; 3 and 4, unabraded 64 to 74μ; 5 and 6, abraded > 149μ (5 is a single grain, 6 is three grains); 7, unabraded 74 to 149μ. Four coarse grain-sized fractions give an upper intercept date of 2.142 ± 0.005 Ga and a lower intercept date of 0.438 ± 0.129 Ga. 2.142 Ga is considered as the minimum crystallization age of the Kuandian granite. Two abraded coarse, one unabraded intermediate, and two unabraded fine grain-sized zircons define a line with a highly suspected upper intercept date of 2.25 ± 0.05 Ga. This line probably resulted from Proterozoic and modern Pb loss.

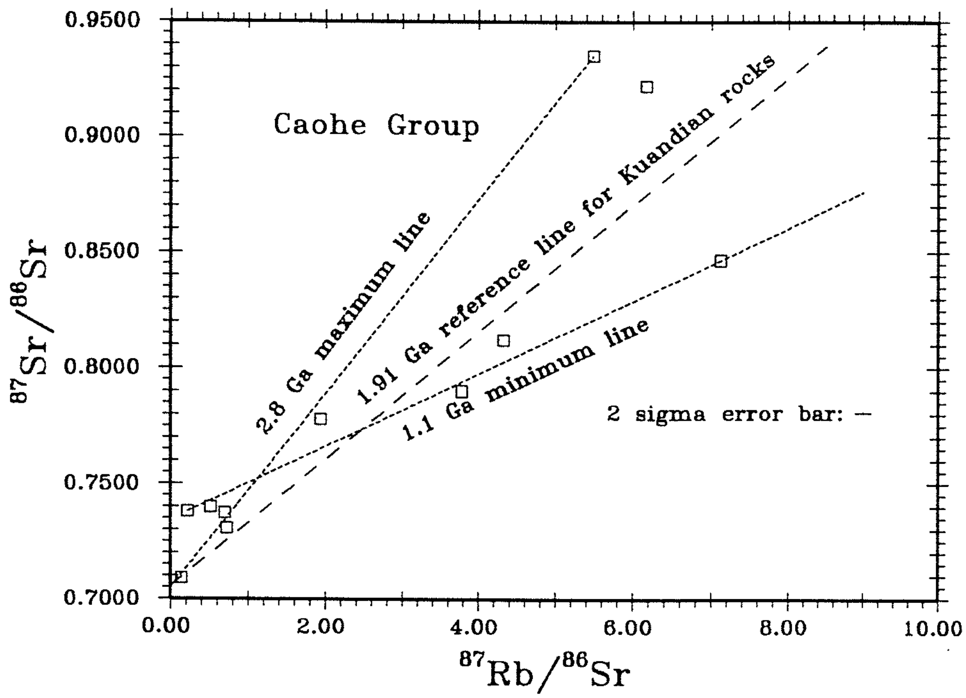

Figure 3-37. Rb - Sr isochron plot for metasedimentary rocks from Caohe Group. The data are virtually indecipherable in terms of Rb-Sr ages.

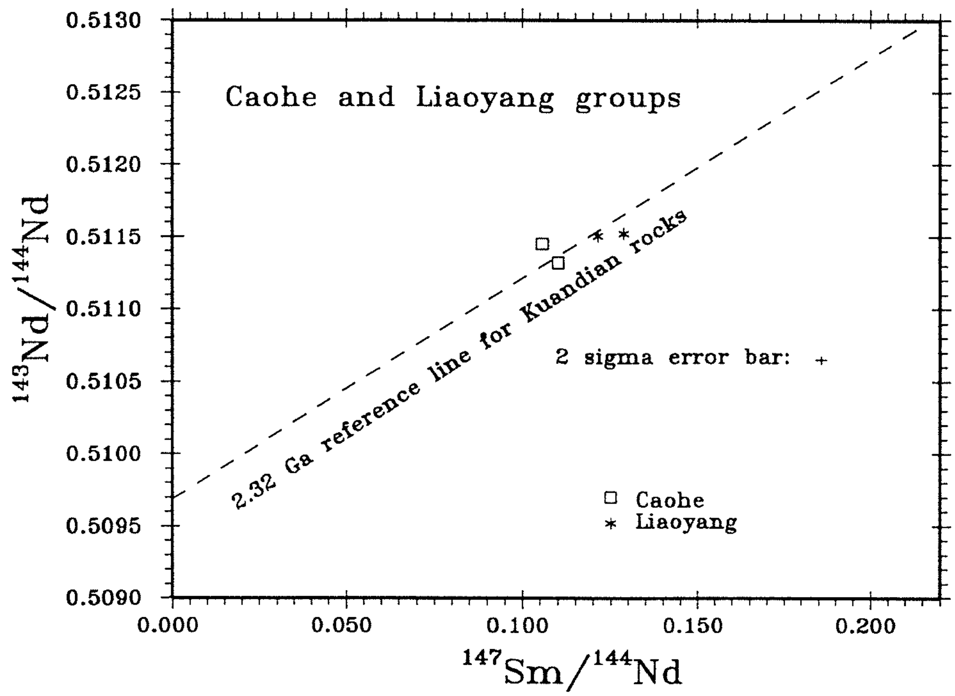

Figure 3-38. Sm - Nd isochron plot for metasedimentary samples from Caohe and Liaoyang groups.

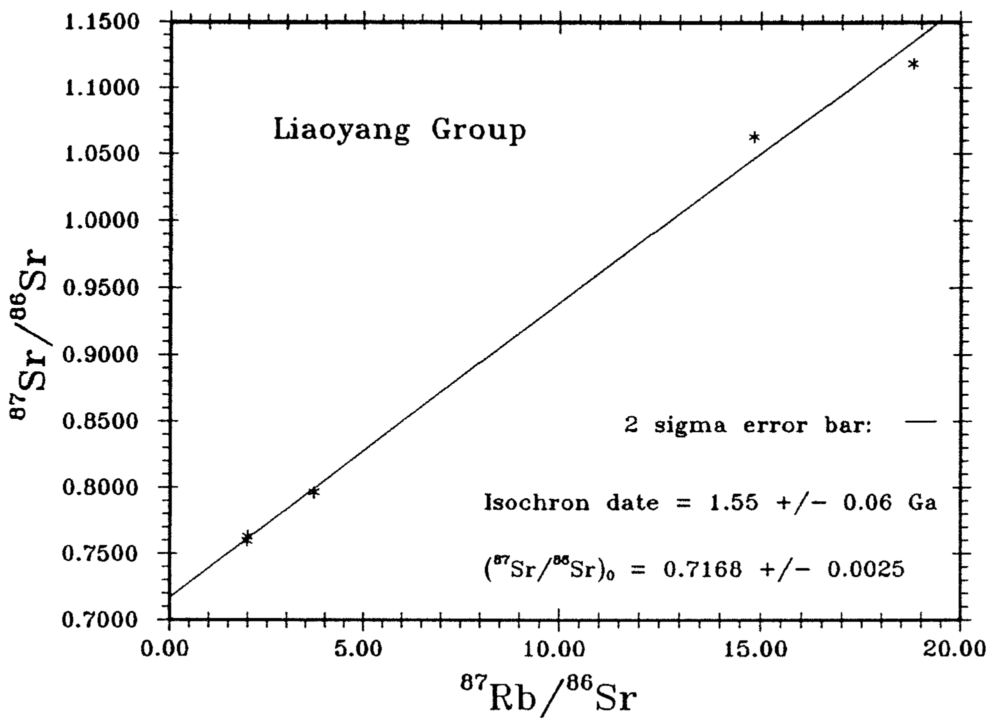

Figure 3-39. Rb - Sr isochron plot for metasedimentary samples from Liaoyang Group.

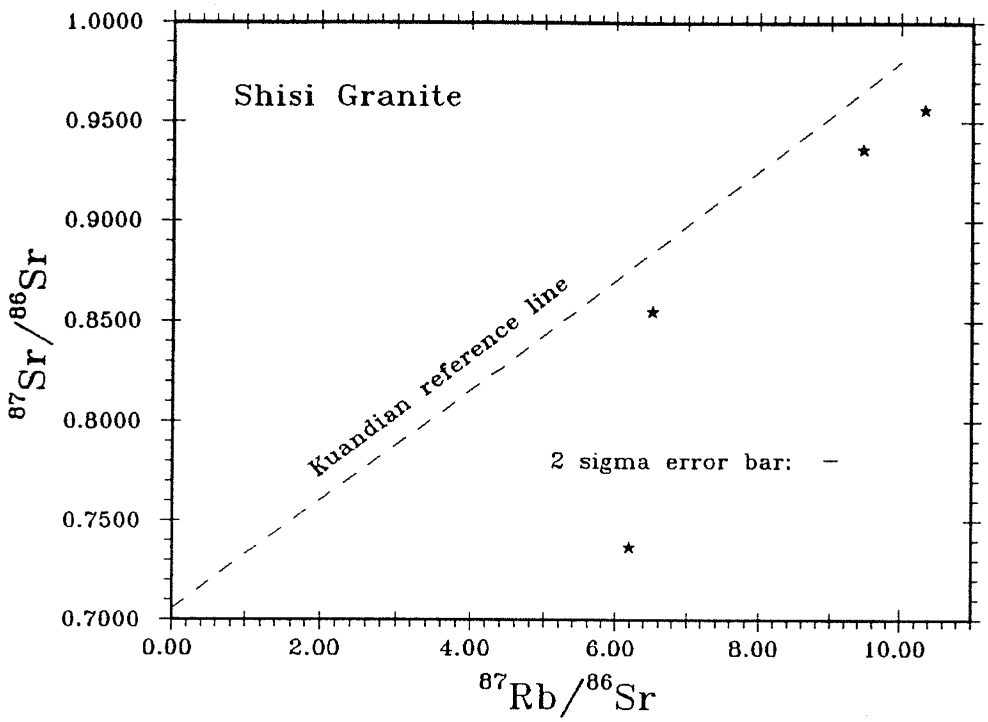

Figure 3-40. Rb - Sr isochron plot for samples from the Shisi Granite.

date, while one odd sample results in a 0.4 Ga model date. Samples from this granite are moderately weathered. K-feldspar and plagioclase are seriously saussuritized. Sr model dates are all younger than inferred from field relationships. We suspect that this granite has been strongly isotopically reset by a post-Proterozoic event or recent weathering. Two samples with the same $^{143}Nd/^{144}Nd$ ratio today give Nd depleted mantle model dates of 2.44 and 3.07 Ga (Fig. 3-4).

Post-Kuandian granite:

Mafeng Granite:

Five whole rock samples define a Rb-Sr isochron of 210 ± 25 Ma with $(^{87}Sr/^{86}Sr)_0$ = 0.7167 ± 0.0003 (Fig. 3-41). Two samples give 2.17 and 2.58 Ga Nd depleted mantle model dates, and define a two point isochron of 0.16 ± 0.10 Ga with $(^{143}Nd/^{144}Nd)_0$ = 0.51138 ± 0.00014 or $\epsilon_{Nd}(T)$ = -20.3 (Fig. 3-4). Four whole rock samples are clustered in a Pb-Pb isotopic plot (Fig. 3-42), close to but left of the geochron. Calculated single stage, first stage μ for one point on the geochron is 8.0, second stage μ's are equal or less.

Felsic dyke intruding the Kuandian Complex:

Two zircon fractions from a felsic dyke intruding the Kuandian Complex have been analyzed. These zircons are colourless, euhedral, prismatic crystals. Length/width ratio is 2 to 3. The intermediate grain-sized zircons plot very close to the concordia at 120 to 125 Ma (Fig. 3-43). The fine-grain zircons show a hint of Pb inheritance, probably from a Precambrian precursor.

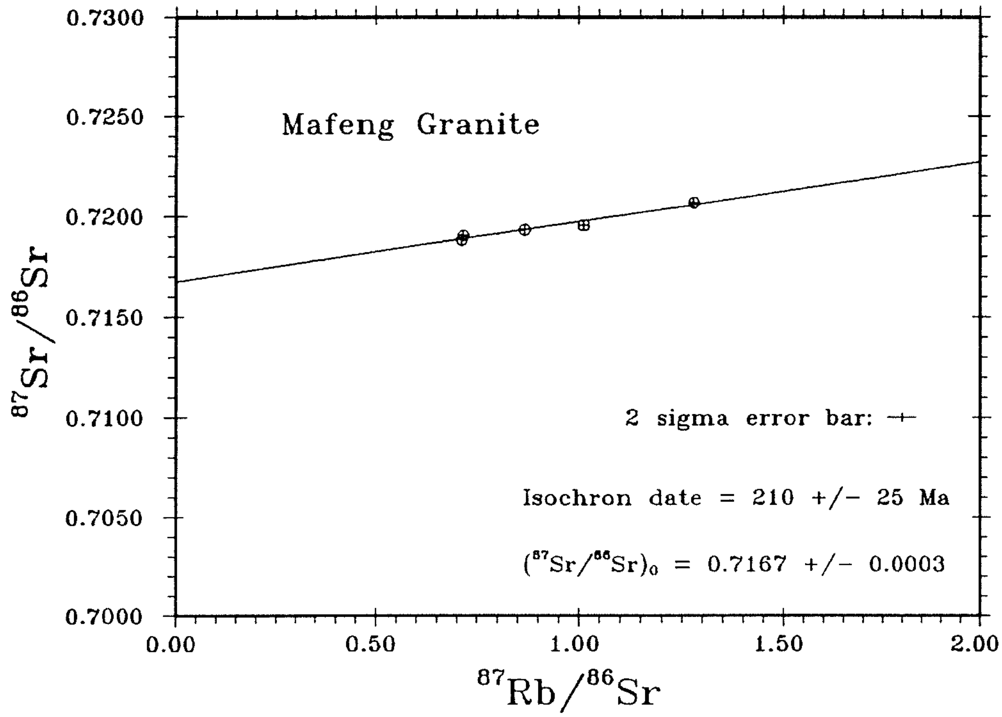

Figure 3-41. Rb - Sr isochron plot for samples from the Mafeng Granite.

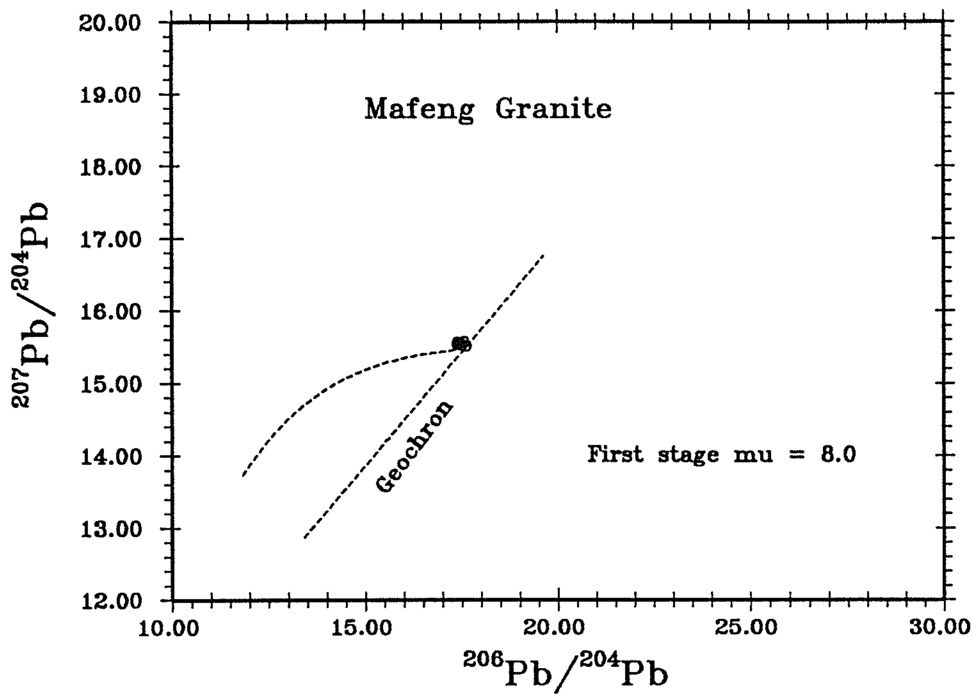

Figure 3-42. Whole rock Pb plot for the Mafeng Granite. a μ value of 8.0 is calculated for the point on the geochron.

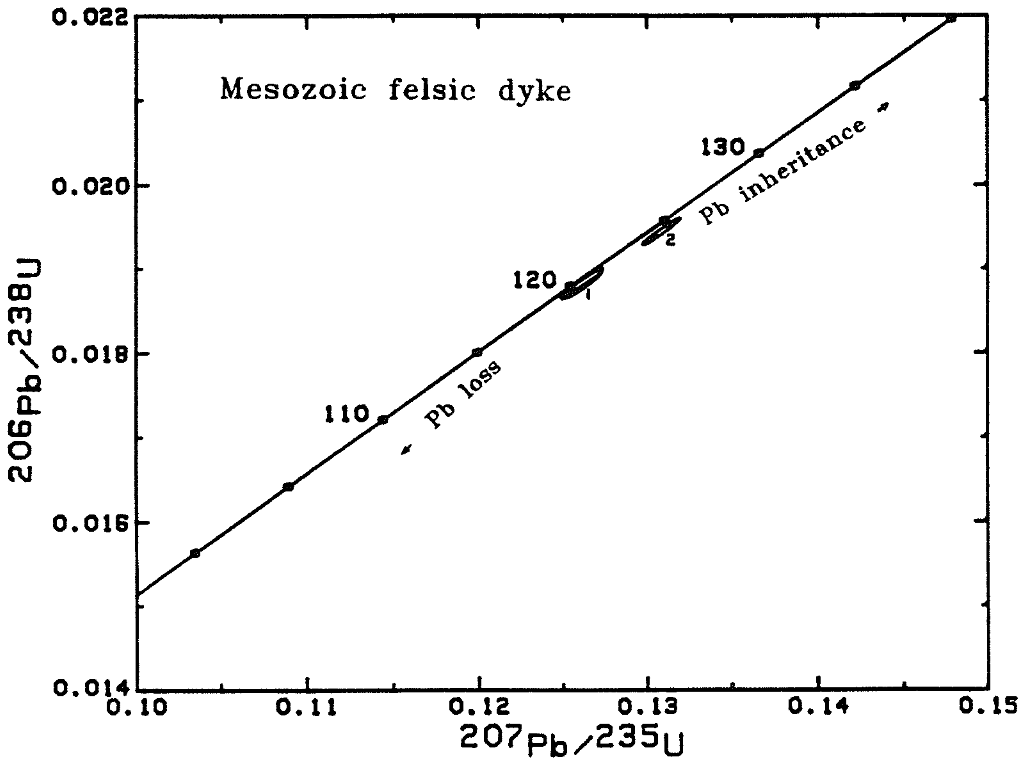

Figure 3-43. U-Pb concordia plot for zircons from a felsic dyke intruding the Kuandian Granite. Zircon fractions: 1, 74 to 149μ, 2, 64 to 74μ.

Age interpretation

Different dating techniques give somewhat inconsistent dates for the Kuandian Complex and associated rocks from the eastern Liaoning Province (Table 3-1). The reason for this could be initial heterogeneity in isotopic composition or isotopic resetting(s) after rock formation. The region was tectonically active over prolonged periods in the Precambrian and was reactivated in the Mesozoic (Yanshanian orogeny) and Cenozoic.

Many studies indicate that zircons can survive late disturbance without completely losing their inherited Pb even up to granulite facies (e.g. Koppel, 1974; Grauert and Wagner, 1975; Schenk, 1980; Vidal et al., 1980; Coolen et al., 1982). So the upper intercept ages of U-Pb zircons have been emphasized when we constrain the minimum formation age of a rock system.

DePaolo (1981) derived a mantle Nd evolution curve by compiling published $\epsilon_{Nd}(T)$ values of samples of known age. The depleted mantle model date is calculated by extrapolating a measured $\epsilon_{Nd}(0)$ value to the mantle evolution curve according to the measured $^{147}Sm/^{144}Nd$ ratio. Nd depleted mantle model dates can be used as an important tool when we constrain the maximum formation age of a rock system.

For an undisturbed Sm-Nd system all cogenetic samples from the depleted mantle source will have the same Nd depleted mantle model dates which are equal to the true mantle separation age and the Sm-Nd isochron date. There are several alternatives to this ideal situation. If the source was more depleted than the mantle curve (i.e. higher $\epsilon_{Nd}(T)$), the calculated model dates will be younger than the true mantle separation age (Fig. 3-44). On the other hand, if the source was less depleted, the calculated model dates will be older than the true mantle separation age.

If samples are contaminated by crustal material during magma ascent, the initial ϵ_{Nd} will decrease and thus give older model dates than the true igneous crystallization age.

If the Sm-Nd isotopic system was reset at a later time T', calculated model dates will all be older than T' and scattered around the true mantle separation age T, either older or younger than T depending on whether the sample Sm/Nd ratio is higher or lower than the average Sm/Nd ratio (Fig. 3-45).

Kuandian Complex:

The minimum crystallization age for the Kuandian Complex is 2.14 Ga, the coarse zircon U-Pb upper intercept date. Considering the movement towards concordia of coarse grain-sized zircons after abrasion, we expect that the intermediate and fine grain-sized grains would also become older and more concordant after abrasion, thus Proterozoic Pb loss event may be better defined.

The Kuandian granites give a Sm-Nd isochron date and a positive initial ϵ_{Nd} similar to those of amphibolites. This could indicate that the Kuandian granite and amphibolites have a common mantle source. The Nd depleted mantle model dates for amphibolites are between 2.46 and 2.75 Ga, those of gneisses are 2.36 to 2.53 Ga. Spread of Nd model dates could be due to the following causes:

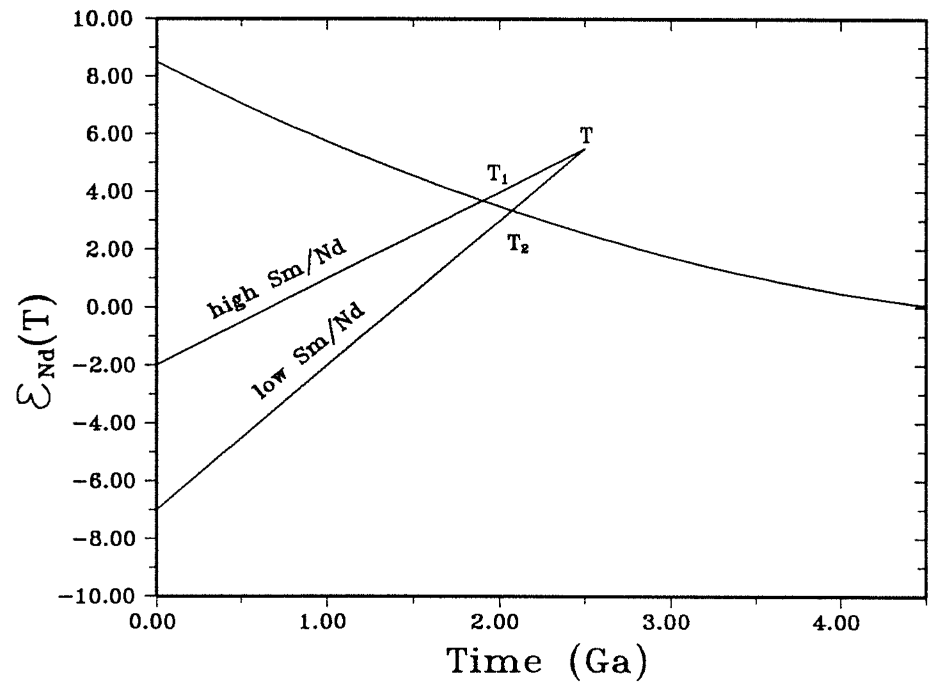

Figure 3-44. Diagram showing younger Nd depleted mantle ages will be calculated if the source region was more depleted than the average mantle evolution curve. T is true age. T_1 and T_2 are calculated Nd model ages. The higher the Sm/Nd ratio of a rock, the lower the calculated Nd model age and greater discrepancy with the true age.

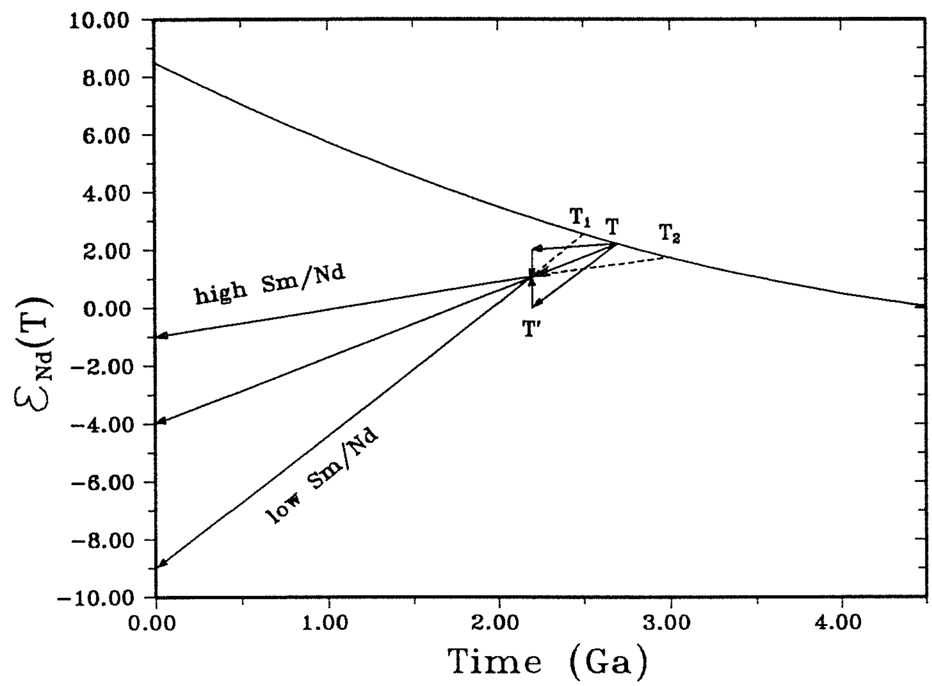

Figure 3-45. Diagram showing how Nd depleted mantle model ages (T_1 and T_2) will be scattered around true age (T), if the Sm-Nd system was homogenized by a later event.

(1). Rocks are initially heterogeneous in isotopic composition or contaminated by crustal material in different degrees. Because the granite is more crustal in chemical composition, erroneously old Nd model ages could arise for the granite. For example, 2.7-2.8 Ga gneiss from Anshan Complex, also in the eastern Liaoning Province, gives Nd model dates up to 3.61 Ga (Qiao et al., 1990, recalculated according to DePaolo, 1981). The Kuandian granites, however, have younger model dates than the amphibolites. This makes heterogeneous source or crustal contamination an unlikely explanation for the spread of Nd dates.

(2). Rocks are from a common source defined by the average mantle evolution curve, but isotopically reset or partially reset by a later metamorphic or alteration event. In this case, the model date calculated from true average Sm/Nd ratio and $\epsilon_{Nd}(0)$ will be identical to the true age. The average Sm/Nd of Kuandian Complex probably lies close to the maximum value of the granites and the minimum value of the amphibolites. So by this interpretation the Kuandian Complex formed around 2.5 Ga. The 2.32 Ga Sm-Nd isochron date is somewhat related to a metamorphic event. Considering the 2.14 Ga coarse zircon U-Pb upper intercept date, however, it is not very likely that the Kuandian Complex is as old as 2.5 Ga.

(3). Rocks are from a common source that is more depleted than that defined by the average mantle evolution curve. For example, 3.5 Ga old amphibolites from Qianxi Complex, Hebei Province, give initial ϵ_{Nd} about +2 higher than the mantle curve

(Huang et al., 1986; Jahn et al., 1987; Qiao et al., 1987). The calculated Nd depleted mantle model date for a rock from this highly depleted source will be younger than the true mantle separation age, which can be defined by Sm-Nd isochron if the system remains closed after rock formation. Moreover, the higher the Sm/Nd ratio of a rock, the younger the model date. However the Sm/Nd isochron date for the Kuandian Complex is younger than the calculated Nd model dates, and the Kuandian amphibolites (with high Sm/Nd ratios) yield old model dates while the Kuandian granite (with low Sm/Nd ratios) give young model dates. This makes the more-depleted source hypothesis unlikely, and rules out the possibility that the Kuandian Complex formed in Archean.

(4). Rocks are from a common source that is more enriched than the average mantle evolution curve. In this case, all the model dates will be older than the true mantle separation age, and the higher the Sm/Nd ratio of a rock, the older the model age. Hence, the true age may be close to the 2.32 Ga Sm-Nd isochron date. Lower initial ϵ_{Nd} than the mantle evolution curve is consistent with this explanation.

(5). Rocks were formed at different times. The Kuandian amphibolite and granite have identical Sm-Nd isochron dates (~2.4 Ga) and initial Nd isotopic compositions. If the Sm-Nd isochrons are related to their formation ages, it is unlikely that the granites are much younger than the amphibolites. The only possibility that the Kuandian amphibolites are much older than the granites is that the amphibolites formed between 2.46

and 2.75 Ga, the Nd depleted mantle model dates, and the Sm-Nd isotopic system was isotopically reset or partially reset during emplacement of the Kuandian granite at 2.4 Ga. In this case, the Kuandian amphibolites could have formed in Late Archean, but younger than 2.7 Ga, the age of underlying Anshan Complex.

From the above reasoning, we derive the following conclusions:

(a). The Kuandian amphibolites and granites are derived from a moderately but not highly depleted mantle source. The mantle depletion is presumably related to Archean crustal formation, but not necessarily creation of the Anshan Complex or in the same area.

(b). The Kuandian Complex, at least the Kuandian granite, formed 2.3 to 2.4 Ga ago, near to the Sm-Nd isochron date and the U-Pb zircon upper intercept date. The 1.9 Ga whole rock Rb-Sr isochron date is related to the isotopic resetting in later metamorphic events. Considering that two metasediments fall on the Rb-Sr isochron and that the two-mineral Sm-Nd isochron date is close to 1.9 Ga, we infer that the Kuandian Complex was metamorphosed about 1.9 Ga ago. This date is also consistent with the oldest K-Ar dates for hornblende (Jiang, 1987).

The 2.1 Ga whole rock Pb-Pb and 2.14 Ga upper intercept U-Pb coarse zircon date are probably the result of partial resetting. An alternative explanation is that they record a pre-1.9 Ga metamorphic event. This date is close to the Rb-Sr (reset) isochron date for the Lishan Granite. Some previous Rb-Sr and U-Pb work also gave 2.1 Ga dates (Jiang, 1987). The confirmation of the later explanation, however, awaits further study of the Kuandian Complex and study of granites intruding the Kuandian Complex.

The first stage growth μ equals 8.21 for the Kuandian whole rock samples. Data plot to the right of the geochron, indicating U/Pb enrichment of the rocks relative to their mantle source which was itself somewhat enriched. This U/Pb enrichment is in accord with the less depleted mantle Nd character of the same source. The only Precambrian rocks nearby with depleted radiogenic Pb are in the granulite-facies Archean Longgang Complex outcropping in Jilin Province (Table 3-6). Whether a basement rock like the Longgang Complex exists beneath the Eastern Liaoning Province, which can balance the Pb budget, is a question worth further investigation.

(c). The initial ϵ_{Nd} of the Kuandian Complex is 1.5 ϵ-units lower than the model mantle evolution curve, indicating a less depleted mantle source. This phenomenon is contrast with the Archean rock systems in Sino-Korean craton, for example, 3.5 Ga Qianxi amphibolites have average ϵ_{Nd} +2.0 higher than the mantle curve, 2.7 Ga amphibolites from Anshan Complex possess an ϵ_{Nd} +1.8 higher than the mantle curve (Jahn et al., 1990; Qiao et al., 1990), 2.7 Ga amphibolites from Taishan Complex, Shandong Province have a ϵ_{Nd} +1.1 higher than the mantle curve (Jahn et al., 1988). This reveals either an important chemical difference between the Archean and the Early Proterozoic mantle under the region, or reflects an increase in direct crustal recycling during Proterozoic magma genesis, or contamination of the

Proterozoic magmas by Archean basement rocks. Modern CFB also have a less-depleted source than MORB or oceanic arc.

Caohe Group:

Rb-Sr data from this study are all scattered. We could not infer the deposit age or metamorphic age for the Caohe Group. Two Nd depleted mantle model dates, 2.23 and 2.53 Ga, imply that the Caohe sediments are derived from Kuandian rocks or from a source with the Kuandian age.

Liaoyang Group:

We obtained a 1.55 ± 0.06 Ga Rb-Sr isochron with $(^{87}Sr/^{86}Sr)_0$ = 0.7168 ± 0.0025. Considering the previous reported 1.6 Ga K-Ar muscovite date of pegmatite intruding the Liaoyang Group, we interpret this as a metamorphic date for the Liaoyang Group. The sedimentation age will be older. The two Nd depleted mantle model dates, 2.54 and 2.73 Ga, could indicate a slightly larger proportion of Archean rocks in their provenance. But again the Kuandian or similar age rocks are likely dominant.

Shisi Granite:

Two Nd model dates have been obtained for the Shisi Granite, i.e. 2.44 and 3.07 Ga. We can only suspect this granite formed about 2.4 Ga ago, consistent with the field relationships and may have involved melting or assimilation of older rocks..

Mafeng Granite:

This granite gives a 210 ± 25 Ma Rb-Sr isochron with initial Sr ratio of 0.7167 ± 0.0003. The two-sample Sm-Nd isochron date, 0.16 Ga, is very similar. We infer that the Mafeng Granite formed in the Mesozoic, about 0.2 Ga ago. The

2.17 and 2.58 Ga Nd depleted mantle model dates imply a Proterozoic to Archean crust as the dominant source of the magma. The Pb isotopic analyses are nearly identical, but plot just to left of the geochron. The first stage μ is 8.0, the second stage μ's are equal or less. This is the only rock suite in the Liaoning Province showing a depleted U/Pb character. They could be derived from U/Pb depleted rocks, such as the granulitic-facies Longgang Complex exposed in the Jilin Province.

A felsic dyke intruding the Kuandian Complex gives a circa 0.12 Ga U-Pb zircon concordia date, showing that it is another result of Mesozoic magmatic activity.

Petrogenesis of Kuandian igneous rocks

(1). Kuandian amphibolite

The Nd isotopic composition indicates that precursor magma of the Kuandian amphibolite is from a mantle source. The low Mg# (49-63) and Fe enrichment are possibly a result of fractional crystallization of pyroxene and olivine, which can be inferred from the AFM plot. The REE data indicate that this fractionation could not be very extensive because the REE pattern is relative primitive.

The high Rb character of the Kuandian amphibolite cannot be explained by fractionation. Rb content in magma can only increase by a factor of 2, with 50% crystallization, although Rb partition coefficients for clinopyroxene, orthopyroxene and olivine are very small. The Rb concentrations of the Kuandian amphibolite are 10 to 60 times higher than an E-MORB mantle source (e.g. Proterozoic Keweenawan basalt). In order to account for the high Rb (and K_2O) contents in the Kuandian amphibolite, we need to invoke crustal contamination of the precursor magma or alkali metasomatism, which either happened in the source region or after emplacement. The crustal contamination hypothesis is not in conflict with the initial Nd isotopic ratio, but it could not explain the relative low Al_2O_3, and the REE pattern of the Kuandian amphibolite. The alternative hypothesis, alkali metasomatism in a multi-stage evolutionary process, can account for the trace element character of the Kuandian amphibolite.

We infer that the precursor magma of the Kuandian amphibolite was less evolved: the high K_2O and Rb character is most likely due to alkali metasomatism either in the mantle magma source or post emplacement. If this interpretation is correct, it leads to the conclusion that the initial Nd isotopic ratio of the Kuandian igneous rocks, more enriched than the Archean amphibolites, reflects an important chemical difference between the Archean and Early Proterozoic mantle in the region. This characteristic is shared by all CFB regardless of age.

(2). Kuandian granite

The Kuandian granite is genetically related to the Kuandian amphibolite, as evidenced by Nd isotopic data, REE pattern, and same geochemical character of bimodal-suite rocks.

Trace element partition model calculations indicate that direct partial melting of the Kuandian amphibolite (202-260 ppm Sr) cannot account for the Sr content in the Kuandian Granite (70-114 ppm Sr), due to an unrealistic bulk partition coefficient ($K_D > 2$). Furthermore, a negative Eu anomaly of the Kuandian granite rules out significant melting of plagioclase. Partial melting of a gabbroic or eclogite rock could not produce a magma with lower Sr content than itself, due to small K_D values of their component minerals. So magma of the Kuandian granite is unlikely to have been derived from partial melting of the Kuandian amphibolite or its chemical equivalent rocks.

Extreme fractional crystallization (>>80%) is needed for Rb and Ba to differentiate Kuandian granite from a parent magma with composition of the Kuandian amphibolite, and those mineral with very small K_D's for Rb and Ba have to be involved (e.g. olivine, pyroxene). However, Cr content of the Kuandian granite will not allow extensive fractionation of pyroxene and Ni content of the Kuandian granite excludes extensive fractionation of olivine. Moderate fractional crystallization of (50-60%) of olivine and/or pyroxene, and plagioclase can explain Cr, Ni, REE and most other elements of the Kuandian granite. We propose that the high Rb and Ba concentrations in the Kuandian granite are due to alkali metasomatism. Although the Kuandian amphibolite is also enriched in Rb compared with world-wide CFB, it is still too low in Rb to be parent of the Kuandian granite. We infer that the Rb enrichment for the Kuandian igneous rocks is most likely a post-emplacement event. This explanation can also account for negative correlation of Rb and SiO_2 in the Kuandian granite.

In order to interpret the anhydrous character of A-type granite, many researchers invoke partial melting of residual granulitic lower crust (e.g. White, 1979; Collins et al., 1982; White and Chappell, 1983; Whalen et al., 1987). They consider the residual lower crust has undergone a previous extraction of an orogenic (M-, I-, or S-type) granite. Nevertheless the overall source μ value of the Kuandian igneous rocks does not indicate a long term U-depleted source. So we do not see evidence for the residual crust anatexis model for the Kuandian granite.

It is worth mention that the only rock suite in the Liaoning Province with a U/Pb depleted source character, the Mafeng Granite, has an I-type granite chemistry. This contradiction invites future study.

Summary

The Kuandian Complex formed 2.3 to 2.4 Ga ago and experienced a major metamorphic overprint about 2.0 Ga ago and more recently.

The Kuandian amphibolite and granite formed in an environment like modern CFB, and are genetically related. They are chemically similar to modern CFB and anorogenic granite, and thus probably were created by a mantle plume (Duncan and Richards, 1991). Nd isotope and REE chemistry indicate that little (if any) crustal contamination was involved in creating the Kuandian igneous rocks. Low Sr content in the Kuandian granite rules out its derivation from partial melting of the Kuandian amphibolites or their chemical equivalents. Fractional crystallization of precursor magma of the Kuandian amphibolites can explain origin of the Kuandian granite. An alkali metasomatism is invoked to explain high Rb character of the Kuandian igneous rocks. Pb isotopic character of the Kuandian granite does not indicate a long term U/Pb-depleted source. This is not favourable to the residual crust anatexis model of A-type granite.

The Kuandian igneous rocks are from a depleted mantle source. However the source is less depleted than DePaolo (1981)'s average mantle Nd evolution curve, which is in contrast with the extremely depleted character of Archean mantle for the Sino-Korean Craton. This is an important chemical difference between the Early Proterozoic and Archean mantle in the region. The same mantle could not have produced both groups of rocks in succession.

Liaoyang Group is older than 1.55 Ga. The Kuandian or rocks of similar chemistry and age are a dominant component in the provenance of Caohe and Liaoyang sedimentary rocks.

Shisi Granite formed in the Early Proterozoic; Mafeng Granite formed in the Mesozoic by partial melting or extensive assimilation of the old lower crust.

IV. EARLY PRECAMBRIAN ROCKS IN WUTAISHAN AND TAIHANGSHAN AREA

Early Precambrian metamorphic rocks are well exposed in the Wutaishan and Taihangshan ("shan" means mountain) areas, Shanxi and Hebei Provinces of China (Fig. 1-1, 1-2, 4-1 and 4-2). A standard "stratigraphic succession" of Early Precambrian rocks has been established in this region by Chinese geologists (e.g. Ma et al., 1957). The lowermost high grade metamorphic complex of grey-gneiss and amphibolite is named "Fuping Group" and assigned to the Archean. The medium to low grade metavolcanic complex is named "Wutai Group" and assigned either to the Early Proterozoic (e.g. Yang et al., 1986) or the Late Archean (Bai, 1986). The low-grade metasediments are named "Hutuo Group" and assigned to the Early Proterozoic. All of these rock systems are overlain by unmetamorphosed, little deformed siliceous dolomites of the Sinian of North China. The unconformities between Fuping and Wutai, Wutai and Hutuo, Hutuo and Sinian are named as Fuping, Wutai and Luliang Movements, respectively. The Fuping Movement is considered to be related to the formation of Chinese continental nuclei. The Wutai Movement is attributed to the initial consolidation of the basement of Sino-Korean Platform. The Luliang Movement is believed to mark the completion of the assembly and stabilization of the Sino-Korean Platform.

IV-1. Geological background and previous isotopic work

Fuping Complex:

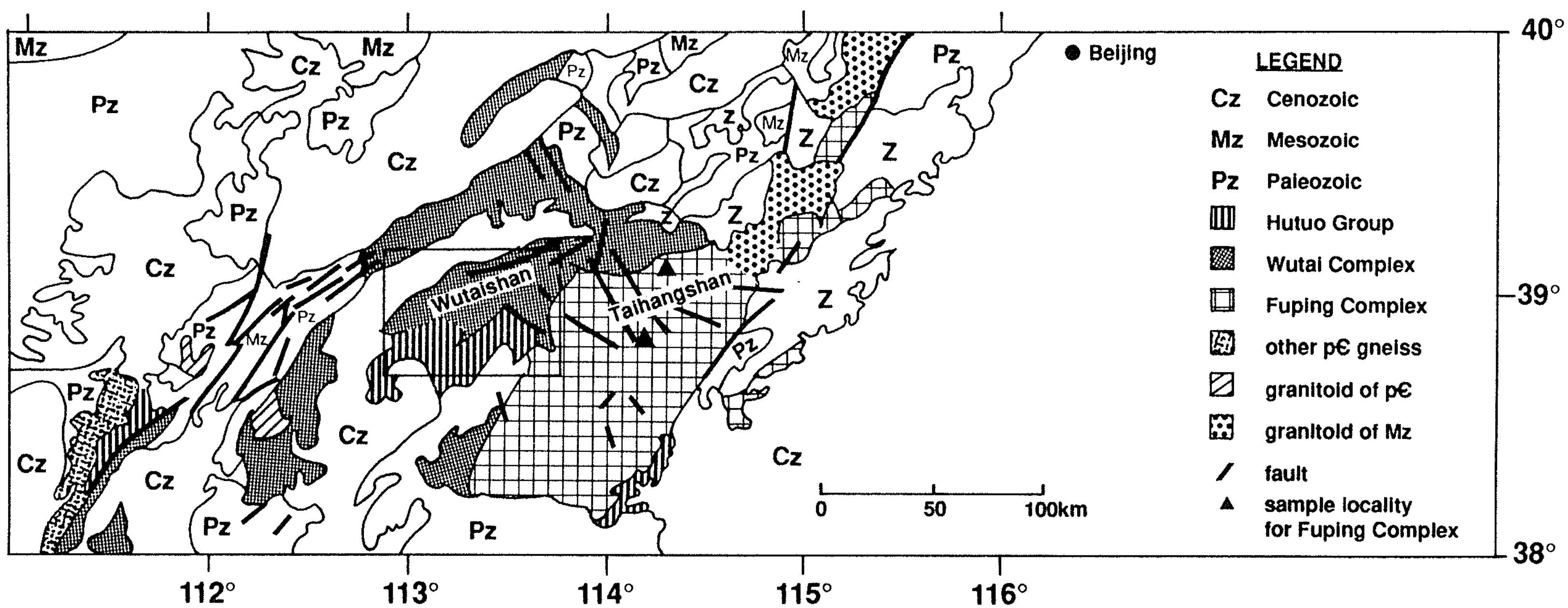

Figure 4-1. Simplified geological map of the region containing the Wutaishan and Taihangshan areas. The area shown in greater detail on Figure 4-2 is outlined by a rectangle. Sample localities for the Fuping Complex are labelled.

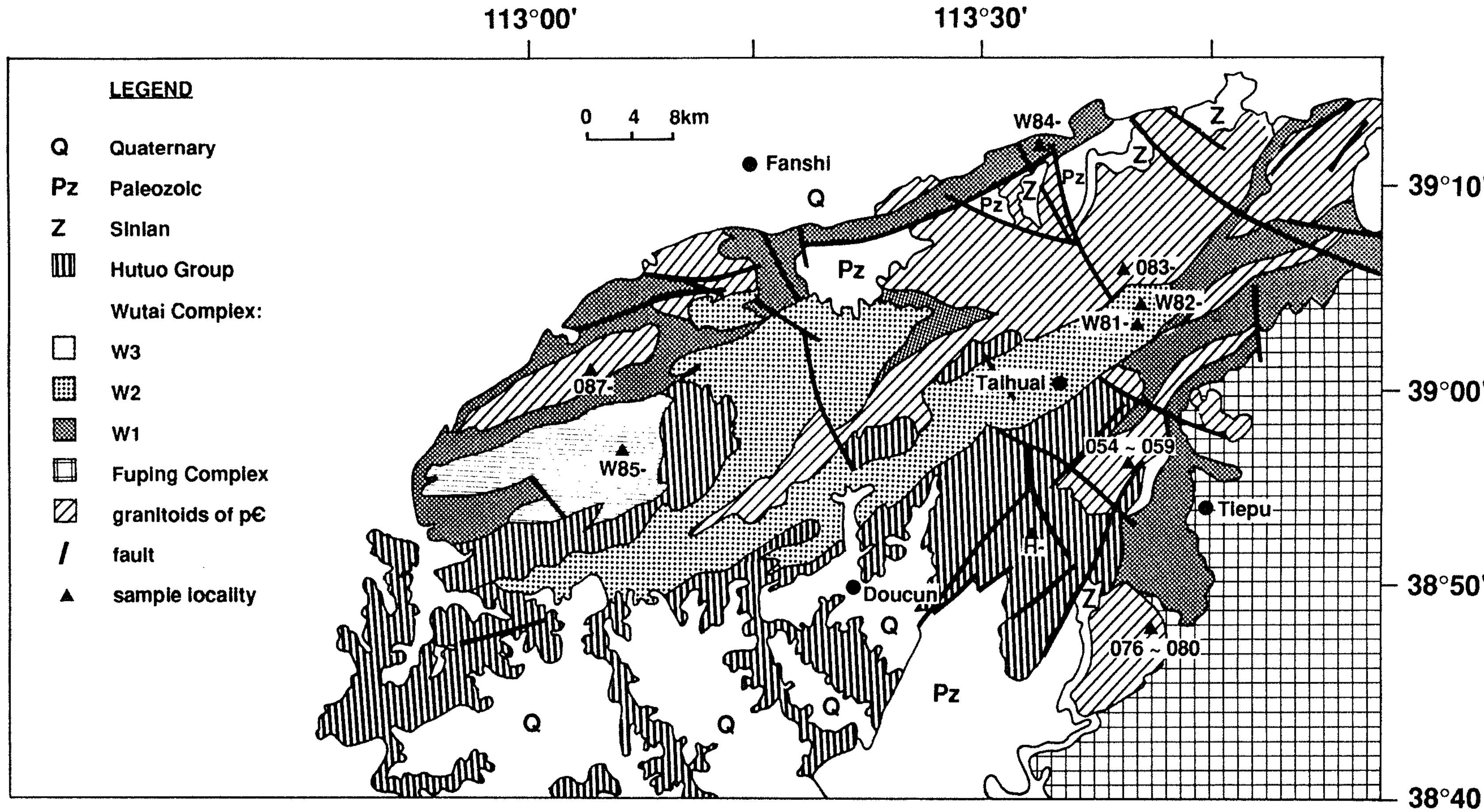

Figure 4-2. Geological map of Wutaishan area. The map shows the field occurrences of the Fuping Complex, Wutai complex, Hutuo Group, and Precambrian granites. Sample localities for the Wutai Complex, Hutuo Group and Precambrian granites are labelled.

Fuping Complex is exposed in Taihangshan region, along the boundary of Hebei and Shanxi Provinces (Fig. 4-1). It contains grey-gneiss, amphibolite, fine-grained gneiss, and some marbles.

The early application of K-Ar dating yielded minimum ages of 2300 Ma (compiled by Liu et al., 1985). Liu et al. (1985) reported zircon U-Pb isotopic analyses of six pink euhedral zircon fractions from a paragneiss sample which define (excluding one analysis) an upper intercept age of 2474 +/- 20 Ma. This was interpreted by the authors as a metamorphic age. Sub-rounded, brownish and colourless detrital zircon fractions from a similar paragneiss yielded an upper intercept age of 2800 $+/-\,^{230}_{150}$ Ma. Thus a 2800 Ma maximum age for the Fuping Complex was assigned by Liu et al. (1985). However, based on the same data, Bai (1986) assigned a minimum age of 2.7 to 2.9 Ga to the Fuping Complex by inferring the possibility of an igneous origin for the "detrital zircon" of Liu et al. (1985).

Wutai Complex:

The Wutai Complex is mainly composed of medium-grade metavolcanic rocks and has been considered as an Archean greenstone belt (Bai, 1986). It can be mapped as W-1, W-2 and W-3, according to the metamorphic grades (Fig. 4-2). The W-1 consists of amphibolite and fine-grained gneiss of medium P and T amphibolite facies. The W-2 consists of rocks of greenschist facies, such as sericite- and chlorite- quartz schists, magnetite quartzite and locally marble. From the previous field and petrochemical studies, two volcanic cycles are recognized in this subdivision (a lower W-2a and an upper W-2b). The W-3 mainly consists of quartzite and metaturbidite of subgreenschist facies.

K-Ar dates for the Wutai Complex are mainly between 1400 and 2000 Ma, with the highest value being 2300 Ma (Bai, 1986). Rb-Sr isochron dates of 1.8 Ga, 2.1-2.3 Ga and 2.5 Ga have been reported (Bai, 1986). Liu et al. (1985) reported a 2522 +/- $^{17}_{16}$ Ma upper intercept date for pink euhedral zircon fractions of a felsic metavolcanic rock (keratophyre) from W-2 and interpreted this as a volcanic crystallization age. They also reported 2508 +/- 2 Ma for purple zircon fractions from a quartofeldspathic fine grained gneiss from the Wutai Complex (W-1) and interpreted it as a metamorphic age.

Previous work indicated that one unconformity is located between the Fuping and "Longquanguan Group", and one between the "Longquanguan" and Wutai Complex. The "Longquanguan Group" consists of augen-gneisses of the same composition as the Fuping Complex. New field observation revealed that the "Longquanguan Group" is a shear zone[1]. In such a case, the two unconformities need to be reexamined, they may be merely structural contacts or zones of rapid changes in ductility. Further careful field work is needed to settle uncertainties about the tectonic settings of Fuping and Wutai Complexes and the tectonic history of the region.

---

[1]Field observation was made during sampling by Min Sun, Kaiyi Wang and Ruqi Liu.

Hutuo Group:

The Hutuo Group is composed of low-grade metasedimentary rocks, including metaconglomerate, quartzite, phyllite, slate, dolomitic marble, and a small amount of metavolcanic rocks. K-Ar dates for the Hutuo Group are between 1250 and 1850 Ma, with a maximum of 1928 Ma (Bai, 1986). One Rb-Sr whole rock date of 1851 Ma was reported by Bai (1986). Wu et al. (1986) reported an upper intercept age of 2366 $+/-\,^{103}_{94}$ Ma for zircon fractions from metabasalts of the lower part of Hutuo Group. They interpreted this age as the maximum formation age of the Hutuo Group. However, it is difficult to exclude the possibility that these zircons are of metamorphic origin.

Granitic intrusions:

In the Wutaishan and Taihangshan region Precambrian granitic intrusions are widely distributed. Liu et al. (1985) analyzed zircon fractions from the Lanzishan Granite, and obtained a 2560 +/- 6 Ma upper intercept age. Their field observation confirmed that the Lanzishan Granite intrudes the Fuping Complex and is unconformably overlain by the Wutai Complex. They inferred 2560 Ma as the minimum age of the Fuping Complex and the maximum age of the Wutai Complex. However, Bai (1986) argued that this intrusion is unconformably overlain by the Hutuo Group and implied that the Wutai Complex is older than 2560 Ma. But they did not make any direct observation of the relation between Wutai Complex and Lanzishan Granite.

Field observation indicates that the Wutai Complex is intruded by many granitic bodies, including the Shifo, Chechang, Wangjiahui and Ekou granites. Some of these granitic bodies have also been dated by U-Pb zircons: Shifo Granite yielded a 2507+/- $^{17}_{16}$ Ma upper intercept age (Bai, 1986), Ekou Granite yielded a 2520 +/- 30 Ma upper intercept age (Liu et al., 1985).

In summary, previous geochronological studies generally agree on an Archean age for both Fuping and Wutai Complexes and an early Proterozoic age for the Hutuo Group.

In this area, there are also some younger Precambrian granitic bodies and mafic dykes intruding the Hutuo Group. These granites can be chemically distinguished from 2.5 Ga granites by higher total alkali and higher K_2O/Na_2O ratio. One granitic body, Fengkuangshan Granite, yields a K-Ar biotite date of 1810 +/- 29 Ma (Bai, 1986). 1.9 Ga was assigned to the Luliang Movement corresponding to metamorphism and deformation of the Hutuo Group (Bai, 1986). Mesozoic granitic intrusions of Yanshanian and Cenozoic plateau basalts are the only younger magmatic units in this area.

IV-2. Petrochemistry of samples from the Wutaishan-Taihangshan region

The results of major and trace element analyses for 46 samples from the Wutaishan and Taihangshan area are presented in Tables 4-1 and 4-2. Immobile elements have been given special attention in this study.

(1). Metabasic samples

Table 4-1. Major element analyses for samples from the Wutaishan and Taihangshan region (recalculated to 100% volatile free)

Sample	SiO_2^*	TiO_2	Al_2O_3	Fe_2O_3(as ΣFe)	MnO	MgO	CaO	Na_2O	K_2O	P_2O_5	L.O.I.$^+$
Fuping Complex											
F1-3	60.0	0.75	14.5	7.7	0.13	4.96	6.42	3.63	1.64	0.25	0.32
F2-2	48.8	1.27	14.6	14.4	0.23	5.95	10.36	2.92	1.32	0.16	0.53
F4-2	48.5	1.00	15.0	13.2	0.24	6.67	11.18	2.84	1.23	0.10	0.65
F4-3	48.8	0.99	14.6	13.9	0.23	6.37	10.72	3.08	1.20	0.10	0.52
F6-1	74.0	0.09	13.5	1.6	0.06	0.17	1.99	3.47	5.13	0.06	0.21
F6-3	73.0	0.12	13.8	1.9	0.05	0.36	2.00	3.40	5.31	0.06	0.25
F6-4	73.6	0.13	13.5	1.7	0.04	0.26	1.83	3.36	5.50	0.05	0.25
F6-5	72.0	0.28	13.9	2.8	0.05	0.73	2.42	3.76	3.92	0.11	0.29
Wutai Complex (W-1)											
W84-1	50.1	1.28	15.3	13.3	0.20	6.35	9.66	3.38	0.25	0.10	0.33
W84-4	53.2	1.08	19.1	8.9	0.18	3.35	11.60	1.97	0.47	0.20	1.65
W84-51(felsic)	44.0	0.53	21.2	9.5	0.28	3.35	18.73	1.73	0.60	0.07	1.86
W84-52(mafic)	49.8	0.60	20.4	9.1	0.21	4.76	11.88	3.06	0.22	0.04	0.36
W84-7	49.7	1.03	15.1	13.7	0.22	6.29	11.14	2.11	0.58	0.12	2.47
W84-8	53.3	0.60	20.7	7.6	0.11	3.26	9.74	3.52	1.02	0.23	0.78
W84-9	65.4	0.63	15.4	6.0	0.09	1.86	4.73	3.76	1.87	0.22	1.25
Wutai Complex (W-2a)											
W82-4	50.2	1.06	17.0	13.0	0.19	6.16	9.64	2.53	0.13	0.09	6.01
W82-5	52.0	0.93	14.7	13.0	0.23	6.54	10.89	1.49	0.10	0.07	2.87
W82-7	50.4	0.97	15.8	13.4	0.20	6.83	9.75	2.44	0.18	0.08	3.13
W82-9	48.8	0.97	15.2	12.0	0.23	5.17	14.84	2.53	0.14	0.08	8.91
Wutai Complex (W-2b)											
W81-1	63.6	0.54	16.5	7.9	0.04	8.64	0.37	0.0	2.33	0.08	5.15
W81-2	64.9	0.55	15.7	7.3	0.06	6.27	1.21	3.05	0.80	0.14	4.30
W81-6	59.3	0.73	18.2	7.4	0.10	3.64	5.05	4.47	0.89	0.19	3.24
W81-7	55.3	1.17	16.7	10.0	0.16	3.24	9.37	3.22	0.67	0.17	5.94
W81-8	55.3	0.79	17.4	8.7	0.13	6.75	6.11	4.48	0.15	0.13	5.13
W81-11	52.3	0.90	18.4	11.0	0.13	5.26	8.91	2.09	0.87	0.16	2.32
Wutai Complex (W-3)											
W85-2	46.5	1.10	18.0	12.8	0.18	7.11	11.44	2.34	0.40	0.09	0.93
W85-4	48.0	1.11	17.6	11.5	0.19	6.53	12.85	1.75	0.41	0.10	0.67
W85-6	48.6	1.03	17.4	12.0	0.17	7.14	10.74	2.54	0.30	0.09	0.88
W85-8	48.1	1.10	17.4	11.6	0.18	7.29	11.23	2.68	0.32	0.10	0.56
Hutuo Group											
H-003	47.1	1.81	19.4	14.1	0.06	9.93	2.57	4.03	0.73	0.32	6.03
H-004	49.3	2.00	17.9	13.4	0.13	8.06	4.95	3.33	0.52	0.35	6.20
H-007	50.0	1.76	18.4	13.9	0.09	10.22	2.31	2.60	0.48	0.31	5.55
H-014	50.4	1.61	17.0	15.7	0.17	9.10	1.80	3.48	0.32	0.40	4.64
H-017	51.5	1.61	17.6	12.6	0.18	7.56	3.07	5.17	0.32	0.40	3.91
Lanzishan Granite											
076	73.6	0.21	13.5	2.1	0.04	0.31	1.39	3.80	4.99	0.07	0.38
077	73.7	0.23	13.4	2.3	0.04	0.36	1.42	3.80	4.69	0.08	0.38
078	73.7	0.19	13.5	2.1	0.04	0.26	1.39	3.93	4.80	0.06	0.31
080	73.4	0.23	13.4	2.3	0.03	0.32	1.45	3.83	4.89	0.07	0.37
Shifo Granite											
054	69.6	0.39	14.0	4.4	0.08	2.09	1.78	3.72	3.84	0.11	0.65
057	70.3	0.34	13.8	3.5	0.07	1.47	2.51	3.62	4.32	0.10	0.82

continued

Chechang Granite											
083-1	73.9	0.23	13.5	3.0	0.05	0.63	2.25	4.73	1.62	0.07	1.27
083-2	72.1	0.26	14.5	3.0	0.06	0.63	3.15	4.52	1.73	0.08	0.73
083-4	72.8	0.26	14.2	2.7	0.03	0.85	2.53	5.24	1.35	0.08	1.00
Wangjiahui Granite											
087-2	72.7	0.45	12.8	3.3	0.03	0.45	1.53	3.74	4.84	0.14	0.41
087-3	72.0	0.45	12.8	3.6	0.03	0.45	1.64	3.70	5.18	0.13	0.35
087-4	73.3	0.43	12.5	3.0	0.03	0.47	1.49	3.58	5.09	0.12	0.40

* All major element analyses are by a Philips PW-1400 XRF spectrometer, on ground fused glass pellets (Michael and Russell, 1989), reported in wt%.
Estimated accuracy (1 σ) from duplicated runs: SiO_2, 1%; K_2O, TiO_2, 2%; Fe_2O_3, 7%; Al_2O_3, MgO, CaO, Na_2O, 5%; MnO, P_2O_5, ±0.01.
\+ L.O.I. = weight loss between 120 and 900°C.

Table 4-2. Trace element concentrations (in ppm) for samples from the Wutaishan and Taihangshan region

	Ba*	Cr	Nb	Ni	Rb	Sr	V	Y	Zr
ERROR (1σ)+	7	8	1	5	1	6	37	1	3
Fuping Complex									
F1-3	345	320	6	147	63	496	97	14	121
F2-2	165	93	6	40	19	134	247	26	110
F4-2	63	153	4	57	20	173	179	20	69
F4-3	70	141	5	57	18	164	183	19	65
F6-1	1181	10	4	0	157	373	26	4	164
F6-3	1044	18	3	1	163	360	25	3	154
F6-4	1101	16	4	1	159	279	24	3	145
F6-5	875	31	5	10	133	369	41	7	185
Wutai Complex (W-1)									
W84-1	114	170	5	74	7	136	235	26	72
W84-4	55	268	8	229	19	189	129	23	92
W84-51(felsic)	134	384	5	228	41	262	149	13	31
W84-52(mafic)	52	472	5	299	6	175	171	15	27
W84-7	228	176	5	76	10	164	182	24	82
W84-8	578	211	5	71	26	1016	114	13	111
W84-9	708	154	7	58	52	501	94	17	142
Wutai Complex (W-2a)									
W82-4	8	227	4	108	5	101	219	25	59
W82-5	13	30	3	70	0	100	177	21	53
W82-7	14	198	4	96	2	76	188	22	52
W82-9	20	208	5	93	3	113	172	19	57
Wutai Complex (W-2b)									
W81-1	435	561	3	139	59	21	134	6	68
W81-2	175	70	4	82	25	72	71	7	104
W81-6	237	73	5	76	21	364	100	16	111
W81-7	67	26	6	20	23	368	159	23	117
W81-8	8	293	5	199	3	351	118	16	91
W81-11	250	122	5	168	34	471	148	22	103
Wutai Complex (W-3)									
W85-2	118	172	5	176	10	299	164	20	82
W85-4	111	173	4	185	8	332	162	18	83
W85-6	78	171	5	174	5	284	168	16	74
W85-8	96	160	5	167	4	311	166	17	84
Hutuo Group									
H-003	360	90	9	134	9	64	214	23	148
H-004	297	93	11	126	6	172	210	21	157
H-007	228	91	10	119	5	44	222	21	144
H-014	30	58	7	100	3	24	234	26	141
H-017	46	56	8	103	5	40	231	26	135
Lanzishan Granite									
076	555	19	9	31	271	157	19	8	137
077	532	17	10	25	197	177	20	10	152
078	399	19	12	24	314	121	12	9	120
080	516	20	8	19	244	158	17	10	134
Shifo Granite									
054	601	132	9	43	180	176	50	9	147
057	796	130	8	51	170	352	43	12	121

continued

Chechang Granite									
083-1	383	20	6	29	49	238	15	6	106
083-2	452	17	4	25	43	287	25	7	114
083-4	244	34	4	34	37	338	18	3	94
Wangjiahui Granite									
087-2	825	8	21	17	259	223	43	32	270
087-3	846	13	21	27	255	236	34	27	257
087-4	724	13	18	16	247	189	35	23	219

* All trace element analyses are by a Philips PW-1400 XRF spectrometer, on pressed powder pellets (Armstrong and Nixon, 1980).

+ Estimated from scatter of standards about working curve.

Essential Classification:

One amphibolite from the Fuping Complex, one amphibolite from the Wutai Complex (W-1) and three greenschists from the bottom cycle of W-2 have andesitic compositions. All the other metabasic samples from the region are basaltic. Major element data indicate that these samples mostly have the chemical signature of subalkaline rocks (Fig. 4-3 and 4-4). The exceptions are that one greenschist from the Hutuo Group is in the alkaline field on an alkali-SiO_2 plot, and that two amphibolites from the Fuping Complex, one felsic sample from W-1 and one greenschist from W-2a plot in the alkaline field in Ol'-Ne'-Q' plot. Amphibolites of the Fuping Complex and the metabasalts of the Hutuo Group have higher alkali than the Wutai Complex. The greenschists from W-2b have the highest total alkali content in the Wutai Complex (Fig. 4-5) and thus the name metaspilite was given by some previous workers (e.g. Li et al., 1988). K_2O/Na_2O ratio of metabasic rocks generally decreases from the Fuping Complex to the Hutuo Group with a minimum at W-2a (Fig. 4-5). Trace elements show a subalkaline character for all the metabasic samples from the region, e.g. Y/Nb > 1.

The few samples that are in alkaline fields can be tentatively explained as due to the mobility of alkali elements in metamorphic processes. We consider that the metabasic samples from the region are essentially subalkaline.

The Fuping amphibolites plot in the tholeiitic field in Al_2O_3 -normative plagioclase plot (Fig. 4-6a), but are in both tholeiitic and calc-alkaline fields in AFM diagram (Fig. 4-7).

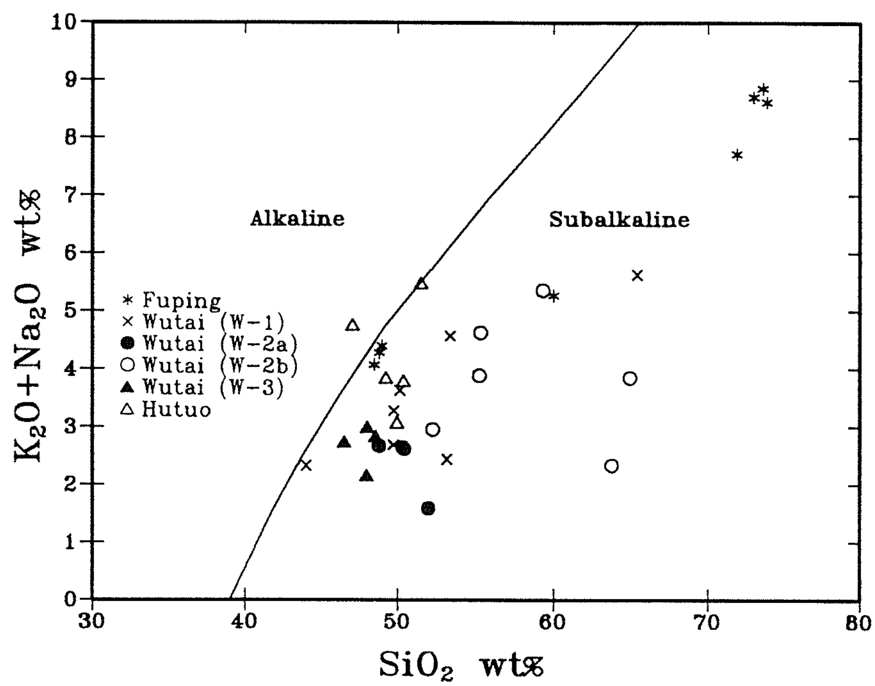

Figure 4-3. Total alkali - SiO_2 plot showing that metavolcanic samples fall in the subalkaline field with one exception from the Hutuo Group. The dividing line is from Irvine and Baragar (1971).

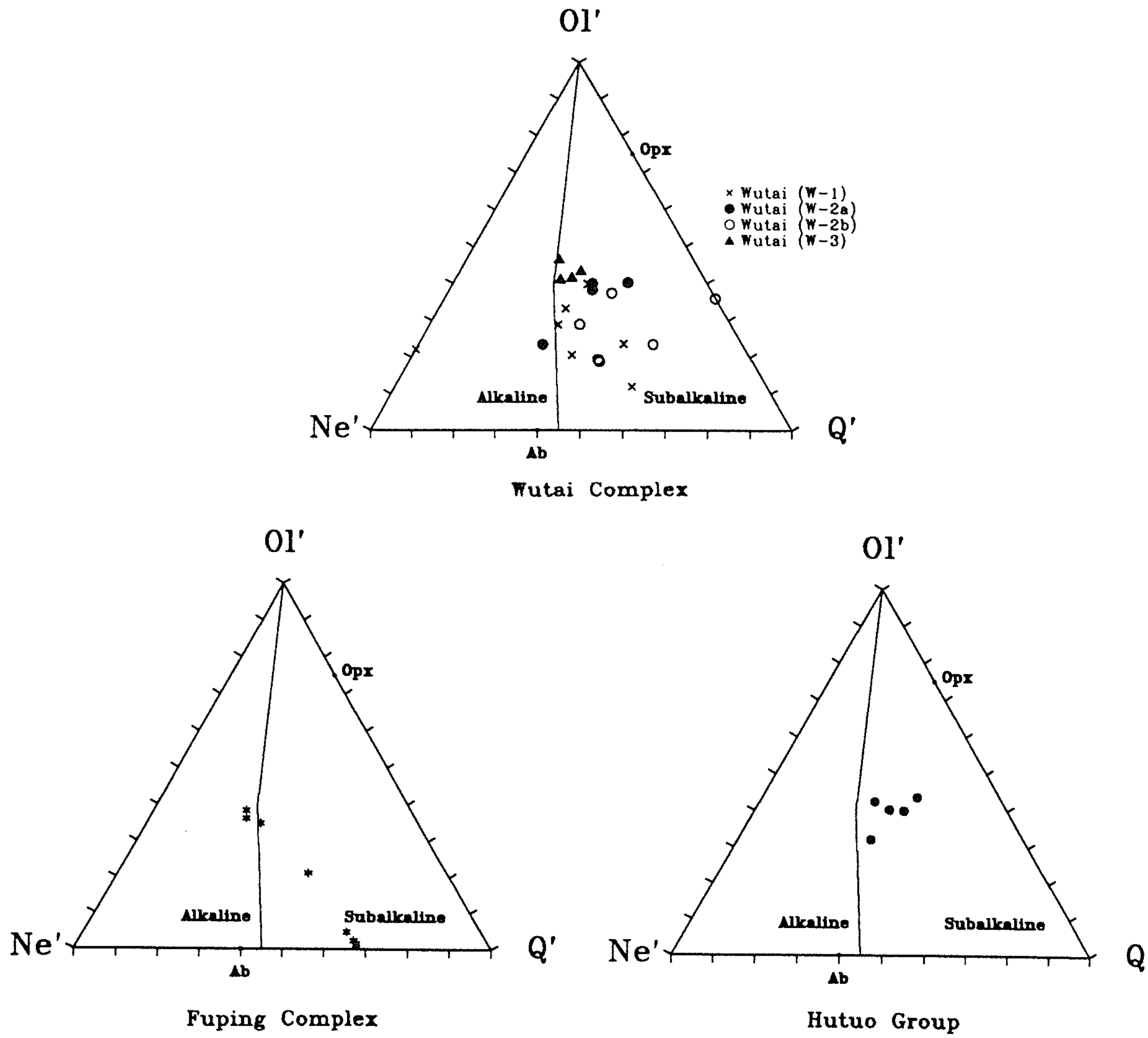

Figure 4-4. Ol'-Ne'-Q' plot showing that most metavolcanic samples fall in the subalkaline field. The dividing line is from Irvine and Baragar (1971). Ol'=Ol+3/4Opx, Ne'=Ne+3/5Ab, Q'=Q+2/5Ab+1/4Opx, cation norms.

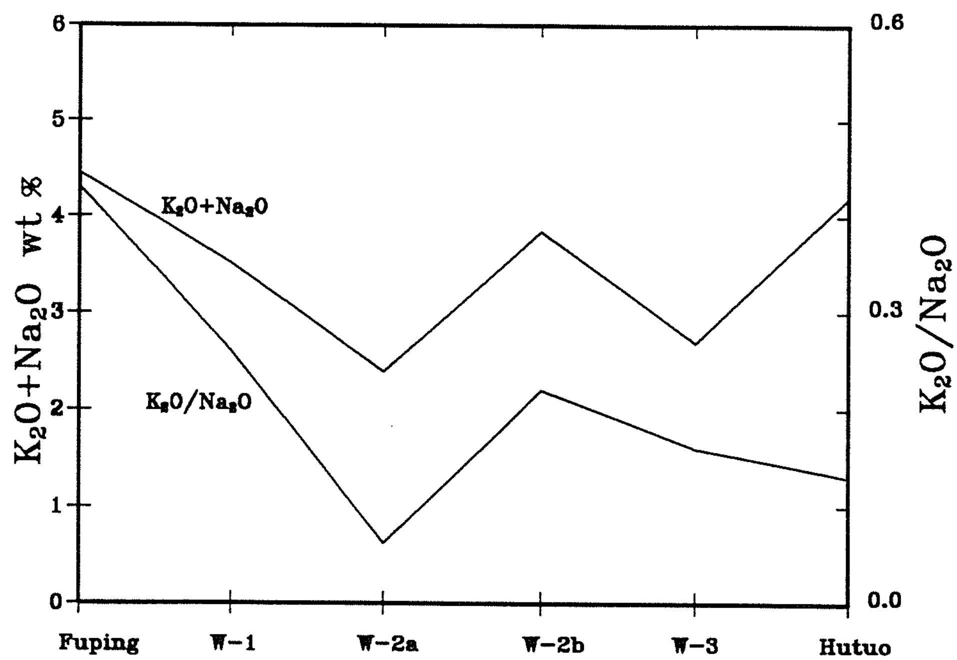

Figure 4-5. Average total alkali and K_2O/Na_2O values of metavolcanic rocks from Fuping Complex, Wutai Complex, and Hutuo Group, all in wt%.

(a)

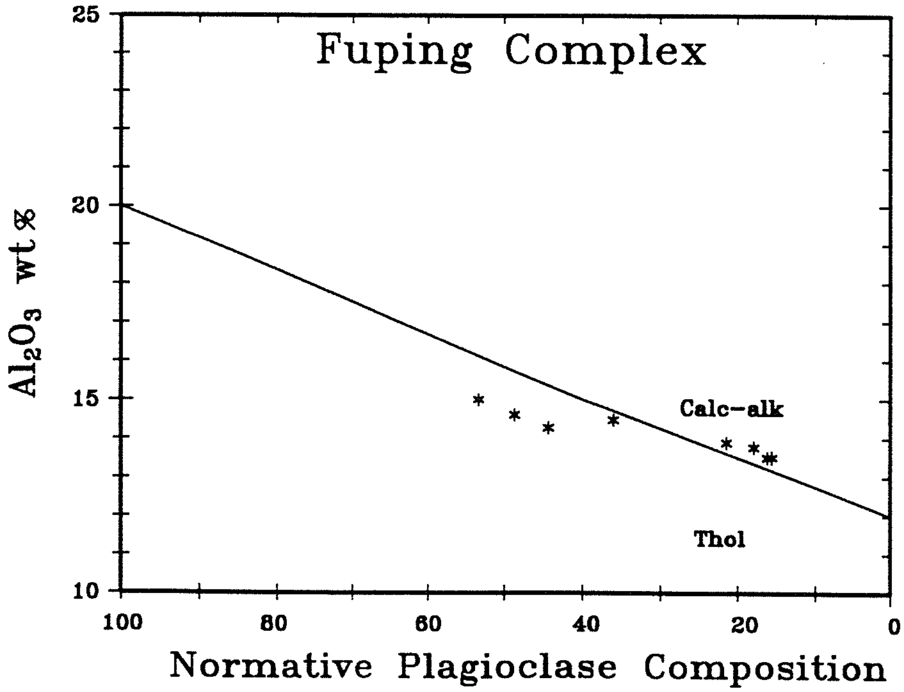

Fuping Complex
Al_2O_3 wt%
25
20
15
10
100
80
60
40
20
0
Calc-alk
Thol
Normative Plagioclase Composition

(b)

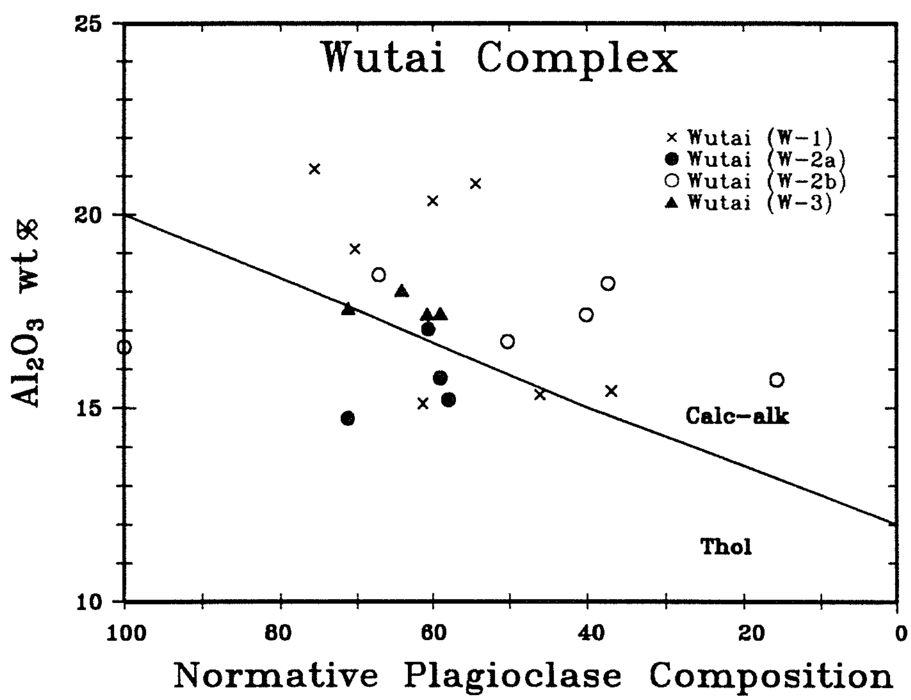

Wutai Complex
× Wutai (W-1)
● Wutai (W-2a)
○ Wutai (W-2b)
▲ Wutai (W-3)
Al_2O_3 wt%
25
20
15
10
100
80
60
40
20
0
Calc-alk
Thol
Normative Plagioclase Composition

(c)

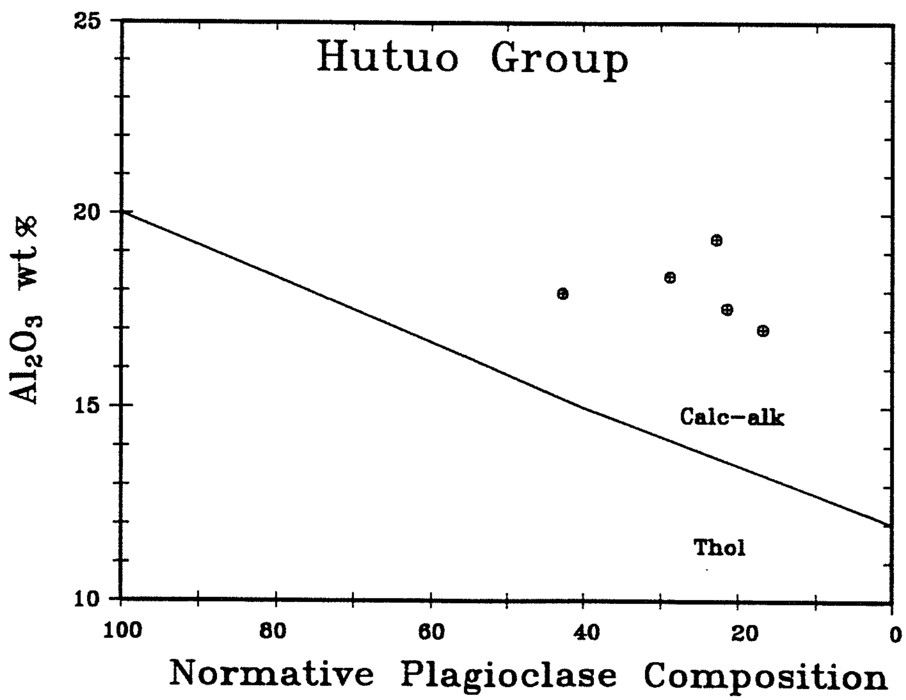

Figure 4-6. Al_2O_3 - Plagioclase plot for metavolcanic samples from (a) Fuping Complex, (b) Wutai Complex, and (c) Hutuo Group. The dividing line is from Irvine and Baragar (1971).

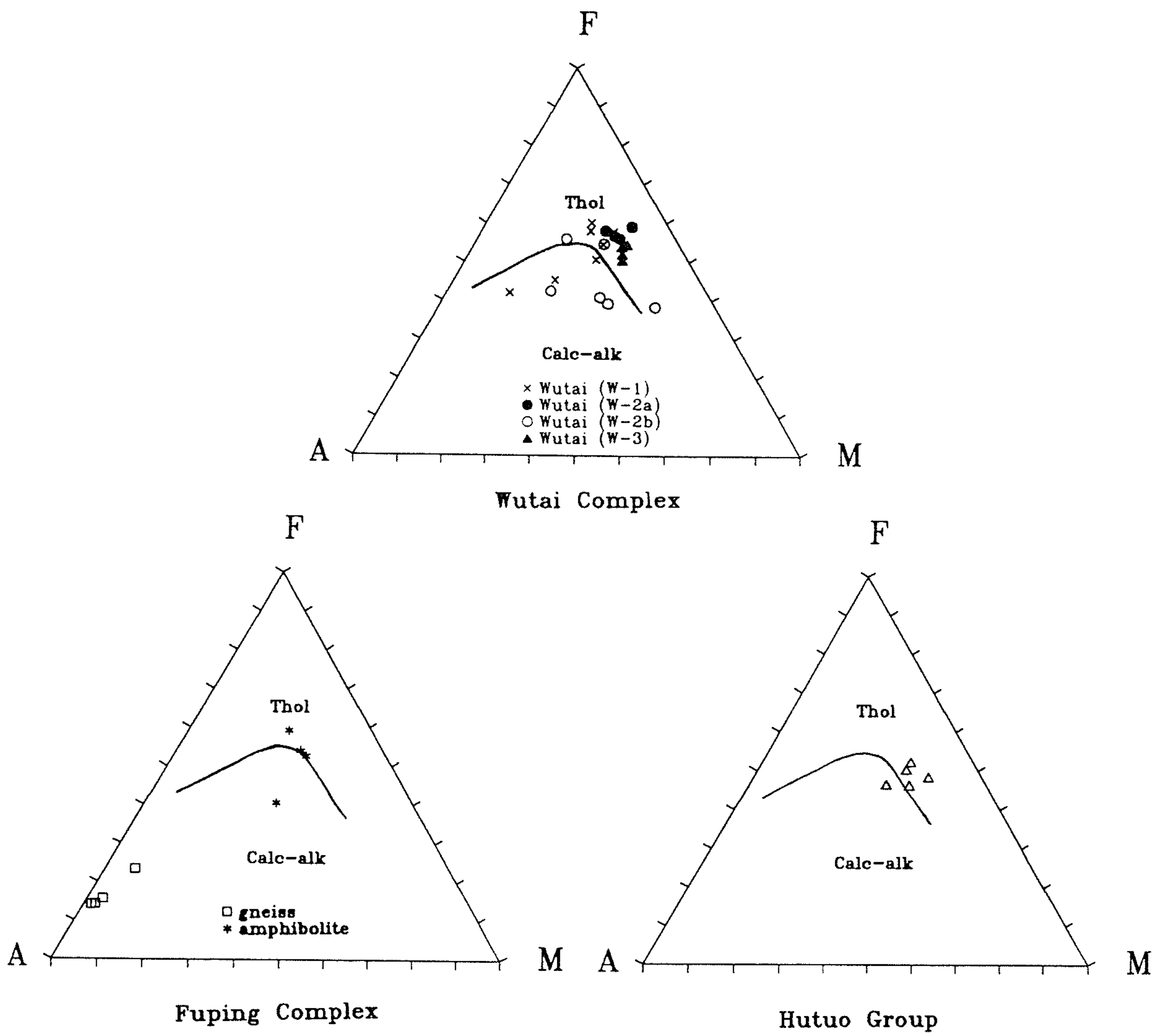

Figure 4-7. AFM plot for metavolcanic samples from Fuping Complex, Wutai Complex, and Hutuo Group. The dividing line is from Irvine and Baragar (1971). $A=K_2O+Na_2O$, $F=\Sigma FeO$, and $M=MgO$, all in wt%.

The amphibolites from W-1 plot mainly in the calc-alkaline field in Al_2O_3 - normative plagioclase plot (Fig. 4-6b), but are in both tholeiitic and calc-alkaline fields in AFM diagram (Fig. 4-7). The greenschists from W-2a plot mainly in tholeiitic field and those from W-2b mainly in the calc-alkaline field in both Al_2O_3 - normative plagioclase and AFM diagrams (Fig. 4-6b and 4-7). The metabasalts from W-3 mainly are in the calc-alkaline field in Al_2O_3 - normative plagioclase plot (Fig. 4-6b), but in contrast fall in the tholeiitic field of the AFM diagram (Fig. 4-7).

Metabasaltic samples from the Hutuo Group plot in the calc-alkaline field in Al_2O_3 - normative plagioclase diagram, but most samples, in contrast, are in the tholeiitic field in AFM diagram (Fig. 4-6c and 4-7).

In summary, Fuping amphibolites are more tholeiitic than calc-alkaline. The greenschists samples from W-1 have more calc-alkaline than tholeiitic character. The greenschists from W-2 show a tholeiitic signature in the bottom cycle (W-2a) and a calc-alkaline character in the upper cycle (W-2b). The metabasaltic samples from W-3 and from the Hutuo Group fall in the contradictory fields in the two different plots (Table 4-3).

Tectonic Discriminant Plots:

All the metatholeiitic samples from the Fuping and the Wutai complexes plot in the IAT field in a FeO^*/MgO - TiO_2 diagram (Fig. 4-8).

Table 4-3. Summary of discrimination test for metavolcanic rocks

Diagrams	Fuping	W-1	W-2a	W-2b	W-3	Hutuo
Alk-SiO_2	Subalk	Subalk	Subalk	Subalk	Subalk	4-Subalk 1-Alk
Ol'-Ne'-Q'	6-Subalk 2-Alk	6-Subalk 1-Alk	3-Subalk 1-Alk	Subalk	Subalk	Subalk
Y/Nb	Subalk	Subalk	Subalk	Subalk	Subalk	Subalk
Al_2O_3-Plag	Thol(am.) CAB(geiss)	2-Thol 5-CAB	3-Thol 1-CAB	1-Thol 5-CAB	3-CAB 1-boundary CAB+Thol	CAB
AFM	Thol & CAB(am.) CAB(gneiss)	4-Thol 3-CAB	Thol	3-Thol 3-CAB	Thol	3-Thol 2-CAB
FeO^*/MgO-TiO_2	IAT	IAT	IAT	N/A	boundary IAT+MORB	MORB near OIB
F_2-F_1	CAB+LKT (C+L)	5-(C+L) 1-WPB	C+L	C+L	C+L	C+L
F_3-F_2	LKT	2-LKT 4-CAB	LKT	4-CAB 1-out	LKT	1-LKT 4-CAB
Spider diagram	CAB-IAT	CAB-IAT	MORB	CAB-IAT	CAB-IAT	WPB
Ti/Y-Nb/Y	VAB+MORB (V+M)	3-MORB 3-(V+M)	V+M	V+M	1-(V+M) 3-bound. MORB+WPB	3-WPB 2-bound. MORB+WPB
Ti/100-Zr-Y*3	non-WPB	non-WPB	non-WPB	non-WPB	boundary WPB+non-WPB	WPB
Zr/Y-Zr	non-WPB	non-WPB	non-WPB	non-WPB	boundary WPB+non-WPB	WPB
Ti/100-Zr-Sr/2	OFB 1-CAB	3-OFB 2-LKT 1-CAB	OFB	CAB	boundary LKT+CAB	N/A
Ni-Y	3-LKT 1-MORB	1-LKT 5-MORB	MORB	N/A	MORB	N/A

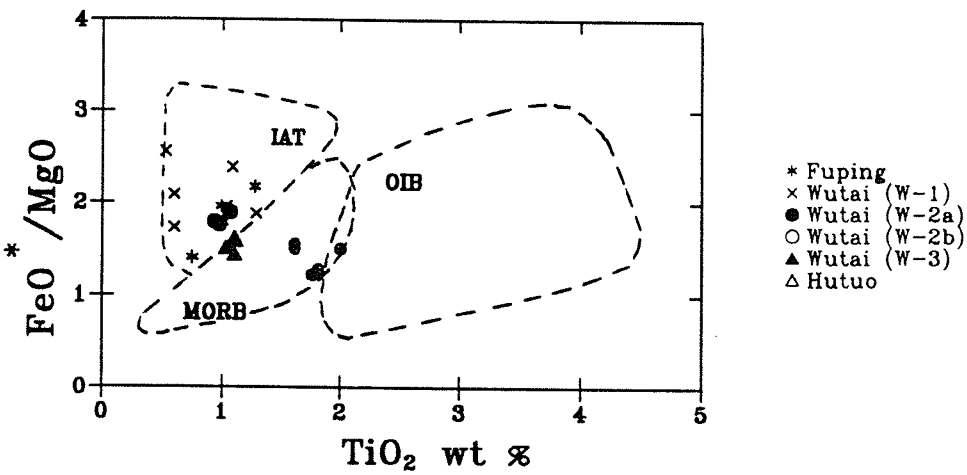

Figure 4-8. FeO^*/MgO - TiO_2 plot for TH basalts (Glassley, 1974). FeO^* represents total iron in FeO form, all in wt%. Tholeiites can be discriminated as MORB, IAT, and OIB in this diagram. Metatholeiitic samples from the Fuping and the Wutai complexes fall in the IAT filed. Samples in MORB field are from W-3 and the Hutuo Group, which are ambiguous in the classification of tholeiitic and calc-alkaline series.

In F_2-F_1 plot, most metabasic samples from the region plot in the field of LKT+CAB (Fig. 4-9). In F_3-F_2 plot, Fuping amphibolites plot mainly in LKT, amphibolites from the W-1 mainly in CAB, greenschists from the W-2a in LKT, greenschists from the W-2b mainly in CAB, metabasaltic samples from the W-3 in LKT, and the Hutuo metabasalts mainly in CAB field (Fig. 4-10).

Fuping amphibolites are highly enriched in K, Rb, and Ba, slightly depleted in Ti, Y and Cr, Zr is close to 1. Two samples show high P and high Sm, respectively. The trace element pattern is between typical calc-alkaline and typical arc tholeiitic basalts (Fig. 4-11a).

Two analyses from the same hand specimen (W84-51 and W84-52, one felsic and one mafic micro-layer) from W-1 show a pattern similar to typical arc tholeiite, but with high Cr values. Other amphibolites from the W-1 behave like the Fuping amphibolites (Fig. 4-11b). The W-2a greenschists show a trace element pattern similar to basalts formed in slow spreading ridges, such as Alula-Fartak trench, but with higher Nb concentrations (Fig. 4-11c). The W-2b and W-3 metavolcanic samples are similar to arc volcanics like the Fuping amphibolites (Fig. 4-11d and 4-11e).

Metabasaltic samples from the Hutuo Group show the trace element pattern of within-plate tholeiites (Fig. 4-11f).

In Ti/Y - Nb/Y (Pearce, 1982) and Ti/100 - Zr - Y*3 (Pearce and Cann, 1973) diagrams, amphibolites from the Fuping Complex and from W-1, and greenschists from W-2 plot in the fields of

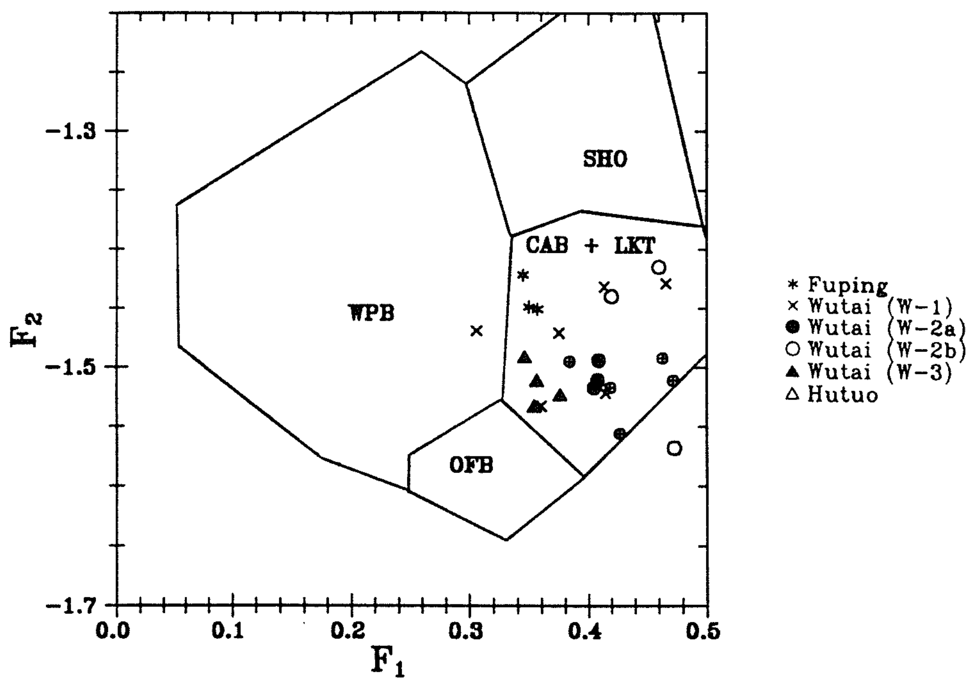

Figure 4-9. F_2 - F_1 plot for basaltic rocks (Pearce, 1976). Most metabasaltic samples from the study region plot in the field of CAB+LKT. $F_1 = 0.0088SiO_2 - 0.0774TiO_2 + 0.0102Al_2O_3 + 0.0066FeO - 0.0017MgO - 0.0143CaO - 0.0155Na_2O - 0.0007K_2O$, $F_2 = -0.0130SiO_2 - 0.0185TiO_2 - 0.0129Al_2O_3 - 0.0134FeO - 0.00300MgO - 0.0204CaO - 0.0481Na_2O + 0.0715K_2O$.

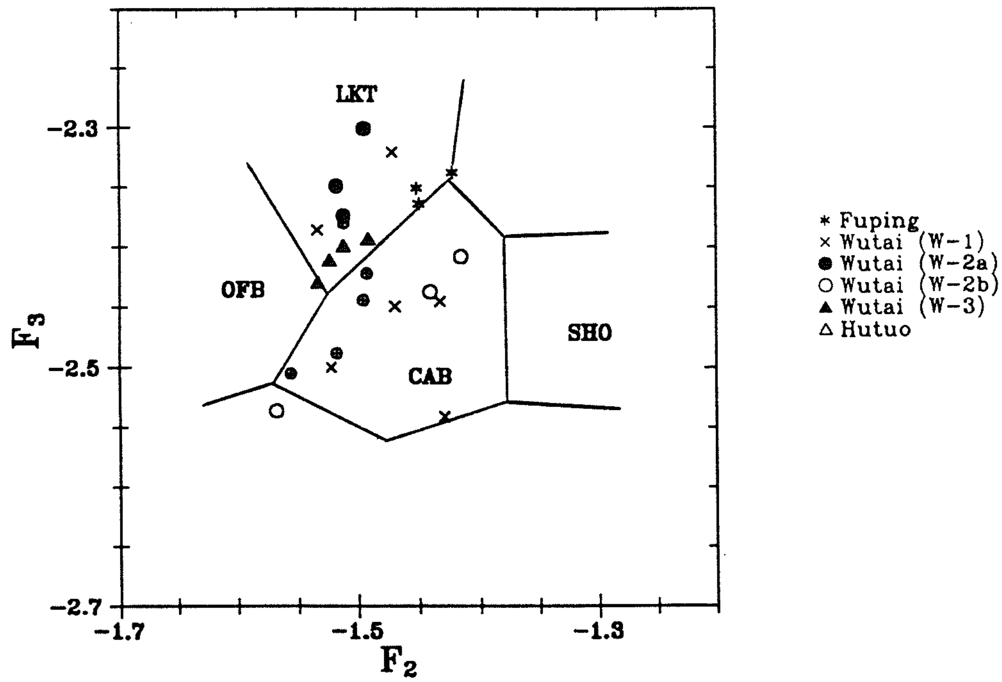

Figure 4-10. F_3 - F_2 plot for basaltic rocks (Pearce, 1976). The Fuping amphibolites, W-2a, and W-3 metabasaltic samples are in the LKT field. W-1, most W-2b, and the Hutuo metabasaltic samples fall in the CAB filed. F3 = $-0.0221SiO_2 - 0.0532TiO_2 - 0.036Al_2O_3 - 0.0016FeO - 0.0310MgO - 0.0237CaO - 0.0614Na_2O - 0.0289K_2O$.

(a)

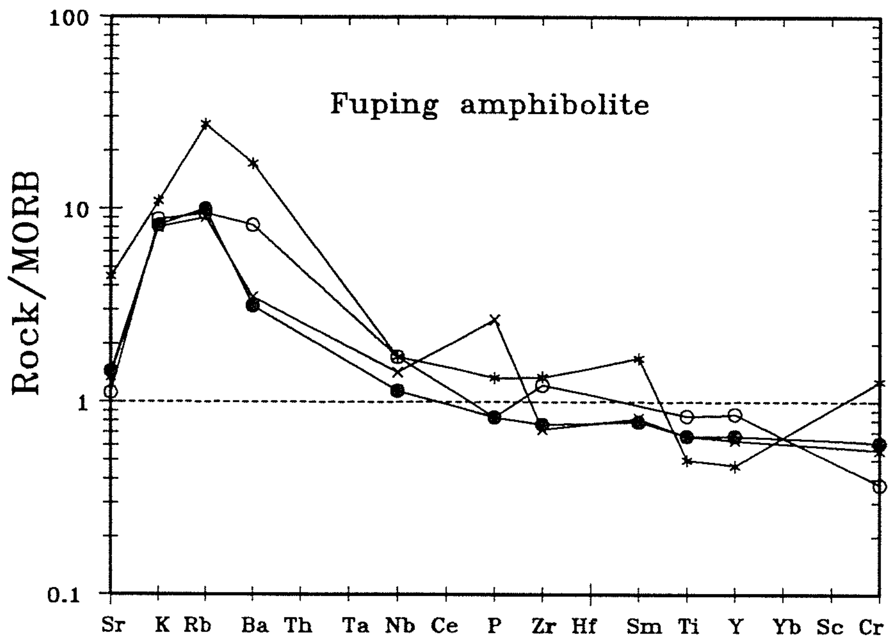

(b)

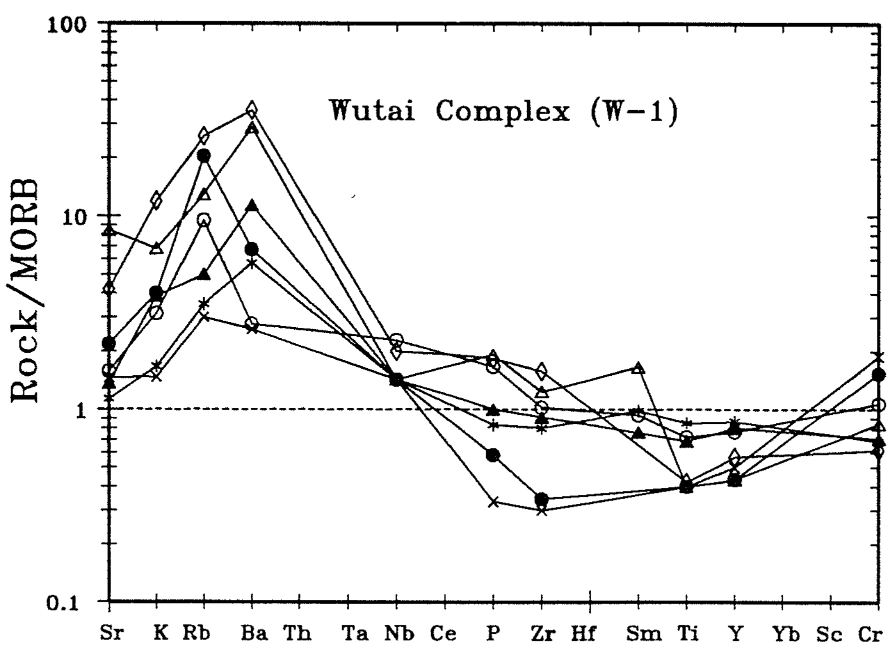

Figures 4-11a and 4-11b, caption in p.140.

(c)

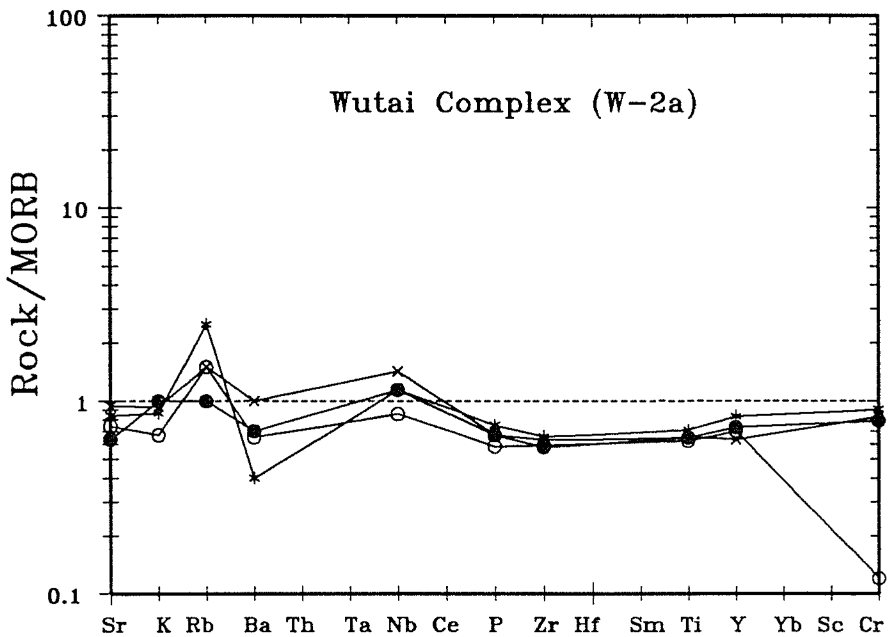

(d)

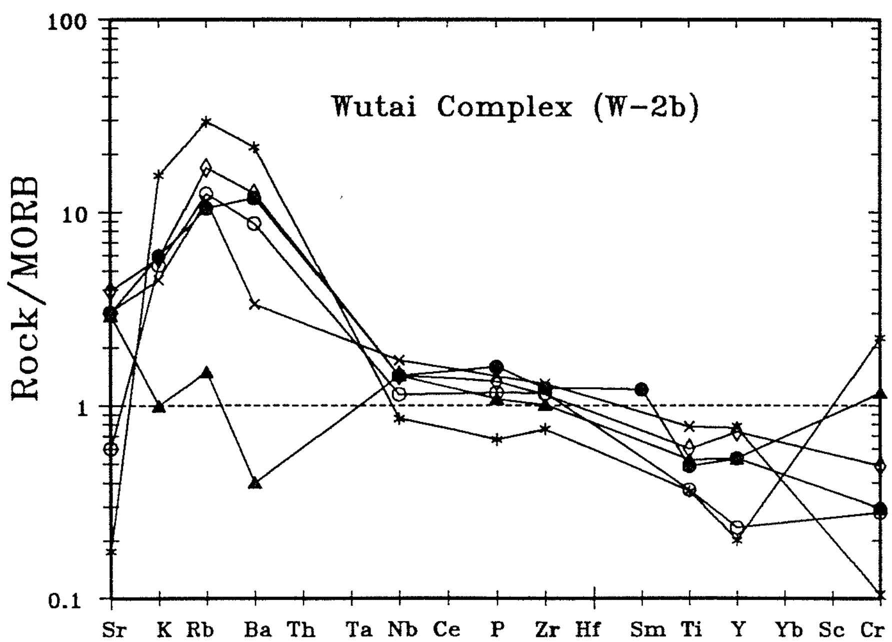

Figures 4-11c and 4-11d, caption in p.140.

(e)

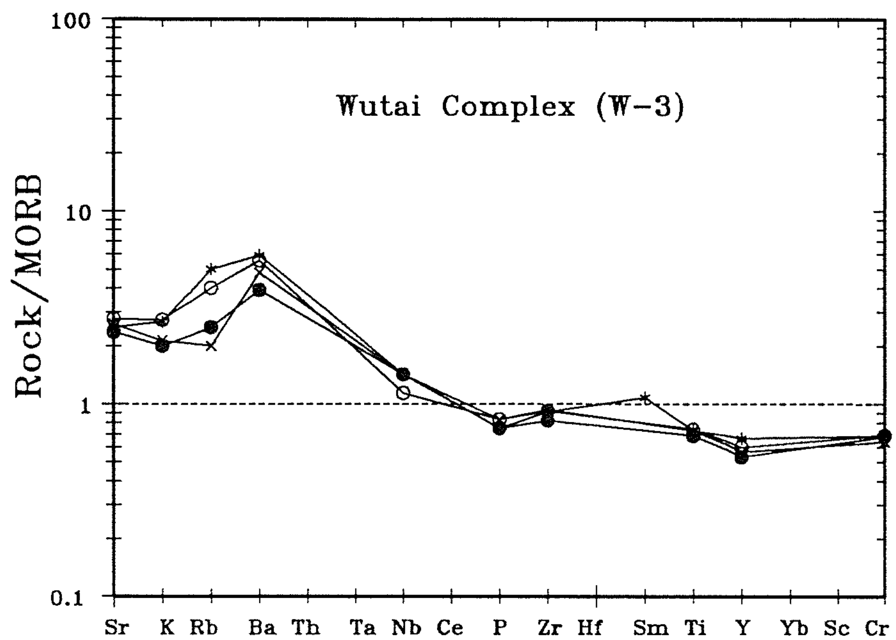

(f)

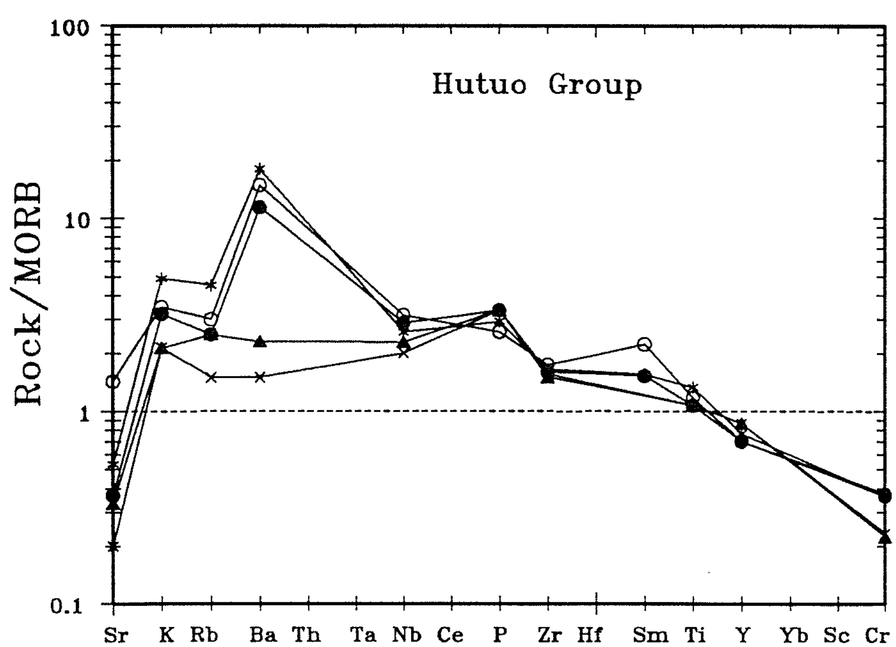

Figure 4-11a to 11f: trace element plots (spider diagrams) for metavolcanic rocks from Fuping Complex, Wutai Complex (four subdivisions), and Hutuo Group.

non-WPB. Metabasalts from the W-3 plot near to the boundary of WPB and non-WPB. The Hutuo metabasaltic samples mostly plot in the WPB field (Fig. 4-12 and 4-13).

In a Zr/Y - Zr plot (Pearce and Norry, 1979), the Fuping amphibolites are in both WPB and non-WPB fields. Amphibolites from the W-1 mainly fall in the non-WPB field. Greenschists from the W-2a plot in the non-WPB field. Two greenschists from W-2b fall in the WPB field and other 4 out of the fields defined by the original paper. Metabasalts from the W-3 plot near to the boundary of WPB and non-WPB and some out of the original fields. The Hutuo metabasalts plot in the WPB field (Fig. 4-14).

Ti/100 - Zr - Sr/2 (Pearce and Cann, 1973) and Ni - Y (Capedri et al., 1980) have been suggested for the further discrimination of non-WPB. The meta-WPB from Hutuo Group are also plotted for comparison although not discussed below. In a Ti/100 - Zr - Sr/2 diagram, most Fuping amphibolites plot in the OFB field. Amphibolites from the W-1 plot in the OFB, CAB, and LKT fields. Greenschists from the W-2a fall in the OFB field, those from the W-2b mainly in the CAB field. Metabasaltic samples from the W-3 plot near to the boundary of OFB and CAB (Fig. 4-15).

In Ni - Y diagram, most Fuping amphibolites plot in the LKT field. Amphibolites from the W-1 mainly plot in MORB field. Greenschists from the W-2a plot in the MORB field, those from the W-2b in both LKT and MORB. Metabasalts from the W-3 fall in the MORB field (Fig. 4-16).

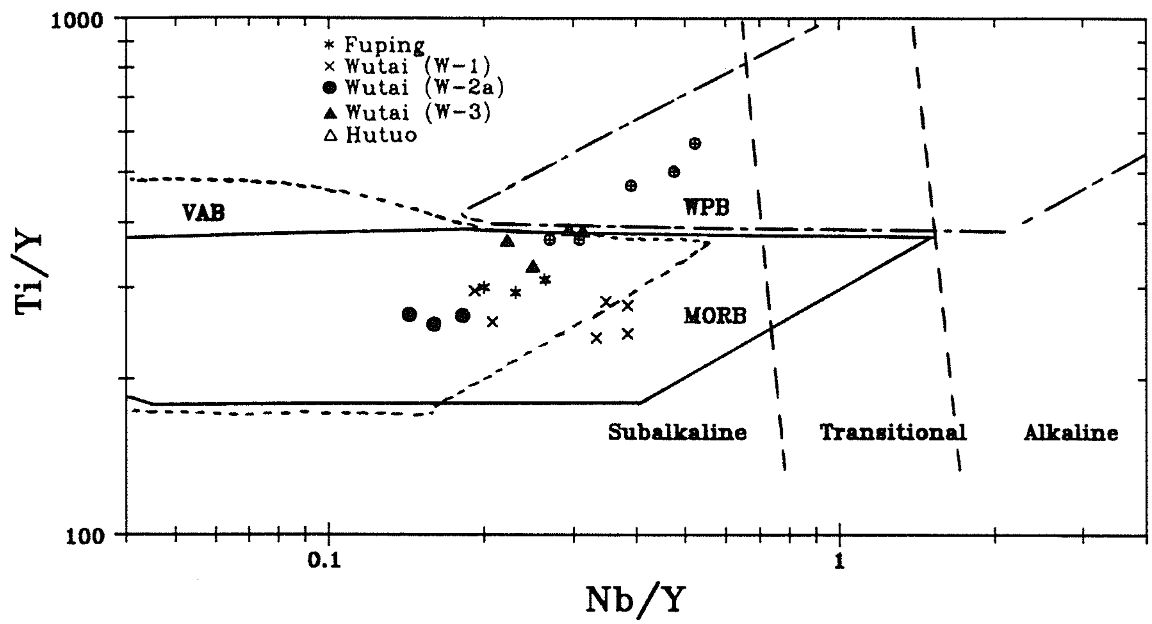

Figure 4-12. Ti/Y - Nb/Y plot for tholeiitic and alkaline basalts (Pearce, 1982). Fields are divided into subalkaline, transitional, and alkaline mainly according to Nb/Y ratios. WPB can be easily discriminated from the non-WPB that includes VAB and MORB. But VAB and MORB fields largely overlap. The amphibolites from the Fuping Complex and Wutai Complex (W-1), greenschists from W-2a are non-WPB. W-3 metabasalts are ambiguous. The metabasaltic samples from the Hutuo Group are WPB. All the metabasic samples are subalkaline, in accord with major element plots.

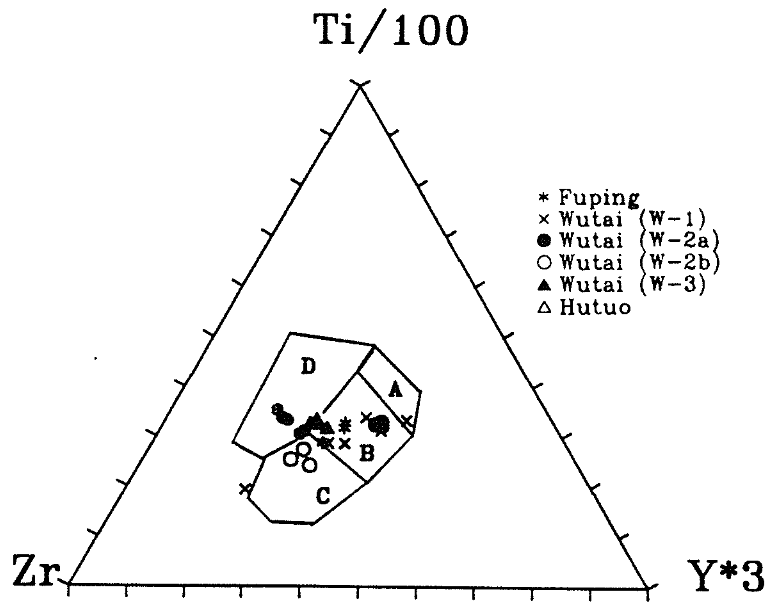

Figure 4-13. Ti/100 - Zr - Y*3 plot for basaltic rocks (Pearce and Cann, 1973). WPB plots uniquely in the field D, thus can be discriminated from non-WPB. The amphibolitesfrom the Fuping Complex and the Wutai Complex (W-1), greenschists from the W-2a and W-2b mostly in non-WPB fields. W-3 metabasalts plot near to the boundary of WPB and non-WPB. The metabasaltic samples from the Hutuo Group fall in the WPB field.

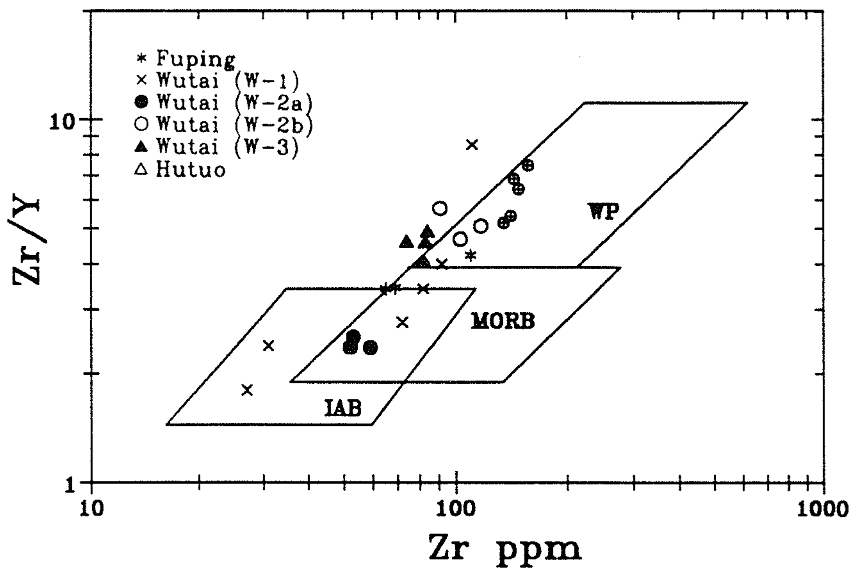

Figure 4-14. Zr/Y - Zr plot for basaltic rocks (Pearce and Norry, 1979). WPB can be distinguished from non-WPB, but the fields of MORB and IAB partly overlap. The Fuping amphibolites plot in both WPB and non-WPB fields. Most W-1, and W-2a fall in non-WPB field. Two W-2b metavolcanic samples plot in WPB field, and other one out of the fields defined by the original paper. W-3 metavolcanic samples fall near to the boundary of WPB and non-WPB, and some out of the original fields. The metavolcanic samples from the Hutuo Group fall in the WPB field.

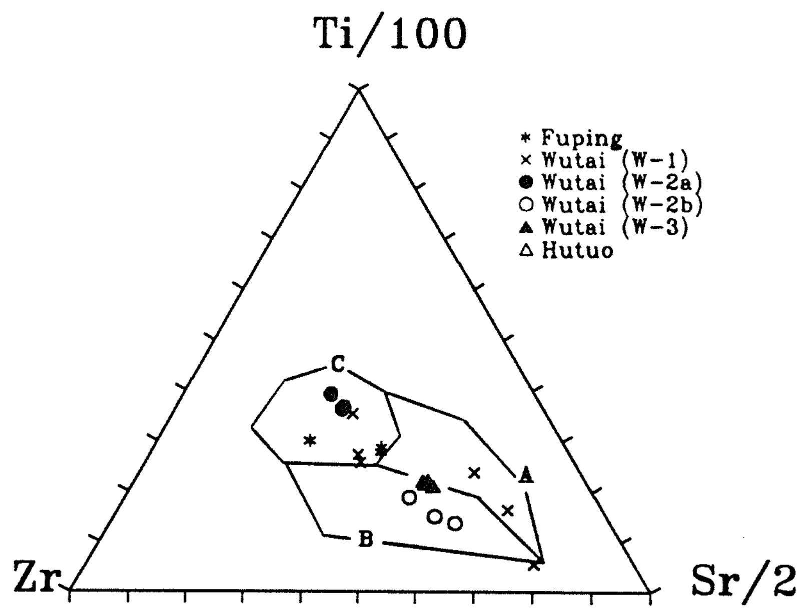

Figure 4-15. Ti/100 - Zr - Sr/2 plot for non-WPB basalts (Pearce and Cann, 1973). Basalts formed in non-WP settings can be easily distinguished, but subject to much uncertainty because of Sr mobility in metamorphic rocks. LKT plots in field A, CAB in field B, and OFB in field C. Most Fuping amphibolites plot in the OFB field. W-1 amphibolites plot in OFB, CAB, and LKT field, greenschists from the W-2a fall in the OFB field and those of W-2b in CAB field, W-3 metavolcanic samples near to the boundary of OFB and CAB.

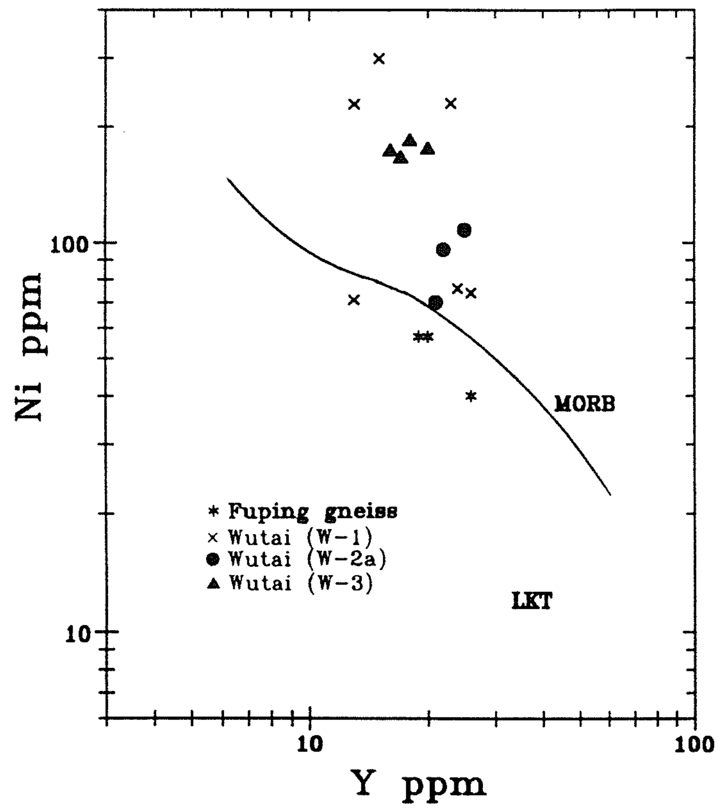

Figure 4-16. Ni - Y plot for TH basalts (Capedri et al., 1980). The fields are divided into MORB and LKT. The Fuping amphibolites plot in the LKT field. Most W-1 amphibolites, and W-2a greenschists fall in the MORB field, W-2b greenschists in both LKT and MORB fields, W-3 metabasalts in the MORB field.

In summary (Table 4-3), the amphibolites from the Fuping Complex and the Wutai Complex (W-1), and greenschists from the upper cycle of the W-2 show the character of island arc tholeiites, but less commonly show a MORB-like signature. The greenschists from the lower cycle of the W-2 fall in MORB field in trace element plots but in contrast fall in the island arc tholeiite field in major element plots. Metabasaltic samples from W-3 plot ambiguously between WPB and non-WPB, with a slight affinity to low-K tholeiites. Metabasaltic samples from the Hutuo Group uniquely plot in the WPB field. Geochemistry clearly indicates that metavolcanic samples from the Wutai and Taihang region formed in a succession of different tectonic environments.

(2). Gneisses and granites

Gneisses from the Fuping Complex and all the granitic bodies that we have analyzed are subalkaline, with a calc-alkaline character. Calculated discriminant function of Shaw (1972) indicates an igneous parentage for the Fuping gneiss. The Fuping gneiss and the Lanzishan, Wangjiahui and Shifo granites plot in the granite field, while the Chechang Granite plots in trondhjemite and tonalite fields in normative An-Ab-Or diagram (Fig. 4-17). These granites are I-type granites according to their chemistry.

In Rb - (Y+Nb) diagram, the Chechang trondhjemite-tonalite falls in the VAG field, the Wangjiahui Granite plots on the boundary of VAG and WPG, the Lanzishan Granite on the VAG syn-COLG boundary and the Shifo Granite nearby, just inside VAG

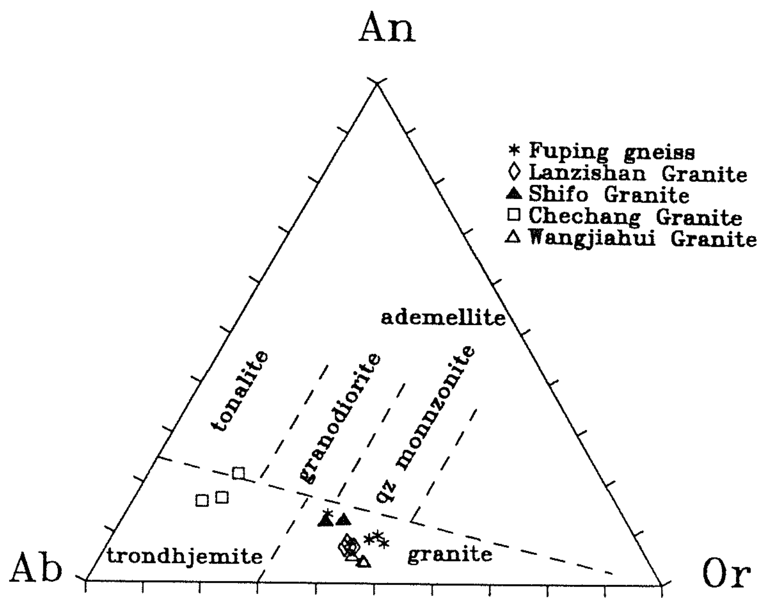

Figure 4-17. An - Ab - Or plot for some Precambrian granites from the Wutaishan and Taihangshan region. The dividing lines are from O'Connor (1965).

(Fig. 4-18).

IV-3. Isotopic results

Rb-Sr isotopic results for samples from the Wutaishan and Taihangshan areas are represented in Table 4-4. Sm-Nd isotopic results are in Table 4-5. Pb isotopic results are in Table 4-6. Our Rb-Sr, Sm-Nd, and Pb-Pb isochron dates, and published U-Pb zircon dates are summarized in Table 4-7.

Fuping Complex:

Two amphibolites and three gneisses are scattered in the Rb-Sr isochron plot (Fig. 4-19). The poorly defined isochron date is 2.3 +/- 0.4 Ga, with $(^{87}Sr/^{86}Sr)_0$ = 0.7036 +/- 0.0029. Three amphibolites and two gneisses define a straight line in the Sm-Nd plot (Fig. 4-20). The isochron date is 2.37 +/- 0.07 Ga with $(^{143}Nd/^{144}Nd)_0$ = 0.50963 +/- 0.00005 or $\epsilon_{Nd}(T)$ = 1.5±0.9 (Fletcher and Rosman, 1982). Nd depleted mantle model dates for amphibolites are 2.48 to 2.60 Ga, and those for gneisses are 2.43 to 2.46 Ga. Three amphibolites and three gneisses define a Pb-Pb isochron of 2.2 +/- 0.2 Ga with a first stage growth μ = 7.73, largely controlled by one sample (Fig. 4-21).

Wutai Complex:

All metavolcanic samples from the Wutai Complex define a Rb-Sr isochron of 2.0 +/- 0.1 Ga with $(^{87}Sr/^{86}Sr)_0$ = 0.7025 +/- 0.0002 (Fig. 4-22) but with large scatter about the line (MSWD = 72). Seven amphibolites from the Wutai Complex (W-1) alone define an isochron of 2.4 +/- 0.4 Ga with $(^{87}Sr/^{86}Sr)_0$ = 0.7021 +/- 0.0008.

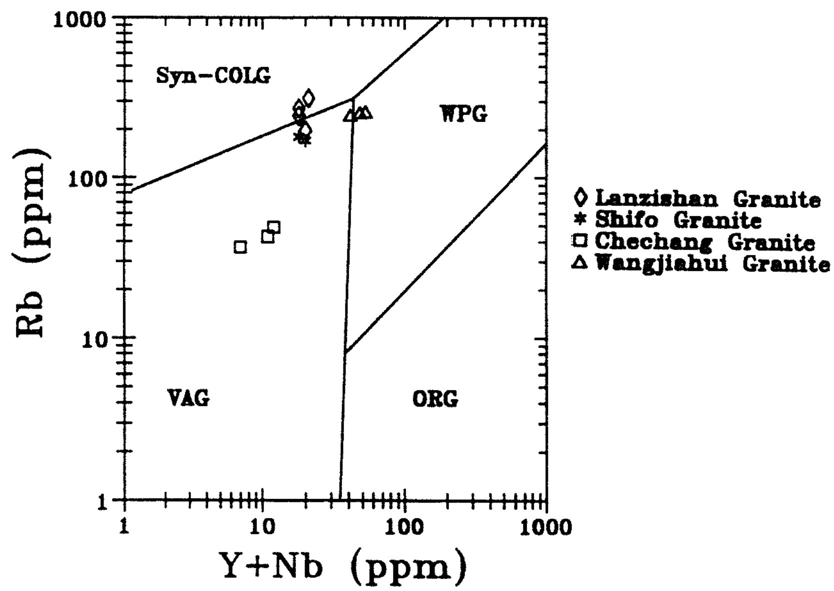

Figure 4-18. Rb - (Y+Nb) plot for some Precambrian granites from the Wutaishan and Taihangshan region. The dividing lines are from Pearce et al. (1984).

Table 4-4. Rb-Sr isotopic data for whole rock samples from the Wutaishan and Taihangshan region

Sample	Rb ppm	Sr ppm	$^{87}Rb/^{86}Sr$	$^{87}Sr/^{86}Sr^{+}$	$\epsilon Nd(0)$	T^{*}_{DM}
Fuping Complex						
F1-3	63.35	496.26	0.3695	0.71305	121.	2.1
				±0.00007	1.	0.2
F4-2	19.62	173.81	0.3268	0.71529	153.	3.0
				±0.00002	0.	0.2
F4-3	20.99	161.19	0.3772	0.71916	208.	3.3
				±0.00001	0.	0.2
F6-1	147.75	348.92	1.2291	0.74116	520.	2.3
				±0.00072	10.	0.8
F6-4	155.68	278.66	1.6245	0.75934	778.	2.5
				±0.00001	0.	0.6
Wutai Complex (W-1)						
W84-1	4.19	128.94	0.0939	0.70479	4.	2.3
				±0.00019	3.	0.2
W84-2	2.43	132.93	0.0531	0.70357	-13.	2.6
				±0.00005	1.	0.2
W84-3	4.71	132.54	0.1028	0.70497	7.	2.2
				±0.00006	1.	0.2
W84-4	20.24	197.96	0.2960	0.70966	73.	1.8
				±0.00005	1.	0.4
W84-52	6.79	168.43	0.1166	0.70689	34.	3.4
				±0.00012	2.	0.2
W84-7	10.55	169.70	0.1788	0.70879	61.	2.9
				±0.00016	2.	0.2
W84-8	27.23	1028.54	0.0766	0.70562	16.	4.1
				±0.00007	1.	0.2
W84-9	55.98	490.23	0.3306	0.71465	144.	2.8
				±0.00006	1.	0.2
Wutai Complex (W-2a)						
W82-4	2.76	113.91	0.0701	0.70374	-11.	1.8
				±0.00008	1.	0.2
W82-5	2.83	89.38	0.0916	0.70658	30.	4.2
				±0.00040	6.	0.4
W82-7	1.36	73.33	0.0536	0.70366	-12.	2.8
				±0.00018	3.	0.4
W82-9	4.05	133.24	0.0880	0.70610	23.	3.9
				±0.00005	1.	0.1
Wutai Complex (W-2b)						
W81-1	54.99	23.66	6.8000	0.89691	2731.	2.0
				±0.00006	1.	3.4
W81-2	24.82	73.64	0.9773	0.73161	385.	2.2
				±0.00006	1.	0.4
W81-3	3.97	60.27	0.1906	0.70745	42.	2.1
				±0.00017	2.	0.2
W81-6	24.16	380.91	0.1836	0.70705	36.	2.0
				±0.00009	1.	0.1
W81-7	28.55	362.98	0.2275	0.70881	61.	2.2
				±0.00002	0.	0.2
W81-8	4.80	472.40	0.0294	0.70438	-2.	8.2
				±0.00005	1.	0.1
W81-11	33.39	471.12	0.2050	0.70773	46.	2.0
				±0.00007	1.	0.2
W81-15	28.39	239.25	0.3434	0.71308	122.	2.3
				±0.00010	1.	0.2

continued

Wutai Complex (W-3)						
W85-1	6.62	302.07	0.0634	0.70440	-1.	3.4
				±0.00005	1.	0.2
W85-2	10.06	231.45	0.1257	0.70497	7.	1.7
				±0.00007	1.	0.1
W85-3	3.25	309.09	0.0305	0.70327	-17.	5.5
				±0.00004	1.	0.2
W85-4	8.72	379.27	0.0665	0.70522	10.	4.4
				±0.00003	1.	0.1
W85-6	3.11	308.68	0.0291	0.70328	-17.	5.8
				±0.00003	1.	0.2
W85-7	9.41	307.72	0.0886	0.70486	5.	2.6
				±0.00003	1.	0.1
W85-8	4.00	231.50	0.0500	0.70380	-10.	3.5
				±0.00022	3.	0.6
Hutuo Group						
H-003	8.54	59.79	0.4135	0.71292	120.	1.9
				±0.00028	4.	0.4
H-004	6.82	170.32	0.1159	0.70572	17.	2.5
				±0.00014	2.	0.2
H-014	3.53	28.57	0.3574	0.71767	187.	3.2
				±0.00006	1.	0.4
H-017	6.87	53.13	0.3744	0.71728	181.	3.0
				±0.00013	2.	0.2
Lanzishan Granite						
076	274.72	161.66	5.0039	0.88848	2612.	2.6
				±0.00005	1.	2.4
077	191.23	269.27	2.0696	0.78185	1098.	2.7
				±0.00015	2.	1.0
078	296.25	155.11	5.6356	0.91017	2919.	2.6
				±0.00013	2.	1.0
079	225.18	125.19	5.3059	0.89718	2735.	2.6
				±0.00019	3.	1.1
080	236.50	160.66	4.3212	0.86033	2212.	2.6
				±0.00019	3.	1.2
Chechang Granite						
083-1	41.25	219.48	0.5445	0.71973	216.	2.3
				±0.00007	1.	0.2
083-2	43.42	232.70	0.5410	0.71677	174.	1.9
				±0.00001	4.	0.6
083-3	43.81	265.41	0.4780	0.71857	200.	2.5
				±0.00008	1.	0.2
083-4	33.82	357.18	0.2740	0.71044	84.	2.2
				±0.00007	1.	0.2
Wangjiahui Granite						
087-1	218.18	214.38	2.9690	0.79264	1251.	2.2
				±0.00006	1.	1.4
087-2	242.86	218.00	3.2542	0.80620	1444.	2.3
				±0.00014	2.	1.4
087-3	239.27	250.78	2.7819	0.78723	1174.	2.2
				±0.00005	1.	1.4

\+ 2σ errors are listed in the table, 0.026% and 2% were used for $^{87}Sr/^{86}Sr$ and $^{87}Rb/^{86}Sr$ in the regression calculation.

* T_{DM}: depleted mantle model date of DePaolo (1981), the following constants have been used in the calculation: $(^{87}Rb/^{86}Sr)_{UR}$=0.0827, $(^{87}Sr/^{86}Sr)^0_{UR}$=0.7045, $\lambda_{^{87}Rb}$=0.0142 AE^{-1}.

Table 4-5. Sm-Nd isotopic data for whole rock samples from the Wutaishan and Taihangshan region

Sample	Sm ppm	Nd ppm	$^{147}Sm/^{144}Nd$	$^{143}Nd/^{144}Nd^{+}$	$\epsilon Nd(0)$	T_{DM}^{*}
Fuping Complex						
F1-3	5.558	29.94	0.1120	0.511317	-25.5	2.59
				±0.000008	0.2	0.02
F4-2	2.597	9.35	0.1678	0.512257	-7.2	2.60
				±0.000016	0.3	0.06
F4-3	2.717	10.05	0.1633	0.512219	-7.9	2.48
				±0.000012	0.2	0.04
F6-1	2.665	27.02	0.0595	0.510586	-39.8	2.43
				±0.000012	0.2	0.08
F6-4	1.962	18.94	0.0625	0.510604	-39.4	2.46
				±0.000016	0.3	0.08
Wutai Complex (W-1)						
W84-1	3.254	9.33	0.2106	0.512900	5.3	--
				±0.000040	0.8	--
W84-4	3.094	11.92	0.1567	0.512052	-11.2	2.65
				±0.000020	0.4	0.10
W84-7	2.509	9.80	0.1546	0.511994	-12.3	2.71
				±0.000006	0.1	0.96
W84-8	5.470	28.76	0.1148	0.511524	-21.5	2.33
				±0.000016	0.3	0.08
Wutai Complex (W-2b)#						
W81-6	3.989	20.40	0.1180	0.511462	-22.7	2.51
				±0.000010	0.2	0.08
W81-15	3.545	13.63	0.1570	0.512114	-10.0	2.48
				±0.000008	0.2	0.16
Wutai Complex (W-3)						
W85-1	3.682	12.63	0.1760	0.512329	-5.8	2.91
				±0.000008	0.2	0.26
W85-2	3.566	12.49	0.1724	0.512356	-5.3	2.52
				±0.000006	0.1	0.32
Hutuo Group						
H-003	5.133	23.38	0.1325	0.511799	-16.1	2.32
				±0.000006	0.1	0.22
H-004	7.344	32.69	0.1356	0.511837	-15.4	2.34
				±0.000014	0.3	0.08
H-007	5.034	21.53	0.1411	0.511795	-16.2	2.62
				±0.000006	0.1	0.08

continued

Lanzishan Granite						
076	2.558	19.11	0.0808	0.510813	-35.4	2.56
				±0.000014	0.3	0.06
077	3.163	23.10	0.0826	0.510953	-32.6	2.43
				±0.000060	1.2	0.10
078	2.988	19.41	0.0929	0.511027	-31.2	2.54
				±0.000008	0.2	0.02
079	1.951	12.93	0.0910	0.510889	-33.9	2.68
				±0.000012	0.2	0.08
080	4.353	33.66	0.0780	0.510803	-35.6	2.52
				±0.000008	0.2	0.10
Chechang Granite						
083-4	2.133	12.01	0.1072	0.511321	-25.5	2.46
				±0.000016	0.3	0.36

\+ $^{146}Nd/^{144}Nd$=0.7219 has been used for normalization, 2σ errors are listed in the table, 0.005% and 1% were used for $^{143}Nd/^{144}Nd$ and $^{147}Sm/^{144}Nd$ in the regression calculation.

* T_{DM}: depleted mantle model date of DePaolo (1981), the following constants have been used in the calculation: $(^{143}Nd/^{144}Nd)^0_{CHUR}$= 0.512626, $(^{147}Sm/^{144}Nd)^0_{CHUR}$=0.1967, $\lambda_{^{147}Sm}$=0.00654 AE^{-1}.

\# Data for six additional samples of W-2 from Li et al. (1990) were also plotted on the Sm-Nd diagram.

Table 4-6. Whole rock Pb isotopic data for samples from the Wutaishan and Taihangshan region

Sample	$^{206}Pb/^{204}Pb$#	$^{207}Pb/^{204}Pb$	$^{208}Pb/^{204}Pb$
Fuping Complex			
F1-3	18.22	15.40	37.75
F4-2	15.00	14.92	35.26
F4-3	15.47	15.06	35.92
F6-1	15.65	15.13	40.61
F6-3	15.71	15.10	42.35
F6-4	15.34	15.03	39.85
Wutai Complex (W-1)			
W84-1	15.59	15.07	35.44
W84-4	15.60	15.01	35.04
Wutai Complex (W-2a)			
W82-7	15.67	15.07	35.27
W82-9	15.44	15.06	35.19
Wutai Complex (W-2b)			
W81-1	21.71	15.84	40.43
W81-2	30.21	17.17	50.53
W81-6	17.80	15.28	37.91
W81-8	18.21	15.48	37.74
W81-11	17.02	15.16	36.58
Wutai Complex (W-3)			
W85-2	17.83	15.42	36.59
W85-8	17.86	15.46	37.16
Hutuo Group			
H-003	21.99	15.91	40.83
H-004	18.79	15.52	38.35
H-007	23.33	15.62	41.09
H-014	18.55	15.52	39.11
H-017	19.23	15.38	39.66
Lanzishan Granite			
076	24.27	16.44	43.96
077	28.67	16.96	46.63
078	28.45	17.12	42.39
079	28.62	16.84	46.87
Chechang Granite			
083-1	30.16	17.00	46.39
083-3	18.81	15.36	38.45
083-4	23.94	16.23	43.10

The 2σ errors for $^{206}Pb/^{204}Pb$, $^{207}Pb/^{204}Pb$ and $^{208}Pb/^{204}Pb$ are 0.10, 0.15, and 0.16%, respectively. Error correlation coefficient (R) between $^{206}Pb/^{204}Pb$ and $^{207}Pb/^{204}Pb$ is 0.8. Pb standard NBS981 gave average ratios, $\pm 2\sigma$, of 16.940±0.003, 15.495±0.003, and 36.731 ±0.017 for $^{206}Pb/^{204}Pb$, $^{207}Pb/^{204}Pb$, and $^{208}Pb/^{204}Pb$, respectively.

Table 4-7. Isotopic dates for Early Precambrian rocks from Wutaishan and Taihangshan region Ga ± 2σ

	Rb-Sr	Pb-Pb	Sm-Nd	Nd model dates	Zircon U-Pb	overall inferred age
Fuping Complex		2.2 ±0.2 μ_1=7.73	2.37 ±0.07 @ϵ_{Nd}(T)=1.5 ±0.9	am. 2.48-2.60 gn. 2.43-2.46	detrital 2.8* ±0.2 euhedral 2.47* ±0.02	~2.6
Lanzishan Granite	2.48 ±0.03 @0.7076 ±0.0014	$1.9^{+0.4}_{-0.6}$ μ_1=8.38		2.52-2.56 & 2.43,2.68	2.560* ±0.006	~2.55
Wutai Complex W-1	2.4 ±0.4 @0.7021 ±0.0008		2.2 ±0.1 @ϵ_{Nd}(T)=0.5 ±1.0	2.33,2.65 & 2.71	2.508* ±0.002	≥2.5
Wutai Complex W-2			2.4 ±0.1 @ϵ_{Nd}(T)=1.2 ±0.9	2.48 & 2.51	2.52* ±0.02	≥2.5
Wutai Complex W-3				2.91,2.52		≥2.5
Wutai Complex as a whole a whole	2.0 ±0.1 @0.7025 ±0.0002	$2.27^{+0.06}_{-0.07}$ μ_1=7.73	2.26 ±0.06 @ϵ_{Nd}(T)=1.1 ±0.5			≥2.5
Ekou Granite					2.52* ±3	≥2.5
Shifo Granite					2.51$ ±2	≥2.5

continued

Chechang Granite	2.3 ±0.5 @0.7011 ±0.0032	2.3 ±0.1 μ_1=7.51	2.46		≥2.3
Wangjiahui Granite	2.2-2.3+				≥2.3
Hutuo Group			2.32,2.34 & 2.62	2.37# $\pm^{0.10}_{0.09}$	~2.4

* data from Liu et al. (1985).
\# data from Wu et al. (1986).
$ data from Bai (1986).
\+ Sr depleted mantle model date.

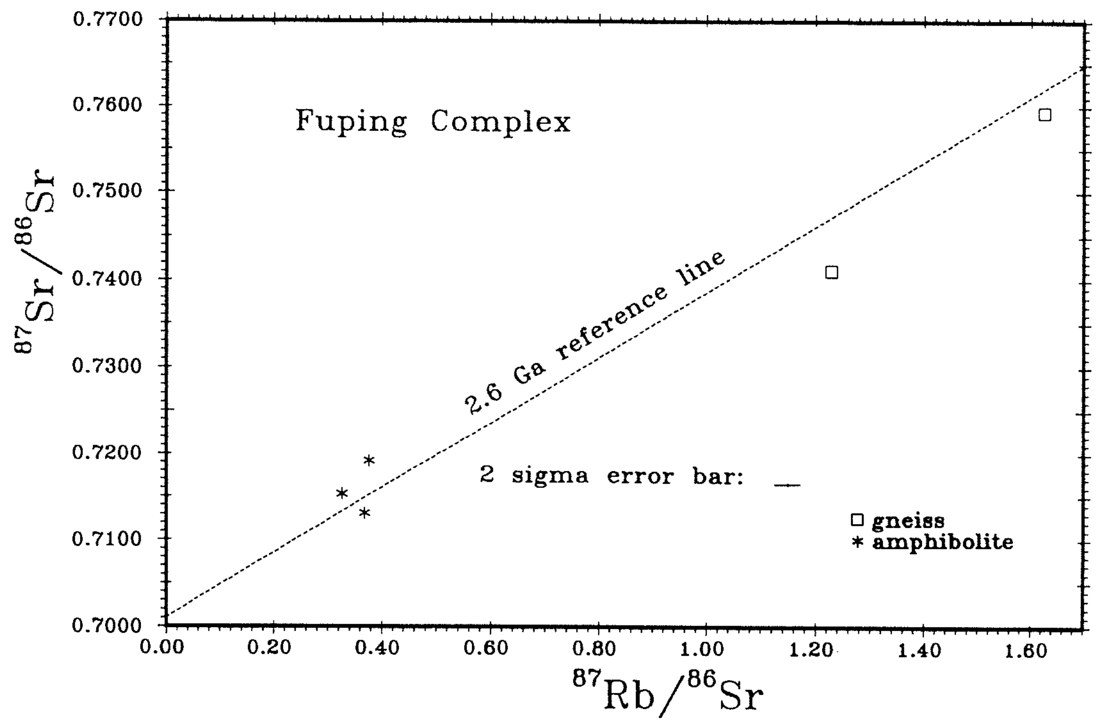

Figure 4-19. Rb - Sr isochron plot for the amphibolites and gneisses from the Fuping Complex.

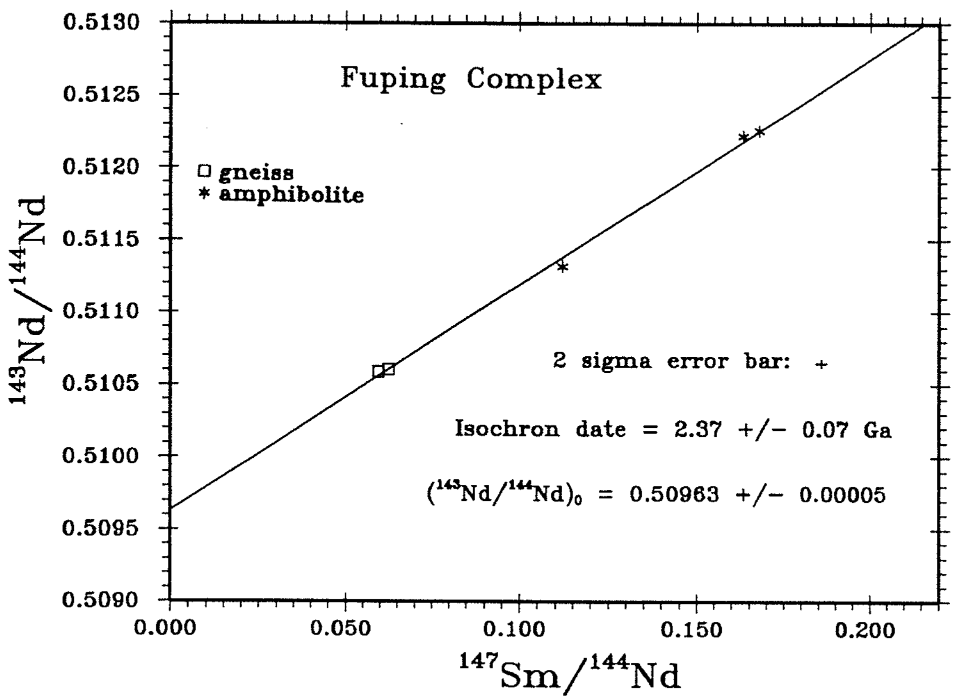

Figure 4-20. Sm-Nd isochron plot for the amphibolites and gneisses from the Fuping Complex.

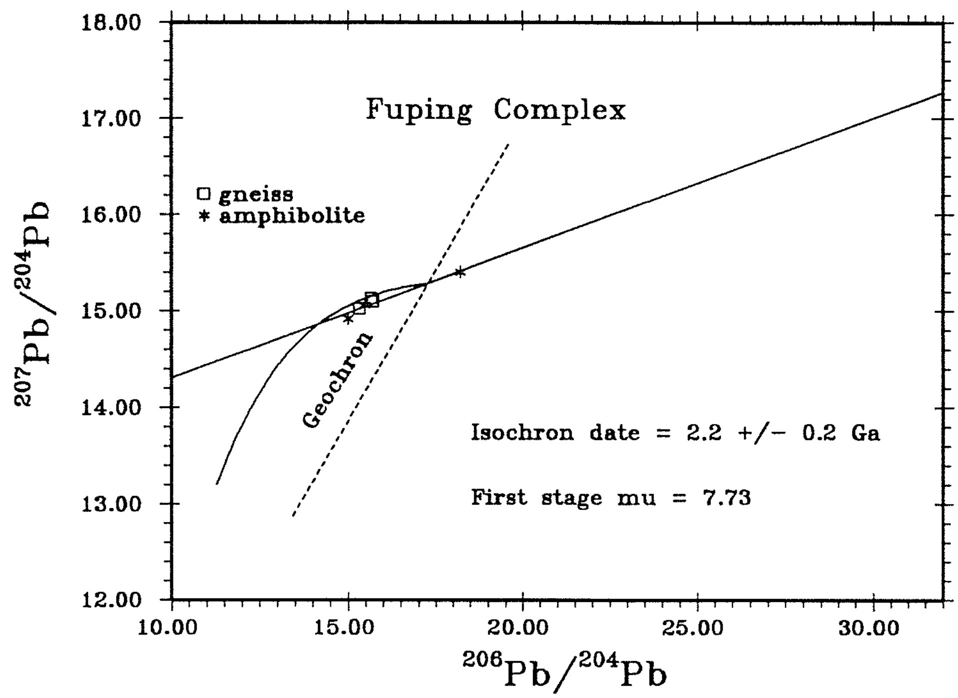

Figure 4-21. Whole rock Pb plot for the amphibolites and gneisses from the Fuping Complex.

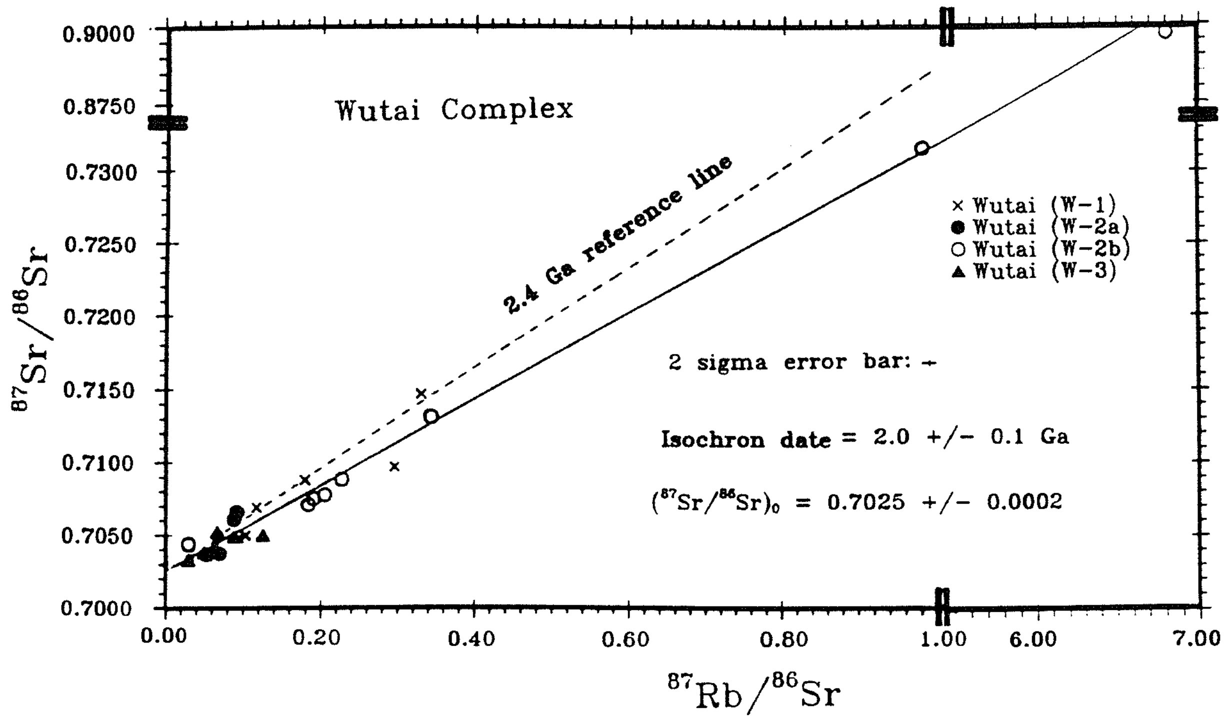

Figure 4-22. Rb - Sr isochron plot for the metavolcanic rocks from the Wutai Complex.

Four amphibolites from the W-1 define a Sm-Nd isochron of 2.2 +/- 0.1 Ga with $(^{143}Nd/^{144}Nd)_0$ = 0.50984 +/- 0.00015 or $\epsilon_{Nd}(T)$ = 0.5±1.0 (Fig. 4-23). Nd depleted mantle model dates are 2.33, 2.65, 2.71 Ga. One sample with Sm/Nd greater than chondrite does not give a realistic model date.

Li et al. (1990) reported a Sm-Nd isochron of 2.25 Ga for W-2b. We analyzed two greenschists from the same volcanic cycle. Combining our data with their data we derive a Sm-Nd isochron of 2.4 +/- 0.1 Ga with $(^{143}Nd/^{144}Nd)_0$ = 0.5096 +/- 0.0001 or $\epsilon_{Nd}(T)$ = 1.2±0.9 (Fig. 4-24). Nd depleted mantle model dates from all these samples are between 2.39 and 2.51, with one exception of 2.73 Ga.

When plotting all the analyses of Wutai complex, including two from metabasalts of the W-3, we derive a composite Sm-Nd isochron of 2.26 +/- 0.06 Ga with $(^{143}Nd/^{144}Nd)_0$ = 0.50974 +/- 0.00006 or $\epsilon_{Nd}(T)$ = 1.1±0.5 (Fig. 4-25).

Two amphibolites from W-1, two greenschists from the W-2a, five from W-2b, and two metabasalts from the W-3 define a Pb-Pb isochron of 2.27 +/- $^{0.06}_{0.07}$ Ga with a first stage growth μ = 7.73. (Fig. 4-26).

Hutuo Group:

Four metabasalts are scattered on the Rb-Sr isochron plot (Fig. 4-27). No Rb-Sr age can be calculated. Three metabasalts are close to one another on the Sm-Nd isochron plot (Fig. 4-28) so no isochron is defined but all lie close to a 2.4 Ga reference line. The Nd depleted mantle model dates are 2.32, 2.34, and 2.62 Ga. Five metavolcanics are scattered on the Pb-

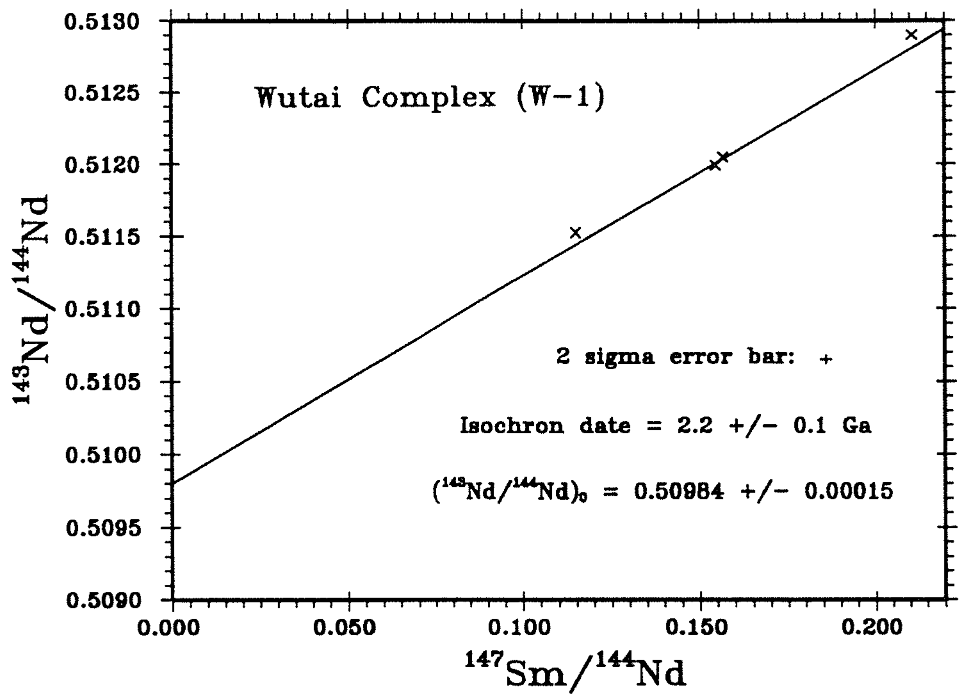

Figure 4-23. Sm - Nd isochron plot for the amphibolites from the Wutai Complex (W-1).

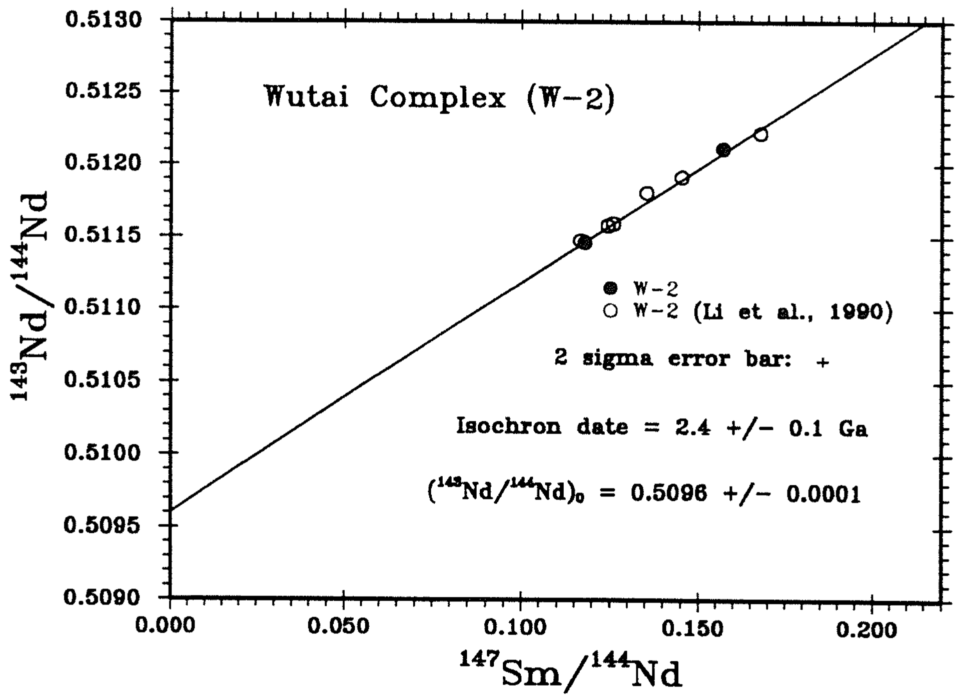

Figure 4-24. Sm - Nd isochron plot for the greenschists from the Wutai Complex (W-2). Six analyses from Li (1986) are also plotted.

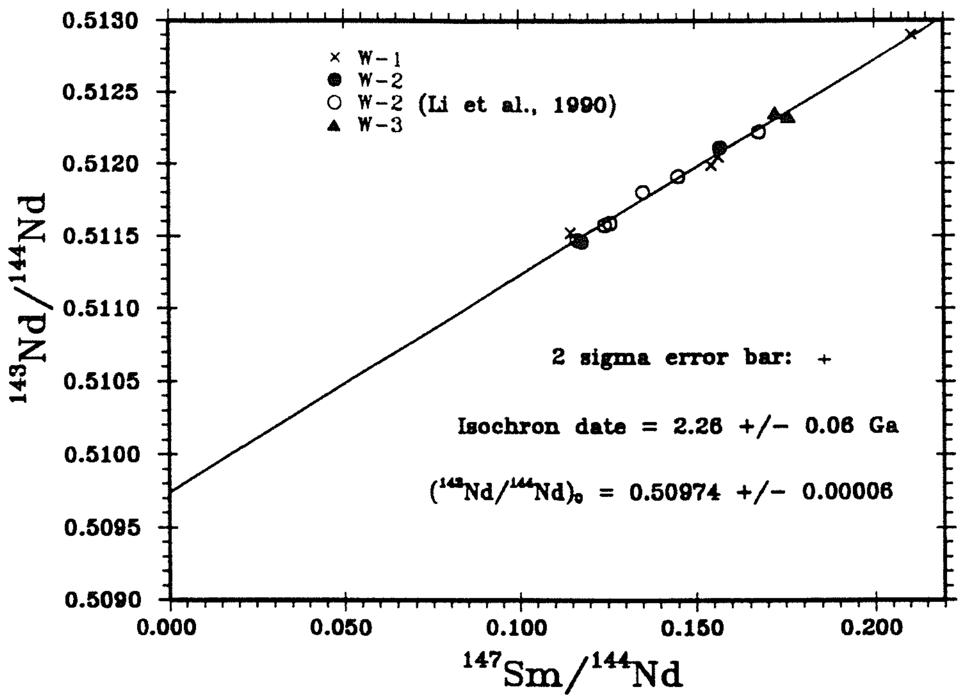

Figure 4-25. Composite Sm - Nd isochron plot for all the metabasic samples from the Wutai Complex.

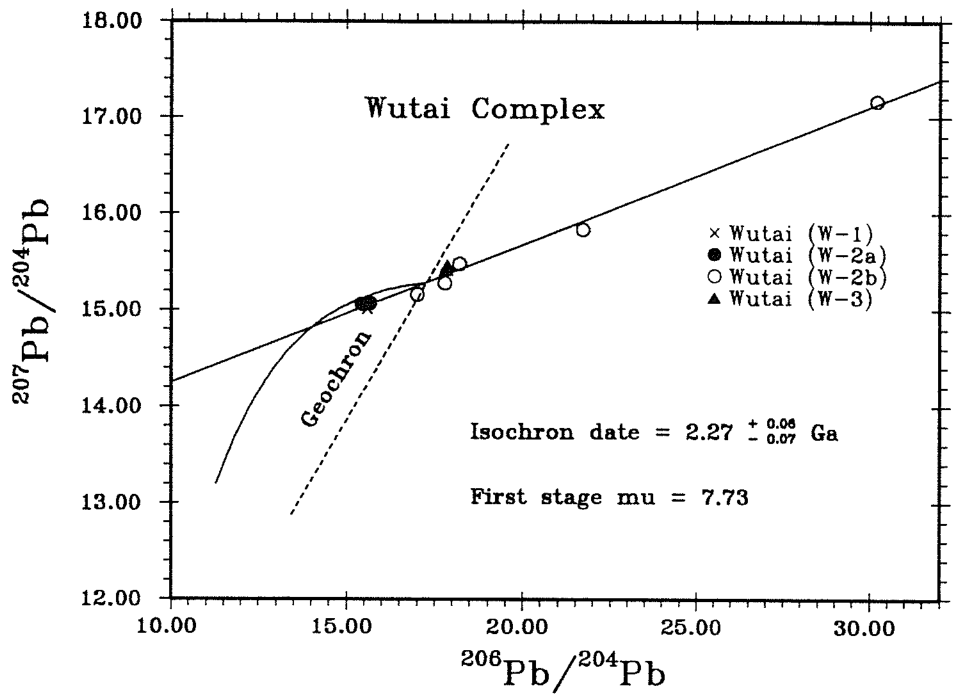

Figure 4-26. Whole rock Pb plot for all the metabasic samples from Wutai Complex.

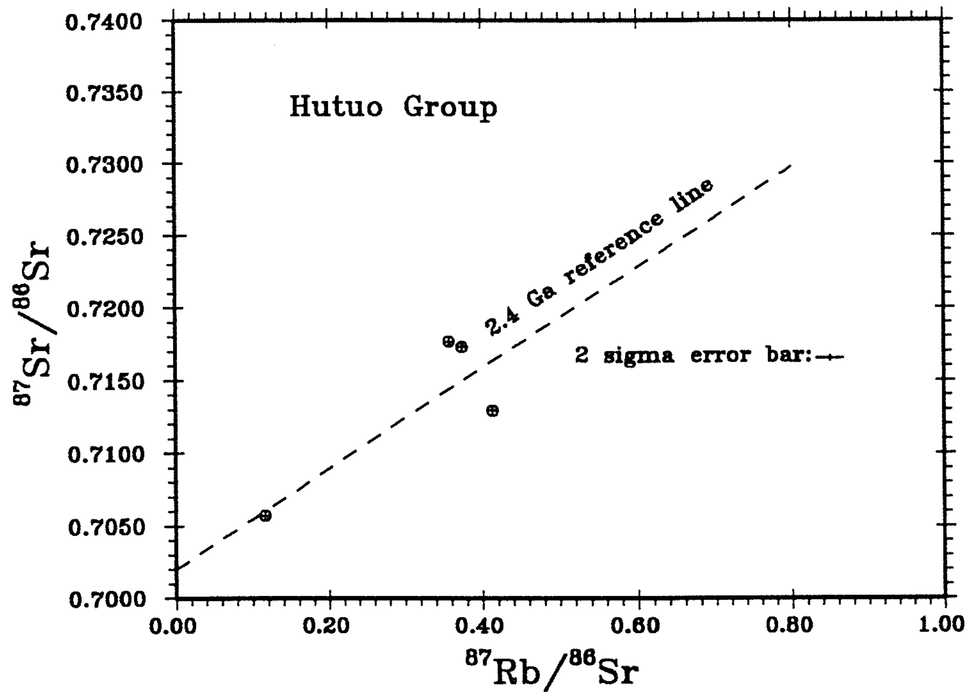

Figure 4-27. Rb - Sr isochron plot for the mebasaltic samples from the Hutuo Group.

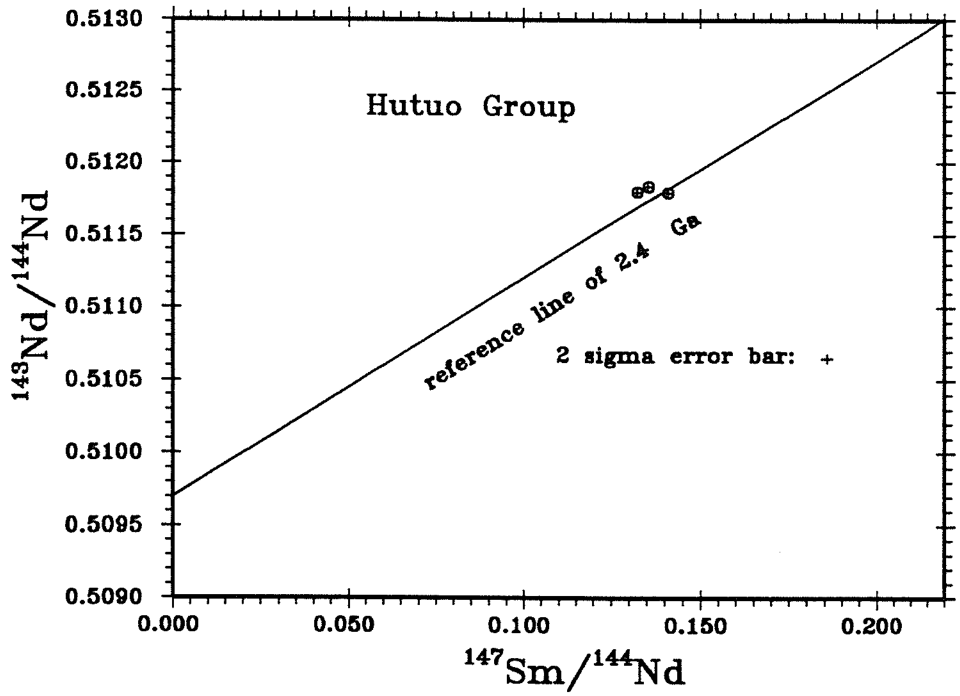

Figure 4-28. Sm - Nd isochron plot for the metabasaltic samples from the Hutuo Group.

Pb plot (Fig. 4-29) so isochron date and model μ cannot be calculated.

Lanzishan Granite:

Five samples from Lanzishan Granite define a 2.48 +/- 0.03 Ga Rb-Sr isochron with $(^{87}Sr/^{86}Sr)_0$ = 0.7076 +/- 0.0014 (Fig. 4-30). Its Sr depleted mantle dates are 2.6 to 2.7 Ga. Five samples from this granite are close to one another in Sm-Nd isochron plot (Fig. 4-31). The Nd depleted mantle model dates are 2.43 to 2.68 Ga. Four samples from the Lanzishan Granite define an isochron on the Pb-Pb plot which gives a date of 1.9 +/- $^{0.4}_{0.6}$ Ga with a first stage growth μ = 8.38 (Fig. 4-32), the line being largely controlled by a single point.

Chechang Granite and Wangjiahui Granite:

Four samples from the Chechang Granite define a 2.3 +/- 0.5 Ga Rb-Sr isochron with $(^{87}Sr/^{86}Sr)_0$ = 0.7011 +/- 0.0032 (Fig. 4-30), largely controlled by one point. Its Sr depleted mantle model dates are 1.9 to 2.5 Ga. Three samples from the Wangjiahui Granite do not define a Rb-Sr isochron with a reasonable initial ratio. A maximum age 2.24 Ga is calculated by assuming an initial ratio 0.701. The Sr depleted mantle model dates are 2.2 to 2.3 Ga (Fig. 4-30). One sample from the Chechang Granite has been analyzed for Sm-Nd isotopic composition which yield a Nd depleted mantle model date of 2.46 Ga. Three samples from Chechang Granite define a Pb-Pb isochron of 2.3 +/-0.1 Ga with a first stage growth μ = 7.51 (Fig. 4-33).

IV-4. Age constraints

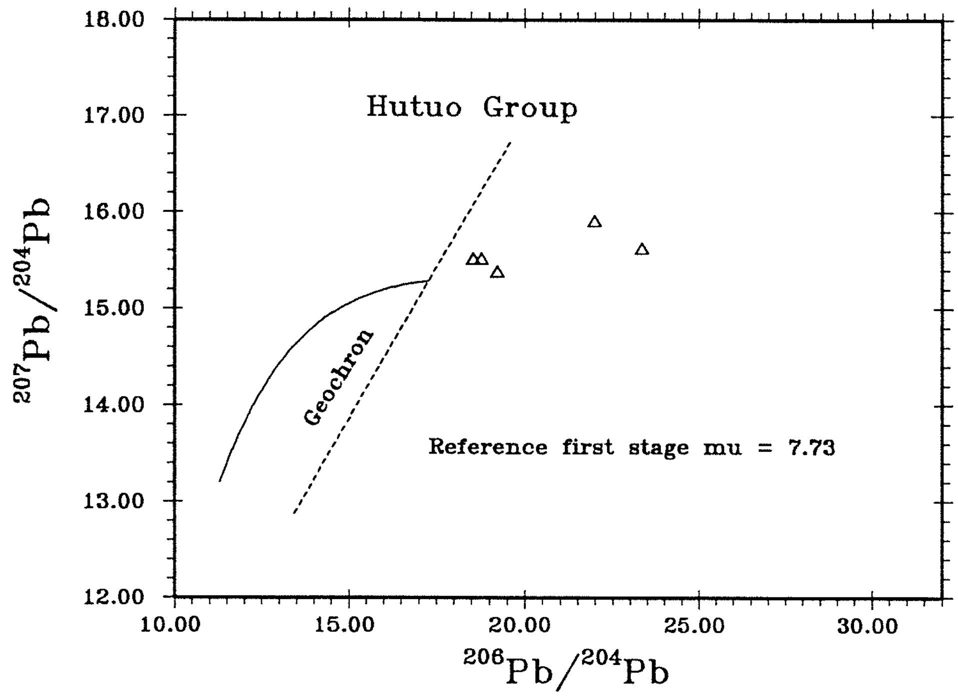

Figure 4-29. Whole rock Pb plot for the metabasaltic samples from the Hutuo Group.

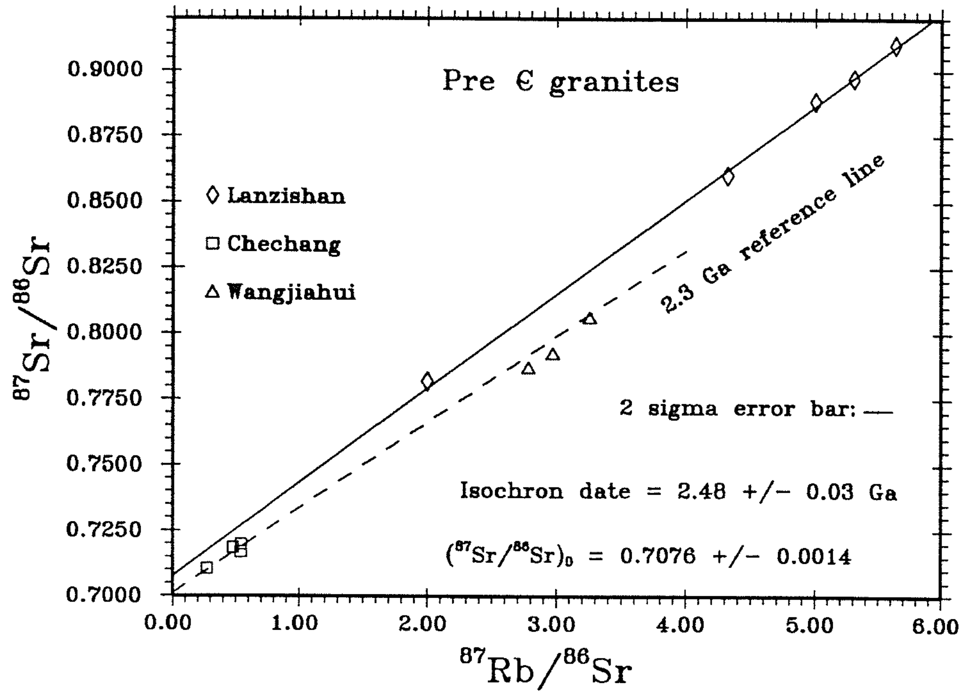

Figure 4-30. Rb - Sr isochron plot for samples from Lanzishan, Chechang, and Wangjiahui granitic bodies. The 2.48 Ga isochron is defined by five samples from the Lanzishan Granite. Four samples from the Chechang Granite give a crude age of 2.3 +/- 0.5 Ga with lower initial ratio 0.7011 +/- 0.0032. A maximum age for the Wangjiahui Granite, represented by three samples, is 2.24 Ga (0.701 initial ratio assumed).

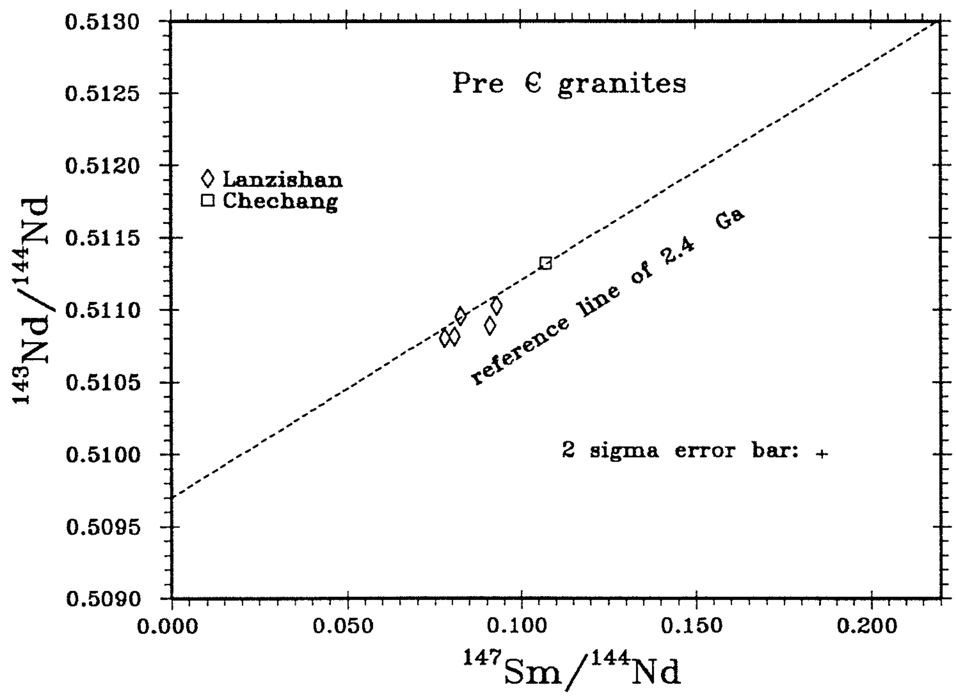

Figure 4-31. Sm - Nd isochron plot for Lanzishan, and Chechang granitic bodies.

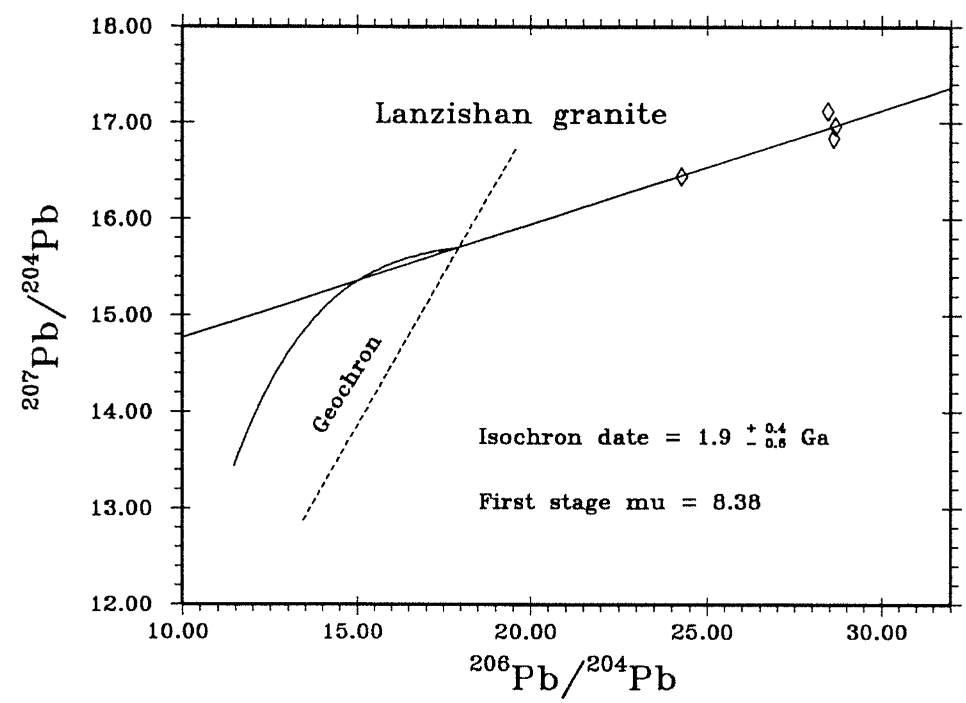

Figure 4-32. Whole rock Pb plot for the Lanzishan Granite.

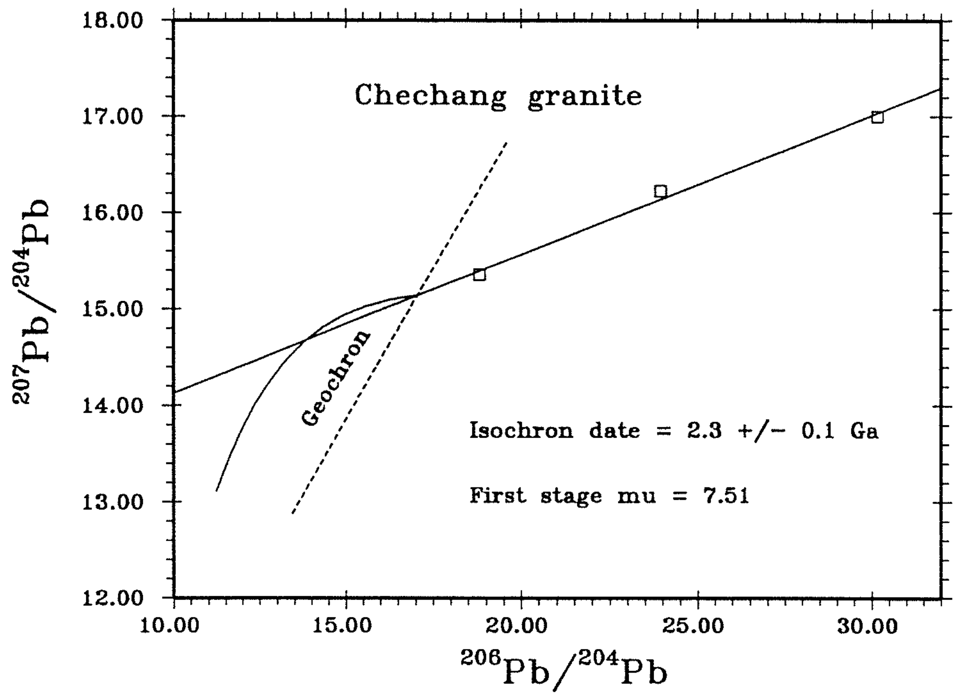

Figure 4-33. Whole rock Pb plot for the Chechang Granite.

Different dating techniques give somewhat inconsistent dates for the Precambrian rock systems in the Wutaishan and Taihangshan region. The reason for this could be, as in case of the Kuandian Complex, isotopic resetting or post magmatic open system behaviour. The region was also tectonically active over prolonged periods in the Precambrian and was reactivated in the Mesozoic (Yanshanian orogeny) and Cenozoic. We will use the same criteria as for the Kuandian Complex to constrain the age of Early Precambrian rocks from the Wutaishan and Taihangshan region.

Fuping Complex:

The maximum depositional age for the Fuping Complex is 2.8 Ga, the detrital zircon U-Pb upper intercept age (Liu et al., 1985). The minimum formation age is 2.47 Ga, the euhedral zircon U-Pb upper intercept age interpreted as a metamorphic event (Liu et al., 1985). The Nd depleted mantle model dates for the amphibolites are between 2.48 and 2.60 Ga, those of gneisses are 2.43 to 2.46 Ga. Spread of Nd model dates could be due to the following causes:

(1). Rocks were formed at different times. Field observations, however, indicate that it is unlikely that the Fuping gneisses are much younger than the amphibolites.

(2). Rocks are heterogeneously contaminated or they came from different sources. Because the gneiss is more crustal in chemical composition, erroneously old Nd model ages could arise for the gneiss. For example, 2.7-2.8 Ga gneiss from Anshan

Complex, Liaoning Province, NE China, gives Nd model dates up to 3.61 Ga (Qiao et al., 1990). The Fuping gneisses, however, have younger model dates than the Fuping amphibolites. This makes contamination an unlikely explanation for the spread of Nd dates.

(3). Rocks are from a common source defined by the average mantle evolution curve, but isotopically reset or partially reset by a later event (Fig. 3-45). In this case, the model date calculated from true average Sm/Nd ratio and $\epsilon_{Nd}(0)$ will be identical to the true age. The average Sm/Nd of Fuping complex probably lies between the ratios of the gneisses and the amphibolites. Thus the Fuping gneiss may yield model date younger than their true mantle separation age, and the Fuping amphibolites may produce model dates older than their true mantle separation age. By this interpretation the formation age of the Fuping Complex is possibly older than 2.46 and younger than 2.60 Ga. It is unlikely that the average Sm/Nd ratio of the protolith of Fuping Complex was higher than that of any amphibolite, which would be required to suggest a true mantle separation age older than 2.6 Ga. This interpretation is also supported by the younger Sm-Nd isochron date (2.37 Ga).

(4). Rocks are from a common source that is more enriched than the average mantle evolution curve. In this case, all the depleted mantle model dates will be older than the true mantle separation age, and the higher the Sm/Nd ratio of a rock, the older the model dates. Given a 2.47 Ga euhedral zircon upper intercept age, it is unlikely that the true age of Fuping

Complex is younger than 2.43 Ga, the youngest Nd model date, so this explanation is ruled out.

(5). Rocks are from a common source that is more depleted than that defined by the average mantle evolution curve (Fig. 3-44). For example, 3.5 Ga old amphibolites from Qianxi Complex, Hebei Province, 450 km northeast of the study region, give initial ϵ_{Nd} about +2 higher than the mantle curve (Huang et al., 1986; Jahn et al., 1987; Qiao et al., 1987). The calculated Nd depleted mantle model date for a rock from this highly depleted source will be younger than the true mantle separation age, which can be defined by Sm-Nd isochron if the system remains closed after rock formation. Moreover, the higher the Sm/Nd ratio of a rock, the younger the model date. However the Sm/Nd isochron date for the Fuping Complex is younger than the calculated Nd model dates, and the Fuping amphibolites (with high Sm/Nd ratios) yield old model dates while the Fuping gneisses (with low Sm/Nd ratios) give young model dates. This makes the more depleted source hypothesis unlikely.

The only possibility that the Fuping Complex is older than 2.6 Ga is that its source was more depleted than the depleted mantle curve (Fig. 3-44) and isotopically reset or partly reset by a later event. In this case, the true age will be older than all the model ages and rocks with higher Sm/Nd ratio may give Nd model ages older than those with low Sm/Nd.

The other Archean rocks from the Sino-Korea Craton show high initial ϵ_{Nd}. The 3.5 Ga Qianxi amphibolites have average ϵ_{Nd} +2.0 higher than the mantle curve. 2.7 Ga amphibolites from

Liaoning and Jilin Provinces, NE China possess an ϵ_{Nd} +1.8 higher than the mantle curve (Jahn and Ernst, 1990; Qiao et al., 1990). 2.7 Ga amphibolites from Taishan Complex, Shandong Province have a ϵ_{Nd} +1.1 higher than the mantle curve (Jahn et al., 1988). The average Fuping Sm/Nd and ϵ_{Nd} extrapolates to 2.62 Ga with ϵ_{Nd} = +4.3, which is +2 higher than the mantle curve. Even if high depleted Archean mantle is present in the Fuping area, we can still conclude that the Complex is very unlikely to be older than 2.62 Ga.

From the above reasoning, we infer that the mantle separation time for the Fuping Complex is about 2.6 Ga, slightly older than the 2.56 Ga Lanzishan Granite. The 2.5 Ga upper intercept U-Pb age of euhedral zircons is probably related to a metamorphic event.

Constrained by the 2.47 Ga U-Pb zircon upper intercept age, and the Nd model dates and their relationship to Sm/Nd ratios, the 2.37 +/- 0.07 Ga Sm-Nd and 2.34 +/- 0.42 Rb-Sr isochron dates can not be treated as true formation age of the Fuping Complex. Instead the isochron dates can be interpreted as a consequence of isotopic resetting at some equal or younger time or artifacts of mixing lines. We infer that the isochron dates probably represent the formation age reset by a later metamorphic event or events, or even recent alteration. The Fuping amphibolite and gneiss, separately, have similar Nd model dates, and this makes a mixing line hypothesis unlikely. Uniform initial Nd isotopic ratios in different rock types have been observed in several studies, for instance, different komatiites of the Onverwacht Group (Hamilton et a., 1979a; Jahn et al., 1982) and amphibolites and gneisses from the Taishan Complex (Jahn et al., 1988).

The 2.2 +/- 0.2 Ga Pb-Pb isochron, likewise, must be the result of younger metamorphic events in the region.

Wutai Complex:

The Nd depleted mantle dates are very close to 2.5 Ga in the W-2 (including data from Li et al., 1988). The 2.3 to 2.4 Ga isochron dates of Sm-Nd and Pb-Pb have probably been reset to some degree by later metamorphic events in the region. An alternative explanation is that the Wutai Complex formed 2.3 to 2.4 Ga ago from partial melting of the underlying Fuping Complex. However, the chemical composition of the Wutai rocks does not favour this suggestion and the two published 2.5 Ga U-Pb zircon upper intercept ages support the conclusion that the Wutai Complex formed 2.5 Ga ago, and is not much younger than the Fuping Complex.

Hutuo Group:

The previously published U-Pb upper intercept age of zircons from a metabasalt is 2.37 Ga (Wu et al., 1986). Nd depleted mantle model dates are 2.32, 2.34 and 2.62 Ga. We infer that the lower part (volcanic series) of the Hutuo Group formed about 2.4 Ga ago, very early in the Proterozoic, in a within-plate environment, as indicated by its petrochemistry. The scatter in Nd model dates, and Rb-Sr, Pb-Pb isochron plots is probably due to crustal contamination and post-emplacement regional metamorphism.

Granitic intrusions:

A 2.48 +/- 0.03 Ga Rb-Sr isochron is well defined for the Lanzishan Granite, with $(^{87}Sr/^{86}Sr)/_0$ = 0.7076 +/- 0.0014. The Nd depleted mantle dates of the Lanzishan Granite are 2.43 to 2.68 and average 2.55 Ga. The published U-Pb zircon age for this granite is 2.56 Ga (Liu et al., 1985). For Rb-Sr system of this granite, only 0.1 Ga is needed to change $^{87}Sr/^{86}Sr$ from the mantle curve to 0.7076 at 2.48 Ga. We thus interpret that this granite was formed around 2.56 Ga, with the Rb-Sr systems reset about 0.1 Ga later. The 2.56 Ga age separates the Fuping Complex and Wutai Complex. The Pb-Pb isochron age for this granite, 1.9 +/- $^{0.4}_{0.6}$ Ga, is presumably reset by later metamorphic events.

As mentioned above, two granites, the Ekou Granite and Shifo Granite, both intruding the Wutai Complex, have 2.52 and 2.51 Ga zircon U-Pb ages, respectively.

We also obtained a 2.46 Ga Nd depleted mantle model date and 2.3 Ga Rb-Sr and Pb-Pb isochron dates for the Chechang Granite. As in other suites, the Rb-Sr and Pb-Pb isochrons are probably somewhat reset by later events.

The maximum Sr model date for the Wangjiahui Granite is 2.24 Ga. Such 2.3 to 2.4 Ga dates are not only shown in these later granites, but they also frequently appear as times of resetting in the Fuping and the Wutai complexes. Widespread resetting evidently ceased at about volcanic eruption time of the Hutuo Group.

There is geochronological evidence that Archean supracrustal rocks are intruded by multiple granites in a relatively short time. For example, both 2.6 Ga and 2.4-2.5 Ga granites intrude the 2.7 to 2.75 Ga Taishan Complex (Jahn et al., 1988). We postulate that in the Wutaishan and Taihangshan area at least three Precambrian granitic events can be inferred, one at 2.56 Ga (intruding the Fuping Complex), others at 2.3 to 2.5 Ga (intruding Wutai Complex), and the final one at 1.9 Ga (high-K, intruding Hutuo Group, Bai, 1986, not studied in this investigation).

IV-5. Discussion

Alkali metasomatism:

The amphibolitic samples from the Fuping and the Wutai complexes (W-1), and the greenschists from the upper cycle of the W-2 possess high alkali, high K_2O/Na_2O ratio, and high Rb content. Sr concentrations are generally comparable with common Archean basalts (e.g. Jahn and Sun, 1979). High-Rb is also observed in the Qianxi amphibolites (Jahn et al., 1987), the Taishan amphibolite (Jahn et al., 1988), and the Kuandian Complex (this study). The cause can be attributed to metamorphic and metasomatic effects of later intrusion of granitic magmas.

For the Fuping gneisses, chondrite normalized Nd_N/Sm_N = 3.11 to 3.26, and Sm_N = 10.22 to 13.88. This might reflect an extremely fractionated REE pattern with HREE depletion. This REE character is typical for Archean gneisses of TTG composition

(Arth and Hanson, 1975; Glikson, 1976, 1979; Tarney et al., 1979). However they plot in the granite (s.s.) field in Ab-An-Or plot of O'Connor (1965). This feature is also found in the Qianxi gneiss (Jahn et al., 1987) and the Lanzishan Granite in this study. Weaver (1980) invoked a metasomatic fluid to explain high K and Rb feature of acid charnockite from Madras. Jahn et al. (1987) interpreted that the Qianxi gneiss had an original TTG composition but was modified through assimilation, contamination, or veining by late granite and pegmatite. We accept this explanation for the Fuping gneiss based on the widely distributed red granitic and pegmatitic veins in the Fuping gneiss.

Resetting of isotopic systems:

An alkali element metasomatic redistribution event can be tentatively invoked as one cause of the isotopic resetting of Rb-Sr, Pb-Pb, and probably Sm-Nd systems in the Archean rocks of study area. Rb-Sr and Pb-Pb isotopic resetting are quite common for high-grade metamorphic rock systems (e.g. Jahn et al., 1987). But the Sm-Nd system can either remain little disturbed up to granulite facies, e.g. in case of the Lewisian gneiss (Hamilton et al., 1979b) and the retrogressed Qianxi amphibolite (Jahn et al., 1987), or significantly disturbed in the granulite facies, e.g. in case of the Napier Complex, Antarctica (DePaolo et al., 1982; McCulloch and Black, 1984).

The Sm-Nd systems of Archean metabasic rocks, either in amphibolite or greenshist facies, from the Wutaishan and

Taihangshan area have been significantly disturbed. The Sm-Nd isochron dates are all younger than the U-Pb zircon upper intercept ages. In contrast, Archean samples from other parts of the Sinokorean Craton mostly give old Sm-Nd isochron dates, i.e. 3.5 Ga Qianxi Complex, the 2.7-2.8 Ga Taishan Complex, and the 2.7-2.8 Ga Anshan Complex.

Although the Sm-Nd systems were disturbed, the reset isochrons still give positive ϵ_{Nd} values for the Fuping and the Wutai complexes. The true initial ϵ_{Nd} at their formation times will be even higher. This indicates that igneous precursors for the Fuping and the Wutai complexes are derived from a depleted mantle source.

Stratigraphic and tectonic revisions:

The high-grade Fuping Complex is not much older than the lower-grade Wutai Complex. This does not agree with the attempt to make the age of Fuping Complex 2.8 Ga or older (Bai, 1986); the Fuping Complex is not one of the older continental nuclei of Sinokorean Craton, as previously suggested by Ren (1987). The old nuclei of the Sino-Korean Craton are 3.5 Ga old Qianxi supracrustal rocks in eastern Hebei Province, and ≥3.0 Ga Qingyuan Complex and Tiejiashan and Lishan granites in the Liaoning Province. The Taishan Complex farther south, and the Anshan Complex farther northeast, formed at 2.7 to 2.8 Ga ago. The Fuping complex to the southwest formed about 2.6 Ga ago. Nd isotopes reveal that there was no significant amount of continental crust present before 2.6 Ga in the Wutaishan and

Taihangshan region.

Some authors have put the Wutai Complex in the Early Proterozoic (e.g. Yang et al., 1986). Accumulated isotopic data render this hypothesis obsolete. The Wutai complex formed at least 2.5 Ga ago, and is thus Archean by modern definitions (Plumb, 1986).

IV-6. Summary

The Fuping Complex was derived from mantle about 2.6 Ga ago and experienced a major metamorphic overprint about 2.4 Ga ago and/or more recently.

The Wutai Complex was derived from mantle ≥ 2.5 Ga ago and was likewise metamorphosed about 2.4 Ga ago and/or more recently.

Metabasaltic rocks of the Hutuo Group were derived from the mantle nearly 2.4 Ga ago.

No significant amount of continental crust existed before 2.6 Ga in this region. From 2.6 to 2.5 Ga is the major continental growth period in the Wutaishan and Taihangshan Area. In this period, Fuping and Wutai complexes formed sequentially from depleted mantle sources. The Fuping Complex and most of the Wutai Complex formed in a modern island arc-like environment, with exception that the lower cycle of the W-2 formed in a modern MOR-like environment (rifted oceanic arc?) and that subgreenschist-facies rocks of the Wutai Complex (W-3) formed in an environment transitional between modern within plate and plate margin settings. Many calcalkaline I-type granitic bodies formed in this region at about 2.55 and 2.50 Ga, the older ones intruding Fuping Complex and the later ones intruding both Fuping and Wutai complexes.

About 2.4 Ga a major period of deformation and metamorphism affected in the region. Some granites may have formed between 2.3 and 2.5 Ga. At that time, the Fuping and the Wutai complexes were under greenschist to amphibolite facies metamorphic conditions. They were deeply eroded before the Hutuo Group metasediments were deposited just after 2.4 Ga ago, with minor associated within-plate volcanic rocks. The Hutuo Group, and presumably its basement, underwent a later low-greenschist metamorphic and high-K granite emplacement event about 1.8 to 1.9 Ga ago.

This study adds new evidence that Chinese Archean mantle has positive $\epsilon_{Nd}(T)$ values. The Archean igneous rocks from the Sinokorean Craton formed at different times from heterogeneous and depleted mantle sources.

V. EARLY PRECAMBRIAN ROCKS IN SHANDONG PROVINCE

The Early Precambrian rocks in the Shandong Province are called Taishan Complex, west of the Tan-Lu Fault, and Jiaodong Complex, east of the Tan-Lu Fault (Fig. 1-1 and 1-2).

V-1. Taishan Complex and associated granitic rocks

The Taishan Complex is exposed in the Taishan, Mengshan and Lushan area, western Shandong Province. It is composed of grey gneiss, amphibolite, fine-grained gneiss, schist and quartzite. These rocks have generally undergone amphibolite-facies metamorphism.

The Taishan gneisses have TTG compositions and have been interpreted by Ying (1980) to be metamorphosed volcano-sedimentary piles, and the amphibolites that occur as enclaves in the Taishan gneiss to be residue of partial melting of the Taishan gneiss. Nevertheless, based on the isotopic and rare earth geochemical character of the Taishan amphibolite and gneiss, Jahn et al. (1988) considered that the Taishan amphibolite and gneiss are a possible bimodal magmatic suite.

Jahn et al. (1988) reported a 2.69 ± 0.08 Ga Rb-Sr isochron, with $(^{87}Sr/^{86}Sr)_0 = 0.7006 \pm 0.0004$, and a 2.70 ± 0.04 Ga Sm-Nd isochron, with $\epsilon Nd(T) = +3.3 \pm 0.3$, for the Taishan amphibolite and gneiss (Table 5-1). The Taishan amphibolite alone defined 2.77 Ga Rb-Sr and 2.74 Ga Sm-Nd isochrons. The authors inferred that the precursor basic and tonalitic magmas of the Taishan Complex were derived from the mantle and emplaced

Table 5-1. Isotopic dates for Early Precambrian rocks from Shandong Province

Rock type	Date (Ga±2σ)	Method	Source
Taishan amphibolite & gneiss	2.69±0.08 @I_{Sr}=0.7006±4	Rb-Sr isochron	Jahn et al., 1988
	2.70±0.04 @εNd(T)=+3.3±0.3	Sm-Nd isochron	Jahn et al., 1988
Taishan amphibolite	2.69	Nd T_{DM}	this study
	2.3±0.2 @I_{Sr}=0.7024±14	Rb-Sr isochron	Sun and Armstrong, 1986
	2.41±0.07	K-Ar hornblende	Sun and Armstrong, 1986
Puzhaosi Diorite & Zhongtainmen Granite	2.6±0.1 @I_{Sr}=0.7008±8	Rb-Sr isochron	Jahn et al., 1988
	2.45 to 2.55	Nd T_{DM}	Jahn et al., 1988
Hushan Granite	2.56±0.01	U-Pb zircon upper intercept	Jahn et al., 1988
Aolaishan Granite	2.49±0.05 @I_{Sr}=0.7028±11	Rb-Sr isochron	Jahn et al., 1988
	2.45±0.14 @εNd(T)=+1.0±1.7	Sm-Nd isochron	Jahn et al., 1988
	2.52 to 2.76	Nd T_{DM}	Jahn et al., 1988
Taishan pegmatite	2.4±0.1 @I_{Sr}=0.733±18	Rb-Sr isochron	Sun and Armstrong, 1986
	2.30±0.06	K-Ar muscovite	Sun and Armstrong, 1986
Jiaodong gneiss	2.6 to 2.8	U-Pb zircon	Liu (unpublished)

about 2.7-2.75 Ga ago. We also obtained a 2.69 Ga Nd T_{DM} for the Taishan amphibolite (Table 5-2). Sun and Armstrong (1986) obtained a 2.3 ± 0.2 Ga Rb-Sr isochron, with $(^{87}Sr/^{86}Sr)_0$ = 0.7024 ± 0.0014, for the Taishan amphibolites (Table 5-1).

The Taishan amphibolites mostly have a flat REE pattern similar to Archean low-K tholeiites. However, the Taishan amphibolites have much more Rb and higher Rb/Sr ratio than modern arc tholeiite. Jahn et al. (1988) considered two possible causes for this phenomenon, mantle metasomatism shortly before the melting event and metamorphic enrichment. In favour of the latter possibility, and considering the low initial Sr isotopic ratio, they proposed that the Rb enrichment is due to amphibolite-facies metamorphism that happened shortly after magma emplacement.

Sun and Armstrong (1986) reported a 2.41 ± 0.07 Ga K-Ar hornblende date for the Taishan amphibolite. This indicates that the amphibolite-facies metamorphism ended by 2.4 Ga ago.

Granitic rocks intruding the Taishan Complex:

Jahn et al. (1988) obtained a 2.6 ± 0.1 Ga Rb-Sr isochron, with $(^{87}Sr/^{86}Sr)_0$ = 0.7008 ± 0.0008 for the Puzhaosi Diorite and Zhongtianmen Granodiorite. The Nd T_{DM}'s of these rocks are between 2.45 and 2.55 Ga. The authors inferred that these dioritic rocks were mantle-derived. They also reported a 2.56 ± 0.01 Ga U-Pb zircon upper intercept date for the Hushan Granite.

Table 5-2. Sm-Nd isotopic data with 2σ errors for samples from Taishan Complex

Sample		Sm ppm$^+$	Nd ppm	$^{147}Sm/^{144}Nd$	$^{143}Nd/^{144}Nd$	$\epsilon Nd(0)$	T_{DM}^*
Taishan Complex							
SYB-5		2.698	8.72	0.1868	0.512562	-1.2	2.73
	+/-	0.002	0.01	0.0003	0.000014	0.3	0.09
SYE-1		2.108	6.22	0.2047	0.512819	3.8	--
	+/-	0.002	0.01	0.0004	0.000014	0.3	--

+ Sm and Nd concentrations were determined by isotopic dilution on a VG-30 mass spectrometer, $^{143}Nd/^{144}Nd$ ratios were measured by a VG-354 at the University of Alberta. 2 sigma errors listed in this table do not include calibration and replication uncertainties. 0.005% and 1.0% were used for $^{143}Nd/^{144}Nd$ and $^{147}Sm/^{144}Nd$ in regression calculations.

* T_{DM}: depleted mantle model date of DePaolo (1981), errors are propagated from standard deviations of $^{147}Sm/^{144}Nd$ and $^{143}Nd/^{144}Nd$.

Jahn et al. (1988) derived a 2.49 ± 0.05 Ga Rb-Sr isochron, with $(^{87}Sr/^{86}Sr)_0$ = 0.7028 ± 0.0011, and a 2.45 ± 0.14 Ga Sm-Nd isochron, with $\epsilon Nd(T)$ = + 1.0 ± 1.7, for the Aolaishan Granite. Nd T_{DM}'s for this granite are between 2.52 and 2.76 Ga. They interpreted the Aolaishan Granite to be derived from the partial melting of the Taishan grey gneisses. Sun and Armstrong (1986) obtained a 2.4 ± 0.1 Ga Rb-Sr isochron, with $(^{87}Sr/^{86}Sr)_0$ = 0.733 ±0.018, and a 2.30 ± 0.06 Ga muscovite K-Ar date for a pegmatite intruding the Taishan Complex.

In summary, the Taishan complex was formed 2.7 to 2.75 Ga ago and has been intruded by mantle-derived granitic rocks ~2.56 Ga ago, and then intruded by the S-type Aolaishan Granite 2.45 to 2.5 Ga ago. The magmatic activity in the area ended ~2.4 Ga ago.

V-2. Jiaodong Complex

The Jiaodong Complex is exposed in eastern Shandong Province. It consists of gneiss, amphibolite, fine-grained gneiss, and some marble. These rocks have undergone amphibolite facies metamorphism.

Recent U-Pb analyses confirmed Archean ages of 2.6 to 2.8 Ga for the Jiaodong Complex (Liu, personal communication).

VI. EARLY PRECAMBRIAN ROCKS IN NORTHERN SLOPE OF QINLING MOUNTAIN BELT

VI-1. Taihua Complex

The Taihua Complex is exposed along the northern slope of the eastern Qinling Mountain Belt in Henan Province and adjacent provinces (Fig. 1-1 and 1-2). The Qinling Mountain Belt has been considered a result of continental collision in the Proterozoic (Xu and Wang, 1990), the Paleozoic (e.g. Mattauer et al., 1985) or the Mesozoic (e.g. Sengor, 1985). Amphibolites from centre of the Qinling Mountain Belt give 1.2 Ga Sm-Nd isochron, with $\epsilon Nd(T) = +5.7$, and 1.13 to 1.19 Ga Nd T_{DM} (Chen et al., 1991).

The Taihua Complex consists primarily of tonalitic gneisses and tectonically interbedded upper amphibolite to granulite grade supracrustals, e.g. metatholeiites, metapelites, and lenses of komatiitic amphibolites (Zhang et al., 1985).

Single-grain evaporation of zircons from a tonalitic gneiss of the Taihua Complex gave dates of 2.84 ± 0.01 and 2.81 ± 0.01 Ga (Kröner et al., 1986, Table 6-1).

We infer that the Taihua Complex formed 2.8 Ga ago.

VI-2. Dengfeng Complex

The Dengfeng Complex, surrounded by the Taihua Complex along the northern slope of the eastern Qinling Mountain Belt in Henan Province and adjacent provinces (Fig. 1-1 and 1-2), consists of amphibolite-grade metavolcanic and metasedimentary rocks. These rocks were intruded by large volumes of TTG and K-

Table 6-1. Isotopic dates for Early Precambrian rocks from Henan Province

Rock type	Date (Ga±2σ)	Method	Source
Taihua tonalitic gneiss	2.84±0.01 & 2.81±0.01	single zircon evaporation	Kröner et al., 1986
Dengfeng amphibolite & acid metavolcanics	2.51±0.03 @ϵNd(T)=2.2±0.8	Sm-Nd isochron	Li et al., 1987
Dengfeng metarhyodacite	2.51±0.02	U-Pb zircon concordia	Kröner et al., 1986
Shipaihe pluton	~2.52	U-Pb zircon upper intercept	Wang et al., 1987

rich granite (Zhang et al., 1985).

Li et al. (1987) obtained a 2.51 ± 0.03 Ga Sm-Nd isochron, with $\epsilon_{Nd}(T)$ = 2.2 ± 0.8, for six amphibolites and two acid metavolcanic rocks from the Dengfeng Complex (Table 6-1). Kröner et al. (1988) derived a 2.51 ± 0.02 Ga concordia U-Pb age for single zircons from a metarhyodacite of the Dengfeng Complex. A monzonite from the Shipaihe pluton intruding the Dengfeng Complex gave a ~2.52 Ga U-Pb upper intercept date (Wang et al., 1987).

We infer that the Dengfeng Complex formed 2.5 Ga ago.

VII. EARLY PRECAMBRIAN ROCKS IN INNER MONGOLIA

Sanggan Complex

The Sanggan Complex is exposed along the eastern Yinshan Range, Inner Mongolia (Fig. 1-1 and 1-2). The Sanggan Complex has been once subdivided into "Jining Group" and "Wulashan Group", which has been proven to be without sound field evidence (Yang et al., 1986).

The Sanggan Complex mainly consists of gneiss, amphibolite, quartzite, marble, semipelitic rocks and cherty iron beds. These rocks have undergone a granulite to amphibolite-facies metamorphism. Migmatite and granitic intrusions are extensive throughout.

Whole rock Rb-Sr dates of 2.45 to 2.6 Ga have been obtained for the Sanggan Complex by previous studies (Cheng et al., 1984, Table 7-1).

Sun et al. (1989) derived a 2.5 ± 0.1 Ga Rb-Sr isochron, with $(^{87}Sr/^{86}Sr)_0 = 0.701 \pm 0.002$, for granulitic rocks from the Sanggan Complex, and a 2.4 ± 0.1 Ga Rb-Sr isochron, with $(^{87}Sr/^{86}Sr)_0 = 0.703 \pm 0.003$ for the amphibolites from the Sanggan Complex. Model dates calculated from the average ratios of $^{87}Rb/^{86}Sr$ and $^{87}Sr/^{86}Sr$ and bulk earth (Cameron et al., 1981) or 0.701 Sr initial ratio (Hart and Brooks, 1977; Glikson, 1979) are both 2.6 Ga for the Sanggan granulites.

We infer that the Sanggan Complex was formed 2.5 to 2.6 Ga ago. Further Sm-Nd and U-Pb zircon work may prove that the Sanggan Complex could be as old as the Fuping Complex or even as old as the Jianping Complex.

Table 7-1. Isotopic dates for Early Precambrian rocks from Inner Mongolia

Rock type	Date (Ga±2σ)	Method	Source
Sanggan Complex	2.45 to 2.6	Rb-Sr isochrons	Cheng et al., 1984
Sanggan amphibolite	2.4±0.1 @I_{Sr}=0.701±3	Rb-Sr isochron	Sun et al., 1989
Sanggang granulite	2.5±0.1 @I_{Sr}=0.701±2	Rb-Sr isochron	Sun et al., 1989

VIII. CRUSTAL ACCRETION HISTORY OF THE SINOKOREAN CRATON IN EARLY PRECAMBRIAN TIME

1. Continental nuclei older than 3.0 Ga

The oldest supracrustal rocks of the Sinokorean Craton are shallow water deposits about 3.5 Ga old in the eastern Hebei Province (Table 2-1 and Fig. 8-1). Extensive basaltic volcanism accompanied the deposition of the sedimentary rocks. Felsic magmas intruded as plutons and erupted as volcanic layers which have been metamorphosed to grey gneiss and fine-grained gneiss. Magmatic and sedimentary processes may have lasted from 3.5 to 3.0 Ga.

Another continental nucleus has been identified in the Qingyuan area where amphibolites and grey gneiss have given ≥3.0 Ga ages (Table 3-1 and Fig. 8-1). This nucleus may extend to the Anshan area to include the ≥3.0 Tiejiashan and Lishan granites (Table 3-1 and Fig. 8-1).

2. Late Archean high-grade metamorphic complexes (2.5 to 2.8 Ga)

The Late Archean high-grade rocks are extensive in the Sinokorean Craton, surrounding the >3.0 Ga nuclei and along the south margin of the craton. These include the 2.7 to 2.8 Ga old Anshan, Longgang, and Jianping complexes in the Liaoning and Jilin provinces, Taishan and Jiaodong Complexes in the Shandong Province, and the Taihua Complex in the Henan Province (Tables 3-1, 5-1, and 6-1, and Fig. 8-2).

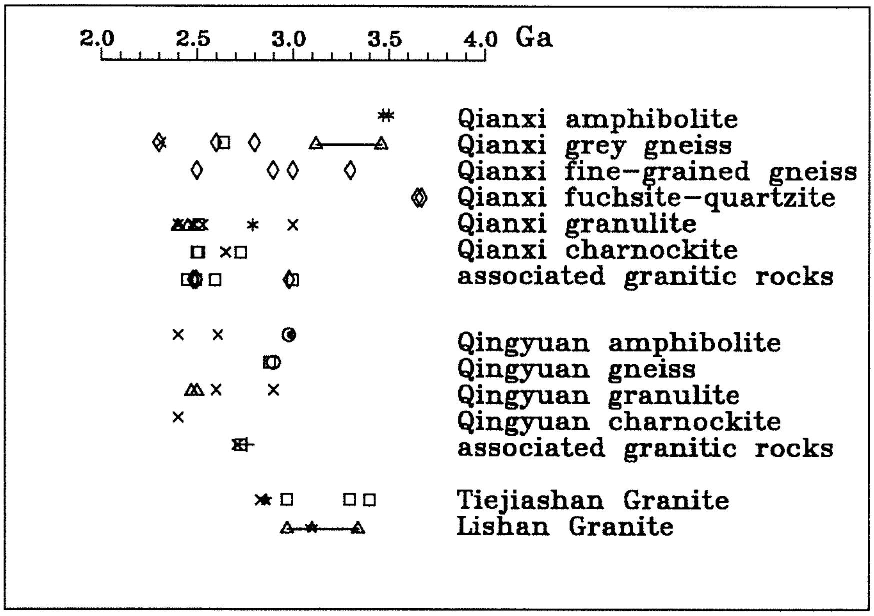

Figure 8-1. Isotopic dating results from different techniques for rocks from the Qianxi, Qingyuan complexes and associated granitic rocks, and Tiejiashan and Lishan granites. Asterisks stand for Sm-Nd isochron dates, triangles for Nd depleted mantle model dates, squares for U-Pb zircon upper intercept dates, diamonds for single zircon evaporation dates, crosses for Rb-Sr isochron dates, open circles for K-Ar dates, solid dots for $^{40}Ar/^{39}Ar$ dates, pluses for Th-Pb dates, stars for Pb-Pb whole rock isochron dates.

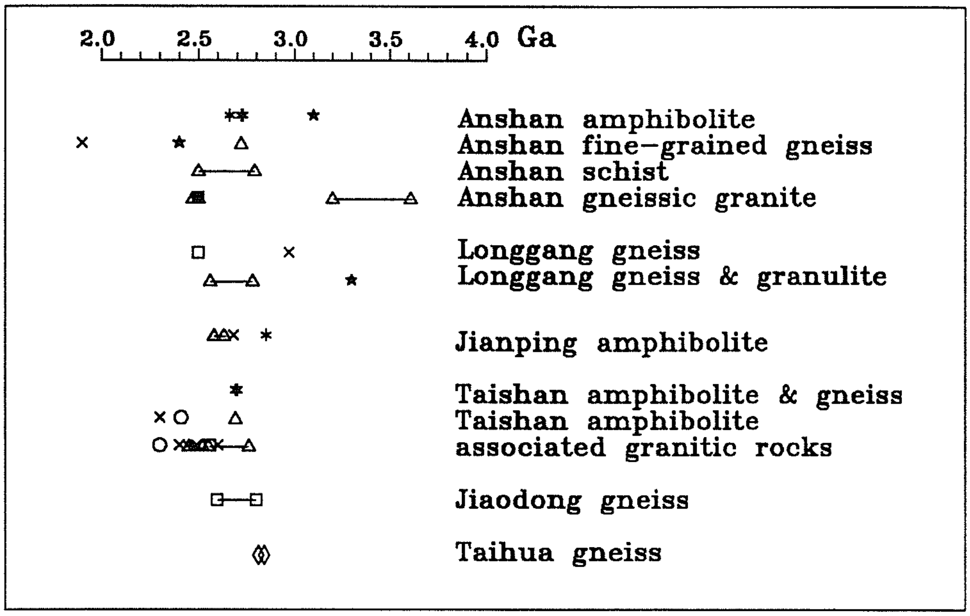

Figure 8-2. Isotopic dating results from different techniques for the Anshan, Longgang, Jianping, Taishan, Jiaodong, and Taihua complexes and associated granitic rocks. Symbols for different techniques are the same as in Figure 8-1.

The > 3.0 Ga continental nuclei have been also intruded by the 2.7 to 2.8 Ga granitic rocks.

The high-grade Fuping Complex formed ~2.6 Ga ago in Shanxi and western Hebei provinces (Table 4-7 and Fig. 8-3). Age of the Dengfeng Complex in Henan and adjacent provinces has been determined by the 2.51 Ga U-Pb zircon concordia date (Table. 6-1 and Fig. 8-3). The Sanggan Complex formed at least 2.5 to 2.6 Ga ago in Inner Mongolia (Table 7-1 and Fig. 8-3).

3. Late Archean greenstone-granite belt (≥2.5 Ga)

The Wutai Complex formed ≥2.5 Ga ago as a greenstone-granite belt in Shanxi Province (Table 4-7 and Fig. 8-3).

4. Terminal Archean granitic magmatism (~2.5 Ga)

Granitic magmatism peaked about 2.5 Ga ago in the Sinokorean Craton. These plutons overprinted all the previously formed complexes. After 2.5 Ga, magmatic activity was greatly restricted in the Sinokorean Craton.

5. Early Proterozoic continental rift (2.3 to 2.4 Ga)

Early Proterozoic volcanic rocks in the Sinokorean Craton are mainly found in the Kuandian Complex in the eastern Liaoning Province, bottom of the Hutuo Group in Shanxi Province, and the Dantazi-Zhuzhangzi Group in eastern Hebei Province.

Metavolcanic rocks of the Kuandian Complex have a composition similar to modern continental flood basalt. Granites from the Kuandian Complex have an anorogenic granite chemistry. The Kuandian Complex formed 2.3 to 2.4 Ga ago (Table 3-1 and Fig. 8-4). The Hutuo metavolcanic rocks have a within-plate character and most likely also formed 2.3 to 2.4 Ga ago (Table

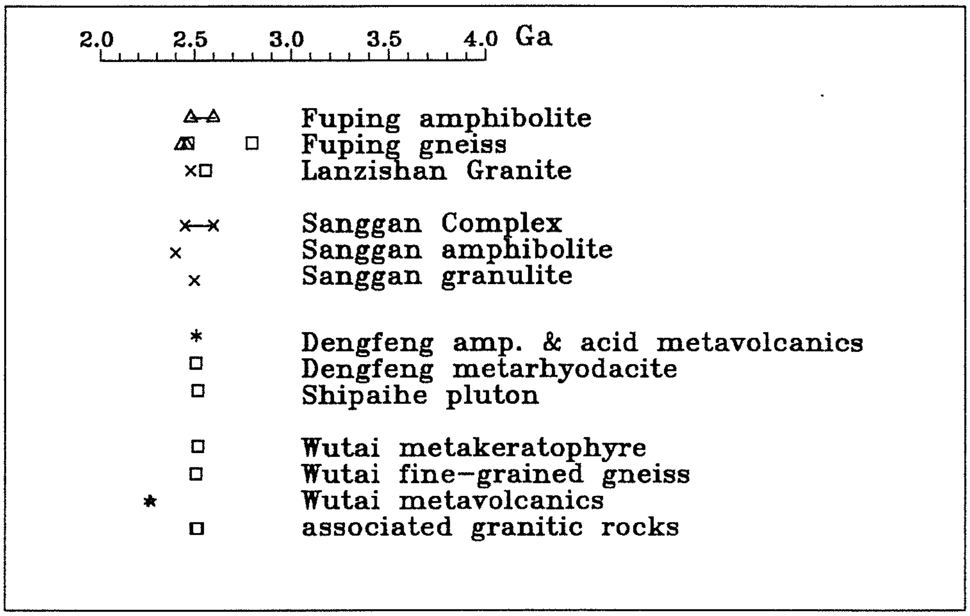

Figure 8-3. Isotopic dating results from different techniques for the Fuping, Sanggan, Dengfeng and Wutai complexes and associated granitic rocks. Symbols for different techniques are same as in Figure 8-1.

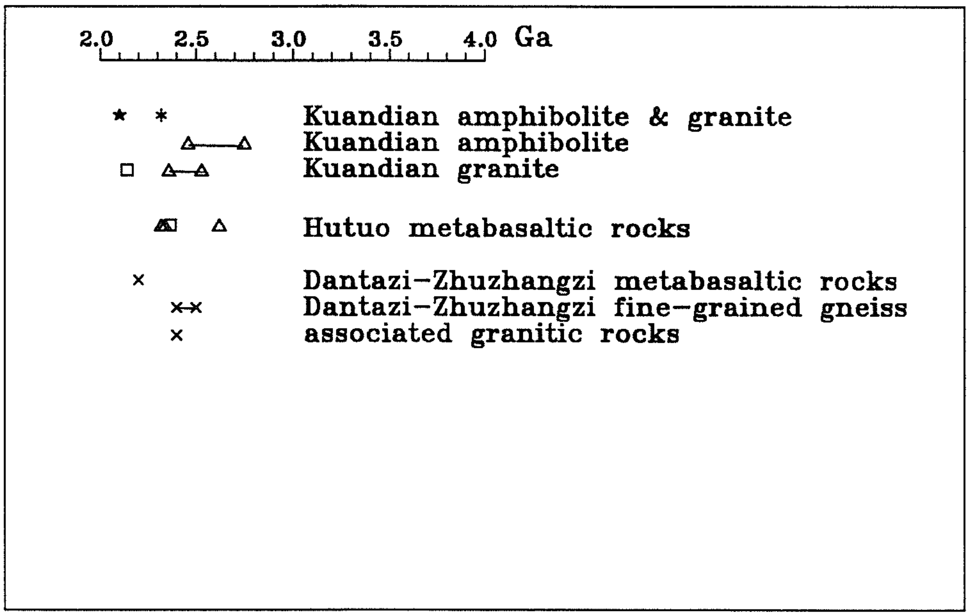

Figure 8-4. Isotopic dating results from different techniques for the Kuandian Complex, Hutuo metabasalts, Dantazi-Zhuzhangzi Group and associated granitic rocks. Symbols for different techniques are same as in Figure 8-1.

4-7 and Fig. 8-4). The Dantazi-Zhuzhangzi Group is less extensively studied. It is younger than 2.5 Ga and probably older than 2.4 Ga (Table 4-7 and Fig. 8-4).

We conclude that the Sinokorean Craton contains relicts of 3.5 Ga crust and was largely consolidated about 2.5 Ga ago. In the Early Proterozoic the craton was only disrupted locally by continental rifts or aulacogens in which Early Proterozoic sedimentary rocks were deposited.

All the Archean and Early Proterozoic rocks in the Sinokorean Craton underwent a thermal event about 1.8 to 1.9 Ga ago, which has been recorded by K-Ar and Rb-Sr isotopic systems. In the Middle and Late Proterozoic times, platform-type carboniferous rocks were deposited along east, southwest margins, and in the Yinshan-Yanshan area (Inner Mongolia-Hebei Province) of the Sinokorean Craton.

IX. ND ISOTOPIC CHARACTER OF THE EARLY PRECAMBRIAN ROCKS IN THE SINOKOREAN CRATON

Initial ϵNd values determined from well defined Sm-Nd isochrons have been plotted in Figure 9-1. Sm-Nd isotopic compositions for individual samples have been plotted in Figure 9-2a, b, c, and d.

Precambrian rocks older than 2.5 Ga in the Sinokorean Craton, whether of basic or granitic composition, plot above DePaolo's (1981) depleted mantle evolution curve (Fig. 9-1), and mostly are above their reference lines, which are drawn through the initial ratios calculated from the mantle curve, on Sm-Nd isochron plots (Fig. 9-2a and b). This indicates that the basic rocks are derived from a mantle source more depleted than that defined by the mantle curve. Granitic rocks are also derived from the depleted mantle source or are products of the former basic rocks with short crustal residence times. The mantle depletion can be related to extraction of old continental materials. The Nd isotopic character, however, implies that preservation of the old continental material was not much before 2.5 Ga ago.

Some ~2.5 Ga granitic rocks in the Sinokorean Craton, especially the Anshan gneissic granite, show an enriched Nd character (Fig. 9-1 and Fig. 9-2c), which can be explained by significant involvement of old continental material in their origin. This indicates that a large proportion of the Sinokorean Craton has been formed since 2.5 Ga ago.

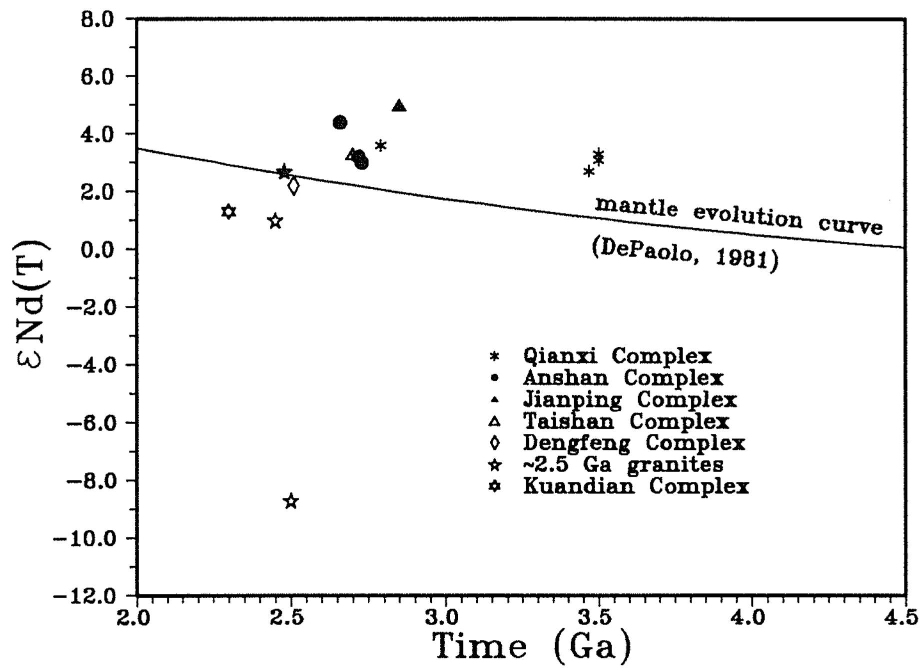

Figure 9-1. εNd evolution diagram for rocks well defining Sm-Nd isochrons. All rocks older than 2.5 Ga show a more depleted character than DePaolo's (1981) depleted mantle curve. Some ~2.5 Ga granitic rocks plot below the mantle curve, which can be explained by involvement of old continental material. The 2.3-2.4 Ga Kuandian Complex came from a mantle source less depleted than that defined by the mantle curve. This is due to contamination of Archean basement or derivation from a different mantle source.

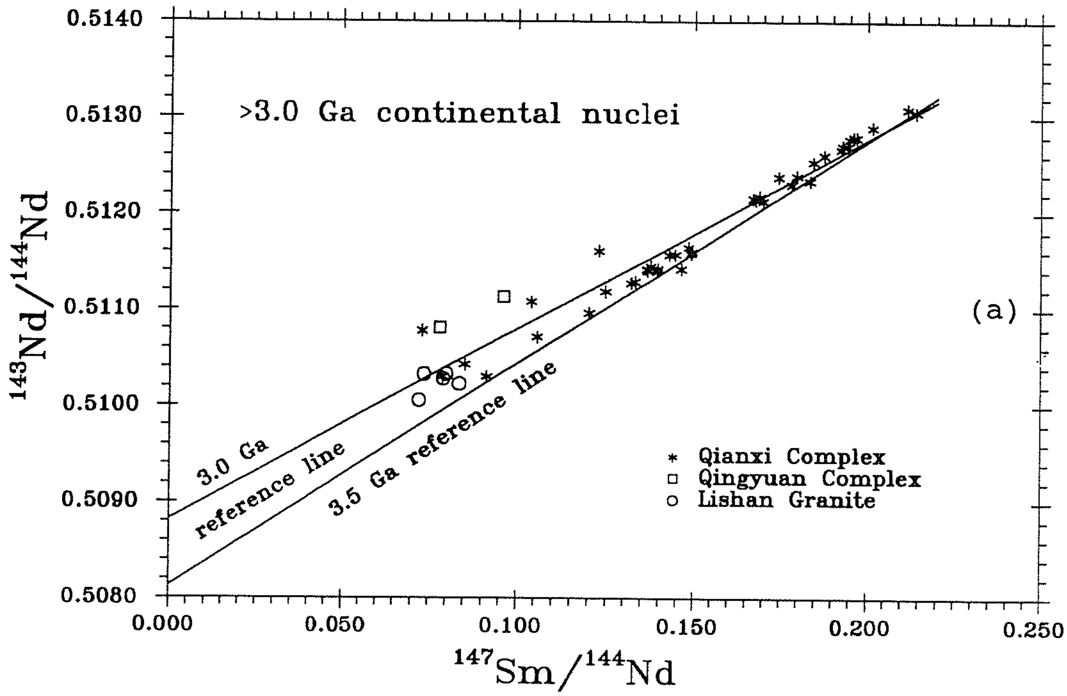

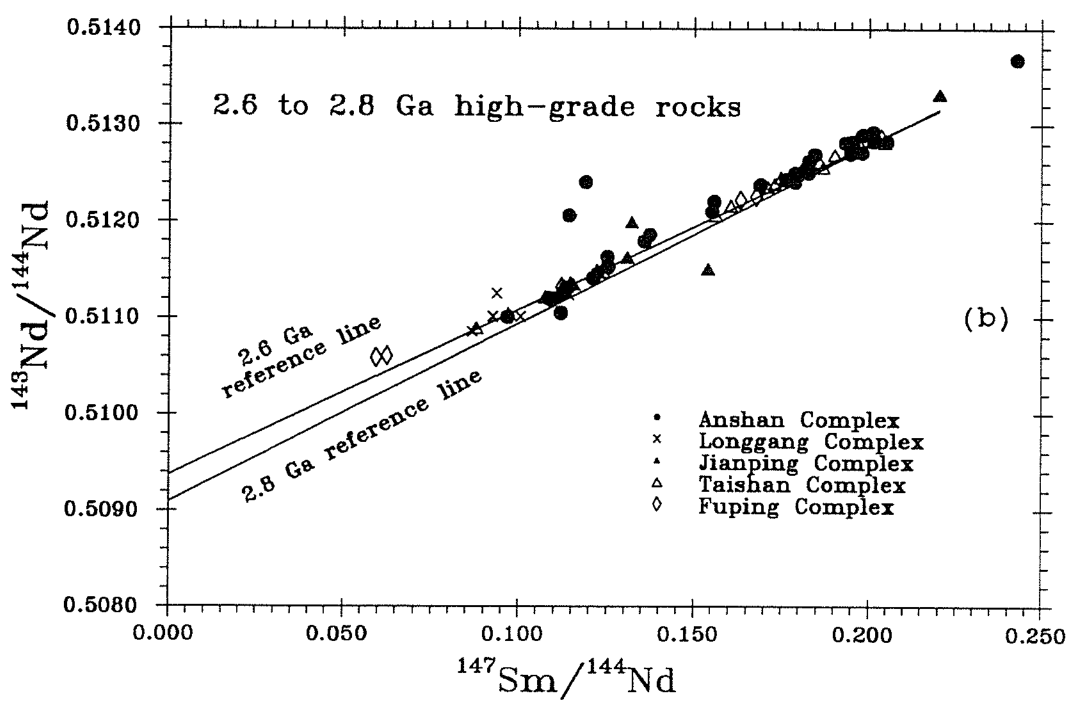

Figures 9-2a and 9-2b, caption in p.206.

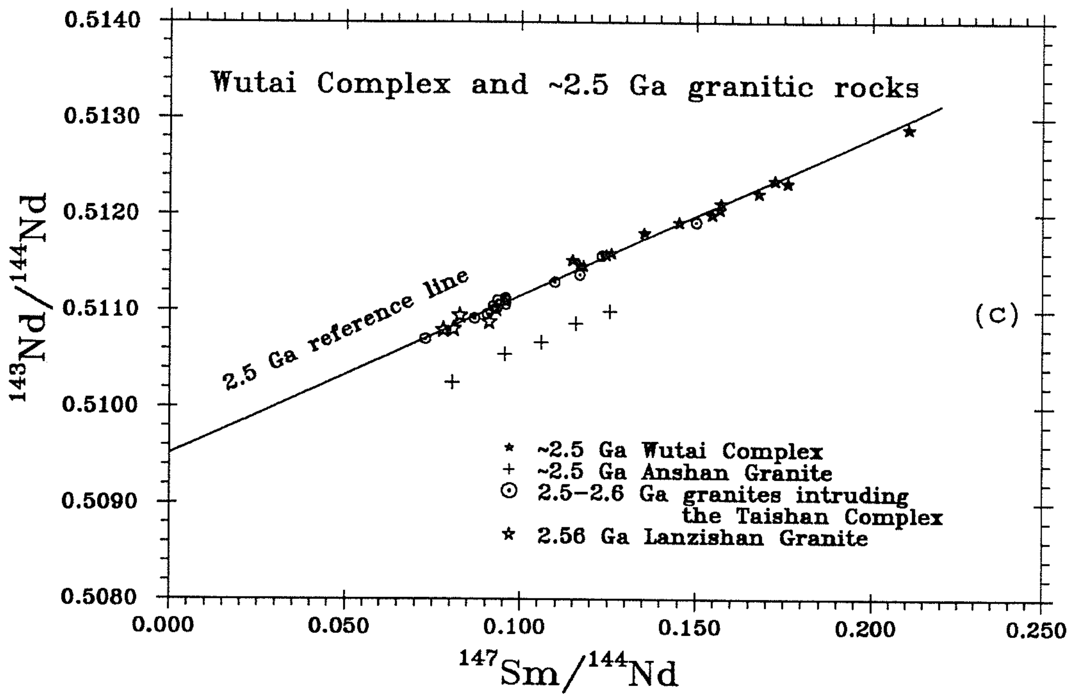

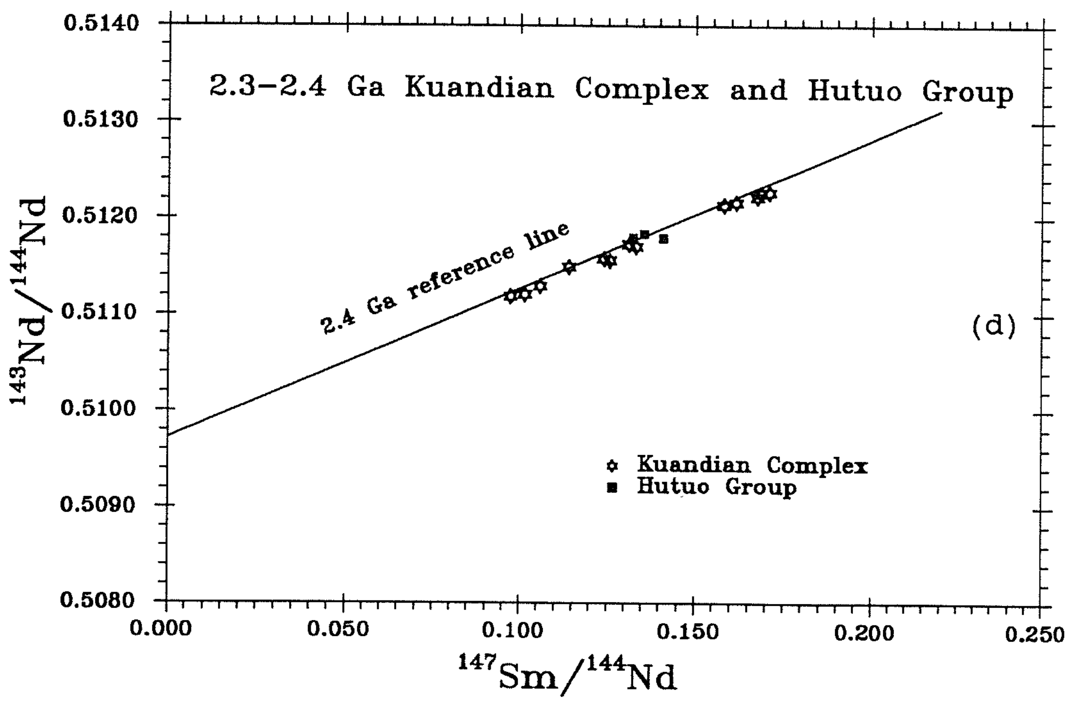

Figure 9-2a, b, c, and d. Sm-Nd isochron plot for individual sample data of (a) Qianxi and Qingyuan complexes, and Lishan Granite; (b) Anshan, Longgang, Jianping, Taishan, and Fuping complexes; (c) Wutai Complex and ~2.5 Ga granitic rocks, and (d) Kuandian Complex and Hutuo Group. The reference lines are drawn through initial Nd isotopic ratios that are calculated from the depleted mantle evolution curve (DePaolo, 1981). Rocks more depleted will plot above their reference lines and those less depleted will plot below their reference lines.

The 2.3 to 2.4 Ga old continental rift-related Kuandian Complex show a Nd isotopic character less depleted than the mantle curve (Fig. 9-1 and 9-2d). This is due to contamination of Archean continental crust or to derivation of a different mantle source.

X. CONCLUSION

Continental nuclei of the Sinokorean Craton include the 3.5 Ga amphibolites and grey gneisses of the Qianxi Complex in the eastern Hebei Province, and the ≥ 3.0 Ga Qingyuan Complex in the eastern Liaoning Province. The latter may extend to the Anshan area to include the ≥ 3.0 Ga Tiejiashan Granite and Lishan Granite. There is little evidence for the existence of the Sinokorean Craton before 3.5 Ga; either not much crustal material formed earlier than 3.5 Ga ago in the area or most of rocks older than 3.5 Ga have been recycled back to the mantle or buried in the lower crust.

Younger Archean rocks in the Sinokorean Craton occur mainly as high-grade metamorphic complexes, including the 2.7 to 2.8 Ga old Anshan Complex in eastern Liaoning Province, Longgang Complex in southern Jilin Province, Jianping Complex in western Liaoning Province, Taishan Complex in western Shandong Province, Jiaodong Complex in eastern Shandong Province, and Taihua Complex in Henan Province; 2.6 Ga Fuping Complex in western Hebei and Shanxi Province; and ≥ 2.5 Ga Sanggan Complex in the Inner Mongolia and Dengfeng Complex in Henan Province. The Wutai Complex and associated granites in Shanxi Province, a well preserved Early Precambrian greenstone-granite belt, are ≥ 2.5 Ga old, and are not of Early Proterozoic age as suggested by Yang et al. (1986). There is no evidence for continental crust before 2.6 Ga in the Wutaishan and Taihangshan regions, and as yet there are no data greater than 2.5 Ga in the Inner Mongolia region.

Nd isotopic data indicate that the Early Precambrian rocks older than 2.5 Ga in the Sinokorean Craton are mainly derived from a very depleted mantle source.

Granitic magmatism peaked about 2.5 Ga ago in the Sinokorean Craton, affecting all previously formed rocks. Some ~2.5 Ga granites are partly derived from older continental crust, as shown by Nd isotopic compositions. After 2.5 Ga, the craton was largely consolidated and magmatic activity was greatly reduced.

In the Early Proterozoic the craton was disrupted locally by continental rifts or aulacogens in which Early Proterozoic sedimentary rocks were deposited. The Early Proterozoic volcanic rocks in the Sinokorean Craton, those in the 2.3 to 2.4 Ga old Kuandian Complex and Hutuo Group, were derived from an intra-continental environment. Nd isotopic compositions indicate that either the mantle source for the Kuandian amphibolite is less depleted than that for the Archean rocks, or precursor magmas were contaminated by Archean basement. Granites from the Kuandian Complex have an anorogenic character. Fractional crystallization of olivine, pyroxene and plagioclase from the precursor magma of the Kuandian amphibolite can produce a magma with a chemical composition similar to that of the Kuandian granite.

All Archean and Early Proterozoic rocks in the Sinokorean Craton were affected by a thermal event about 1.8 to 1.9 Ga ago, as shown by K-Ar and Rb-Sr isotopic systems. In Middle and Late

Proterozoic times, platform-type carbonates were deposited along the eastern, southwestern margins of the Sinokorean Craton, and the Yinshan-Yanshan area (Inner Mongolia-Hebei Province).

BIBLIOGRAPHY

Allègre, C. J. and Rousseau, D., 1984. The growth of the continent through geological time studied by Nd isotopic analysis of shales. Earth Planet. Sci. Lett., 67: 19-34.

Anderson, J. L., 1983. Proterozoic anorogenic granite plutonism of North America. In: L. G. Medaris, Jr., C. M. Byers, D. M. Mickelson and W. C. Shanks (Editors), Proterozoic geology: Selected papers from an international Proterozoic symposium, Geol. Soc. Am. Mem., 161, pp.133-154.

Armstrong, R. L. and Nixon, G. T., 1980. Chemical and Sr-isotopic composition of igneous rocks from DSDP legs 59 and 60. In: Initial Reports of the Deep Sea Driling Project. U.S. Government Printing Office, Washington, D. C.

Arth, J. G. and Hanson, G. N., 1975. Geochemistry and origin of the early Precambrian crust of northeastern Minnesota. Geochim. Cosmochim. Acta, 39:325-362.

Bai, J., 1986. The Early Precambrian geology of Wutaishan. Tianjin Science and Technology Press, Tianjin, 475pp.

Bailey, M. M., 1989. Revisions to stratigraphic nomenclature of the Picture George Basalt Subgroup, Columbia River Basalt Group. In: S. P. Reidel and P. R. Hooper (Editors), Volcanism and tectonism in the Columbia River flood-basalt province, Geol. Soc. Am. special paper 239, pp. 67-84.

Baker, B. H., Goles, G. G., Leeman, W. P. and Lidstrom, M. M., 1977. Geochemistry and petrogenesis of a basalt-benmoreite-trachyte suite from the southern part of the Gregory Rift, Kenya. Contrib. Mineral. Petrol., 64: 303-332.

Barberi, F., Ferrara, G., Santacroce, R., Treuil, M. and Varet, J., 1975. A transitional basalt-pantellerite sequence of fractional crystallization, the Boina Centre, (Afar Rift, Ethiopia). J. Petrol., 16: 22-56.

Barberi., F., Santacroce, R. and Varet, J., 1982. Chemical aspects of rift magmatism. In: Continental and oceanic rifts, G. Pálmason (Editor), Washington, D. C.: Am. Geophys. Union Series 8, 259-270.

Basalt volcanism study project, 1981. Basaltic volcanism on the terrestrial planets. Pergamon Press Inc., New York, pp.1286.

Cameron, M., Collerson, K. D., Compston, W. and Morton, R., 1981. The statistical analysis and interpretation of imperfectly-fitted Rb-Sr isochrons from polymetamorphic terrains. Geochim. Cosmochim. Acta, 45: 1087-1097.

Capedri, S., Venturelli, G., Bocchi, G., Dostal, J., Garuti, G.

and Rossi, A., 1980. The geochemistry and petrogenesis of and ophiolitic sequence from Pindos, Greece. Contrib. Mineral. Petrol., 74: 189-200.

Chen, Y. W. and Zhong, F. D., 1981. Pb isotopic dating of Precambrian rocks in North China: Geological time scale of Chinese Precambrian. Geochemistry 3: 209-219.

Chen, Y. W., Zhong, F. D., Liu, J. Y., Mao, C. X. and Hong, W. X., 1981. Study of Pb isotopes of Precambrian rocks in North China and Chinese isotopic geological scale. Geochimica, 3: 209-219.

Chen, N. S., You, Z. D., Han, Y. Q. and Sun, M., 1991. Whole rock Sm-Nd and Rb-Sr, hornblende $^{40}Ar/^{39}Ar$ and single grain zircon ^{207}Pb-^{206}Pb dating from central complex of eastern Qinling orogenic belt, western Henan: implications for its crustal evolution. Submitted to Geochimica.

Cheng, Y. Q., Sun, D. Z. and Wu, J. S., 1984. Evolutionary mega-cycles of the Early Precambrian proto-North China Platform. J. Geodynamics, 1, 251-277.

Chinese Academy of Geological Sciences, 1973. Geological atlas of the Peoples' Republic of China. Publishing House of Geological Maps, Beijing, 149pp.

Collins, W. J., Beams, S. D., White, A. J. R. and Chappell, B. W., 1982. Nature and origin of A-type granites with particular reference to southern Australia. Contrib. Mineral. Petrol., 80: 189-200.

Compston, W., Zhong, F. D., Foster, J. J., Collerson, K. D., Bai, J. and Sun, D. Z., 1983. Rubidium-strontium geochronology of Precambrian rocks from the Yenshan region, North China. Precambrian Res., 222: 175-202.

Condie, K.C., 1982. Plate tectonics and crustal evolution, Pergamon Press, New York, pp. 310.

Coolen, J.J.M.M.M., Priem, H.N.A., Verdurmen, E.A.Th. and Verschure, R.H., 1982. Possible zircon U-Pb evidence for Pan-African granulite-facies metamorphism in the Mozambique belt of southern Tanzania. Precambrian Res., 17: 31-40.

DePaolo, D. J., 1981. Neodymium isotopes in the Colorado Front Range and crust-mantle evolution in the Proterozoic. Nature, 291: 193-196.

Duncan, R. A. and Richards, M. A., 1991. Hotspots, mantle plumes, flood basalts, and true polar wander. Rev. Geophys, 29: 31-50.

Eby, G. N., 1990. The A-type granitoids: A review of their occurrence and chemical characteristics and speculations on their petrogenesis. Lithos, 26: 115-134.

Ewart, A., 1979. A review of the mineralogy and chemistry of Tertiary - Recent dacitic, rhyolitic and related sialic volcanic rocks. In: F. Barker (Editor), Trondhjemites, dacites and related rocks, Elsevier, Amsterdam, 13-121.

Ewart, A., 1982. Petrogenesis of the Tertiary anorogenic volcanic series of southern Queesland, Australia, in the light of trace element geochemistry and O, Sr and Nd isotopes. J. Petrol., 23: 344-382.

Fabriès, J. and Latouche, L., 1973. Presence de fuchsite dans les quartzites de la série charnockitique des Gour Oumelalen, nord-est de l'Ahaggar, Algérie. Bull. Soc. Fr. Mineral. Cristallogr., 96: 148-149.

Fletcher, I. R. and Rosman, K. J. R., 1982. Precise determination of initial ϵ_{Nd} from Sm-Nd isochron data. Geochim. Cosmochim, Acta, 46:1983-1987.

Glassley, W., 1974. Geochemistry and tectonics of the Crescent Volcanic Rocks, Olympic Peninsula, Washington. Geol. Soc. Am. Bull., 85: 785-794.

Glikson, A.Y., 1976. Trace element geochemistry and origin of early precambrian acid igneous series, Barberton Mountain Land, Transvaal. Geochim. Cosmochim. Acta, 40:1261-1280.

Glikson, A. Y., 1979. Early Precambrian tonalite-trondhjemite sialic nuclei. Earth Sci. Rev., 15: 1-73.

Glikson, A.Y., Prider, C., Jahn, B., Davy, R. and Hickman, A. H., 1986. RE and HFS elements evolution of Archean mafic-ultramafic volcanic suites, Pilbara Block, Western Australia. Australian Bur. Min. Resources, Rec. 1986-No.6, 85pp.

Grauert, B. and Wagner, M.E., 1975. Age of the granulite-facies metamorphism of the Wilmington Complex, Delaware - Pennsylvania Piedmont. Am. J. Sci., 275: 683-691.

Hamilton, P.J., Evensen, N.M., O'Nions, R.K., Smith, H.S. and Erlank, A.J., 1979a. Sm-Nd dating of Onvercht Group volcanics, Southern Africa. Nature, 279: 298-300.

Himilton, P.J., Evensen, N.M., O'Nions, R.K. and Tarney, J., 1979b. Sm-Nd systematics of Lewisian gneisses: implications for the origin of granulites. Nature, 277: 25-28.

Hart, S. R., Brooks, C., 1977. The geochemistry and evolution of Early Precambrian mantle. Contrib. Mineral. Petrol., 61: 109-128.

Huang, X., Bi, Z. and DePaolo, D. J., 1986. Sm-Nd isotope study of early Archean rocks, Qianan, Hebei Province, China. Geochim. Cosmochim. Acta, 50: 625-631.

Irvine, T. N. and Baragar, W.R.A., 1971. A guide to the chemical classification of the common volcanic rocks. Can. J. Earth Sci., 8: 523-548.

Jahn, B. M., 1990a. Origin of granulites: geochemical constraints from Archean granulite facies rocks of the Sino-Korean Craton, China. In: D. Vielzeuf and P. Vidal (Editors), Granulites and Crustal Differentiation (NATO ASI Ser.). Kluwer, Dordrecht, pp. 471-492.

Jahn, B. M., 1990b. Early Precambrian basic rocks of China. In: R. P. Hall and D. J.Hughes (Editors), Early Precambrian Basic Magmatism. Blackie & Son, Glasgow and London, pp. 294-316.

Jahn, B.M. and Sun, S.S., 1979. Trace element distribution and isotopic composition of Archean greenstones. In: L.H. Ahrens (Editor), Origin and Distribution of the Elements. Second Symp. Pergmon Press., Oxford, 597-618.

Jahn, B.M., Glickson, A.Y., Peucat, J.J. and Hickman, A.H., 1981. REE geochemistry and isotopic data of Archean silisic volcanics and granitoids from the Pilbara Block, Western Australia: implications for the early crustal evolution. Geochim. Cosmochim. Acta, 45: 1633-1652.

Jahn, B.M., Gruau, G. and Glickson, A.Y., 1982. Komatiites of the Onverwacht Group, S. Africa: REE geochemistry, Sm/Nd age and mantle evolution. Contrib. Mineral. Petrol., 80: 25-40.

Jahn, B. M. and Zhang, Z. Q., 1984. Radiometric ages (Rb-Sr, Sm-Nd, U-Pb) and REE geochemistry of Archean granulite gneisses from Eastern Hebei Province, China. In: A. Kröner (Editor), Archean Geochemistry. Springer-Verlag, Heidelberg, pp. 204- 234.

Jahn, B. M., Auvray, B., Cornichet, J., Bai, Y. L., Shen, Q. H. and Liu, D. Y., 1987. 3.5 Ga old amphibolites from Eastern Hebei Province, China: field occurrence, petrography, Sm-Nd isochron age and REE geochemistry. Precambrian Res., 34: 311-346.

Jahn, B. M., Auvray, B., Shen, Q. H., Liu, D. Y., Zhang, Z. Q., Dong, Y. J., Ye, X. J., Zhang, Q. Z., Cornichet, J. and Macé, J., 1988. Archean crustal evolution in China: The Taishan Complex and evidence for juvenile crustal addition from long-term depleted mantle. Precambrian Res., 38: 381-403.

Jahn, B. M. and Ernst, W. G., 1990. Late Archean Sm-Nd isochron age for mafic-ultramafic supracrustal amphibolites from the

Northeastern Sino-Korean Craton, China. Precambrian Res., 46: 295-306.

Jiang, C. C., 1981. On Precambrian of Eastern Liaoning. J. of Shenyang Inst. of Geol. and Mineral Resources, 2:No.1, 56-83.

Jiang, C. C., 1984. On Precambrian stratigraphy and comparison of Eastern Liaoning: Deliberation on usage of "Liaohe Group". Bull. of Chinese Academy of Geol. Sci., 9: 157-167.

Jiang, C. C., 1987. Precambrian geology of Eastern Liaoning and Jilin Provinces. Science and Technology Publishing House of Liaoning, 321pp.

Jiang, G. Y. and Shen, H. D., 1980. Archean division and comparison in the Liaoning and Jilin region. Bull. Shenyang Geol. Mineral Resources, 1: 41-63.

Kröner, A., Compston, W., Zhang, G. W., Guo, A. L. and Todt, W., 1988. Age and tectonic setting of late Archean greenstone-gneiss terrain in Henan Province, China, as revealed by single-grain zircon dating. Geology, 16: 211-215.

Köppel, V., 1974. Isotopic U-Pb ages of monazites and zircons from the crust-mantle transition and adjacent units of the Ivrea and Ceneri zones (Southern Alps, Italy). Contrib. Mineral. Petrol., 43: 55-70.

Li, J. L., Wang, K. Y., Wang, Q. C., Liu, X. H. and Zhao, Z. Y., 1990. Early Proterozoic collision orogenic belt in Wutaishan area, China. Scientia Geologica Sinica, 1: 1-11.

Li, S. G., Hart, S. R., Guo, A. L. and Todt, W., 1987. Whole-rock Sm-Nd isotopic age of the Dengfeng Group, central Henan, and its tectonic significance. Science Bull., 22: 1718-1731.

Li S. G., Hart, S.R., Wu T-S, 1990. Rb-Sr and Sm-Nd Isotopic Dating of an Early Precambrian Spilite - Keratophyre Sequence in the Wutaishan Area, North China: Preliminary evidence for Nd-isotopic Homogenization in the mafic and felsic lavas during low-grade metamorphism. Precambrian Res., 47: 191-203.

Liu, H. Y., Hu, H. G., Hu, S. L. and Qi, Z. L., 1981. Rb-Sr and K-Ar dating and ages of some Precambrian and Mesozoic volcanic rocks. Scientia Geologica Sinica, 4: 303-313.

Liu D-Y, Page R.W., Compston, W. and Wu J-S., 1985. U-Pb Zircon geochronology of late Archean Metamorphic Rocks in the Taihangshan-Wutaishan Area, North China. Precambrian Res., 27: 85-109.

Liu, D. Y., Shen, Q. H., Zhang, Z. Q, Jahn, B. M. and Auvray, B., 1990. Archean crustal evolution in China: U-Pb geochronology of the Qianxi Complex. Precambrian Res., 48: 223-244.

Luo, X. Q., Shen, Q. H., Xia, M. X., Liu, D. Y. and Liu, F. X.,1982. Rb-Sr geochronological study of Proterozoic rocks in the Qinglong region of the Hebei Province. In: Abstracts of the second symposium of national isotopic geochemistry, Geol. Publ. House, Beijing, pp. 273-274.

Lu, G. Y. and Huang, G. H., 1987. Rb-Sr isotopic results of low-grade metamorphic rocks from Eastern Hebei Province and the geologic significance. Chinese Regional Geology, 3: 219-244.

Ma X-Y, Ji Y-C, Wei B-H and Zhou D-R, 1957. Basic character of geotectonics in Wutai Mountain area. Geological Publ. House, China.

Macdonald, R., Davies, G. R., Bliss, C. M., Leat, P. T., Bailey, D. K. and Smith, R. L., 1987. Geochemistry of high-silica peralkaline rhyolites, Naivasha, Kenya Rift Valley. Jour. Petrol., 28: 979-1008.

Martin, H., Chauvel, C. and Jahn, B.M., 1983. Major and trace element geochemistry and crustal evolution of Archean granodioritic rocks from eastern Finland. Precambrian Res., 21:159-180.

Mattauer, M. S., 1985. Tectonics of the Qinling Belt: buildup and evolution of Eastern Asia. Nature, 317: 496-500.

McDonough, W. F., 1990. Constraints on the composition of the continental lithosphere mantle, Earth Planet. Sci. Lett., 101: 1-18.

Michael, P. J. and Russell, J. K., 1989. Petrogenetic studies of plutons in the Southern Cordillera, British Columbia. In: Project Lithoprobe, Southern Canadian Cordillera Transect Workshop, University of British Columbia.

O'Connor, J.T., 1965. A classification for quartz-rich igneous rocks based on feldspar ratio. U. S. Geol. Surv. Prof. Paper, 525B: 79-84.

Pearce, J. A., 1976. Statistical analysis of major element patterns in basalts. J. Petrol., 17: 15-43.

Pearce, J.A., 1982. Trace element characteristics of lavas from destructive plate boundaries. In: R. S. Thorpe (Editor), Andesites, John Wiley & Sons, New York, pp.525-547.

Pearce J.A. and Cann, J.R., 1973. Tectonic setting of basic volcanic rocks determined using trace element analyses. Earth Planet. Sci. Lett., 19: 290-300

Pearce, J. A. and Norry M.J., 1979. Petrogenetic implications of Ti, Zr, Y and Nb variations in volcanic rocks. Contrib. Mineral.Petrol., 69: 33-47.

Pearce, J. A., Harris, N.B.W. and Tindle, A.G., 1984. Trace element discrimination diagrams for the tectonic interpretation of granitic rocks. J. Petrol., 25: 956-983.

Peltzer, G., Tapponnier, P., Zhang, Z. T. and Xu, Z. Q., 1985. Neogene and Quaternary faulting in and along the Qinling Shan. Nature, 317: 500-505.

Peucat, J. J., Jahn, B. M. and Cornichet, J., 1986. High precision zircon U-Pb age of a tonalite from the Archean granite greenstone terrain, Qingyuan, NE China. Proc. Int. Symp. Precamb. Crust. Evol. 3, Geol. Publ. House, Beijing, 222-229.

Pidgeon, R. T., 1980. 2480 Ma old zircons from granulite facies rocks from east Hebei Province, North china. Geol. Rev., 26: 198-207.

Plumb, K. A., 1986. Subdivision of Precambrian time: recommendations and suggestions by the Subcommision on Precambrian Stratigraphy. Precambrian Res., 32:65-92.

Qiao, G. S., Wang, K. Y., Guo, A. F. and Zhang, G. T., 1987. Sm-Nd dating of Caochuang early Archean supracrustals, eastern Hebei. Scientia Geologica Sinica, 1: 86-92.

Qiao, G. S., Zhai, M. G. and Yan, Y. H., 1990. Geochronology of Anshan-Benxi Archean metamorphic rocks in Liaoning Province, NE China. Scientia Geologica Sinica, 2: 158-165.

Ren, J.S., 1987. Geotectonic evolution of China. Beijing: Science Press; Berlin: Springer-Verlag.

Schenk, V., 1980. U-Pb and Rb-Sr radiometric dates and their correlation with metamorphic events in the granulite facies basement of the Serre, southern Calabria (Italy). Contrib. Mineral. Petrol., 73: 23-38.

Sengor, A. M. C., 1985. East asia tectonic collage. Nature, 318: 16-17.

Shaw, D.M. 1972. The origin of the Apsby gneiss, Ontario. Can. J. Earth Sci., 9: 18-35.

Shen, Q. H., Zhang, Z. Q., Xia, M. X., Wang, X. Y. and Lu, J. Y., 1981. Rb-Sr age determination on the late Archean ferrosiliceous rocks series in Sijiaying, Luanxian, Hebei. Geol. Rev., 27: 207-212.

Shen, Q. H., Liu, D.Y., Wang, D., Gao, G. F. and Zhang, Y. F.,

1987. U-Pb and Rb-Sr isotope age study of the Jining Group from Inner Mongolia of China. Bull. Chin. Acad. Geol. Sci., 16: 165-178.

Sigvaldason, G. E. and Óskarsson, L., 1986. Fluorine in basalts from Iceland. Contrib. Mineral. Petrol., 94: 263-271.

Sun, J. S., 1987. On the boundary age of Qianxi Group and Dantazi Group, East Hebei Province. In: The Working Group on the Geological Time Scale of China, MGMR (Editors), A Geological Time Scale of China, Geol. Publ. House, Beijing pp. 29-31.

Sun, M., Armstrong, R. L. and Lambert, R. St J., 1991a. Petrochemistry and Sr, Pb Nd isotopic geochemistry of Early Precambrian rocks, Wutaishan and Taihangshan areas, China. Precambrian Res., in press.

Sun, M. Armstrong, R. L. and Lambert, R. St J., Jiang, C. C. and Wu, J. H., 1991b. Petrochemistry and Sr, Pb and Nd isotopic geochemistry of Early Proterozoic Kuandian Complex, East Liaoning Province, China. Submitted to Precambrian Res.

Sun, R. G., Armstrong, R. L. and Scott, K., 1985. Rb-Sr geochronology of Archean rocks from the eastern Hebei Province, Science Bull., 22: 1725-1728.

Sun, R. G. and Armstrong, R. L., 1986. Isotopic geochronology of the Taishan Group in western Shandong Province. Geol. Review, 32: 426-432.

Sun, R. G., Armstrong, R. L. and Scott, K., 1989. Rb-Sr chronology of cratonization of Sino-Korea Plate. Geochimica, 3: 233-240.

Sun, S. S., 1980. Lead isotopic study of young volcanic rocks from mid-ocean ridges, ocean islands and island arcs. Phil. Trans. R. Soc. Lond., A297: 409-445.

Tarney, J., Weaver, B. and Drury, A., 1979. Geochemistry of Archean trondhjemitic and tonalitic gneisses from Scotland and east Greenland. In: F. Barker (Editor), Trondhjemites, Dacites and Related Rocks. Elsevier, Amsterdam, 275-299.

Thompson, B. N., Esson, J. and Dunham, A. C., 1972. Major element chemical variation in the Eocene lavas of the Isle of Skye, Scotland. J. Petrol., 13: 219-253.

Thompson, R. N., Gibson, I. L., Marriner, G. F., Mattey, D. P. and Morrison, M. A., 1980. Trace-element evidence of multistage mantle fusion and polybaric fractional crystallization in the Palaeocene lavas of Skye, NW Scotland. J. Petrol., 21: 265- 293.

Thompson, R. N., Morrison, M. A., Dickin, A. P. and Hendry, G. L., 1983. Continental flood basalts...arachnids rule OK? In: C. J. Hawkesworth and M. J. Norry (Editors), Continental basalts and mantle xenoliths, Shiva, Nantwich, pp.158-185.

van der Heyden, 1989. U-Pb and K-Ar geochronometry of the coast plutonic complex, 53°N to 54°N British Columbia, and implications for the Insula-intermontane Superterrane boundary. Unpubl. Ph D thesis, University of British Columbia, Vancouver, pp.392.

Vidal, Ph., Peucat, J. J. and Lasnier, B., 1980. Dating of granulites involved in the Hercynian fold-belt of Europe: An example taken from the granulite-facies orthogneisses at la Picherais, Southern Armorican Massif, France. Contrib. Mineral. Petrol., 72: 283-289.

Wang, K. Y., Yan, Y. H., Yang, R. Y. and Chen, Y. F., 1985. REE geochemistry of Early Precambrian charnockites and tonalitic-granodioritic gneisses of the Qianan Region, eastern Hebei, North China. Precambrian Res., 27: 63-84.

Wang, K. Y., Windley, B. F., Sills, J. D. and Yan, Y. H., 1990. The Archean gneiss complex in E. Hebei Province, North China: geochemistry and evolution. Precambrian Res., 48: 245-265.

Wang, Q. C., 1988. The stratigraphical ages, division and correlation of the Early Precambrian in the Taihang-Watai Area, the Yanshan area and the Eastern Sector of the Yinshan Mountains. Acta Geol. Sinica, 1: 16-30.

Wang, S. S., Zhai, M. G., Hu, S. L., Sang, H. Q. and Qiu, J., 1986. $^{40}Ar/^{39}Ar$ age spectrum for biotite separated from Qingyuan tonalite, NE China. Scientia Geol. Sinica, 1: 97-99.

Wang, S. S., Hu, S. L., Zhai, M. G., Sang, H. Q. and Qiu, J., 1987. An application of the $^{40}Ar/^{39}Ar$ dating technique to the formation time of the Qingyuan granite-greenstone terrane in NE China. Acta Petrol. Sinica, 11: 55-62.

Wang, Z. J., Shen, Q. H. and Jin, S. W., 1987. Petrology, geochemistry and U-Pb isotopic dating of the Shipaihe 'metadiorite mass' in Dengfeng County, Henan Province, China. Bull. Chin. Acad. Geol. Sci., 16: 215-225.

Weaver, B.L., 1980. Rare earth geochemistry of Madras granulites. Contrib. Mineral. Petrol., 71:271-279.

Weaver, B.L. and Tarney, J., 1980. Rare earth element geochemistry of Lewisian granulite-facies gneisses, northwest Scotland: implications for the petrogenesis of the Archean lower continental crust. Earth Planet. Sci.

Let., 51: 279-296.

Whalen, J. B., Currie, K. L. and Chappell, B. M., 1987. A-type granites: Geochemical characteristics, discrimination and petrogenesis. Contrib. Mineral. Petrol., 95: 407-419.

White, A. J. R. and Chappell, B. W., 1983. Granitoid types and their distribution in the Lachland fold belt, southeastern Australia. Geol. Soc. Am. Mem., 159: 21-34.

Wood, D. A., 1978. Major and trace element variations in the Tertiary lavas of eastern Iceland and their significance with respect to the Icelandic geochemical anomaly. J. Petrol., 19: 393-436.

Wu J-S, Lin D-Y, Jin L-G, 1986. The zircon U-Pb age of metabasic lavas from the Hutuo Group in the Wutai Mountain Area. Geol. Rev., 32(2): 178-184.

Xu, G. Z. and Wang, Y. F., 1990. On the characteristics of Precambrian structural evolution of the east Qinling Mountain. Scientia Geologica Sinica., 2: 102-112.

Yan, E., Li, X. Q. and Han, G. G., 1981. Geological character of Archean greenstone belt in Qingyuan region. J. Liaoning Geology., 1: 158-177.

Yang, Z. Y., Cheng, Y. Q. and Wang, H. Z., 1986. The Geology of China. Clarendon Press, Oxford, 303pp.

Yin, Q. Z., 1988. The petrology geochemistry and geochronology of the Shuichang charnockites and related rocks, Qianan County, eastern Hebei, China. M. S. thesis. Inst. Geol. Chin. Acad. Geol. Sci., Beijing, pp.79.

Ying, S. H., 1980. The Taishan Complex. Science Publishing House, Beijing, 83pp.

York, D., 1969. Least squares fitting of a straight line with correlated errors. Earth Planet. Sci. Lett., 5: 320-324.

Zhai, M. G., Yang, R. Y., Lu, W. J. and Zhou, J., 1985. Geochemistry and evolution of the Qingyuan Archean granite-greenstone terrain, NE China. Precambrian Res., 27: 37-62.

Zhai, M. G., Windley, B. F. and Sills, J. D., 1990. Archean gneisses, amphibolites and banded ion-formations from the Anshan area of Liaoning Province, NE China: their geochemistry, metamorphism and petrogenesis. Precambrian Res., 46: 195-216.

Zhang, G. W., Bai, Y. B., Sun, Y., Gui, A. L., Zhou, D. W. and Li, T. H., 1985. Composition and evolution of the Archean crust in central Henan, China. Precambrian Res., 27: 7-35.

Zhang, Q. S., 1984. Chinese Early Precambrian Geology and Mineralization. Jilin People's Publishing House, Changchun, 536pp.

Zhao, Z. P., 1988. Subdivision of Precambrian time and rock-stratigraphic units of Eastern China: Inference from Precambrian crustal evolution of Eastern Hebei Province. Scientia Geol. Sinica., 4: 301-312.

Zhong, F. D., 1984. Geochronological study of Archean granite-gneisses in Anshan area, Northeast China. Geochimica, 1: 195-205.

APPENDIX 1
SAMPLE DESCRIPTION

Sample	Locality	Latitude Longitude	Description
Qianxi Complex			
HTB-4	Taipingzhai, Qianxi, Hebei	40°15' 118°36'	Grey plagioclase granulite.
HTB-5	Same as above.		Grey plagioclase granulite.
Qingyuan Complex			
LG-2	Gounaidianzi, Qingyuan, Liaoning	42°4' 124°54'	Biotite granulite. Migmatitic.
LG-3	Same as above.		Biotite granulite/gneiss. Leucocratic.
Tiejiashan Granite			
T-1	Tiejiashan, Anshan, Liaoning.	41°6' 123°2'	Leucocratic granite.
Lishan Granite			
r86-159	Lishan Park Anshan, Liaoning.	41°8' 123°2'	Dark-grey trondhjemite.
r86-163	Same as above.		Same as above.
r86-164	Same as above.		Same as above.
r86-165	Same as above.		Same as above.
r86-166	Same as above.		Same as above.
Longgang Complex			
LG-001	Laojinchang Huadian Jilin.	42°53' 127°27'	Light-grey granulite. Medium grain sized.
LG-003	Same as above.		Light-reddish granulite.
LG-009	Same as above.		Granulite.
LG-011	Same as above.		Same as above.
LG-014	Erdaogou, Huadian, Jilin.	42°51' 127°17'	Biotite-hornblende-plagioclase gneiss. Coarse grain sized.
LG-033	Quanhuizhan, Huadian, Jilin.	42°48' 127°14'	Grey gneiss. Medium grain sized
LG-034	Same as above.		Dark-grey gneiss.
LG-035	Same as above.		Light-grey gneiss.
Anshan Complex			
A86-002	Cigou, Anshan, Liaoning.	41°3' 123°30'	Magnetite amphibolite.
A86-005	Same as above.		Amphibolite. Fine grain sized.

A86-008	Same as above.		Same as above.
A86-010	Same as above.		Same as above.
A86-120	Dagushan, Anshan, Liaoning.	41°3' 123°3'	Fine-grained gneiss.
A86-121	Same as above.		Same as above.
A86-128	Xidabei drilling core-110, Anshan, Liaoning.		Plagioclase amphibolite. Fine grain sized.
A86-129	Same as above.		Same as above.
A86-130	Same as above.		Same as above.
A86-133	Same as above.		Plagioclase amphibolite.
A86-136	Same as above.		Same as above.
A86-137	Same as above.		Same as above.
A86-143	Xidabei drilling core-130, Anshan, Liaoning.		Biotite fine-grained gneiss.
A86-144	Same as above.		Same as above.
A86-147	Same as above.		Same as above.
Jianping	Complex		
6302	Liushubozi, Jianping, Liaoning.	41°18' 118°50' 118°50'	Garnet-diopside-plagioclase-amphibolite.
6303	Same as above.		Biotite-hypersthene-orthoclase-plagioclase-granulite.
6341	Same as above.		Olivine-orthopyroxene-clinopyroxene pyroxenite. Medium grain sized.
6354	Same as above.		Orthopyroxene-clinopyroxene amphibolite.
6441	Same as above.		Garnet-biotite-clinopyroxene-orthopyroxene-plagioclase-granulite.
6496	Same as above.		Amphibolite.
Kuandian	Complex		
K86-026	Wenjiagou, Fengcheng, Liaoning.	40°43' 123°56'	Gneissic granite. Fine grain sized.
K86-027	Same as above.		Same as above.
K86-086	Simenzi Bridge, Fengcheng, Liaoning.	40°44' 123°49'	Same as above.
K86-088	Same as above.		Same as above.
K86-089	Same as above.		Same as above.
K86-090	Same as above.		Same as above.
K86-091	Same as above.		Same as above.
K86-093	Same as above.		Same as above.
K86-083	Linjiapu, Fengcheng, Liaoning.	40°46' 113°34'	Plagioclase amphibolite.
K86-084	Same as above.		Plagioclase amphibolite.

K86-243	Yujiapu, Yingkou, Liaoning.	40°32' 122°43'	Plagioclase amphibolite.
K86-244	Same as above.		Plagioclase amphibolite.
K86-246	Same as above.		Quartz amphibolite. Light colour layer.
K86-248	Same as above.		Plagioclase amphibolite.
K87-079	Shangying, Reservoir, Haicheng, Liaoning.	40°50' 122°56'	Cordierite-biotite schist.
K87-125	Same as above.		Biotite-hornblende gneiss.
Caohe Group			
C86-019	Huanggou, Liaoyang, Liaoning.	41°1' 123°34'	Albite fine-grained gneiss. Leucocratic.
C86-020	Same as above.		Same as above.
C86-032	Tongyuanpu, Fengcheng, Liaoning.	40°46' 123°55'	Biotite fine grained-gneiss.
C86--37	Same as above.		Same as above.
C86-098	Longchang, Liaoyang, Liaoning.	40°55' 123°11'	Fine-grained gneiss. Leucocratic.
C86-099	Same as above.		same as above.
C86-207	Qinghuayu, Dashiqiao, Liaoning.	40°40' 122°44'	Graphite-tremolitite. Fine grain-sized.
C87-020	Gaojiayu, Dashiqiao, Liaoning.	40°44' 122°44'	Biotite-schist.
C87-076	Huaziyu, Dashiqiao, Liaoning.	40°43' 122°44'	Graphite-tremolitite. Fine grain-sized.
C87-091	Baijiapu, Dashiqiao, Liaoning.	40°40' 122°45'	Staurolite-biotite-schist.
C87-098	Same as above.		Biotite-schist. Fine grain sized.
Liaoyang group			
L86-213	Luoshan, Dashiqiao, Liaoning.	39°49' 122°34'	Spotted phyllitic slate. Blue-greenish.
L86-218	Same as above.		Same as above.
L86-222	Same as above.		Same as above.
L87-107	Xiaosigou, Dashiqiao, Liaoning.	40°40' 122°34'	Phyllitic slate. Grey-greenish.
L87-108	Same as above.		Same as above.
Shisi Granite			
r86-172	Shizhugou, Shisi, Haicheng,	40°54' 123°0'	Reddish granite. Medium grain sized.

	Liaoning.		
r86-173	Same as above.		Same as above.
r86-174	Same as above.		Same as above.
r86-175	Same as above.		Same as above.
r86-176	Same as above.	40°55'	Same as above.
		123°57'	Same as above.
r86-178	Same as above.		Same as above.
Mafeng Granite			
r86-180	Shianzui, Mafeng, Haicheng, Liaoning.	40°48' 123°57'	Porphyritic biotite-granite. Coarse grain sized.
r86-183	Same as above.		Same as above.
r86-184	Same as above.		Same as above.
r86-187	Same as above.		Same as above.
r86-188	Same as above.		Same as above.
Dading granite			
rD-002	Dading, Fengcheng, Liaoning.	40°43' 123°41'	Trondhjemite
rD-005	Same as above.		Same as above.
rD-008	Same as above.		Same as above.
Fuping	Complex		
F1-3	Shuibao, Laiyuan, Shanxi.	39°05' 114°21'	Biotite-hornblende-plagioclase amphibolite.
F2-2	Zhifu Bridge, Laiyuan, Shanxi.	39°04' 114°19'	Plagioclase amphibolite.
F4-2	60km of Road Lianshanguan to Fuping.	39°00' 114°16'	Amphibolite, sericitized.
F4-3	Same as above	38°54'	Amphibolite.
F6-1	100m west of Xicaokou, Fuping, Hebei	114°08'	Grey gneiss.
F6-3	Same as above		Grey gneiss.
F6-4	Same as above		Grey gneiss.
F6-5	Same as above		Grey gneiss.
Wutai Complex (W-1)			
W84-1	Road of Nanyukou to tongziya Fanzhi, Shanxi.	39°11' 113°34'	Plagioclase amphibolite. Fine grain-sized.
W84-2	Same as above		Plagioclase amphibolite.
W84-3	Same as above		Plagioclase amphibolite.
W84-4	Same as above		Plagioclase amphibolite. Chloritized and sericitized.
W84-51	Same as above		Epidote amphibolite. Light colour layer.
W84-52	Same as above		Amphibolite. Interlayered

			with W84-51.
W84-7	Same as above		Amphibolite.
W84-8	Same as above		Amphibolite. Biotite around hornblende.
W84-9	Same as above		Amphibolite. Biotite around hornblende.
Wutai Complex (W-2a)			
W82-4	SE 2km of Taipinggou, Fanzhi, Shanxi.	39°05' 113°39'	Chlorite greenschist. Also consists of epidote, plagioclase, quartz and calcite. Fine-grain sized. Micro-veins of calcite.
W82-5	Same as above		Epidote-chlorite greenschist.
W82-7	Same as above		Chlorite greenschist. Fine-grain sized. Poor schistosity.
W82-9	Same as above		Chlorite greenschist. Micro-folded. Calcite veins.
Wutai Complex (W-2b)			
W81-1	SE 6km of Taipinggou, Fanzhi, Shanxi.	39°04' 113°41'	Chlorite greenschist. Good schistosity.
W81-2	Same as above		Chlorite greenschist. Good schistosity.
W81-3	Same as above		Chlorite greenschist. Fair schistosity.
W81-6	Same as above		Chlorite greenschist. Poor schistosity.
W81-7	Same as above		Chlorite greenschist. Poor schistosity.
W81-8	Same as above		Chlorite greenschist. Medium-grain sized.
W81-11	Same as above		Chlorite greenschist. Poor schistosity.
W81-15	Same as above		Chlorite greenschist.
Wutai Complex (W-3)			
W85-1	NE 700m of Yaozichun, Daixian, Shanxi	38°58' 113°04'	Actinolite amphibolite. Also consists of epidote, plagioclase, quartz. Fine-grain sized.
W85-2	Same as above		Actinolite amphibolite. medium-grain sized.
W85-4	Same as above		Actinolite amphibolite. medium-grain sized.
W85-6	Same as above		Actinolite amphibolite. medium-grain sized.
W85-8	Same as above		Actinolite amphibolite. medium to coarse-grain sized.

Hutuo Group			
H-003	S 100m of Huilongdi, Wutai, Shanxi.	38°51' 113°35'	Chlorite greenschist.
H-004	S 150m of Huilongdi, Wutai, Shanxi.	38°51' 113°40'	Chlorite greenschist.
H-007	Same as above		Chlorite greenschist. Fine-grain sized. Poor schistosity.
H-014	E 500m of Liudingsi, Wutai, Shanxi.	38°01' 113°34'	Chlorite greenschist.
H-017	Same as above		Chlorite greenschist. Well preserved ophitic texture.
Lanzishan Granite			
076	E 500m of Changchengling, Wutai, Shanxi.	38°45' 113°45'	Gneissic granite.
077	Same as above		Gneissic granite. Medium-grain sized.
078	Same as above		Gneissic granite.
079	Same as above		Gneissic granite.
080	Same as above		Gneissic granite.
Shifo Granite			
054	SW 500m of Xiaomati, Wutai, Shanxi.	38°55' 113°38'	Granitic gneiss.
057	Same as above		Granitic gneiss.
Chechang Granite			
083-1	Taipinggou, Fanzhi, Shanxi.	39°06' 113°38'	Gneissic trondhjemite-tonalite.
083-2	Same as above		Gneissic trondhjemite-tonalite.
083-3	Same as above		Gneissic trondhjemite-tonalite.
083-4	Same as above		Gneissic trondhjemite-tonalite.
Wangjiahui Granite			
087-1	SW 4km of Wangjiahui, Daixian, Shanxi.	39°01' 113°06'	Granitic gneiss.
087-2	Same as above		Granitic gneiss.
087-3	Same as above		Granitic gneiss.
087-4	Same as above		Granitic gneiss.
Taishan Complex			
SYB-5	0.5 km S of Yanlingguan, Xintai, Shandong.	36°5' 117°30'	Plagioclase amphibolite.

SYE-1	1 km N of Yanlingguan, Xintai, Shandong	Plagioclase amphibolite.

APPENDIX 2.

ANALYTICAL METHODS FOR RB-SR, SM-ND and PB-PB ISOTOPES:

Rb-Sr and Sm-Nd:

Optimum amounts of ^{87}Rb and ^{84}Sr spikes were added to 200 mg of whole rock powder for Rb and Sr isotopic dilution and Nd isotopic ratio analyses. Sm and Nd isotopic dilution analyses were done separately, using another 200 mg whole rock powder aliquot mixed with an optimum amount of mixed spike containing ^{149}Sm and ^{145}Nd.

Samples were digested with double-distilled HF and 16 N HNO_3 (7:3) in a 15 ml screw-capped Savillex vial on a hot plate for over 24 hours. After drying the dissolved samples were extracted in 2.3 N HCl and any residue was treated with more HF and HNO_3 in the closed Savillex vial on a hot plate for over 5 hours for a complete dissolution and taken up again in 2.3 N HCl after drying.

After the sample had been totally dissolved in 2.3 N HCl, the solution was dried again and then redissolved in 2 ml 2.3 HCl and centrifuged. The supernatant was loaded into a cation exchange resin column (20 cm long 1 cm wide) for Rb, Sr and REE separation by elution with 2.3 N and 6 N HCl.

The REE aliquot was dried on a hot plate and loaded in 0.1 N HCl into a second cation exchange resin column (30 cm long 0.1 cm wide) for Sm and Nd separation by MLA elution. The flow rate was controlled by adjusting the height of MLA reservoir. An automatic counting collector was used for Sm and Nd collection.

Rb, Sr, Sm, and Nd fractions were dried and further cleaned by using a small cation resin column (7 cm long 0.5 cm wide) and HCl elution.

Rb, Sr, Sm, and Nd isotopic dilution analyses were made using a VG - MM30 mass spectrometer at the University of Alberta. Nd isotopic ratio was measured using a VG - 354 mass spectrometer, equipped with a multiple collector, at the University of Alberta. Double Re filaments were used for Rb, Sr, Sm and Nd isotopic analyses. $^{87}Sr/^{86}Sr$ ratios are normalized to $^{88}Sr/^{86}Sr$ = 8.3752 and corrected for ^{87}Rb ($^{87}Rb/^{85}Rb$ ratio of the same spiked sample was used, Rb in any Sr run was negligible). Sr standard NBS-987 gave an average $^{87}Sr/^{86}Sr$ = 0.71020 +/- 0.00002 (2σ) during the course of this work. $^{143}Nd/^{144}Nd$ was normalized to $^{146}Nd/^{144}Nd$ = 0.7219. La Jolla standard Nd metal $^{143}Nd/^{144}Nd$ gave an average 0.511856 +/- 0.000004 (2σ) during the course of this work. The 2σ precisions estimated from duplicated runs are as follows: 2.0% for $^{87}Rb/^{86}Sr$, 1.0% for $^{147}Sm/^{144}Nd$, 0.026% for $^{87}Sr/^{86}Sr$ and 0.005% for $^{143}Nd/^{144}Nd$. The blanks for the total procedure are 0.2-0.3 ng for Rb, 3-4 ng for Sr, 0.2-0.3 ng for Sm, and 0.5-0.9 ng for Nd.

Whole rock Pb:

200 mg of rock powder was dissolved by the same method described above using triple distilled HF and 16 N HNO_3. The sample was taken up in 5 ml dilute HNO_3 and centrifuged. 1 ml purified $BaNO_3$ solution was added to the supernatant for Pb coprecipitation. The precipitate was taken up in 1.5 N HCl and

loaded into an anion exchange resin column (5 cm long 0.5 cm wide) for Pb separation by 1.5 N HCl and H_2O elution.

A silica gel - phosphoric acid loading method was used when measuring the Pb isotopic ratios on a VG - MM30 mass spectrometer at the University of Alberta. The 2σ precision estimated from duplicated runs is 0.10%, 0.15%, and 0.16% for $^{206}Pb/^{204}Pb$, $^{207}Pb/^{204}Pb$, and $^{208}Pb/^{204}Pb$ respectively. Error correlations between any two of these ratios are 0.8. Pb standard NBS-981 gave average ratios, +/- 2σ, of 16.940 +/- 0.003, 15.495 +/- 0.003, and 36.731 +/- 0.017 for $^{206}Pb/^{204}Pb$, $^{207}Pb/^{204}Pb$, $^{208}Pb/^{204}Pb$, respectively. Blank for the total procedure is 2 ng.